THE BIOGENESIS OF TAIL-ANCHORED MEMBRANE PROTEINS AT THE ENDOPLASMIC RETICULUM

A thesis submitted to The University of Manchester for the degree of Doctor of Philosophy in the Faculty of Life Sciences

2010

Pawel J. Leznicki

Faculty of Life Sciences
The University of Manchester

CONTENTS

Word count: 53,752

ABSTRACT

Tail anchored (TA) proteins constitute an evolutionarily-conserved group of integral membrane proteins that are characterised by the presence of a single C-terminal transmembrane segment (TMS), which acts as both a membrane anchor and a targeting signal. In eukaryotes, TA-proteins localise to most intracellular membranes with the endoplasmic reticulum (ER) being the entry site for TA-proteins destined for the compartments of the secretory pathway and the plasma membrane. Notably, distinct routes for TA-protein delivery to the ER have been identified, and the pathway preference seems to be determined by a relative hydrophobicity of the TMS.

In the present study I demonstrate that two major routes for TA-protein delivery to the ER membrane, the TRC40-dependent and "unassisted"/chaperone-mediated pathways, both rely on the action of cytosolic factors which are extremely flexible and can accommodate substrates with TMSs that have been extensively modified (Chapters 2.1 – 2.3). Moreover, the ability of PEGylated forms of the TRC40 client Sec61β to become membrane-integrated correlates very well with the calculated changes in free energy that are associated with its partitioning into a lipid bilayer, supporting a thermodynamics-driven mode of membrane insertion for TA-proteins (Chapter 2.1). The use of fluorescently-labelled recombinant cytochrome b5 (Cytb5), a model TA-protein exploiting the "unassisted"/chaperone-mediated pathway, strongly suggests the involvement of cytosolic components during its biogenesis, whilst the accessibility of novel cysteine residues to the reagent mPEG-5000 indicates a role for peripheral membrane proteins during Cytb5 membrane integration (Chapter 2.2). Importantly, pull down assays using recombinant TA-proteins as bait, followed by mass spectrometric analysis, allowed me to identify a number of cytosolic interacting partners of TA-proteins (Chapters 2.3 and 2.4). The function of one such a factor, Bat3, was further investigated, and it was found to act prior to TRC40 and facilitate the loading of TA-protein substrates onto this targeting factor (Chapter 2.3). Based on these results and available published data, a hypothetical protein-protein interaction network is presented, and I speculate about the role of individual components during TA-protein biogenesis (Discussion).

DECLARATION

No portion of the work referred to in the thesis has been submitted in support of an application for another degree or qualification of this or any other university or other institute of learning.

COPYRIGHT STATEMENT

i. The author of this thesis (including any appendices and/or schedules to this thesis) owns certain copyright or related rights in it (the "Copyright") and s/he has given The University of Manchester certain rights to use such Copyright, including for administrative purposes.

ii. Copies of this thesis, either in full or in extracts and whether in hard or electronic copy, may be made only in accordance with the Copyright, Designs and Patents Act 1988 (as amended) and regulations issued under it or, where appropriate, in accordance with licensing agreements which the University has from time to time. This page must form part of any such copies made.

iii. The ownership of certain Copyright, patents, designs, trade marks and other intellectual property (the "Intellectual Property") and any reproductions of copyright works in the thesis, for example graphs and tables ("Reproductions"), which may be described in this thesis, may not be owned by the author and may be owned by third parties. Such Intellectual Property and Reproductions cannot and must not be made available for use without the prior written permission of the owner(s) of the relevant Intellectual Property and/or Reproductions.

iv. Further information on the conditions under which disclosure, publication and commercialisation of this thesis, the Copyright and any Intellectual Property and/or Reproductions described in it may take place is available in the University IP Policy (see http://www.campus.manchester.ac.uk/medialibrary/policies/intellectual-property.pdf), in any relevant Thesis restriction declarations deposited in the University Library, The University Library's regulations (see http://www.manchester.ac.uk/library/aboutus/regulations) and in The University's policy on presentation of Theses

ACKNOWLEDGEMENTS

I would like to begin by thanking my supervisor Prof. Stephen High for all his help and advice throughout my PhD studies, and for giving me enough independence to try and carry out my own ideas even though I am sure that he must have had doubts about some of them. He is truly an example of the kind of supervisor I hope to become one day.

I would also like to thank all the current and past members of the High lab for their help, advice and kind words. I feel lucky that I had a chance to work with such wonderful people. In particular, I would like to thank Catherine Rabu for everything she taught me and Peri Roboti for always keeping my spirits up.

I am also grateful to Drs Martin Lowe, Martin Pool, Blanche Schwappach, Lisa Swanton, Dave Thornton and Phil Woodman for their comments on manuscripts in preparation, and advice regarding day-to-day experimental work.

I would like to thank my friends Matthew Stroud, Andromachi Malandraki and Raimondo Guerra for making my stay in Manchester so enjoyable.

I also thank my wonderful family: my parents, Stanislawa and Antoni Lezniccy, my brother Marcin, and aunt Janina Pietrykowska, for always believing in me and supporting me, even though I know that sometimes they would have preferred me to have made difference choices.

Most of all, I would like to thank my lovely fiancée, Maja Mackiewicz, who encouraged me to study in Manchester in the first place and who stood by me all these years regardless of the circumstances. May we love and support each other in the years to come at least as much as till now.

CO-AUTHOR CONTRIBUTION

Chapter 2.1

Construct preparation, protein expression, purification and chemical modification, and all the biochemical experiments were carried out by the author. Bioinformatic modelling of the modified TA-proteins and calculations of the thermodynamic cost of TA-protein partitioning into a lipid bilayer were done by Jim Warwicker (equivalent to Figures 7A and 7B, and part of the Supplementary Data). Stephen High supervised and co-ordinated the work.

Chapter 2.2

Construct preparation, protein expression, purification and labelling as well as biochemical and fluorescence-based experiments were done by the author. Peter U. Mayerhofer and Arthur E. Johnson provided the author with appropriate technical input and training in fluorescence spectroscopy-based techniques. Stephen Rigby together with the author carried out the EPR-based experiments, whilst Stephen High supervised and co-ordinated the work.

Chapter 2.3

All data presented in Figures 1-5 and Figure 7a, and the preparation of all DNA constructs used were performed by the author whilst Anne Clancy and Blanche Schwappach contributed the fluorescence microscopy results shown in Figures 6 and 7b. Blanche Schwappach and Stephen High supervised and co-ordinated the work. All four authors contributed to writing the resulting research paper.

Chapter 2.4

All biochemical experiments together with sample processing for mass spectrometric measurements and subsequent data analysis were done by the author. The mass spectrometric measurements were done by the staff of Biomolecular Analysis Facility, Faculty of Life Sciences, University of Manchester. Stephen High supervised the work.

ABBREVIATIONS

BAG domain	Bcl-2 associated athanogene domain
Bat3	HLA-B-associated transcript 3
Bcl-2	B-cell lymphoma 2
BMB	1,4-bis(maleimido)butane
BMH	bis(maleimido)hexane
BMOE	bis(maleimido)ethane
CAR	constitutive androstane receptor
CHIP	C-terminus of Hsc70 interacting protein
Cytb5	cytochrome b5
DDM	dodecyl-β-D-maltopyranoside
DSS	disuccinimidyl suberate
EndoH	endoglycosidase H
EPR	electron paramagnetic resonance
ER	endoplasmic reticulum
FC-16	Fos-Choline-16
GET pathway	guided entry of tail-anchored proteins pathway
GFP	green fluorescent protein
GST	glutathione S-transferase
HC	hydrocarbon core
HisTrx	Histidine-Thioredoxin
Hsc	constitutively induced heat-shock protein
Hsp	heat-shock protein
IFR	interfacial region
IPTG	isopropyl-β-D-1-thiogalactopyranoside
LDAO	lauryldimethylamine-N-oxide
Lyso-FC-16	LysoFos-Choline-16
MOM	mitochondrial outer membrane
mPEG-5000	polyethylene glycol 5000 maleimide
MTSSL	(1-Oxyl-2,2,5,5-tetramethylpyrroline-3-methyl) methanethiosulfonate
NBD	7-nitrobenz-2-oxa-1,3-diazole-4-yl

NBD	nucleotide binding domain
NEM	N-ethylmaleimide
NiNTA	nickel-nitrilotriacetic acid
NLS	nuclear localisation signal
OG	octyl-β-D-glucopyranoside
OPG tag	opsin-derived glycosylation tag
PC	phosphatidylcholine
PTP1B	protein tyrosine phosphatase 1B
RAMP4	ribosome-associated membrane protein 4
RNC	ribosome nascent chain complex
SGTA	small glutamine-rich tetratricopeptide repeat-containing protein alpha
SMCC	Succinimidyl 4-[*N*-maleimidomethyl]cyclohexane-1-carboxylate
SNARE	soluble N-ethylmaleimide-sensitive factor attachment protein receptor
SR	SRP receptor
SRP	signal recognition particle
Syb2	synaptobrevin 2
Syn1A	Syntaxin 1A
TA	tail-anchored
TMS	transmembrane segment
TPR	tetratricopeptide repeat
TRC40	transmembrane domain recognition complex of 40 kDa
TX-100	Triton X-100
UBA	ubiquitin-associated domain
UBL	ubiquitin-like domain

CHAPTER ONE

Introduction

1. Co-translational protein translocation across, and integration into, the ER membrane.

The endoplasmic reticulum (ER) serves as the primary entry site to the eukaryotic secretory pathway for both soluble proteins destined for export, and membrane proteins localising to the compartments of the secretory pathway and the plasma membrane. The most common mechanism of protein translocation/insertion at the ER membrane is the co-translational pathway where the synthesis of a polypeptide is coupled to its translocation/insertion. The importance of this process is reflected by its evolutionary conservation in both eukaryotes and prokaryotes with the latter utilising this pathway for protein insertion into the inner membrane.

Co-translational protein translocation across/insertion into the ER membrane is typically initiated from the early stages of nascent chain synthesis. Hence, after the first ~ 40 amino acid residues of a polypeptide destined for secretion has been synthesised, an N-terminal ER targeting signal sequence will have emerged from the ribosomal exit tunnel and have been recognised by a ribonucleoprotein complex known as the Signal Recognition Particle or SRP. Membrane proteins destined for the ER will also have a signal sequence or signal peptide that is recognised by SRP as the nascent chain leaves the ribosome. A key feature of ER targeting signals is a core of hydrophobic residues and whilst many secretory proteins have cleavable signals that are removed after SRP-dependent targeting, the transmembrane segments of some membrane proteins can serve a dual role mediating both targeting and membrane integration (High and Dobberstein, 1992). Importantly, the association of SRP with the nascent chain can attenuate further protein translation by inducing a so-called elongation arrest in a heterologous *in vitro* system (Walter and Blobel, 1981) and delaying the rate of synthesis *in vivo* (Lakkaraju et al., 2008; Mason et al., 2000). The ribosome-nascent chain complex (RNC) together with SRP in its "GTP-bound" form are next targeted to the ER where SRP associates with its membrane bound receptor (SR) composed of two subunits, SRα and SRβ. Subsequent interactions between SRP and SR lead to transfer of the RNC to the protein-conducting channel of the ER membrane known as the translocon. SRP and SR mutually stimulate their GTPase activities, and GTP hydrolysis causes SRP to dissociate from the RNC, which in turn

enables translation to resume, and translocation across/integration into the ER membrane to begin (Pool, 2003; Pool, 2005) (Figure 1.1).

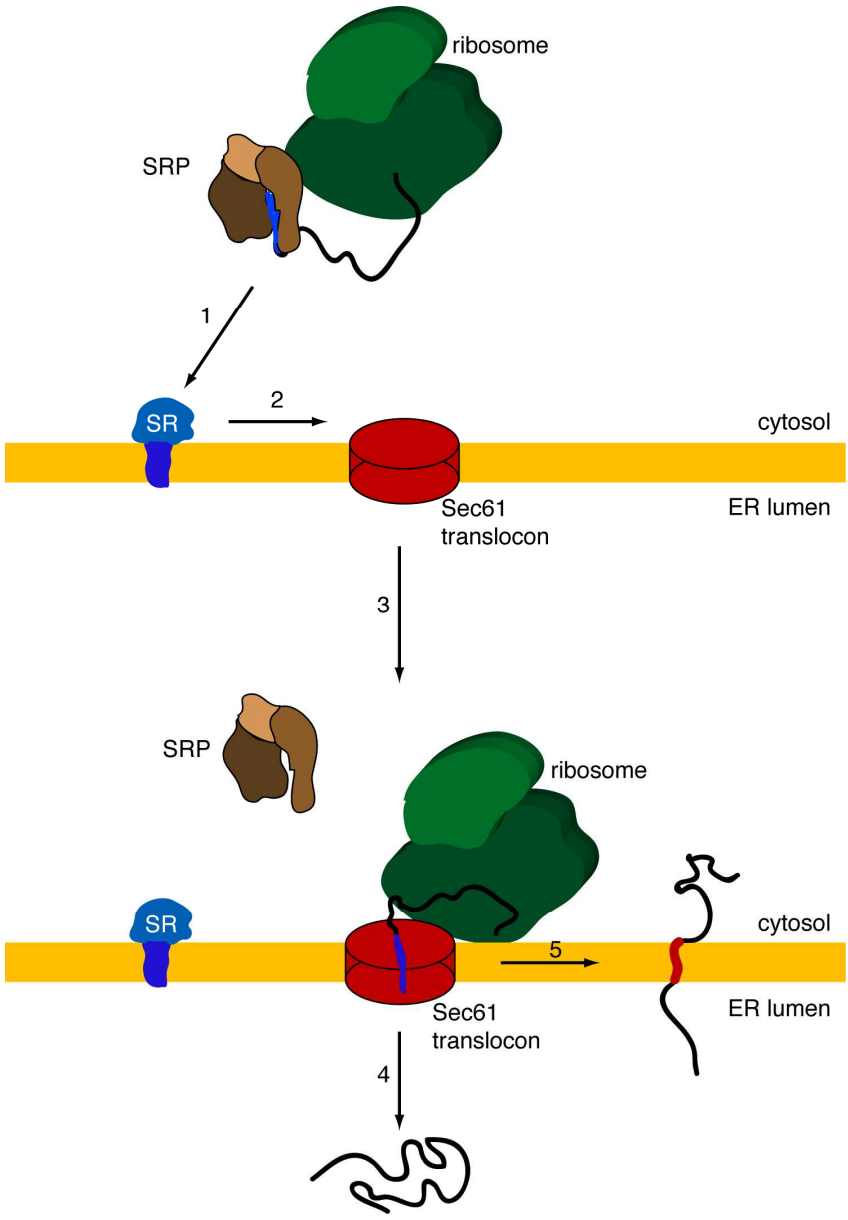

Figure 1.1 Co-translational protein translocation/integration at the ER membrane. During protein translation an N-terminally localised signal peptide (blue) or the transmembrane segment of a membrane protein (not shown) is recognised by the signal recognition particle (SRP) resulting in a slowing of translation or even an "elongation-arrest". The whole ribosome-nascent-chain (RNC)-SRP complex is targeted to the ER membrane-bound SRP receptor (SR) (1) and the RNC then transferred to the Sec61 channel (2). SRP subsequently dissociates from SR, and translation resumes (3). Nascent secretory proteins are translocated into the ER lumen (4), whilst membrane proteins are released into the lipid bilayer (5) via a lateral opening of the Sec61 translocon.

The important contribution of the ribosome to protein translocation across and integration into the ER membrane is demonstrated by the finding that the ribosome is capable of discriminating between nascent secretory and membrane polypeptides, and that it actively induces folding of the latter type of nascent polypeptides (Woolhead et al., 2004). Moreover, the ribosome can recruit SRP very early during protein synthesis, even when a transmembrane segment that acts as the ER targeting signal is still buried inside the ribosomal tunnel; thus maximising the opportunity for signal sequence recognition in an intracellular environment where there is a molar excess of ribosomes over SRP (Berndt et al., 2009). Recently, it has been shown that SRP plays a crucial role in co-translational protein translocation/integration *in vivo*. Not only because it mediates the targeting of the RNC to the translocon, but also because the evolutionary conserved elongation arrest (Mason et al., 2000) induced by SRP allows for co-ordination of protein translation and availability of the SR (Lakkaraju et al., 2008). Given that different signal sequences most likely vary in their affinity for SRP, elongation arrest could also have a regulatory function that would ensure that high-affinity signal sequences are preferentially targeted to the ER (Lakkaraju et al., 2008). A structural basis for SRP binding to an ER-like targeting signal has recently been described (Janda et al., 2010), whilst SRP function and evolution have been comprehensively reviewed by Pool (2005).

Protein transfer across the ER membrane has been the subject of intensive studies for more than 30 years, and significant progress towards understanding the molecular details of this process has been made. Fluorescence-based experiments (Crowley et al., 1993) and electrophysiology-based approaches (Simon and Blobel, 1991) combined with findings that a nascent chain could be extracted from the ER membrane with aqueous perturbants such as 4 M urea and alkaline pH (Gilmore and Blobel, 1985), all provided indirect evidence that translocating proteins pass through an aqueous environment, strongly suggesting that the process is protein-mediated. Cross-linking studies and the use of reconstituted proteoliposomes identified a protein complex composed of three integral membrane proteins (Sec61α, Sec61β, Sec61γ) as the core component of the protein-conducting channel (Gorlich and Rapoport, 1993; High et al., 1993; Oliver et al., 1995). The Sec61 complex also functions as the main ribosome-binding site at the ER membrane under physiological-like conditions

(Kalies et al., 1994) and digitonin-solubilised purified yeast Ssh1 complexes (homologous to Sec61 complexes, see below) interact with ribosomes when these two are mixed (Becker et al., 2009). The involvement of other components in the translocation/integration of proteins across/into the ER membrane was also addressed and another integral membrane protein, translocating chain-associating membrane (TRAM) protein, was found to be either necessary or at least stimulatory for most substrates tested (Gorlich and Rapoport, 1993; Oliver et al., 1995). The lumenal content of the ER has also been implicated in protein transfer across the ER membrane with the Hsp70 homologue, BiP, playing a major role (Nicchitta and Blobel, 1993; Tyedmers et al., 2003).

Structural studies of the archeal SecYEG complex (a functional homologue of the mammalian Sec61 complex) showed that ten transmembrane helices of SecY (Sec61α) form the "walls" of the translocon and suggested that opening of the channel between helices TM2b-3 and TM7-8 allows for the lateral release of transmembrane segments into the lipid bilayer (Van den Berg et al., 2004). Even though the exact mechanisms of translocon opening are not fully understood, it is clear that the protein-conducting channel is a highly dynamic structure and its diameter varies from ~ 9-15 Å in a resting state (Hamman et al., 1998) to ~ 40-60 Å when engaged in translocation (Hamman et al., 1997; Wirth et al., 2003). Moreover, both protein translocation and membrane integration appear to be co-ordinated with the gating of the ER translocon either by the ribosome on the cytosolic side of the membrane or by BiP on the lumenal side (Crowley et al., 1994; Haigh and Johnson, 2002; Liao et al., 1997). Such strict regulation of the Sec61 complex is believed to be required in order to maintain the permeability barrier of the ER and prevent, for example, calcium ion leakage (but see also (Le Gall et al., 2004)).

Interestingly, in the yeast *Saccharomyces cerevisiae* an alternative, post-translational pathway for protein translocation across the ER membrane has been identified (Ngosuwan et al., 2003). Substrates of this novel mode of translocation are targeted to the ER membrane after they have been fully synthesised and released from the ribosome, a feature that appears to preclude the involvement of SRP which in eukaryotes binds primarily to signal sequences when the nascent chain is still

associated with a ribosome (Plath and Rapoport, 2000). Instead, it has been shown that cytosolic molecular chaperones can function to keep the polypeptides in an unfolded or translocation-competent state (Ngosuwan et al., 2003). Even though mechanistically different, these co- and post-translational pathways of protein translocation across the ER membrane both use the Sec61 channel. However, post-translational translocation requires some additional components which co-operate with the conserved Sec61α, Sec61β and Sec61γ homologues of *S. cerevisiae*. These include the integral membrane proteins Sec62p, Sec63p and Sec71p, the cytoplasmic peripheral membrane protein Sec72p and the soluble lumenal chaperone Kar2p (equivalent to mammalian BiP) thought to provide energy required for polypeptide transfer (Panzner et al., 1995). Protein translocation across the yeast ER membrane is, however, complicated by the fact that yeast posses two distinct functional ER translocons (Wilkinson et al., 1997). Whilst the evolutionarily conserved Sec61p/Sbh1p/Sss1p complex participates in both the co- and post-translational protein translocation, the Ssh1p/Sbh2p/Sss1p complex functions only in the co-translational mode (Wittke et al., 2002). The amino acid sequence of the main component of this alternative ER translocon, Ssh1p (Sec sixty-one homologue 1), differs quite significantly from the sequence of Sec61p (Wilkinson et al., 1997), illustrating that essentially the same function can be fulfilled by seemingly distinct proteins. For the same reason it is difficult to predict whether an equivalent of the Ssh1p complex is present in higher eukaryotes. Moreover, the fact that homologues of Sec71p and Sec72p have not yet been identified in higher organisms questions the relative contribution of post-translational protein translocation across the ER membrane in other eukaryotes (but see also (Zimmermann et al., 1990)).

2. General features of tail-anchored (TA) proteins.

In 1993 a short review highlighted the existence of a novel class of membrane proteins predicted to be unable to use the previously identified co-translational pathway for membrane insertion at the ER (Kutay et al., 1993). This class of proteins posses a single hydrophobic amino acid stretch at or very near the C-terminus, usually within the last ~ 40 amino acids, that acts as both a targeting signal and a membrane anchor. Because of its location, this transmembrane segment (TMS) is still buried

inside the ribosome when translation terminates meaning that it cannot be co-translationally recognised by SRP; therefore, a RNC-SRP complex cannot be targeted to the membrane-bound SRP receptor (cf. section 1). Thus, it was speculated that TA-proteins integrate into the ER membrane post-translationally (Kutay et al., 1993), a hypothesis later experimentally validated (Kutay et al., 1995) and consistent with TA-proteins being synthesised on free ribosomes (Rachubinski et al., 1980) and not undergoing an SRP-induced elongation arrest (Anderson et al., 1983).

Function	Examples	Localisation
Enzymatic	Cytochrome b5 Mitochondrial isoform of cytochrome 5 Heme oxygenase I and II UBC6	ER Mitoch. Outer Membrane ER ER
Protein translocation	Sec61β, Sec61γ TOM5, TOM6 Pex15p	ER Mitoch. Outer Membrane Peroxisomes
Vesicular traffic		
SNARE proteins	Target SNAREs (syntaxins) Vesicular SNAREs (e.g., synaptobrevins)	Target membranes for fusion
Tethering proteins	Giantin	Transport vesicles Golgi complex
Regulation of apoptosis (Bcl-2 family)	Bcl-2 Bcl-X_L Bax	Mitoch. Outer Membrane and ER Mitoch. Outer Membrane Cytosol and Mitoch. Outer Membrane
Constituents of viral envelope	Us9 protein of herpes viruses	Trans-Golgi network
Constituents of bacterial cell membrane	Flagellar regulator flk	Bacterial cell membrane

Table 1.1 Examples of function and localisation of different TA-proteins. Adapted from Borgese et al., 2003.

Members of the TA-protein family have been found in virtually all cell membranes, of both prokaryotes and eukaryotes (Borgese et al., 2003b; Borgese and Righi, 2010), and a bioinformatic analysis of the human genome (Kalbfleisch et al., 2007) predicted

the existence of 411 TA-proteins, derived from 325 unique genes. Many of the already characterised TA-proteins have been shown to function in crucial intracellular processes such as vesicular transport (SNAREs), protein translocation across the ER and mitochondrial outer membranes (Sec61β, γ and TOM5, 6, respectively), and the regulation of apoptosis (members of Bcl-2 and Bax families) (see also Table 1.1).

Given that TA-protein insertion occurs independently of protein synthesis, and only after release of the polypeptide from the ribosome, it was theoretically possible that many of these proteins destined for the secretory pathway might be integrated directly into their target membrane rather than first entering the ER membrane and then undergoing vesicular transport to reach their final destination within the cell. However, it was quickly established that synaptobrevin (a SNARE protein) and giantin (a Golgi protein) first enter the ER and are then transported to their final destinations (Kutay et al., 1995; Linstedt et al., 1995) as is typically observed for proteins synthesised via the co-translational pathway. The present consensus is that TA-proteins can be directly inserted into the ER membrane, the mitochondrial outer membrane (MOM) and, in plants, the chloroplast outer envelope (Borgese et al., 2003a; Borgese et al., 2001; High and Abell, 2004).

3. The biophysical properties of TA-proteins dictate their targeting and integration at the ER and MOM.

Most TA-proteins are capable of some level of *in vitro* insertion into ER-derived microsomes (Borgese et al., 2001; Kim et al., 1999) even though *in vivo* they generally localise exclusively to either the ER membrane or the mitochondrial outer membrane (MOM) (Borgese et al., 2003b; Borgese et al., 2001). Discrimination between these two possible sites of membrane integration has been shown to depend primarily on the physicochemical properties of the TA-protein transmembrane segment and, to a lesser extent, the nature of the residues located C-terminal of the TMS (Borgese et al., 2001; Honsho et al., 1998). Hence, shorter transmembrane segments with basic residues located C-terminal of this region tend to confer a MOM localisation, whereas longer hydrophobic TMSs, especially when followed by acidic residues, typically mediate ER membrane insertion (Borgese et al., 2001). Thus, the

introduction of basic residues into the lumenal domain of cytochrome b5 results in the displacement of this protein from the ER membrane and its redistribution to the MOM, whereas substitution of the same C-terminal amino acids with neutral threonine leads to a dual ER-MOM localisation *in vivo* (Borgese et al., 2001). A similar relationship between TMS length, the identity of neighbouring charged residues and protein localisation has also been observed for different isoforms of Vamp1 (or Synaptobrevin 1) (Isenmann et al., 1998). Interestingly, it seems that the overall length and hydrophobicity of TMSs, but not the specific amino acid sequence, play a role in TA-protein targeting (Brambillasca et al., 2006; Honsho et al., 1998). The fact that mitochondrial isoforms of TA-proteins are efficiently inserted into ER-derived microsomes *in vitro* suggests that the ER may act as the "default site" for their integration, although there are clearly signals/motifs that can apparently direct such TA-proteins to the MOM *in vivo* (Borgese et al., 2001).

Studies of the cytochrome b5 TMS fused to the green fluorescent protein (GFP) suggest that the deletion of the entire cytoplasmic region of several TA-proteins does not affect their intracellular localisation (Bulbarelli et al., 2002). On the other hand, the substitution of a few amino acids directly N-terminal to the TMS of Vamp proteins completely abolishes their membrane association (Kim et al., 1999). Similarly, whilst GFP fused to the last 35 amino acid residues of microsomal aldehyde dehydrogenase (msALDH) localises to the ER membrane when expressed in or microinjected into mammalian cells, it remains cytosolic when fused to the TMS alone (Masaki et al., 2003) suggesting that signals other than the TMS are also responsible for intracellular localisation of TA-proteins. For msALDH two short amino acid stretches directly N- and C-terminal from the TMS have been proposed to act as the ER-localisation motifs; however, the relative importance of each of these regions in localising the GFP-msALDH fusion construct has not been investigated. Interestingly, in the case of ER-targeted Vamp isoforms it has been suggested that a conserved region directly N-terminal to the TMS might be responsible for recognition by a potential ER membrane-bound receptor (Kim et al., 1999). However, in most cases the exact role of cytoplasmic domains during TA-protein targeting and insertion has not been studied in great detail, and at present the primary targeting information is believed to reside in the transmembrane and lumenal domains (Borgese et al., 2003b).

The same features that mediate targeting to either the ER or the MOM are also responsible for the residence of TA-proteins in their target membranes. For example, increasing the length of the cytochrome b5 transmembrane domain from 19 to 22 amino acids results in the escape of the protein from the ER membrane and its appearance at the plasma membrane (Bulbarelli et al., 2002; Honsho et al., 1998). Whether this redistribution results from the TMS length *per se* or from an increase in overall hydrophobicity that is caused by this alteration is currently uncertain (Bulbarelli et al., 2002). It has also recently been shown that asymmetry in amino acid composition can strongly influence the post-ER sorting of membrane proteins, and that this relationship also holds to a lesser degree for the SNARE members of the TA-protein family (Sharpe et al., 2010)

This distinct sorting of TA-protein variants differing only in transmembrane domain length/hydrophobicity within the context of the secretory pathway might result from alterations in the protein-lipid interactions of these isoforms (see also (Sharpe et al., 2010)). Thus, differential scanning calorimetry revealed that two cytochrome b5 versions, the wild-type protein and a mutant with an extended TMS that localises to plasma membrane, interact differently with reconstituted liposomes composed of POPC/PS (palmitoyloleyl-phosphatidylcholine/phosphatidylserine) and POPC/CER (palmitoyloleyl-phosphatidylcholine/C16-ceramide) lipid mixtures (Ceppi et al., 2005). Interestingly, the association of these cytochrome b5 variants with liposomes also depends on the lipids used for reconstitution, as exemplified by their indistinguishable interaction with POPC/DSPC (palmitoyloleyl-phosphatidylcholine-distearoylphosphatidylcholine) liposomes. Moreover, the finding that the integration of cytochrome b5 was abolished when the cholesterol content of ER-derived membranes was artificially increased, together with the fact that cholesterol levels increase along the secretory pathway, could explain the retention of some TA-proteins at the ER and their inability to reach later compartments of the secretory pathway (Brambillasca et al., 2005).

4. Topology of TA-proteins – historical perspective.

Even though TA-proteins were known to localise to intracellular membranes, the topology of their membrane binding segment was initially unknown and it was

originally proposed that it might either fully span the lipid bilayer or form a hairpin loop in the membrane with both the N- and C-termini exposed to the cytosol (Kutay et al., 1993) (Figure 1.2). The main difficulty in establishing the location of the C-terminus of TA-proteins results from the fact that there are typically only a few amino acids that extend beyond the TMS, making it extremely difficult to carry out the commonly used protease protection assay with any degree of certainty. Evidence that TA-proteins completely span the lipid bilayer emerged from studies using *in vitro* synthesised polypeptides with a C-terminus containing a tag that included an N-glycosylation site. Thus, first Synaptobrevin 2 (Kutay et al., 1995) and then several other TA-proteins carrying this extension (Abell et al., 2007; Brambillasca et al., 2005; Favaloro et al., 2008; Favaloro et al., 2010; Rabu et al., 2008; Whitley et al., 1996) were shown to be efficiently modified by the ER-localised N-glycosylation machinery, proving that the tag was translocated into the ER lumen. Similarly, by extending the C-terminus of cytochrome b5 (Cytb5) it was also possible to employ the protease protection assay and show that this extended segment was inaccessible to protease digestion consistent with it being in the ER lumen (Brambillasca et al., 2005). Even though these small tags have proved extremely useful experimental tools, one should remember that their addition might alter the properties of the TA-proteins

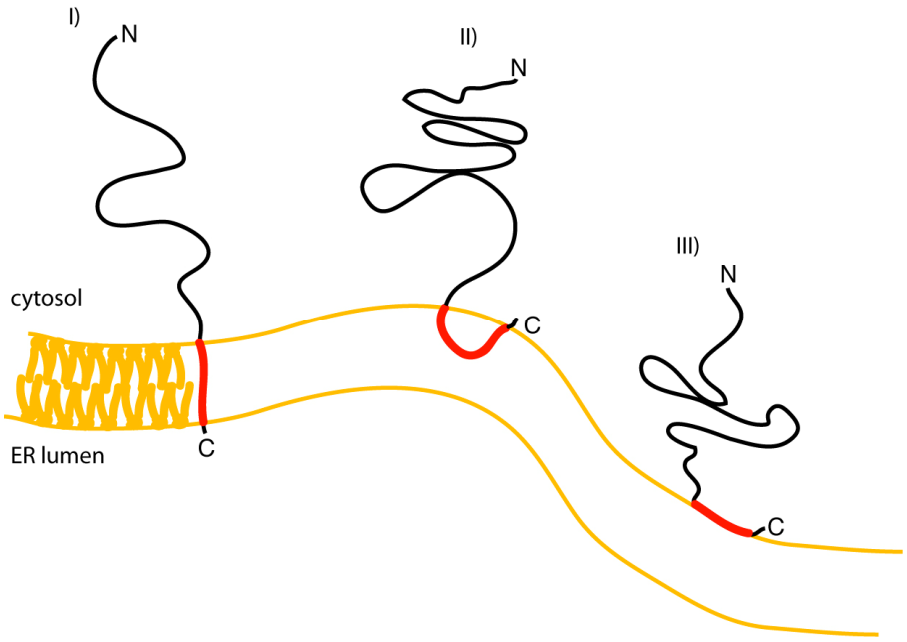

Figure 1.2 Potential membrane associations of a TA-protein. Possible conformations of a TA-protein are shown with I) and II) representing a biochemically "tight" membrane association and III) a "loose" or peripheral association. See text for more details.

being studied, or that the observed insertion efficiency may be underestimated since, for example, the efficiency of N-glycosylation can be influenced by factors such as the distance of the modified Asn residue from the membrane surface (Abell et al., 2007; Nilsson and von Heijne, 1993).

Interestingly, the topology of the transmembrane segment of Cytb5 had been studied in detail long before TA-proteins had been classified as a distinct grouping. Following the identification of the non-polar peptide that anchors Cytb5 to the lipid bilayer (Spatz and Strittmatter, 1971), it was established that this segment is located at the C-terminus of the polypeptide chain (Dailey and Strittmatter, 1978; Strittmatter et al., 1972) and a number of biochemical and biophysical experiments were carried out to resolve its structure and topology. CD spectra of the isolated non-polar peptide region indicated that, both in solution and when tethered to lipid vesicles, the central part of this segment adopts a largely α-helical structure, most likely corresponding to a degenerate 3_{10} helix, whereas the N- and C-terminal regions of five residues each are characterised by a β-sheet conformation (Dailey and Strittmatter, 1978). An interesting feature of such a model is the possibility of these two flanking segments forming an intramolecular antiparallel β-sheet within the non-polar peptide that could stabilise a hairpin loop conformation, and place both the N- and C-termini at the same side of a lipid bilayer (Figure 1.2).

Subsequently, it was shown that, depending on the type of membrane and experimental procedure used, purified Cytb5 reconstituted into lipid vesicles can associate with a lipid bilayer in two distinct forms, identified as “tight” and “loose” (Enoch et al., 1979) (cf. Figure 1.2). The “tight” form was characterised by resistance to protease treatment and a lack of intermembrane protein transfer when the reconstituted vesicles were mixed with another population of membranes. By contrast, the “loose” form of Cytb5 was sensitive to protease and readily transferable (Enoch et al., 1979). Importantly, when purified Cytb5 was mixed with biological membranes or dimyristyl phosphatidylcholine vesicles, it preferentially bound in a “tight” conformation, whilst the “loose” form predominated when other lipids (including microsomal lipid extract) were used (Enoch et al., 1979). Although these results indicated that the “tight” association represents the biologically relevant form of

Cytb5 binding, they did not discriminate between conformations of the TMS. The apparent protease-resistance of the non-polar peptide in the "tight" form could be explained either by assuming that it fully spans the membrane or that in the hairpin loop topology the charged C-terminal residues of Cytb5 are buried, and thus protected, inside the lipid polar headgroups (Dailey and Strittmatter, 1981b; Enoch et al., 1979) (Figure 1.2). Moreover, when the last 6 amino acids of Cytb5 were removed or their anionic charge modified, bound Cytb5 was converted from the "tight" to the "loose" form, further supporting the hairpin loop hypothesis (Dailey and Strittmatter, 1981b) (Figure 1.2).

Further studies identified a single fluorescent tryptophan residue in the non-polar region of cytochrome b5 from bovine liver, and from the quenching of its fluorescence it was established that this residue is located around 20-22 Å inside the lipid bilayer (Fleming et al., 1979). Moreover, ionisation of the C-terminally located tyrosine residues indicated that these amino acids were located in the outer leaflet of the lipid bilayer (Dailey and Strittmatter, 1981a), with one of them being in the polar head group region as judged by its reactivity with a membrane impermeable diazotized sulfonic acid (Dailey and Strittmatter, 1981a). These data prompted Dailey and Strittmatter (1981) to propose a model where the Cytb5 TMS forms a hairpin loop with both the N- and C-termini exposed to the cytosol (cf. Figure 1.2). The cross-linking of membrane bound Cytb5 to [^{3}H]taurine, a carboxyl-reactive nucleophile, also indicated that the location of the C-terminal tetrapeptide was on the outer side of the membrane (Arinc et al., 1987), consistent with structural analyses using Cytb5 asymmetrically reconstituted in a "tight" conformation into phosphatidylcholine (Rzepecki et al., 1986) and dimyristoylphosphatidylcholine (Chester et al., 1992) vesicles.

In practice, all of the biochemical and biophysical data outlined above appear to have been undermined by subsequent *in vitro* and *in vivo* studies (Kuroda et al., 1996) which all suggest that the C-terminus of Cytb5 is fully translocated into the ER lumen, and this is the prevailing model at present (Borgese et al., 2003b). Nevertheless, it is still possible that the topology of Cytb5 TMS differs depending on its precise membrane environment and/or is influenced by C-terminal extensions.

5. Pathways of TA-protein integration into the ER membrane.

The post-translational mode of TA-protein insertion into target membranes excludes their delivery to the ER via the SRP-mediated targeting of a ribosome-nascent chain complex. Not surprisingly, the mechanisms that underlie TA-protein delivery to the ER membrane have therefore received considerable attention, and the research carried out over the past few years has resulted in significant advancements in our understanding of this remarkably complex process.

5.1. An "unassisted" pathway for TA-protein delivery to the ER membrane.

The release of a hydrophobic tail anchor from the ribosome upon completion of translation poses a significant challenge to a cellular machinery that must presumably prevent the protein from aggregating and ensure the delivery of the newly synthesized TA-protein to the correct intracellular compartment. The events underlying this process have largely been studied by the *in vitro* synthesis of different model TA-proteins in cell-free systems combined with experiments designed to address the requirements for their targeting and subsequent membrane integration. Cytochrome b5 (Cytb5) is one of the model substrates that has been used extensively to study TA-protein delivery to the ER membrane, and the route that it employs for its membrane integration is comparatively well defined.

Thus, it has been established that the integration of Cytb5 into the ER membrane does not rely on components of the Sec61 complex or any other known factors that normally facilitate the translocation of secretory proteins (Brambillasca et al., 2005; Yabal et al., 2003). Furthermore, protease treatment of ER-derived microsomes does not inhibit Cytb5 membrane insertion as judged by its membrane association and the N-glycosylation of a tagged version of the protein, suggesting that its integration is independent of any membrane-bound proteins (Abell et al., 2004; Favaloro et al., 2010; Kim et al., 1997). This hypothesis is strengthened by the observation that when a C-terminally extended variant of Cytb5 is incubated with protein-free liposomes the extension is protected from an externally added protease (Brambillasca et al., 2006; Brambillasca et al., 2005; Colombo et al., 2009). Furthermore, the Cytb5 TMS alone supports the translocation of long, hydrophilic regions of polypeptide across a lipid

bilayer (Brambillasca et al., 2006). Based on these data a protein-independent mechanism for the integration of at least some TA-proteins into the ER membrane has been proposed, and this is commonly referred to as the "unassisted" pathway.

Even though it is reasonably well documented that Cytb5 does not require a membrane-bound receptor(s) for its integration into a lipid bilayer, the precise basis for its targeting from the ribosome to the ER membrane is still not entirely clear. It has been speculated that cytosolic molecular chaperones may bind to the newly synthesized Cytb5, prevent its aggregation and keep the polypeptide in an "insertion-competent" state (Abell et al., 2007; Rabu et al., 2009; Rabu et al., 2008; Yabal et al., 2003). The precise role for these putative chaperones is unclear, with hypotheses ranging from a purely "unfolding" action (Yabal et al., 2003) to a more specific delivery of a substrate to the ER membrane (Rabu et al., 2009) (Figure 1.3). Paradigms for both modes of action has already been established for secretory and membrane proteins (Ngosuwan et al., 2003; Wiech et al., 1993) and, importantly, in both cases chaperones of the Hsp/Hsc70 and Hsp40 families have been implicated in the translocation/integration process. Indeed, recent analyses revealed that membrane insertion of TA-proteins can be stimulated by the Hsp70/Hsp40 system (Abell et al., 2007; Rabu et al., 2008), and small molecule inhibitors of Hsp/Hsc70 chaperones specifically target the delivery of Cytb5 (Rabu et al., 2008). The role of chaperone proteins in delivering Cytb5 to the ER membrane is also supported by the well documented ATP requirement for this process, albeit that the concentrations of nucleotide sufficient to promote Cytb5 membrane insertion are extremely low being in the nanomolar range (Brambillasca et al., 2006; Yabal et al., 2003).

However, these conclusions appear at odds with another recent study where the membrane integration of recombinant Cytb5 was investigated. In this case, Cytb5 integration into both microsomes, and protein-free liposomes, was shown to be as efficient in the absence of any cytosolic components as in the presence of cell lysate (Colombo et al., 2009). The apparent nucleotide-independent membrane integration of recombinant Cytb5 (Colombo et al., 2009; Favaloro et al., 2010) would not support a role for classical chaperones during the ER delivery step, and such a pathway is indeed consistent with a previous report (Kim et al., 1997). To rationalise these data, it has been suggested that after leaving the ribosomal exit tunnel Cytb5 forms

oligomers that remain in a dynamic equilibrium with a monomeric form that is capable of spontaneous insertion into the ER membrane (Colombo et al., 2009). However, it may be that in the cell there are mechanisms that prevent the formation of such oligomers since they would be potentially harmful, for example, by nucleating further protein aggregation reminiscent of the processes underlying neurodegenerative diseases such as Huntington's disease (Leznicki, 2005; Ross and Poirier, 2004).

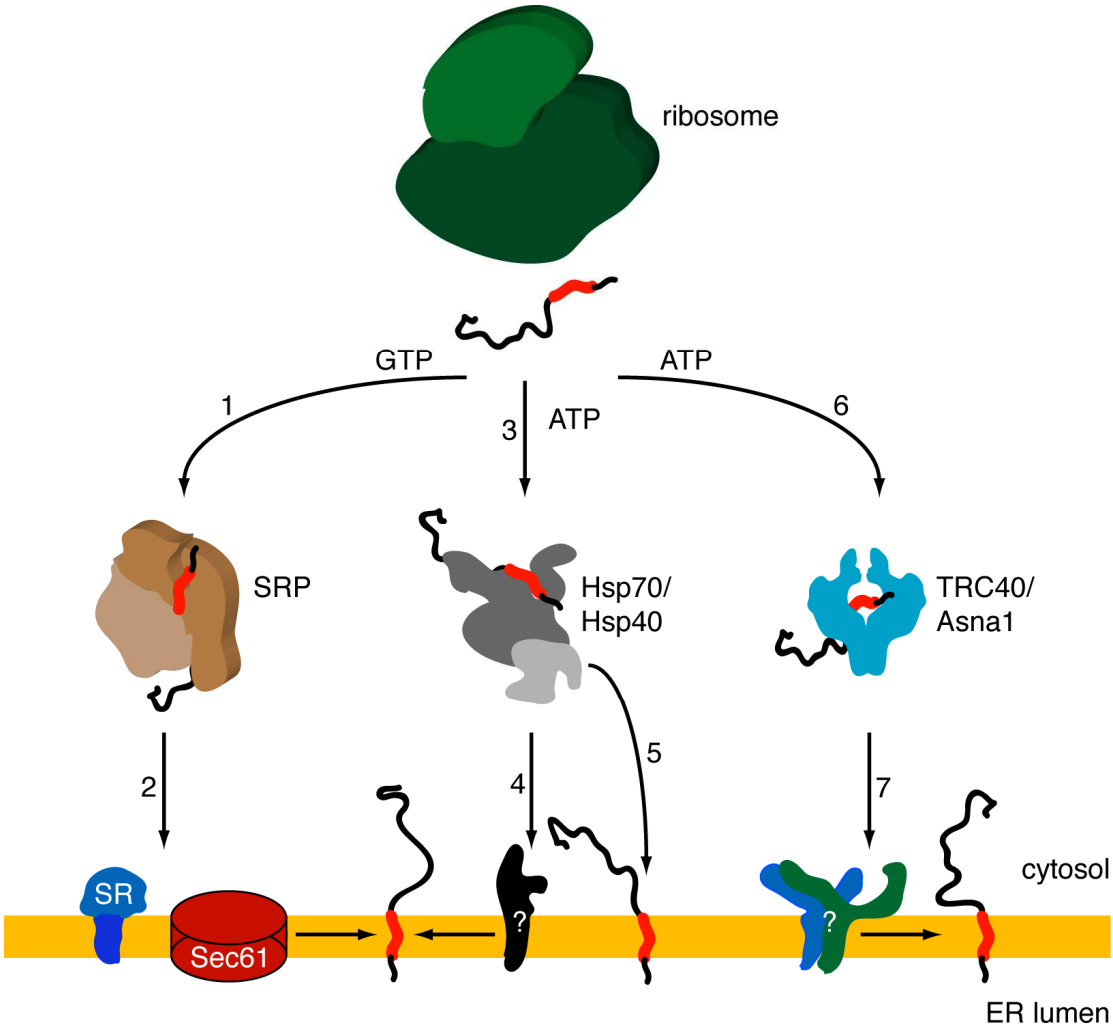

Figure 1.3 Pathways of TA-protein delivery to the mammalian ER membrane. Following release from the ribosome, a TA-protein can be delivered to the ER membrane by one of at least three distinct pathways (Rabu et al., 2009). Substrates with a very hydrophobic TMS are preferentially recognised by SRP (1), targeted to the SR (2) and integrated into the lipid bilayer, potentially via the Sec61 translocon. TA-proteins bearing a relatively hydrophilic TMS are bound by chaperones of the Hsp70/Hsp40 family (3) and integrated into the ER membrane either by a specific interaction with a putative membrane-bound receptor (4), or via direct partitioning into the lipid bilayer in an "unassisted" manner (5). Most TA-proteins (Kalbfleisch et al., 2007) have a TMS with a net hydrophobicity that falls between these two extremes, and these appear to preferentially associate with TRC40/Asna1 (6) that targets these precursors to a putative ER membrane-localised receptor (7), which facilitates the subsequent membrane integration step.

Recently, the determinants for the "unassisted" membrane integration of TA-proteins have been investigated in more detail, and the relatively low hydrophobicity of the TMS found to be of crucial importance (Brambillasca et al., 2006; Rabu et al., 2009; Rabu et al., 2008). Based on this criterion, a second TA-protein, protein phosphatase 1B (PTP1B), was identified and also shown to spontaneously insert into lipid bilayers (Brambillasca et al., 2006). However, most TA-proteins have a significantly more hydrophobic membrane-spanning region, and these precursors use a distinct pathway for both their targeting to, and integration into, the ER membrane (Kalbfleisch et al., 2007; Rabu et al., 2009).

5.2. Protein-dependent routes for TA-protein targeting to and insertion into the ER membrane.

TA-protein delivery to the ER membrane in higher eukaryotes

Most of the TA-proteins studied to date rely on proteinaceous factors during their targeting to and insertion into the ER membrane. This is illustrated by the block in their membrane integration when either protease-treated microsomes (Abell et al., 2004; Favaloro et al., 2008; Favaloro et al., 2010; Kutay et al., 1995) or liposomes (Stefanovic and Hegde, 2007) are used in place of "normal" microsomes, and is also consistent with the requirement for ATP during precursor delivery to the ER membrane (Abell et al., 2007; Kutay et al., 1995; Stefanovic and Hegde, 2007).

Initially, it was hypothesised that the Sec61 translocon might comprise the protease-sensitive component at the ER membrane and function as an entry site for TA-proteins destined for the ER and compartments of the secretory pathway. Indeed, evidence that components of the canonical, co-translational, pathway could be involved in TA-protein delivery to and integration into the ER membrane comes from cross-linking experiments that showed that early in their integration Syb2 and syntaxin 1A (Syn 1A) contact Sec61α and Sec63 (Abell et al., 2003). However, an involvement of the Sec61 translocon has been largely discounted by two criteria. Firstly, proteoliposomes lacking components of the Sec61 translocon and/or its associated proteins are still competent for the integration of TA-protein substrates

(Brambillasca et al., 2005; Kutay et al., 1995; Stefanovic and Hegde, 2007) and, secondly, yeast microsomes prepared from strains depleted for, or expressing conditional mutants of, Sec61 components are also functional for TA-protein integration (Steel et al., 2002; Yabal et al., 2003). At present, the identity of the putative ER membrane-bound receptor/integrase in higher eukaryotes is unknown.

In contrast to membrane insertion, there is fairly detailed knowledge regarding the protein-dependent targeting route that TA-proteins use for the delivery to the ER membrane. By carrying out large-scale *in vitro* translation, followed by cross-linking and mass spectrometric analysis a novel interacting partner of TA-proteins was independently identified by two groups (Favaloro et al., 2008; Stefanovic and Hegde, 2007). In mammalian systems this protein had previously been named Asna-1 because of its amino acid sequence similarity to a bacterial arsenite transporter (see (Rabu et al., 2009)). However, following the discovery of its involvement in TA-protein biogenesis, the alternative name of TRC40 (Transmembrane Domain Recognition Complex of 40 kDa) was proposed (Stefanovic and Hegde, 2007). TRC40 binds to the transmembrane segment of a TA-protein, and its association is abolished by the presence of detergent such as Triton X-100 or upon the addition of ER-derived membranes (Favaloro et al., 2008; Stefanovic and Hegde, 2007). The latter observation and the fact that considerable amounts of TRC40 are found associated with ER-derived microsomes (Stefanovic and Hegde, 2007), indicate that TRC40 may function during TA-protein delivery to the ER membrane. In this scenario, interactions between TRC40 and a putative membrane-bound receptor would lead to release of the TA-protein substrate and its integration into a lipid bilayer (Figure 1.3). Furthermore, when recombinant model TA-proteins are co-expressed in *E. coli* with either TRC40, or its yeast homologue Get3, and the resulting complexes purified, the membrane integration of these TA-proteins does not need any additional cytosolic components (Bozkurt et al., 2009; Favaloro et al., 2010). In fact, only the addition of adenine nucleotides is necessary, consistent with TRC40/Get3 having an ATPase activity (Bozkurt et al., 2009; Favaloro et al., 2010). These findings strongly suggest that TRC40 acts at very late steps of TA-protein delivery to the ER membrane, but do not exclude a role for other cytosolic components, for example to load TRC40 with its TA-protein substrate. Consistent with this hypothesis, TRC40 is found in high molecular weight complexes (Stefanovic and Hegde, 2007) and was identified as part

of a protein network that contains mammalian orthologues of yeast Get4 and Get5 (Sowa et al., 2009) (see below). It has been suggested that such additional components might facilitate the rapid transfer of a TA-protein substrate from the ribosome to TRC40, and/or regulate delivery of the complex to the target membrane (Rabu et al., 2009).

Independent biochemical studies also identified an association between a newly synthesised TA-protein, synaptobrevin 2 (Syb2), and SRP (Abell et al., 2004), leading to a suggestion that SRP might have a novel, previously unappreciated, role in post-translational protein delivery to the ER membrane (Figure 1.3). Such a hypothesis is supported by the increased association of SRP with ribosomes translating membrane proteins, even before the transmembrane segment to which SRP binds has emerged from the ribosomal exit tunnel (Berndt et al., 2009), and is also consistent with the ability of SRP to maintain purified secretory proteins, proOmpA and pre-pro-α-factor, in a translocation-competent state (Sanz and Meyer, 1988).

The availability of multiple pathways for TA-protein targeting/membrane integration (Figure 1.3) raises the question of what factor(s) dictate the route(s) a particular precursor follows. Recent studies have established that the delivery and insertion pathways can be defined by the relative hydrophobicity of the transmembrane segment. Hence, the least hydrophobic segments favour the “unassisted” integration pathway, the bulk of TA-proteins with moderately hydrophobic TMSs rely on the TRC40 route and the TA-proteins with the most hydrophobic TMSs can also exploit SRP via a novel post-translational pathway (Brambillasca et al., 2006; Rabu et al., 2009; Rabu et al., 2008) (Figure 1.3). It should be noted that these distinct pathways are not mutually exclusive, and at least some precursors are capable of using more than a single biosynthetic route (Abell et al., 2004; Rabu et al., 2009; Rabu et al., 2008). Consistent with this hypothesis, a recent bioinformatic analysis identified organisms that lack functional homologues of either TRC40 or Hsp70/Hsp40 although their genomes encode a variety of TA-proteins (Borgese and Righi, 2010).

Targeting of TA-proteins to the yeast ER membrane

By exploiting yeast genetics it has been possible to identify, and extensively characterise, several components involved in the biogenesis of TA-proteins (Figure 1.4). Soon after the identification of Asna-1/TRC40 as a principal targeting factor for TA-protein delivery to the ER membrane in the mammalian system, the yeast homologue, Get3, together with its membrane-bound receptor, were described (Schuldiner et al., 2008). These proteins, cytosolic ATPase Get3 and the membrane-associated Get1/Get2 complex, were previously implicated in Golgi-to-ER trafficking on the basis of a high-throughput analysis of the *S. cerevisiae* genome (Schuldiner et al., 2005). These components form a relatively stable complex that is resistant to high salt and pH treatments (Auld et al., 2006; Jonikas et al., 2009; Schuldiner et al., 2005). Immunofluorescence analysis and experiments with microsomes derived from *Δget1*/*Δget2* strains, and the use of reconstituted proteoliposomes showed that Get1 and Get2 are both necessary and sufficient for the membrane recruitment of Get3 in an ATP-independent manner (Auld et al., 2006; Schuldiner et al., 2008). Further work established that Get3 associates with TA-proteins in a TMS-dependent manner, and showed that the loss of Get3 results in an increase in a cytosolic pool of model TA-proteins (Schuldiner et al., 2008). Similarly, deletion of Get1 and Get2 disrupts TA-protein delivery to the ER membrane and results in the proteins being localised to cytosolic aggregates that also contain Get3 (Schuldiner et al., 2008) (Figure 1.4). Furthermore, in the absence of Get1/Get2 the mislocalisation of ER-destined TA-proteins to mitochondria was observed (Schuldiner et al., 2008). Complementary *in vitro* experiments using components derived from yeast cells devoid of Get3 and/or Get1/Get2 confirmed that all three components are necessary for the authentic insertion of *in vitro* synthesised TA-protein precursors (Schuldiner et al., 2008). To date, mammalian equivalents of Get1/Get2 have not been identified (Table 1.2; (Rabu et al., 2009)).

Interestingly, an earlier study indicated that Get3 is linked to the ubiquitin-proteasome system, as shown by a partial rescue of ER associated degradation (ERAD) in an *npl4-1* strain expressing a mutant form of Get3 (Auld et al., 2006). Moreover, GET3 expression is co-regulated with the transcription of genes of the ubiquitin-proteasome

system, especially under conditions relating to sporulation (Auld et al., 2006). Therefore, Get3 may have a dual role, facilitating TA-protein biogenesis via its association with the Get1/Get2 receptor, and contributing in some other way to protein degradation. Alternatively, both roles might be linked, although in what fashion is presently unclear.

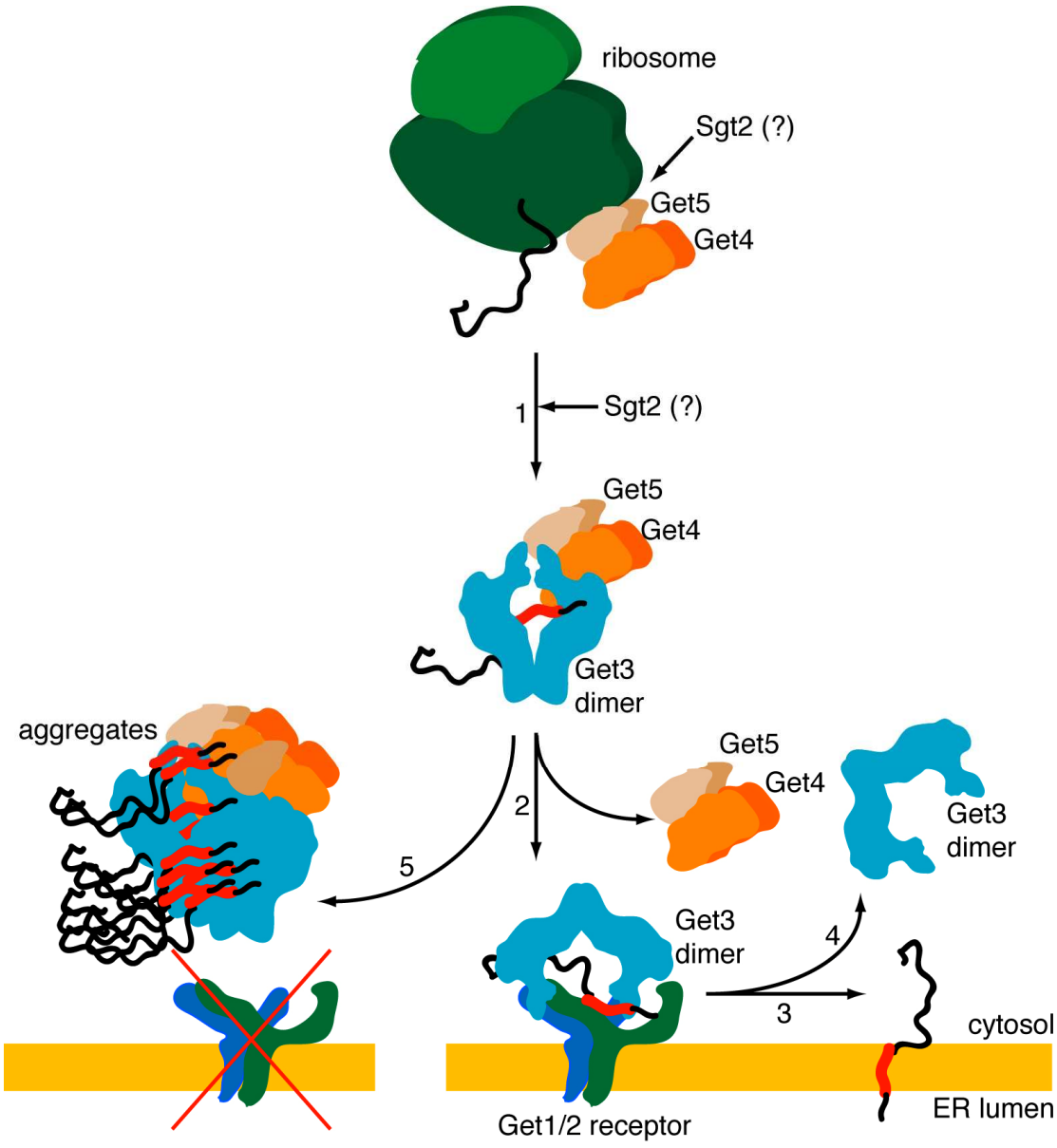

Figure 1.4 GET-mediated delivery of TA-proteins to the yeast ER. A newly synthesised TA-protein is most likely recognised by a ribosome-associated Get4/Get5 complex and then transferred to the Get3 factor (1). Get3 targets the TA-protein to the ER membrane (2) where interactions with the membrane-bound receptor, Get1/2, allow for TA-protein membrane integration (3) and recycling of Get3 back to the cytosol (4). In the absence of Get1/2 TA-proteins form aggregates that contain cytosolic components of the GET pathway (5).

Shortly after the role of Get1, Get2 and Get3 in TA-protein biogenesis was described, two further high-throughput screens identified additional components of the Get pathway (Copic et al., 2009; Jonikas et al., 2009). Cytosolic proteins Yor164c and its interacting partner Mdy2 were both shown to be necessary for TA-protein delivery to the ER membrane, and were thus tentatively renamed to Get4 and Get5, respectively (Jonikas et al., 2009) (Table 1.2). Moreover, the co-localisation of Get3 with TA-protein aggregates formed in the absence of the membrane-bound Get1/Get2 receptor was shown to be dependent on the presence of Get4/Get5 suggesting that these two proteins load Get3 with a TA-protein substrate (Jonikas et al., 2009) (cf. Figure 1.4). This is consistent with an earlier finding that Get4 and Get5 are peripherally associated with the ribosome (Fleischer et al., 2006), and hence conveniently located to bind newly synthesised TA-proteins and transfer them to targeting factors such as Get3.

Yeast Get component	Other name	Mammalian equivalent	Other names
Get1	Mdm39p	Unknown	-
Get2	Rmd7p, Hur2p	Unknown	-
Get3	Arr4p	TRC40	ASNA-1, ARSA
Get4	Yor164c	C7orf20	CEE
Get5	Mdy2, Tma24p	UBL4A	DXS254E, GDX
Sgt2	-	SGTA	SGT, SGT1

Table 1.2 Components of the yeast GET pathway and their mammalian equivalents.

Interactions of the cytosolic Get proteins have now been investigated in more detail, particularly in the context of ongoing structural studies (see below) (Bozkurt et al., 2010; Chang et al., 2010; Chartron et al., 2010). Biochemical and yeast two-hybrid approaches showed that the N-terminus of Get5 binds to the C-terminus of Get4 whilst the N-terminus of Get4 interacts with Get3, presumably in a nucleotide-dependent manner (Chang et al., 2010; Chartron et al., 2010). Interesting, whilst the Get4 surface that mediates association with Get3 is conserved in higher eukaryotes, the N-terminal region of Get5 implicated in binding to Get4 seems to be fungi-

specific, suggesting that in multicellular organisms additional components might participate in the formation of the GET-like complexes (Chartron et al., 2010). It was also established that Get4 and Get5 form higher ordered assemblies containing two copies of each protein and this "dimerisation" was shown to occur via the C-terminal domain of Get5 (Chartron et al., 2010). The importance of a stable Get4-Get5 interaction is also illustrated by the increased degradation of Get5 in a *Δget4* deletion strain (Chang et al., 2010).

Interestingly, links between the GET pathway and a "classical" chaperone machinery have recently been described. Hence, an Hsp70 co-chaperone Sgt2 was shown to interact genetically with components of the GET machinery (Battle et al., 2010; Costanzo et al., 2010), and mass spectrometric analysis confirmed its physical association with Get4, Get5 and members of the Hsp70 (Sse1 and Sse2) and Hsp20 (Hsp42) families (Costanzo et al., 2010). Further biochemical investigation revealed that Sgt2 forms a complex with Get4/Get5 via its N-terminal domain that binds to Get5 fragments containing a ubiquitin-like domain (Chang et al., 2010). The role of Sgt2 in TA-protein biogenesis is supported by mislocalisation of model TA-protein substrates, Pex15 (Costanzo et al., 2010) and Sed5 (Battle et al., 2010), in the *Δsgt2* strain, reminiscent of the targeting defect observed in yeast cells lacking cytosolic components of the GET pathway. The precise role for Sgt2 is, however, unclear and various hypotheses have been formulated. Thus, because the association of Sgt2 with Get4/Get5 is only transient, Chang et al. (2010) suggested that it is unlikely that Sgt2 forms the core of a ribosome-associated complex involved in recognising a TA-protein as it leaves the ribosomal exit tunnel. On the other hand, statistical analysis of genetic interactions of Sgt2 placed it upstream of Get4/Get5 components, and clearly indicated that all these factors contribute to the same "linear" pathway (Battle et al., 2010).

By analysing genetic interactions of the Get proteins it was also discovered that cytosolic Get3, Get4 and Get5 components associate with Ydj1, a major *S. cerevisiae* Hsp40 chaperone, thus establishing another link between the Get-mediated pathway for TA-protein delivery to the ER membrane and a postulated chaperone-dependent route (Abell et al., 2007; Chang et al., 2010; Rabu et al., 2009). Finally, it should be

noted that whilst the deletion of components of the GET pathway results in the mislocalisation of selected model TA-proteins and/or the formation of intracellular protein aggregates, there is no pronounced phenotype in the absence of additional perturbations. This has led to the suggestion that yeast must posses one or more alternative pathways for TA-protein delivery to the ER membrane (Rabu et al., 2009).

Structural analysis of TA-protein recognition and delivery by Get3

Recently, a better understanding of the action of the Get3 protein has emerged from a number of structural studies (Bozkurt et al., 2009; Hu et al., 2009; Mateja et al., 2009; Suloway et al., 2009; Yamagata et al., 2010). When crystallised, the protein was typically found to form dimers, consistent with its elution profile upon gel filtration chromatography (Suloway et al., 2009; Yamagata et al., 2010) and sedimentation during analytical ultracentrifugation (Bozkurt et al., 2009). The Get3 monomer proved to be composed of two distinct domains, a highly conserved nucleotide binding domain (NBD) and less conserved α-helical domain, also termed the finger domain (Hu et al., 2009). These monomers associate in a head-to-head orientation forming a symmetric homodimer that is stabilised by a zinc ion, coordinated by pairs of cysteines from each monomer. This metal binding site, located within the NBD, forms a primary dimerisation interface of Get3, as reflected by an absolute conservation of the cysteine residues (Yamagata et al., 2010). Additional protein-mediated contact sites between monomers have also been suggested (Yamagata et al., 2010) but these do not appear to play as important a role as the zinc-stabilised association. Another point of contact between the two monomers of the Get3 dimer may occur via nucleotides that are bound both *in cis* and *in trans* by residues from both monomers (Bozkurt et al., 2009; Mateja et al., 2009), although not all current structures confirm this observation (Yamagata et al., 2010).

The α-helical domain of Get3, although not as conserved as the NBD, is nonetheless characterised by a high content of methionines, glycines and other non-polar residues (Bozkurt et al., 2009; Mateja et al., 2009; Suloway et al., 2009), leading to speculation that this domain might take part in TA-protein recognition and binding via a mechanism akin to that responsible for signal sequence binding by the 54 kDa subunit

of SRP (Janda et al., 2010; Pool, 2005). This hypothesis is supported by the fact that the α-helical domain appears intrinsically difficult to crystalise, with regions absent from all published structures indicative of high flexibility – a feature consistent with a domain that has to accommodate a variety of relatively diverse transmembrane segments. This flexibility was also confirmed by hydrogen-deuterium exchange experiments which indicated that this protein segment is highly dynamic and solvent-exposed (Bozkurt et al., 2009). Mutational analysis further supported the role of this region in TA-protein recognition, and showed that residues essential for TRC40 binding to a model TA-protein often cluster to helix 8, which is part of a so-called "TRC40 insert" (Mateja et al., 2009). This region is absent in bacterial homologues of TRC40 but, strikingly, has been identified in archea indicating that whilst bacterial TRC40 homologues most likely function to provide resistance to toxic metals, in archea and eukaryotes TRC40 may have gained a novel function, i.e. it participates in TA-protein delivery to target membrane (Borgese and Righi, 2010).

The various structures solved by different groups allow us to model potential conformational changes in Get3 as it progresses through its presumed ATPase cycle, and to relate these changes to TA-protein delivery to the ER membrane (Figure 1.5). Hence, at least two different conformations of the Get3 dimer can be distinguished: nucleotide-free or "open" and nucleotide-bound or "closed". In the "open" state the α-helical domains appear to be separated by ~ 20 Å and their exposed surface is relatively charged, and thus unsuitable for substrate binding (Mateja et al., 2009). In contrast, the binding of nucleotides brings the α-helical domains of two monomers into close proximity, with different variations of the "closed" state currently attributed to the Get3 dimer at distinct stages of the ATPase cycle. Hence, whilst the structures of the dimer in the AMP-PNP and ADP bound states, assumed to represent pre- and post-hydrolysis steps respectively, are relatively similar (Bozkurt et al., 2009); the presumptive transition state, solved in the presence of ADP•AlF_4^-, is characterised by a further closure of the dimer interface and the stabilisation of the α-helical domain (Bozkurt et al., 2009; Mateja et al., 2009). This latter intermediate was also confirmed by cross-linking experiments (Yamagata et al., 2010). It seems that the presence of both nucleotide and Mg^{2+} are necessary to induce the "closed" conformation (Bozkurt et al., 2009; Suloway et al., 2009), and it has been suggested that dimer closure may

be communicated to the ATPase domain via a so called DTAPTGH motif (Yamagata et al., 2010).

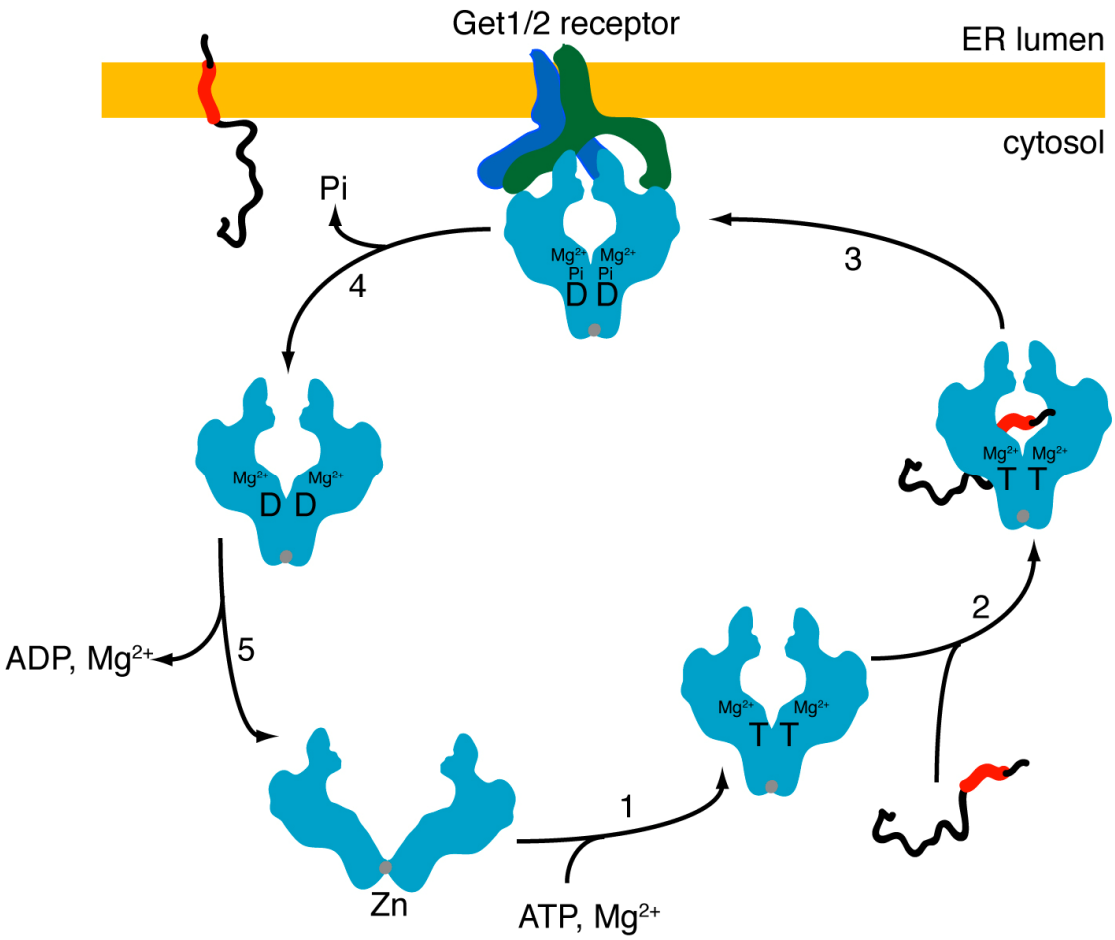

Figure 1.5 ATPase cycle of Get3 is coupled to TA-protein delivery to the ER. Binding of ATP and Mg^{2+} (1) converts a Get3 dimer to a "closed" conformation that can then accept a TA-protein substrate. Binding of a TA-protein (2) and/or an interaction with the Get1/2 receptor (3) triggers an even more compact conformation of the dimer, and receptor-induced ATP hydrolysis enables release of the TA-protein and integration into the lipid bilayer. Inorganic phosphate then dissociates (4) causing relaxation of the Get3 structure and subsequent release of ADP and Mg^{2+} (5) leading to the "open" state of the Get3 dimer.

Such structural data led Bozkurt et al. (2009) to propose a unified model for Get3-mediated TA-protein recognition and delivery to the ER membrane (cf. Figure 1.5). They suggest that the binding of ATP and Mg^{2+} by Get3 leads to the dimer assuming a "closed" conformation that can then accept a TA-protein substrate. Interaction with the ER membrane-bound receptor, Get1/Get2, would induce even further closure, as seen in the transition state structure, followed by ATP hydrolysis that would initiate a

structural relaxation enabling TA-protein substrate release and thereby facilitating both insertion into the ER membrane and recycling of Get3. Subsequent release of ADP would convert the dimer back into the "open" form, which can then enter a new cycle of TA-protein delivery to the ER membrane.

Even though the published structural data from various groups are fundamentally consistent, some observations are difficult to reconcile. For example, it is proposed that the formation of the "closed" dimer upon nucleotide binding causes rearrangements in the α-helical domains that lead to formation of a solvent-exposed, hydrophobic groove spanning both monomers and acting as the TA-protein recognition site (Bozkurt et al., 2009; Mateja et al., 2009). However, dimerisation-deficient Get3 mutants when co-expressed with a model TA-protein in bacteria are still capable of binding to substrates, suggesting that TA-protein recognition can be dimer-independent (Yamagata et al., 2010). Similarly, Get3 mutants believed to have impaired ATP binding and Mg^{2+} coordination still co-purify with a model substrate, again questioning the necessity of acquiring a "closed" dimer conformation prior to TA-protein binding (Yamagata et al., 2010).

The oligomeric state of Get3 when bound to its substrate is also not completely clear. Whilst the transmembrane domain of a TA-protein substrate can easily be accommodated by the hydrophobic groove of the Get3 dimer (Mateja et al., 2009), analytical ultracentrifugation indicated that substrate-bound Get3 is present mainly as a tetramer and, to a much lesser extent, hexamer (Bozkurt et al., 2009). Interestingly, the presence of hexameric Get3 in a crystal structure was also reported (Suloway et al., 2009), and it was suggested that the hexamer might represent a stable, resting form of the protein that is later converted into a dimer. Clearly, although our knowledge of the mechanistic details of Get3 action has increased significantly, many questions still remain unanswered.

6. Aims of my study.

TA-proteins are a large and important group of membrane proteins that utilise distinct pathways for their targeting to, and integration into, the ER membrane. The main aim of this study was to provide a detailed characterisation of the identity and role of cytosolic factors involved in TA-protein delivery to the ER. To this end, a new methodology, relying on bacterially expressed and chromatographically purified recombinant substrates, was developed and is extensively described in Chapter 2.1. By exploiting the advantages of this system, a remarkable flexibility of the components responsible for TA-protein biogenesis was identified (Chapter 2.1). Building on this approach, the model TA-protein, cytochrome b5, was site-specifically labelled with an environmentally-sensitive fluorescent probe and this modified protein used to obtain evidence in support of a role for cytosolic factors during the membrane integration of cytochrome b5 (Chapter 2.2). Pull-down experiments using immobilised recombinant TA-proteins led to the identification, and subsequent characterisation, of the novel component Bat3 as a facilitator of TA-protein biogenesis via the TRC40 pathway (Chapter 2.3; see also (Leznicki et al., 2010)). The identities of other cytosolic factors interacting with TA-proteins in a transmembrane segment-dependent manner are also presented (Chapter 2.4), and the potential role of several cytosolic factors during TA-protein biogenesis is discussed (Chapter 3). Taken together, I believe that the results presented in this thesis have significantly increased our understanding of TA-protein biogenesis, and opened new avenues for future studies, both in terms of available methodologies and specific cellular components for further investigation.

CHAPTER TWO

Results

CHAPTER 2.1

Plasticity of the components mediating tail-anchored protein biogenesis

(manuscript submitted to the Journal of Cell Science)

Plasticity of the components mediating tail-anchored protein biogenesis

Pawel Leznicki, Jim Warwicker and Stephen High*

Faculty of Life Sciences, University of Manchester, Oxford Road, Manchester, M13 9PT, UK.

*To whom correspondence should be addressed: stephen.high@manchester.ac.uk

Page heading title: *Plasticity of TA-protein biogenesis*

Key words: *Cytochrome b5, endoplasmic reticulum, PEGylation, Sec61β, TRC40*

SUMMARY

Tail-anchored (TA) proteins utilise distinct biosynthetic pathways, including TRC40-mediated, chaperone-dependent and/or unassisted routes to the endoplasmic reticulum (ER) membrane. We have addressed the mechanism of action and flexibility of cellular components participating in these pathways by exploiting recombinant forms of Sec61β and Cytb5 bearing covalent modifications within their transmembrane segments. Efficient membrane insertion of both recombinant polypeptides relied on cytosolic factors that were shown to be capable of accommodating remarkably diverse TA-protein variants. Analysis of membrane integration of Sec61β derivatives established that the cytosolic delivery factor TRC40 could bind a singly PEGylated substrate but not a doubly modified version of the same TA-protein, supporting current structural models for the TRC40 substrate binding site. Whilst singly PEGylated Sec61β was efficiently membrane integrated, inability to bind TRC40 precluded insertion of the doubly modified polypeptide. Strikingly, relocation of a single PEG moiety within Sec61β left TRC40 binding unaffected but prevented subsequent membrane insertion. Our modelling indicates that this downstream effect results from the increased energetic cost of insertion into the lipid bilayer. We propose that the membrane integration of TA proteins delivered via TRC40 is strongly dependent upon underlying thermodynamics, and speculate about the physiological significance of plasticity during TA-protein biosynthesis.

INTRODUCTION

Tail anchored (TA) proteins constitute a group of integral membrane proteins characterised by the presence of a single, C-terminally localised, stretch of hydrophobic amino acids that acts as both the sub-cellular targeting signal and membrane anchor (Kutay et al., 1993). Whilst TA-proteins are found in most, if not all, intracellular membranes, the endoplasmic reticulum (ER) acts as the entry site for TA-proteins destined for the various compartments of the secretory pathway (Behrens et al., 1996; Borgese et al., 2001; Kutay et al., 1995; Linstedt et al., 1995). Importantly, the C-terminal location of the membrane-spanning region precludes its co-translational recognition by the signal recognition particle (SRP), ensuring that TA-protein targeting to, and insertion into, the ER membrane are post-translational (Kutay et al., 1995).

The precise route of TA-protein delivery to the ER membrane is precursor-dependent, and correlates to the relative hydrophobicity of the transmembrane segment (TMS) of the tail-anchor region (Brambillasca et al., 2006; Rabu et al., 2009; Rabu et al., 2008). Thus, comparatively hydrophilic tail-anchors, such as those of cytochrome b5 (Cytb5) and protein tyrosine phospatase 1B, define a pathway(s) that is either mediated by Hsp70/Hsp40 chaperones (Abell et al., 2007; Rabu et al., 2008) and/or does not utilise any cytosolic components (Colombo et al., 2009). This pathway(s) does not rely on a specific receptor at the ER membrane, hence, protease-treated microsomes are still fully capable of accepting the TA-protein substrate (Abell et al., 2004; Brambillasca et al., 2006). At the other extreme is a small group of TA-proteins such as synaptobrevin 2 (Syb2) that are characterised by the pronounced hydrophobicity of their TMS. Cross-linking, biochemical studies and a recent phylogenetic analysis all suggest that the SRP can facilitate the post-translational membrane delivery of such precursors (Abell et al., 2004; Borgese and Righi, 2010; Rabu et al., 2009).

The majority of TA-proteins have a TMS with a predicted hydrophobicity that falls between these two extremes (Kalbfleisch et al., 2007), as exemplified by RAMP4 and Sec61β, and these precursors use a specialised targeting factor, known as TRC40 (Asna1)

in mammalian cells (Favaloro et al., 2008; Stefanovic and Hegde, 2007) and Get3 in *Saccharomyces cerevisiae* (Schuldiner et al., 2005; Schuldiner et al., 2008), for their delivery to the ER membrane. The TRC40/Get3 pathway requires additional cytosolic factors (Battle et al., 2010; Costanzo et al., 2010; Jonikas et al., 2009) and a membrane-bound receptor that in yeast has been defined as the Get1/2 complex (Schuldiner et al., 2008). Recent structural analyses of the Get3 protein (Bozkurt et al., 2009; Hu et al., 2009; Mateja et al., 2009; Suloway et al., 2009; Yamagata et al., 2010), and associated components (Chang et al., 2010; Chartron et al., 2010), have provided new insights into the relationship between its ATPase cycle and TA-protein delivery to the ER membrane and identified the likely substrate-binding site. However, since none of the current Get3 structures were obtained as a complex with a TA-protein substrate, several aspects of substrate recognition by Get3 remain to be elucidated (Simpson et al., 2010).

Crucially, the different pathways for TA-protein biogenesis are not mutually exclusive, and at least some precursors appear capable of exploiting multiple routes for their delivery to the ER membrane (Abell et al., 2004; Rabu et al., 2009; Rabu et al., 2008). Furthermore, a recent bioinformatic analysis identified species that appear to have no functional GET pathway, or lack Hsp70/Hsp40 components, yet their genomes encode a range of TA-proteins; further supporting the evolution of multiple mechanisms for the biogenesis of this distinct class of membrane proteins (Borgese and Righi, 2010).

To date many biochemical studies addressing the biogenesis of TA-proteins at the ER membrane have relied upon substrates generated by *in vitro* translation using cell lysates that contain essential cytosolic factors (see (Rabu et al., 2009)). However, a bacterial system has recently been exploited to co-express model TA-proteins with TRC40/Get3 (Bozkurt et al., 2009; Favaloro et al., 2010) and the resulting complexes shown to be sufficient for facilitating membrane insertion, indicating that TRC40/Get3 acts at a very late stage of TA-protein delivery to the ER. Studies using purified recombinant TA-proteins expressed in the absence of known cytosolic interacting partners are limited (Masaki et al., 2003), and have largely focused on Cytb5 (Ceppi et al., 2005; Colombo et al., 2009). The use of recombinant TA-proteins allows polypeptide synthesis to be

physically and temporally separated from the ER delivery and membrane insertion steps, facilitating studies of the components involved in these processes. Indeed, we have recently taken this approach to study Sec61β biogenesis, and identified a novel role for Bat3 during TRC40-dependent ER delivery (Leznicki et al., 2010). Notwithstanding the potential advantages of using recombinant forms of TA-proteins (Henderson et al., 2007), this approach has not been exploited extensively to date.

In the current study, we describe the successful production of recombinant TA-proteins and address the role of detergents and lipid for both purification and substrate competency for membrane integration. A comparison of the insertion kinetics of recombinant Sec61β and Cytb5 emphasises previously reported differences between the pathways utilised by these two precursors for their delivery to the ER membrane (see (Rabu et al., 2009) and references therein). However, by chemically modifying these recombinant TA-protein substrates we show that both routes are surprisingly flexible, and the distinct cellular components that mediate their respective biogenesis can accommodate substrates with significantly modified transmembrane domains. Hence, TRC40 is able to accommodate substrates with a PEGylated TA region. Remarkably, PEGylated forms of both Sec61β and Cytb5 can also be efficiently integrated into the ER membrane, and we provide models for how such modified TA-proteins might associate with TRC40 and be accommodated in the phospholipid bilayer.

RESULTS

Optimisation of tail anchored protein expression and purification.

In order to optimise the production of model TA-proteins in a bacterial system, and thus facilitate the use of purified, recombinant, polypeptides to study their biogenesis, we compared the effects of two different N-terminal affinity tags on the expression and solubility of RAMP4. A short extension derived from bovine opsin (OPG) and containing an N-glycosylation site (Brambillasca et al., 2005; Favaloro et al., 2008; Kutay et al., 1995; Rabu et al., 2008) was added at the C-terminus of the protein, such that its modification could later serve as a reporter for authentic membrane integration.

We found that HisTrx-RAMP4OPG was produced more efficiently than GST-RAMP4OPG, as judged by analysing total protein extracts (cf. Figures 1A and 1B, Coomassie panel, lanes 1 and 2). Furthermore, the GST tagged RAMP4OPG was found to be partially degraded upon immunoblotting (Figure 1A, marked as "Tag-TA-deg."). When the solubility of the two fusion proteins was tested in the absence of detergent, both GST-RAMP4OPG and HisTrx-RAMP4OPG were exclusively found in the insoluble fraction (Figures 1A and 1B, lanes 3-6). The inclusion of 1 % (v/v) Triton X-100 (TX-100) during the cell lysis step resulted in a majority of HisTrx-RAMP4OPG being recovered in the soluble fraction whilst GST-RAMP4OPG remained insoluble even in the presence of detergent (Figures 1A and 1B, lanes 8-11). Hence, on the basis of both yield and solubility we concluded that the HisTrx-based fusion was superior for RAMP4OPG production.

Recombinant TA-proteins are inserted into the ER membrane.

Having established a system for the high-level expression of TA-proteins in a detergent-soluble form, we went on to purify and characterize several model recombinant TA-proteins. We initially chose RAMP4, Sec61β, Syb2 and Cytb5 since these TA-proteins each appear to favour one of the three distinct pathways implicated in TA-protein biogenesis at the ER membrane (see Introduction and (Borgese and Righi, 2010; Favaloro et al., 2008; Rabu et al., 2009; Rabu et al., 2008; Stefanovic and Hegde, 2007)). Cells

expressing recombinant TA-proteins were lysed in the presence of detergent, soluble fractions incubated with NiNTA agarose and, after washing the beads with buffer containing a low concentration of detergent, the various proteins were released from the tag (see Table S1) by thrombin-mediated cleavage ((Ceppi et al., 2005; Colombo et al., 2009), see also Materials and Methods and Table S1). During these solubilisation and initial wash steps, dodecyl-β-D-maltopyranoside (DDM) was used in place of TX-100 because of its increased homogeneity and lack of absorbance in the UV range. DDM was then exchanged for octyl-β-D-glucopyranoside (OG), since its high critical micelle concentration makes it easily removable by dialysis prior to subsequent reconstitution studies (Jackson and Litman, 1982a; Jackson and Litman, 1982b; Niu et al., 2002). Coomassie Blue staining of the proteins resolved by SDS-PAGE showed an acceptable level of protein purity, with only a minor fraction of Sec61βOPG and Cytb5OPG being present in truncated forms (Figure 2A, lanes 3 and 4, see "■" and "□").

To test the capacity of the recombinant proteins to be inserted into ER-derived membranes in the presence of eukaryotic cytosol, a well-established N-glycosylation assay that relies on the C-terminal opsin-derived epitope tag was used (Abell et al., 2004; Brambillasca et al., 2005; Favaloro et al., 2008; Rabu et al., 2008). Crucially, this modification can only take place when the protein spans the membrane and the tag has entered the ER lumen consistent with authentic membrane integration. The recombinant TA-proteins were mixed with cytosol in the form of rabbit reticulocyte lysate, ER-derived membranes were added, and the N-glycosylation status of the proteins determined. Substantial levels of endoglycosidase H (EndoH)-sensitive protein species for both Sec61βOPG and Cytb5OPG were observed (Figure 2B, cf. lanes 5 and 6, 7 and 8), clearly indicating that these two precursors are efficiently integrated into the ER membrane. A small amount of membrane-integrated Cytb5OPG that appears to be a dimer was also observed (Figure 2B, lanes 7 and 8, marked as " "). By the same criteria, the insertion of RAMP4OPG was rather inefficient (Figure 2B, lanes 1-2), whilst Syb2OPG did not even appear to associate with the microsomes, suggesting that it was not effectively delivered to the ER membrane (Figure 2B, lanes 3-4).

Detergent choice and inclusion of phospholipid can influence membrane integration.

Previous studies have shown that the biological activity of purified membrane proteins can depend on both the detergent used during purification, and the inclusion of phospholipids throughout the purification procedure, most likely via effects on protein folding and/or conformation (Banerjee et al., 1995; Knol et al., 1998). To establish whether such factors might contribute to the apparently inefficient membrane insertion of RAMP4OPG and Syb2OPG, both proteins were purified in the presence of various detergents, with and without egg yolk phosphatidylcholine (PC) (see Materials and Methods).

As for other membrane proteins (Banerjee et al., 1995; Knol et al., 1998), the efficiency of RAMP4OPG purification proved to be strongly dependent upon detergent choice and was also affected by the presence of PC (Figure 3A). When the cytosol-dependent membrane insertion of these various RAMP4OPG preparations was tested, only protein purified in the presence of DDM and lauryldimethylamine-N-oxide (LDAO) displayed substantial levels of membrane integration as judged by N-glycosylation (Figure 3B, cf. lanes 1 and 2, 5 and 6, see "+gly" species). The other detergents tested resulted in only low level integration (Figure 3B, lanes 9-15) or no detectable insertion into the ER-derived membranes (Figure 3B, lanes 17 and 18). Interestingly, with some combinations higher molecular weight RAMP4OPG species, most likely corresponding to a protein dimer, were also observed, and in two cases they appeared to be N-glycosylated (Figure 3B, non-glycosylated dimer marked as " ", glycosylated one as "*"). The inclusion of PC during purification typically reduced the efficiency of RAMP4OPG membrane integration, and in several cases increased the proportion of dimer observed (Figure 3B).

When a similar analysis was carried out for Syb2OPG, the efficiency of protein purification was largely unaffected by detergent choice or the inclusion of PC (Figure

3C). However, none of the preparations tested for membrane integration showed any substantial N-glycosylation, with only protein prepared in DDM, OG and LDAO showing a trace level of modification (Figure 3D, cf. lanes 1, 2, 5, 6, 9 and 10). Hence, we could not find conditions to effectively reconstitute Syb2OPG integration using the purified recombinant protein.

Recombinant Sec61β and Cytb5 are inserted into the ER membrane with different kinetics.

Current data strongly suggest that Sec61β and Cytb5 use distinct pathways for their targeting to, and insertion into, the ER membrane (Favaloro et al., 2010; Leznicki et al., 2010; Rabu et al., 2008; Stefanovic and Hegde, 2007), and recombinant forms of both proteins could be efficiently integrated *in vitro* (this study). To establish whether differences between their delivery routes are retained with the recombinant proteins, we compared the kinetics of membrane insertion of purified Sec61βOPG and Cytb5OPG. Previously, N-glycosylation of the opsin-derived tag has been reported to occur almost immediately after translocation into the ER lumen (Brambillasca et al., 2005), indicating that the appearance of N-glycosylated forms of TA-proteins accurately reflects the kinetics of their membrane integration. By this criterion, the membrane insertion of recombinant Sec61βOPG was found to increase steadily after the addition of cytosol and microsomes (Figures 4A and 4C) with membrane integration continuing for at least four hours of incubation (Figure 4C, cf. lanes 5 and 7). In contrast, ~ 50 % of Cytb5OPG is N-glycosylated within the first 30 minutes of a similar time course (Figure 4B, lane 4), and this proportion does not noticeably increase with longer incubations (Figure 4D, cf. lanes 1 and 7). Thus, the recombinant TA-proteins reflect previously reported differences between distinct pathways for TA-protein delivery to the ER membrane (Favaloro et al., 2010; Kim et al., 1997; Leznicki et al., 2010; Rabu et al., 2008; Stefanovic and Hegde, 2007).

Chemically modified TA-proteins are efficiently inserted into the ER membrane.

Purified Sec61βOPG and Cytb5OPG, both bearing single cysteines within their transmembrane segments (Sec61βOPG^{S77C} and Cytb5OPG^{S119C}, see Table S1), were site-specifically modified with a variety of thiol-reactive probes differing in size and physicochemical properties (Figure 5A and 5C). Where appropriate, labelling was confirmed by a shift in electrophoretic mobility (see Figure 5A and 5C) or a colourimetric analysis (for BODIPY, data not shown). Treatment with the biotinylation reagent also resulted in the generation of higher molecular weight species that we conclude to be covalently linked dimers of Sec61βOPG resulting from trace amounts of bifunctional cross-linking reagent present in the commercial preparation used for biotinylation (Figure 5A, lane 2, see " "). This conclusion is strongly supported by the fact that we can generate apparently identical species upon treatment with a bifunctional maleimide (Figure 5A, lane 7, see " "). Treatment with mPEG-5000 and BMH also generated even larger species (Figure 5A, lanes 5 and 7, see "?" and "○", respectively), but since these derivatives were not recovered in the membrane fraction after further analysis (cf. Figure 5B, lanes 9 and 10, 13 and 14) they were not further characterised. In the case of Cytb5OPG, an SDS-stable dimer was observed in the absence of any additional treatment, and similar species became more prominent after incubation with both mPEG-5000 and BMH (Figure 5C). Both the monomeric and dimeric forms of Cytb5OPG appeared to be modified with mPEG-5000 (Figure 5C, lane 2, see "◊" and "□", respectively). Additional high molecular weight species were also observed with BMH (Figure 5C, lane 3, see "○"), but as for Sec61βOPG, little if any of these unassigned species were recovered in association with ER-derived membranes (cf. Figure 5D). Hence, our analysis showed that cysteine residues introduced into the TMSs of both recombinant TA-proteins can be covalently modified by PEGylation and cross-linking reagents, whilst Sec61βOPG can also accept a number of other thiol-reactive probes. To examine the flexibility of cytosolic components involved in the biogenesis of these two TA-proteins, we tested integration of the modified recombinant polypeptides into ER-derived membranes in the presence of cell lysate.

Remarkably, none of the reagents that were covalently attached to a cysteine residue within the TMS of the two TA-proteins resulted in a complete block of membrane integration (Figure 5B, lanes 1-12 and Figure 5D, cf. lanes 3 and 4, 7 and 8). In fact, even homodimers of both Sec61βOPG and Cytb5OPG were still measurably inserted into the lipid bilayer (Figure 5B, cf. lanes 3, 4, 13 and 14 and Figure 5D, cf. lanes 3, 4, 11 and 12). Membrane integration of a Cytb5OPG dimer occurred both with and without prior BMH treatment, suggesting that the close proximity of the two TMSs of the protein monomers does not preclude membrane integration of a Cytb5OPG dimer (Figure 5D, cf. lanes 3 and 4, 11 and 12). A more detailed analysis of Sec61βOPG dimers generated by using cross-linking reagents of different spacer lengths also revealed that its membrane integration is not qualitatively affected by the distance between individual subunits (Figure S1A). Moreover, partial EndoH digestion of the membrane-associated material showed that both subunits of Sec61βOPG and Cytb5OPG dimers are N-glycosylated indicating that both polypeptides are fully inserted into the ER membrane (Figures S1B and S1C).

Remarkably, even the addition of large hydrophilic ER membrane-impermeable probes (Le Gall et al., 2004), including PEG-5000 (Figure 5B, cf. lanes 9 and 10, see "*", and Figure 5D, lanes 7 and 8, see "∞") and, for Sec61βOPG, PEG-20000 (Figure 5B, cf. lanes 11 and 12), to the TMS did not prevent authentic membrane insertion of the recombinant TA-proteins. Perhaps most strikingly, a Cytb5OPG dimer modified with mPEG-5000 was still capable of being efficiently inserted into the ER membrane (Figure 5C, lane 2, and Figure 5D, cf. lanes 7 and 8, marked as "Δ"). Consistent with our previous analysis of Sec61βOPG membrane integration (Leznicki et al., 2010), we find that the membrane integration of both modified and unmodified Cytb5 derivatives is dependent upon the addition of cytosol to the *in vitro* system (Figure 5D, see also Discussion).

PEGylation of Sec61βOPG affects distinct stages of its membrane integration.

Delivery of Sec61β to the ER membrane is mediated by the TRC40 protein (Stefanovic and Hegde, 2007), and if the latter is removed the TA-protein fails to reach its target destination efficiently (Colombo et al., 2009; Leznicki et al., 2010). Crystal structures of TRC40 (Bozkurt et al., 2009; Mateja et al., 2009; Suloway et al., 2009) reveal that it has a deep groove at the dimer interface that most likely acts as a TA-protein recognition site. On the basis of our results (cf. Figure 5B), TRC40 can presumably accommodate a Sec61β polypeptide modified with a single mPEG-5000 moiety. To further investigate the apparent flexibility of substrate binding by TRC40, we mutated both Ser77 and Leu79 of the Sec61βOPG TMS into cysteines and modified this polypeptide with mPEG-5000. Assuming that the transmembrane region adopts an α-helix-like conformation, this double modification would yield a TA-protein with two PEG-5000s extending from opposite sides of the polypeptide chain (Figure 6A). Immunoblotting analysis confirmed the efficient labelling of Sec61βOPG^{S77C,L79C} yielding populations bearing both one and two mPEG-5000 molecules (Figure 6B, cf. lanes 1 and 2). When membrane insertion was tested both unmodified and singly PEGylated forms of Sec61βOPG^{S77C,L79C} were visibly N-glycosylated in agreement with our previous results (Figure 6C, cf. lanes 3 and 4; cf. Figure 5B, lanes 1 and 2, 9 and 10). However, no N-glycosylation of Sec61βOPG^{S77C,L79C} labelled with two mPEG-5000 molecules was seen even after prolonged exposure of the immunoblot (Figure 6C, cf. lanes 3 and 4; and data not shown).

The lack of any membrane-inserted Sec61βOPG^{S77C,L79C} that had been modified with two PEG-5000 species could result from either its inefficient delivery to the ER membrane or an inability to be integrated into the phospholipid bilayer. To address this issue we tested the association of the PEG-labelled Sec61βOPG^{S77C,L79C} with TRC40 by immunoisolation and quantitative immunoblotting. We found that the addition of two PEG probes to a single transmembrane segment of Sec61βOPG^{S77C,L79C} almost completely abolished TA-

protein binding to TRC40 (Figure 6D, cf. lanes 6 and 7 and Figure 6E). This analysis also revealed that the attachment of even a single PEG probe to Sec61βOPG^{S77C,L79C} reduced its binding to TRC40 to about half the level observed with the unmodified protein (Figure 6E). This is consistent with a qualitative reduction in the membrane integration of the singly modified chain when compared to the unmodified version of Sec61βOPG (Figure 6C, cf. lanes 3 and 4, "*0xPEG*" and "*1xPEG*").

We next established whether a TA-protein with a TMS modified with two PEG-5000 molecules predicted to be located on the same side of an alpha helix-like conformation can be bound by TRC40 and delivered to the ER membrane. To this end, a third derivative of Sec61βOPG with both Ser77 and Val84 mutated to cysteines (Figure 6A) was purified and the protein modified with mPEG-5000. The covalent attachment of PEG-5000 probes was confirmed by immunoblotting (Figure 6F, cf. lanes 1 and 2), and a quantitative analysis revealed that a higher proportion of Sec61βOPG^{S77C,V84C} was recovered as a singly PEGylated species than had been observed with Sec61βOPG^{S77C,L79C} (data not shown). This most likely reflects the enhanced modification of the cysteine located at residue 84 where it is adjacent to a polar serine residue (see (Miranda, 2003) and Table S1). When the membrane integration of the two double cysteine variants of Sec61βOPG was compared, surprisingly little if any N-glycosylation of even singly PEGylated Sec61βOPG^{S77C,V84C} could be detected under conditions where the singly modified Sec61βOPG^{S77C,L79C} was reproducibly integrated (Figure 6G). When the binding of Sec61βOPG^{S77C,V84C} to TRC40 was analysed, the interaction of the 1xPEG-5000-Sec61βOPG^{S77C,V84C} species was unperturbed, although association of the doubly PEGylated species was clearly diminished (Figures 6H and 6I). Hence, although TRC40 binding is relatively tolerant of the addition of a single PEG-5000 moiety to the Sec61β TMS, a subsequent step of the membrane insertion process appears much more sensitive to the precise location of such a probe and PEGylation of Cys84 appears not to be tolerated.

DISCUSSION

In the present study we have investigated the use of recombinant TA-proteins as a tool for better understanding the biogenesis of this important class of membrane proteins at the endoplasmic reticulum. To this end, we first compared two distinct systems for the production of TA-proteins in bacteria: one relying on the addition of the N-terminal glutathione S-transferase (GST) tag (cf. (Ceppi et al., 2005; Colombo et al., 2009)), the other on the presence of the Histidine-Thioredoxin (HisTrx) tag (cf. (Leznicki et al., 2010)). Whilst both tags are commonly used to increase the solubility of their fusion partners and facilitate purification of recombinant polypeptides (Hammarstrom et al., 2006; Kim and Lee, 2008; Terpe, 2003), we observed distinct effects on the production of a model TA-protein, RAMP4. Specifically, expression levels were higher for the HisTrx-based system and, more importantly, the resulting fusion protein was largely recovered in a soluble form when detergent was included during the cell lysis step. This was not the case for our GST-RAMP4 fusion protein, although in the case of Cytb5, a GST fusion protein could be partially solubilised using 2 % (v/v) TX-100 in the cell lysis buffer (Colombo et al., 2009). Alternatively, Favaloro and colleagues have recently shown that a HisZZ-tagged form of RAMP4 can be maintained in a soluble form by co-expression with TRC40 (Asna-1) and purification of the resulting complex (Favaloro et al., 2010). The approach we describe here is particularly well suited to the site-specific incorporation of biochemical probes into the purified recombinant TA-protein in order to study its subsequent membrane delivery and integration.

Our main objective was to use the recombinant proteins to better understand TA-protein integration at the ER. We find that the purified recombinant proteins can be integrated into pancreatic microsomes, albeit with varying degrees of efficiency, whilst the yield of purified recombinant protein and the efficiency of membrane insertion can be strongly influenced by detergent choice. Amongst many parameters, the detergent can influence protein conformation thereby affecting proteolytic removal of the affinity tag, and it may

also have an effect on the ability of specific cytosolic factors to bind to TA-proteins (Favaloro et al., 2008). In our studies we were able to recapitulate the interaction between TRC40 and recombinant Sec61β, thereby enabling subsequent membrane integration (see Figure 6). The precise choice of detergent for the production of other insertion-competent TA-proteins will need to be determined empirically.

We find that the membrane integration of both Sec61βOPG (Leznicki et al., 2010), and Cytb5OPG (this study), is dependent upon the presence of cytosol as judged by our N-glycosylation assay. In the case of Sec61β we can correlate this requirement to a need for TRC40/Asna-1 (Favaloro et al., 2008; Stefanovic and Hegde, 2007), and other cytosolic factors including Bat3 (Leznicki et al., 2010) and the mammalian homologues of Get4 and Get5 (Mariappan et al., 2010). The role of cytosolic factors in the membrane integration of Cytb5 remains controversial (Colombo et al., 2009; Rabu et al., 2009; Rabu et al., 2008). Nevertheless, in this study we can only detect an N-glycosylated membrane integrated form of the protein in the presence of lysate, consistent with a role for one or more soluble components during the delivery and/or membrane integration of Cytb5 (cf. (Rabu et al., 2009)). When a time course of membrane integration is carried out, Sec61βOPG and Cytb5OPG show quite different kinetics, with Sec61β integration progressing much more slowly than that of Cytb5. This observation suggests that the loading of recombinant Sec61βOPG onto TRC40 may be the rate-limiting step in our system. This view is supported by the fact that the membrane integration of Sec61βOPG preloaded onto TRC40 displays much faster kinetics (Favaloro et al., 2010), and that the addition of recombinant Get3 to a wild-type yeast *in vitro* system can significantly enhance membrane insertion (Schuldiner et al., 2008). The loading of TRC40 with TA-protein substrates *in vivo* is presumably facilitated by the actions of other associated components that enable binding to occur immediately after synthesis is complete (Leznicki et al., 2010; Mariappan et al., 2010; Rabu et al., 2009).

Sec61β is able to tolerate the covalent attachment of a variety of reagents to a single cysteine residue located within its TMS, whilst retaining the ability to be integrated into the ER membrane. Similarly, the membrane integration of Cytb5 is not blocked by the

addition of a PEG-5000 moiety close to the middle of its TMS or by the formation of a protein dimer. In the case of Sec61β, polypeptides with several different hydrophobic and hydrophilic reagents, PEG-5000 and even PEG-20000, could all be shown to be post-translationally integrated suggesting that the components that mediate its delivery to and integration into the ER membrane can accommodate a range of non-physiological modifications of this substrate without a substantial perturbation of their function. For Sec61β, we found that the attachment of two PEG-5000 molecules both located towards the centre of the TMS was sufficient to prevent membrane integration. By analysing the effect of PEGylation upon Sec61β binding to the cytosolic delivery factor TRC40, we show that a singly PEGylated version of Sec61β^{S77C,L79C} can still bind to TRC40 with substantial efficiency, whilst a doubly modified form cannot. When this PEGylated TMS is modelled into the substrate-binding site of TRC40, our data are in good agreement with the proposed deep pocket (Bozkurt et al., 2009; Hu et al., 2009; Mateja et al., 2009; Suloway et al., 2009) that could accommodate the addition of one centrally localised PEG-5000 to the substrate, but not two (see Figure 7A).

Interestingly, when an alternative cysteine was used to generate a doubly PEGylated variant, Sec61β^{S77C,V84C}, the singly modified form was still capable of binding efficiently to TRC40, but was no longer membrane-integrated. Our interpretation of this observation is that the modification of cysteine 84 results in the specific perturbation of a biosynthetic step occurring after TRC40 binding, for example the failure of TRC40 to release the modified substrate, or a defect in the subsequent membrane integration step (Figure 7C). Our calculations of the changes in free energy resulting from the insertion of a PEG polymer into a lipid bilayer favour the latter possibility. Hence, the free energy associated with the transfer of the unmodified Sec61βOPG transmembrane segment into a lipid bilayer can be estimated as -11.5 kcal/mol (see Supplementary Data) assuming a non-Sec61 translocon mediated pathway for insertion (Hessa et al., 2007; Rabu et al., 2009; Wimley et al., 1996). By the same criteria, the integration of Sec61β PEGylated at cysteine 77 has an estimated energetic cost of -4 kcal/mol, and hence remains favourable (Figure 7B, S77C). In contrast, the energetic cost of integrating Sec61β PEGylated at cysteine 84 is +1 kcal/mol (Figure 7B, V84C, see Supplementary Data for detailed

calculations). Thus, our modelling supports the idea that the membrane integration efficiency of a PEGylated Sec61β TMS is dependent on the precise location of the probe relative to the lipid bilayer (Figure 7B). The distinct behaviour of the differently PEGylated Sec61β TMSs is also consistent with a partitioning-based model for their membrane insertion. In this scenario a putative membrane-bound receptor for TRC40 would act to deliver TA-proteins to the surface of the ER membrane, but subsequent integration would rely on the favourable thermodynamics of TA-protein partitioning into the lipid bilayer and a specialised integrase would not be required (Figure 7C, cf. (Rabu et al., 2009)).

In the case of Cytb5, whilst a role for TRC40 akin to that performed during Sec61β biogenesis seems unlikely (Colombo et al., 2009; Favaloro et al., 2008; Favaloro et al., 2010; Leznicki et al., 2010; Stefanovic and Hegde, 2007), the precise identity of the components that mediate its membrane delivery and integration are uncertain. Nevertheless, we see an equally flexible pathway for Cytb5 biogenesis that can tolerate both PEGylation and enforced dimerisation. We conclude that any cytosolic components that facilitate Cytb5 integration can tolerate these species without substantial perturbation (Figure 5). Once at the membrane, the rate at which the PEGylated Cytb5 can be N-glycosylated appears to be substantially faster than that of Sec61β consistent with different pathways of integration into the ER membrane where the insertion of Cytb5 is primarily mediated by phospholipids (Brambillasca et al., 2005; Kim et al., 1997; Rabu et al., 2009).

Whether the flexibility of the post-translational pathways that underlie TA-protein biogenesis is of physiological significance remains to be determined. However, our results are in good agreement with the finding that certain viral proteins are palmitoylated within their transmembrane segments prior to the membrane integration step (Caballero et al., 1998; Ochsenbauer-Jambor et al., 2001). Moreover, our data are also consistent with the proposal that soluble SNAP25 is initially targeted to the ER membrane in a complex with the TA-protein syntaxin (Vogel et al., 2000), presumably via the binding of the complex to TRC40 prior to ER delivery (Stefanovic and Hegde, 2007). It may even

be the case that TRC40 can bind to covalently modified TA-proteins that are generated *in vivo* such as ubiquitinated species, consistent with both the possibility for co-translational ubiquitination of membrane proteins (Sato et al., 1998) and known links between the yeast homologue of TRC40, Get3, and the ubiquitin-proteasome system (Auld et al., 2006).

MATERIALS AND METHODS

Materials. Bacterial expression vector pHisTrx was a gift from Dr Richard Kammerer (University of Manchester). Rabbit polyclonal antisera recognising TRC40 was a gift from Bernhard Dobberstein (ZMBH, Heidelberg, Germany) and the monoclonal anti-opsin tag antibody was provided by Paul Hargrave (Department of Ophthalmology, University of Florida, USA). All detergents were supplied by Anatrace, except for Triton X-100 which was obtained from Sigma. Cross-linking reagents and EZ-link-biotin were purchased from Pierce whilst BODIPY and IASD from Molecular Probes. PEG-5000 and PEG-20000 maleimides were from Nektar. Nuclease-treated rabbit reticulocyte lysate was supplied by Promega.

Expression of TA-proteins bearing an N-terminal tag. Single cysteine mutants of TA-protein cDNAs, including a region encoding an in frame opsin-derived tag at the 3' end (see Table S1 for amino acid sequences of the proteins used), were cloned into the pGEX4T-1 and pHisTrx expression vectors downstream of sequences encoding the GST and 6xHis-Thioredoxin polypeptides, respectively. The resulting plasmid constructs were verified by sequencing, and then used to transform *E. coli* BLR(DE3) pLysS cells which were grown in LB medium supplemented with ampicillin (100 g/ml) and glucose (1 % w/v) to $OD_{600} \approx 0.45$-0.8. Gene expression was then induced with 0.4 mM IPTG and growth continued for 3 h at 30 C. Cells were harvested, resuspended in buffer A (50 mM Tris-Cl, pH 7.4; 300 mM NaCl; 10 mM $MgCl_2$; 10 mM imidazole; 5 mM 2-ME; 1 mM PMSF; 10 % (v/v) glycerol), snap-frozen in liquid nitrogen and stored at -80 C. To test the solubility of the fusion proteins, bacteria were thawed, lysozyme and DNase I added to final concentrations of 0.2 mg/ml and 15 U/ml respectively. The cell suspension was divided, and Triton X-100 at 1 % (v/v) final concentration added to one half. Samples were incubated for 1 h at room temperature followed by sonication in a water bath at 4 C (two 20 min sonication steps with 30 min gap). Bacterial lysate was spun at 10,000 x g (30 min; 4 C) to pellet any intact cells and cell debris, and the resulting supernatant was

then re-centrifuged at 100,000 x g (1h; 4 C) to sediment protein aggregates and membrane fragments. Samples from each step were analysed by SDS-PAGE followed by Coomassie Brilliant Blue staining.

Purification of TA-proteins. Suspension of *E. coli* cells expressing recombinant TA-proteins was thawed, supplemented with 0.2 mg/ml lysozyme, 15 U/ml DNase I, complete protease inhibitor cocktail (Roche), 1 mM PMSF and 1 % (w/v) dodecyl-β-D-maltopyranoside (DDM) and was incubated for 1 hour at room temperature. Insoluble material was pelleted (10,000 x g; 30 min; 4 C), the soluble fraction incubated with NiNTA agarose for 3 hours at 4 C and the resin washed with buffer B (50 mM Tris-Cl, pH 7.4; 300 mM NaCl; 10 mM imidazole; 10 % (v/v) glycerol) supplemented with 0.1 % (w/v) DDM. At this stage DDM was exchanged by extensively washing the beads with buffer B supplemented with 0.75 % (w/v) octyl-β-D-glucopyranoside (OG), 0.1 % lauryldimethylamine-N-oxide (LDAO), or other detergent to a concentration of 0.05 – 0.1 % (w/v) as indicated. Resin was resuspended in buffer B with the specified detergent, and TA-proteins released by adding thrombin to a final concentration of 15 U/ml and incubating the suspension overnight at room temperature (Ceppi et al., 2005). Beads were re-isolated by centrifugation, and thrombin either inactivated by the addition of 1mM PMSF or removed by incubation with Benzamidine Sepharose (1h; 4 C). Potential aggregates formed during the cleavage reaction were removed by centrifugation at 100,000 x g for 1 hour at 4 C. Protein concentration was calculated from the absorbance at 280 nm, using extinction coefficients predicted from the amino acid sequence. Proteins were aliquoted, snap-frozen in liquid nitrogen and stored at -80 C.

It was determined empirically that OG and LDAO were most suited to the purification of Sec61βOPG and Cytb5OPG in a form that was competent for subsequent membrane integration (see below). To test which detergents supported membrane integration (see below) of recombinant RAMP4OPG and Syb2OPG both proteins were purified as described above but, where indicated, DDM was exchanged into one of the following: 0.75 % (w/v) OG, 0.1 % (w/v) LDAO, 0.05 % Fos-Choline-16 (FC-16) or 0.05 % (w/v) LysoFos-Choline-16 (Lyso-FC-16) (cf. Figure 3). Both proteins were also purified in the

presence of 0.4 mg/ml egg yolk phosphatidylcholine using the same procedure except that concentrations of FC-16 and Lyso-FC-16 was increased to 0.1 % (w/v).

Membrane integration reaction of recombinant TA-proteins. Integration reactions comprising of 0.6 – 2.5 M TA-protein (1/40th total reaction volume), 5 l sheep pancreatic microsomes (final concentration of ~ 3.5 OD_{280} per ml) and rabbit reticulocyte lysate or buffer R (50 mM HEPES-KOH, pH 7.5, 40 mM KOAc, 5 mM $MgCl_2$) supplemented with the ATP/GTP regeneration system (1 mM ATP, 100 M GTP, 10 mM creatine phosphate and 100 g/ml creatine phosphokinase) made up to 30 l were incubated for 4 hours at 30 C unless stated otherwise. Membranes were isolated by centrifugation through an HSC cushion (750 mM sucrose; 500 mM KOAc; 5 mM $Mg(OAc)_2$; 50 mM HEPES-KOH, pH 7.9) at 120,000 x g for 10 min at 4 C, the resulting pellet was resuspended in LSC buffer (250 mM sucrose; 100 mM KOAc; 5 mM $Mg(OAc)_2$; 50 mM HEPES-KOH, pH 7.9) and either first subjected to Endoglycosidase H (EndoH) digestion or solubilised directly in Laemmli buffer. All samples were analysed by SDS-PAGE followed by immunoblotting with the anti-opsin tag antibody.

For the time-course analysis of Sec61βOPG and Cytb5OPG membrane integration assays were performed as above and at the times indicated the reactions were stopped by immediate centrifugation through an HSC cushion. For the 1 min time point, the samples were placed on ice and the membrane fraction recovered by centrifugation together with the samples from the 5 min time point.

Chemical modification of recombinant TA-proteins. Thiol-reactive probes as indicated were mixed with solutions of single cysteine mutants of Sec61βOPG (77 M) in buffer B with 0.75% (w/v) OG and Cytb5OPG (25 M) in buffer Q (50 mM HEPES-KOH, pH 7.9, 50 mM KOAc, 200 mM NaCl, 10 % (v/v) glycerol, 0.1 % (w/v) LDAO) (cf. Table S1) using the reagents at a final concentration of 1-3 mM and incubating for 2 hours at room temperature in the dark. Reactions were quenched by addition of 20 mM 2-mercaptoethanol and further incubation for 10 min. Modified proteins were resolved by SDS-PAGE, and then stained with Coomassie Brilliant Blue or immunoblotted with the

anti-opsin tag antibody, or they were used for membrane integration reactions. The Sec61βOPG double cysteine mutants (see Table S1) were purified and labelled as described using 1.5 mM mPEG-5000 for 1 hour at 25°C. After quenching, labelled proteins were analysed as before or used for integration assays. For comparison of the membrane integration of double cysteine variants of Sec61βOPG (cf. Figure 6G), the amounts of both proteins were normalised to the concentration of their respective singly PEGylated forms.

Binding of PEGylated Sec61βOPG to TRC40. PEGylated Sec61βOPG variants (1 – 1.9 M) were incubated with 140 l of rabbit reticulocyte lysate for 30 min at 30°C, the reaction was split in two and each half added to 20 l (50 % (v/v) suspension) of Protein A Sepharose coated with 7.5 l of rabbit anti-TRC40 or anti-PDI antisera. The lysate was incubated with Protein A Sepharose-antibody beads for 1 h at 4°C, the resin washed extensively with buffer R supplemented with 0.5 M NaCl and bound proteins eluted with buffer R containing 0.5 % (v/v) TX-100 (cf. (Favaloro et al., 2008)). The eluate was mixed with the Laemmli sample buffer, samples resolved on SDS-PAGE and immunoblotted with the anti-opsin tag antibody. Quantitative analysis was carried out using a LiCor Biosciences system (see below). The non-specific binding of the indicated Sec61βOPG variants to anti-PDI antibody-coated Protein A Sepharose beads was subtracted from the results obtained using anti-TRC40 antibody-coated Protein A Sepharose, and the resulting values were normalised to the amount of each Sec61βOPG species present in the starting material.

Quantitative immunoblotting. Following transfer of the samples onto a low-fluor PVDF membrane and incubation with a primary anti-opsin epitope tag antibody, a secondary anti-mouse fluorescent-dye conjugated antibody was added at 1:10000 dilution. The membrane was incubated for 1 hour at room temperature, scanned using a LiCor Biosciences system and the results quantified with Odyssey 2.1 software.

ACKNOWLEDGEMENTS

This work was supported by a PhD studentship from the Wellcome Trust (PL). We thank Richard Kammerer for the pHisTrx expression vector, Paul Hargrave for the anti-opsin epitope tag antibody, and Bernhard Dobberstein, Vincenzo Favaloro and Fabio Vilardi for the anti-TRC40 serum. We are grateful to Lisa Swanton and Martin Pool for their comments during manuscript preparation, and to all of our colleagues who provided reagents and advice.

REFERENCES

Abell, B. M., Pool, M. R., Schlenker, O., Sinning, I. and High, S. (2004). Signal recognition particle mediates post-translational targeting in eukaryotes. *Embo J* **23**, 2755-64.

Abell, B. M., Rabu, C., Leznicki, P., Young, J. C. and High, S. (2007). Post-translational integration of tail-anchored proteins is facilitated by defined molecular chaperones. *J Cell Sci* **120**, 1743-51.

Auld, K. L., Hitchcock, A. L., Doherty, H. K., Frietze, S., Huang, L. S. and Silver, P. A. (2006). The conserved ATPase Get3/Arr4 modulates the activity of membrane-associated proteins in Saccharomyces cerevisiae. *Genetics* **174**, 215-27.

Banerjee, P., Joo, J. B., Buse, J. T. and Dawson, G. (1995). Differential solubilization of lipids along with membrane proteins by different classes of detergents. *Chem Phys Lipids* **77**, 65-78.

Battle, A., Jonikas, M. C., Walter, P., Weissman, J. S. and Koller, D. (2010). Automated identification of pathways from quantitative genetic interaction data. *Mol Syst Biol* **6**, 379.

Behrens, T. W., Kearns, G. M., Rivard, J. J., Bernstein, H. D., Yewdell, J. W. and Staudt, L. M. (1996). Carboxyl-terminal targeting and novel post-translational processing of JAW1, a lymphoid protein of the endoplasmic reticulum. *J Biol Chem* **271**, 23528-34.

Borgese, N., Gazzoni, I., Barberi, M., Colombo, S. and Pedrazzini, E. (2001). Targeting of a tail-anchored protein to endoplasmic reticulum and mitochondrial outer membrane by independent but competing pathways. *Mol Biol Cell* **12**, 2482-96.

Borgese, N. and Righi, M. (2010). REMOTE ORIGINS OF TAIL-ANCHORED PROTEINS. *Traffic*.

Bozkurt, G., Stjepanovic, G., Vilardi, F., Amlacher, S., Wild, K., Bange, G., Favaloro, V., Rippe, K., Hurt, E., Dobberstein, B. et al. (2009). Structural insights into tail-anchored protein binding and membrane insertion by Get3. *Proc Natl Acad Sci U S A* **106**, 21131-6.

Brambillasca, S., Yabal, M., Makarow, M. and Borgese, N. (2006). Unassisted translocation of large polypeptide domains across phospholipid bilayers. *J Cell Biol* **175**, 767-77.

Brambillasca, S., Yabal, M., Soffientini, P., Stefanovic, S., Makarow, M., Hegde, R. S. and Borgese, N. (2005). Transmembrane topogenesis of a tail-anchored protein is modulated by membrane lipid composition. *Embo J* **24**, 2533-42.

Caballero, M., Carabana, J., Ortego, J., Fernandez-Munoz, R. and Celma, M. L. (1998). Measles virus fusion protein is palmitoylated on transmembrane-intracytoplasmic cysteine residues which participate in cell fusion. *J Virol* **72**, 8198-204.

Ceppi, P., Colombo, S., Francolini, M., Raimondo, F., Borgese, N. and Masserini, M. (2005). Two tail-anchored protein variants, differing in transmembrane domain length and intracellular sorting, interact differently with lipids. *Proc Natl Acad Sci U S A* **102**, 16269-74.

Chang, Y. W., Chuang, Y. C., Ho, Y. C., Cheng, M. Y., Sun, Y. J., Hsiao, C. D. and Wang, C. (2010). Crystal structure of Get4/Get5 complex and its interactions with Sgt2, Get3 and Ydj1. *J Biol Chem* **285**, 9962-70.

Chartron, J. W., Suloway, C. J., Zaslaver, M. and Clemons, W. M., Jr. (2010). Structural characterization of the Get4/Get5 complex and its interaction with Get3. *Proc Natl Acad Sci U S A*.

Colombo, S. F., Longhi, R. and Borgese, N. (2009). The role of cytosolic proteins in the insertion of tail-anchored proteins into phospholipid bilayers. *J Cell Sci* **122**, 2383-92.

Costanzo, M., Baryshnikova, A., Bellay, J., Kim, Y., Spear, E. D., Sevier, C. S., Ding, H., Koh, J. L., Toufighi, K., Mostafavi, S. et al. (2010). The genetic landscape of a cell. *Science* **327**, 425-31.

Favaloro, V., Spasic, M., Schwappach, B. and Dobberstein, B. (2008). Distinct targeting pathways for the membrane insertion of tail-anchored (TA) proteins. *J Cell Sci* **121**, 1832-40.

Favaloro, V., Vilardi, F., Schlecht, R., Mayer, M. P. and Dobberstein, B. (2010). Asna1/TRC40-mediated membrane insertion of tail-anchored proteins. *J Cell Sci* **123**, 1522-30.

Hammarstrom, M., Woestenenk, E. A., Hellgren, N., Hard, T. and Berglund, H. (2006). Effect of N-terminal solubility enhancing fusion proteins on yield of purified target protein. *J Struct Funct Genomics* **7**, 1-14.

Heller, H., Schaefer, M. and Schulten, K. (1993). Molecular dynamics simulation of a bilayer of 200 lipids in the gel and in the liquid crystal phase. *J Phys Chem* **97**, 8343-60.

Henderson, M. P., Billen, L. P., Kim, P. K. and Andrews, D. W. (2007). Cell-free analysis of tail-anchor protein targeting to membranes. *Methods* **41**, 427-38.

Hessa, T., Meindl-Beinker, N. M., Bernsel, A., Kim, H., Sato, Y., Lerch-Bader, M., Nilsson, I., White, S. H. and von Heijne, G. (2007). Molecular code for transmembrane-helix recognition by the Sec61 translocon. *Nature* **450**, 1026-30.

Hu, J., Li, J., Qian, X., Denic, V. and Sha, B. (2009). The crystal structures of yeast Get3 suggest a mechanism for tail-anchored protein membrane insertion. *PLoS One* **4**, e8061.

Jackson, M. L. and Litman, B. J. (1982a). Rhodopsin-phospholipid reconstitution by dialysis removal of octyl glucoside. *Biochemistry* **21**, 5601-8.

Jackson, M. L. and Litman, B. J. (1982b). Rhodopsin-Phospholipid Reconstitution from Octyl Glucoside-solubilized Samples. *Biophys J* **37**, 93-94.

Jonikas, M. C., Collins, S. R., Denic, V., Oh, E., Quan, E. M., Schmid, V., Weibezahn, J., Schwappach, B., Walter, P., Weissman, J. S. et al. (2009). Comprehensive characterization of genes required for protein folding in the endoplasmic reticulum. *Science* **323**, 1693-7.

Kalbfleisch, T., Cambon, A. and Wattenberg, B. W. (2007). A bioinformatics approach to identifying tail-anchored proteins in the human genome. *Traffic* **8**, 1687-94.

Kim, P. K., Janiak-Spens, F., Trimble, W. S., Leber, B. and Andrews, D. W. (1997). Evidence for multiple mechanisms for membrane binding and integration via carboxyl-terminal insertion sequences. *Biochemistry* **36**, 8873-82.

Kim, S. and Lee, S. B. (2008). Soluble expression of archaeal proteins in Escherichia coli by using fusion-partners. *Protein Expr Purif* **62**, 116-9.

Knol, J., Sjollema, K. and Poolman, B. (1998). Detergent-mediated reconstitution of membrane proteins. *Biochemistry* **37**, 16410-5.

Kutay, U., Ahnert-Hilger, G., Hartmann, E., Wiedenmann, B. and Rapoport, T. A. (1995). Transport route for synaptobrevin via a novel pathway of insertion into the endoplasmic reticulum membrane. *Embo J* **14**, 217-23.

Kutay, U., Hartmann, E. and Rapoport, T. A. (1993). A class of membrane proteins with a C-terminal anchor. *Trends Cell Biol* **3**, 72-5.

Le Gall, S., Neuhof, A. and Rapoport, T. (2004). The endoplasmic reticulum membrane is permeable to small molecules. *Mol Biol Cell* **15**, 447-55.

Leznicki, P., Clancy, A., Schwappach, B. and High, S. (2010). Bat3 promotes the membrane integration of tail-anchored proteins. *J Cell Sci* **123**, 2170-8.

Linstedt, A. D., Foguet, M., Renz, M., Seelig, H. P., Glick, B. S. and Hauri, H. P. (1995). A C-terminally-anchored Golgi protein is inserted into the endoplasmic reticulum and then transported to the Golgi apparatus. *Proc Natl Acad Sci U S A* **92**, 5102-5.

Mariappan, M., Li, X., Stefanovic, S., Sharma, A., Mateja, A., Keenan, R. J. and Hegde, R. S. (2010). A ribosome-associating factor chaperones tail-anchored membrane proteins. *Nature*. In press.

Masaki, R., Kameyama, K. and Yamamoto, A. (2003). Post-translational targeting of a tail-anchored green fluorescent protein to the endolpasmic reticulum. *J Biochem* **134**, 415-26.

Mateja, A., Szlachcic, A., Downing, M. E., Dobosz, M., Mariappan, M., Hegde, R. S. and Keenan, R. J. (2009). The structural basis of tail-anchored membrane protein recognition by Get3. *Nature* **461**, 361-6.

Miranda, J. J. (2003). Position-dependent interactions between cysteine residues and the helix dipole. *Protein Sci* **12**, 73-81.

Niu, L., Kim, J. M. and Khorana, H. G. (2002). Structure and function in rhodopsin: asymmetric reconstitution of rhodopsin in liposomes. *Proc Natl Acad Sci U S A* **99**, 13409-12.

Ochsenbauer-Jambor, C., Miller, D. C., Roberts, C. R., Rhee, S. S. and Hunter, E. (2001). Palmitoylation of the Rous sarcoma virus transmembrane glycoprotein is required for protein stability and virus infectivity. *J Virol* **75**, 11544-54.

Rabu, C., Schmid, V., Schwappach, B. and High, S. (2009). Biogenesis of tail-anchored proteins: the beginning for the end? *J Cell Sci* **122**, 3605-12.

Rabu, C., Wipf, P., Brodsky, J. L. and High, S. (2008). A precursor-specific role for Hsp40/Hsc70 during tail-anchored protein integration at the endoplasmic reticulum. *J Biol Chem* **283**, 27504-13.

Sato, S., Ward, C. L. and Kopito, R. R. (1998). Cotranslational ubiquitination of cystic fibrosis transmembrane conductance regulator in vitro. *J Biol Chem* **273**, 7189-92.

Schuldiner, M., Collins, S. R., Thompson, N. J., Denic, V., Bhamidipati, A., Punna, T., Ihmels, J., Andrews, B., Boone, C., Greenblatt, J. F. et al. (2005). Exploration of the function and organization of the yeast early secretory pathway through an epistatic miniarray profile. *Cell* **123**, 507-19.

Schuldiner, M., Metz, J., Schmid, V., Denic, V., Rakwalska, M., Schmitt, H. D., Schwappach, B. and Weissman, J. S. (2008). The GET complex mediates insertion of tail-anchored proteins into the ER membrane. *Cell* **134**, 634-45.

Simpson, P. J., Schwappach, B., Dohlman H. G. and Isaacson, R. L. (2010). Structures of Get3, Get4, and Get5 provide new models for TA membrane protein targeting. (in press)

Sowa, M. E., Bennett, E. J., Gygi, S. P. and Harper, J. W. (2009). Defining the human deubiquitinating enzyme interaction landscape. *Cell* **138**, 389-403.

Stefanovic, S. and Hegde, R. S. (2007). Identification of a targeting factor for posttranslational membrane protein insertion into the ER. *Cell* **128**, 1147-59.

Suloway, C. J., Chartron, J. W., Zaslaver, M. and Clemons, W. M., Jr. (2009). Model for eukaryotic tail-anchored protein binding based on the structure of Get3. *Proc Natl Acad Sci U S A* **106**, 14849-54.

Terpe, K. (2003). Overview of tag protein fusions: from molecular and biochemical fundamentals to commercial systems. *Appl Microbiol Biotechnol* **60**, 523-33.

Vogel, K., Cabaniols, J. P. and Roche, P. A. (2000). Targeting of SNAP-25 to membranes is mediated by its association with the target SNARE syntaxin. *J Biol Chem* **275**, 2959-65.

Wimley, W. C., Creamer, T. P. and White, S. H. (1996). Solvation energies of amino acid side chains and backbone in a family of host-guest pentapeptides. *Biochemistry* **35**, 5109-24.

Yamagata, A., Mimura, H., Sato, Y., Yamashita, M., Yoshikawa, A. and Fukai, S. (2010). Structural insight into the membrane insertion of tail-anchored proteins by Get3. *Genes Cells* **15**, 29-41.

FIGURE LEGENDS

Figure 1. Expression and solubility of N-terminally tagged RAMP4OPG.
E.coli BLR (DE3) pLysS expressing GST-RAMP4OPG (A) and HisTrx-RAMP4OPG (B) were harvested and fusion protein solubility tested (see Materials and Methods). Bacteria were lysed in the absence/presence of TX-100 as shown and the resulting lysate centrifuged at 10,000 x g yielding a pellet (P1) and supernatant (S1). This supernatant was re-centrifuged at 100,000 x g to give a second pellet (P2) and supernatant (S2). Fractions were analysed by SDS-PAGE, and gels either stained with Coomassie Brilliant Blue (Coomassie panel) or immunoblotted with the anti-opsin epitope tag antibody (Immunoblotting panel). Migration of the fusion proteins is indicated as "Tag-TA" with probable degradation products of GST-RAMP4OPG labelled as "Tag-TA-deg. (?)" for the Coomassie stained gel and as "Tag-TA-deg" after immunoblotting. A minor high molecular weight HisTrx-RAMP4OPG species likely corresponding to a dimer is also indicated (2xTag-TA).

Figure 2. Purification and membrane insertion of recombinant TA-proteins.
A) TA-proteins as indicated were expressed with the N-terminal HisTrx tag, purified in the presence of 0.75 % (w/v) octyl-β-D-glucopyranoside, and 10 l of each protein preparation resolved by SDS-PAGE and stained with Coomassie Brilliant Blue. Truncated forms of Sec61βOPG (■) and Cytb5OPG (□) are indicated. B) Insertion of the purified recombinant TA-proteins into the ER-derived membranes was analysed as described in Materials and Methods. The N-glycosylation status of recombinant substrates was addressed by EndoH digestion with the membrane fraction resolved by SDS-PAGE followed by immunoblotting for the opsin-derived epitope tag. N-glycosylated protein species (∗) and a faint presumed Cytb5OPG dimer ( ) are indicated. The lack of any detectable Syb2OPG species most likely results from the inefficient association of the protein preparation used with the ER-derived microsomes.

Figure 3. Choice of detergent and inclusion of lipid affect yield and membrane insertion of recombinant TA-proteins.

RAMP4OPG (A, B) and Syb2OPG (C, D) were purified as previously (see Figure 2A) except that, after cell lysis and initial wash steps, dodecyl-β-D-maltopyranoside was exchanged for the detergents indicated. Where shown (+PC), 0.4 mg/ml phosphatidylcholine was included throughout the purification procedure. Samples from each protein preparation were resolved by SDS-PAGE and stained with Coomassie Brilliant Blue (A, C). Migration of the purified TA-proteins in SDS-PAGE is indicated (>). Purified RAMP4OPG (B) and Syb2OPG (D) were also used for membrane integration assays as previously (see legend to Fig. 2). A larger EndoH-resistant RAMP4OPG species most likely represents a protein dimer ( ) and in some cases is N-glycosylated (*). For full details of all detergents see Materials and Methods.

Figure 4. Recombinant Sec61βOPG and Cytb5OPG are inserted into the ER-derived membranes with different kinetics.

Membrane integration reactions with 1.9 M Sec61βOPG (A, C) and 2.5 M Cytb5OPG (B, D) were performed over a range of incubation times using N-glycosylation of the recombinant proteins to report integration following detection by immunoblotting as previously described. Where indicated samples were digested with EndoH prior to analysis. A truncated version of Sec61βOPG (■) and its glycosylated form are indicated (◀).

Figure 5. Chemically modified TA-proteins are integrated into ER-derived membranes.

Variants of Sec61βOPG (A) and Cytb5OPG (C) with single cysteines located in their transmembrane segments (see Table S1) were modified with thiol-reactive probes or the homobifunctional crosslinking reagent, BMH, as indicated and the products analysed by immunoblotting. Full length Sec61βOPG (>), a truncated form (■) and cross-linked dimers (●) are indicated, as are the monomer and dimer of Cytb5OPG (1xb5 and 2xb5, respectively). PEG-5000 and PEG-20000 modified Sec61βOPG (▲ and ♦ respectively), and PEGylated Cytb5OPG monomer (◊) and dimer (□) are shown. Other products

assumed to represent abberant cross-linked species (? and ○) were not competent for membrane integration and their precise identity was not pursued (see panels B and D). N-glycosylated species are indicated with an asterisk (*) except the N-glycosylated, PEG-modified Cytb5OPG dimer (Δ) (see Panel D, lane 7). A product corresponding to the PEGylated Cytb5OPG dimer, and an N-glycosylated, non-PEGylated dimer that comigrate is also indicated (∞).

Figure 6. PEGylation of Sec61βOPG transmembrane segment at different sites blocks membrane integration at distinct stages.

Double cysteine variants of Sec61βOPG were generated as indicated (see also Table S1) and the purified proteins modified with mPEG-5000. A schematic representation of such doubly labelled polypeptides is presented assuming an alpha helix-like conformation of the transmembrane region (A). Covalent attachment of PEG-5000 was confirmed by immunoblotting (B and F) and membrane integration by EndoH sensitivity (C and G). Small amounts of Sec61βOPG species most likely corresponding to a dimer formed during protein purification were observed (B, D and F, (●)). Binding of PEG-modified and control-treated Sec61βOPG variants to TRC40 was addressed by pre-incubating the proteins (1 - 1.9 M) with rabbit reticulocyte lysate followed by their co-immunoprecipitation with anti-TRC40 or control anti-PDI antibodies. Bound Sec61βOPG was eluted and detected by immunoblotting (D and H). Quantitative blotting was carried out to estimate the association of the unmodified and PEG-modified forms of Sec61βOPG to TRC40 (E and I). Non-specific binding to Protein A Sepharose coated with anti-PDI antibody was subtracted from the binding to anti-TRC40 antibody-coated Protein A Sepharose, and the resulting values were normalised to the amount of each Sec61βOPG species. The values shown are the average from two independent experiments.

Figure 7. Membrane delivery and integration of PEG-modified Sec61β.

A) A comparative structure of human TRC40 was modelled using the *S. cerevisiae* Get3 dimer structure as a template (PDB identifier 2woj) (left panel). A 23 amino acid alpha-helical transmembrane segment of Sec61β (green) is shown in the proposed binding

groove and the surface of the TRC40 dimer (viewed approximately along the dimer axis) is colour-coded according to amino acid polarity: grey/non-polar, red/negatively-charged, blue/positively-charged, yellow/polar-uncharged. Groove hydrophobicity, reported in the Get3 crystal structures, is maintained. A schematic representation for the association of PEGylated Sec61β to TRC40 (right panel) showing binding of polypeptides modified with a single PEG molecule at residue 77 or 84, but not of a doubly labelled Sec61β^{S77C,L79C} variant. B) Estimated energy changes (see Supplementary Data) for the incorporation of different singly PEG-modified transmembrane regions of Sec61β into a lipid bilayer (left panel). The relative ΔG values for PEGylation at residues 77 and 84 are indicated. Representation of PEGylated Sec61β TMSs within a model lipid bilayer using membrane coordinates taken from Heller et al. (1993) (right panel). Experiments confirm membrane integration of a Sec61β TMS PEGylated on Cys77 but not on Cys84. C) Working model for the delivery of PEGylated Sec61β to the ER membrane. A variety of upstream components including Bat3, SGTA and the mammalian equivalents of Get4 and Get5 (Chartron et al., 2010; Leznicki et al., 2010; Sowa et al., 2009) facilitate TRC40-mediated delivery to the mammalian ER membrane via a putative receptor protein (Favaloro et al., 2008; Favaloro et al., 2010; Schuldiner et al., 2008; Stefanovic and Hegde, 2007). Any role for a membrane integrase remains hypothetical (cf. (Rabu et al., 2009)). Covalent modification of the TMS of Sec61β in principle could perturb any one of the steps illustrated.

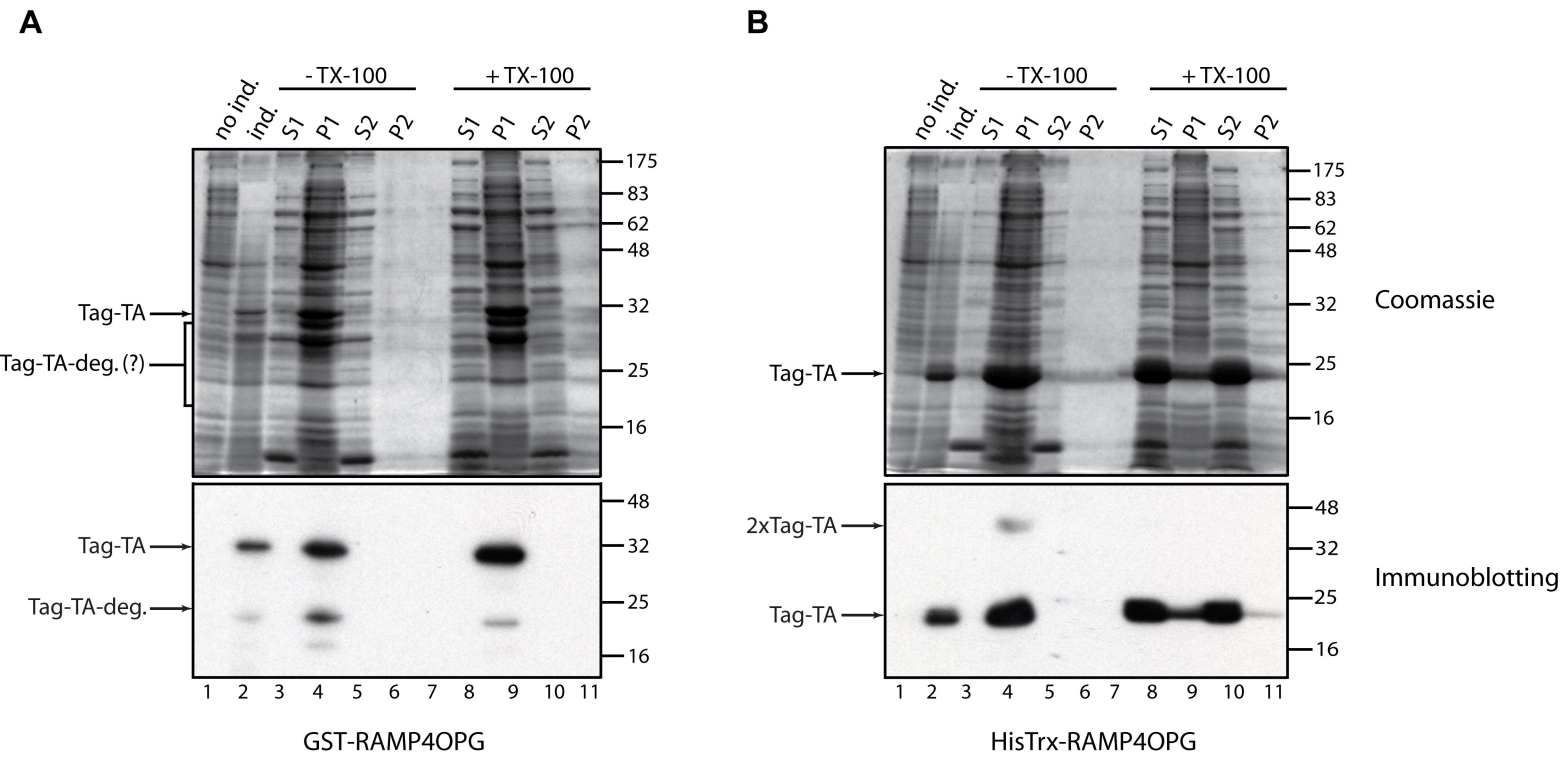
A
no ind.
ind.
-TX-100
+TX-100
S1
P1
S2
P2
175
83
62
48
32
25
16
Tag-TA
Tag-TA-deg. (?)
Tag-TA
Tag-TA-deg.
1 2 3 4 5 6 7 8 9 10 11
GST-RAMP4OPG
B
Coomassie
Immunoblotting
2xTag-TA
HisTrx-RAMP4OPG

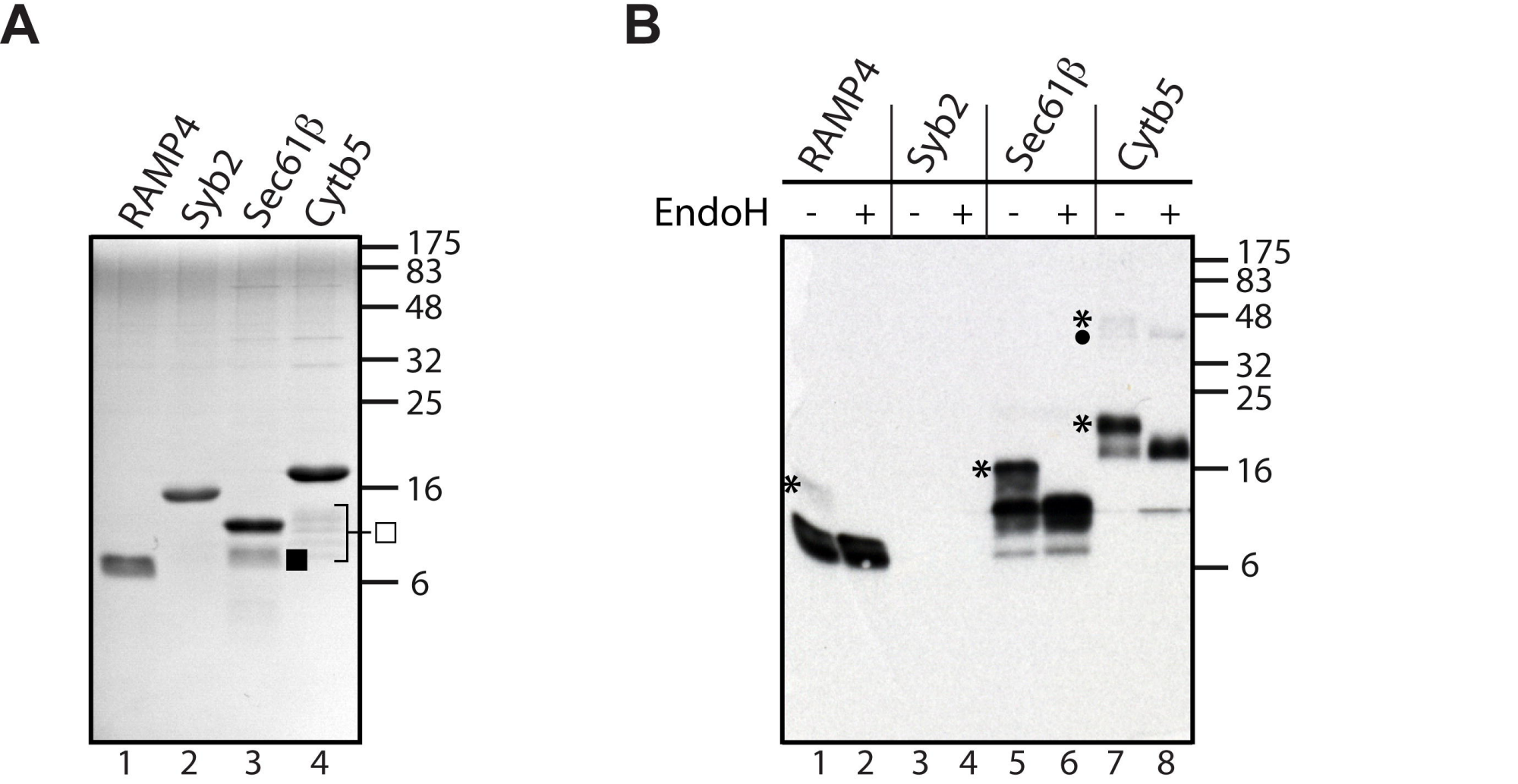
A
RAMP4
Syb2
Sec61β
Cytb5
175
83
48
32
25
16
6
1
2
3
4
B
RAMP4
Syb2
Sec61β
Cytb5
EndoH
- + - + - + - +
175
83
48
32
25
16
6
1 2 3 4 5 6 7 8

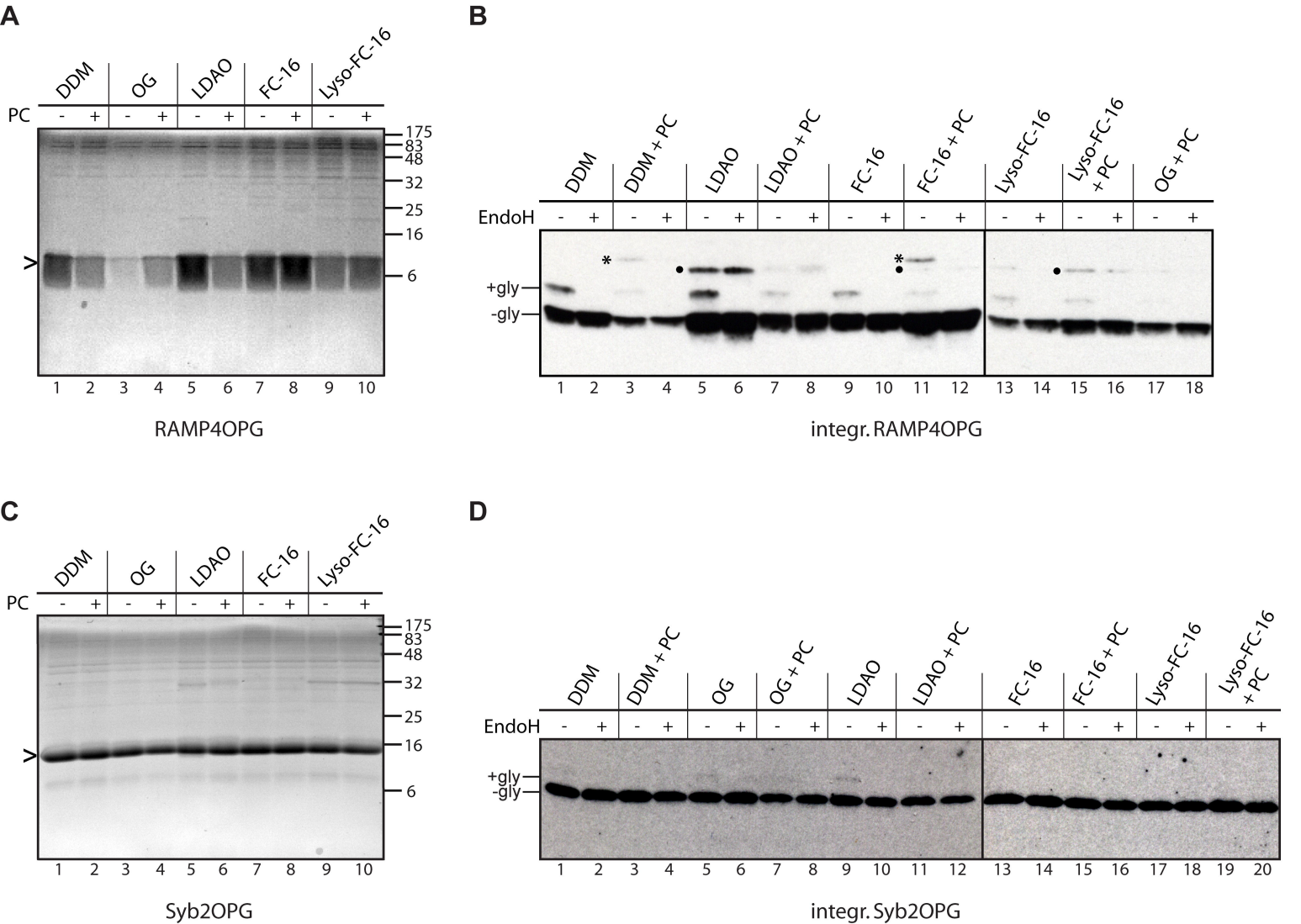
A
DDM
OG
LDAO
FC-16
Lyso-FC-16
PC
- + - + - + - + - +
175
83
48
32
25
16
6
1 2 3 4 5 6 7 8 9 10
RAMP4OPG
B
DDM
DDM + PC
LDAO
LDAO + PC
FC-16
FC-16 + PC
Lyso-FC-16
Lyso-FC-16 + PC
OG + PC
EndoH
+gly
-gly
1 2 3 4 5 6 7 8 9 10 11 12 13 14 15 16 17 18
integr. RAMP4OPG
C
DDM
OG
LDAO
FC-16
Lyso-FC-16
PC
175
83
48
32
25
16
6
1 2 3 4 5 6 7 8 9 10
Syb2OPG
D
DDM
DDM + PC
OG
OG + PC
LDAO
LDAO + PC
FC-16
FC-16 + PC
Lyso-FC-16
Lyso-FC-16 + PC
EndoH
+gly
-gly
1 2 3 4 5 6 7 8 9 10 11 12 13 14 15 16 17 18 19 20
integr. Syb2OPG

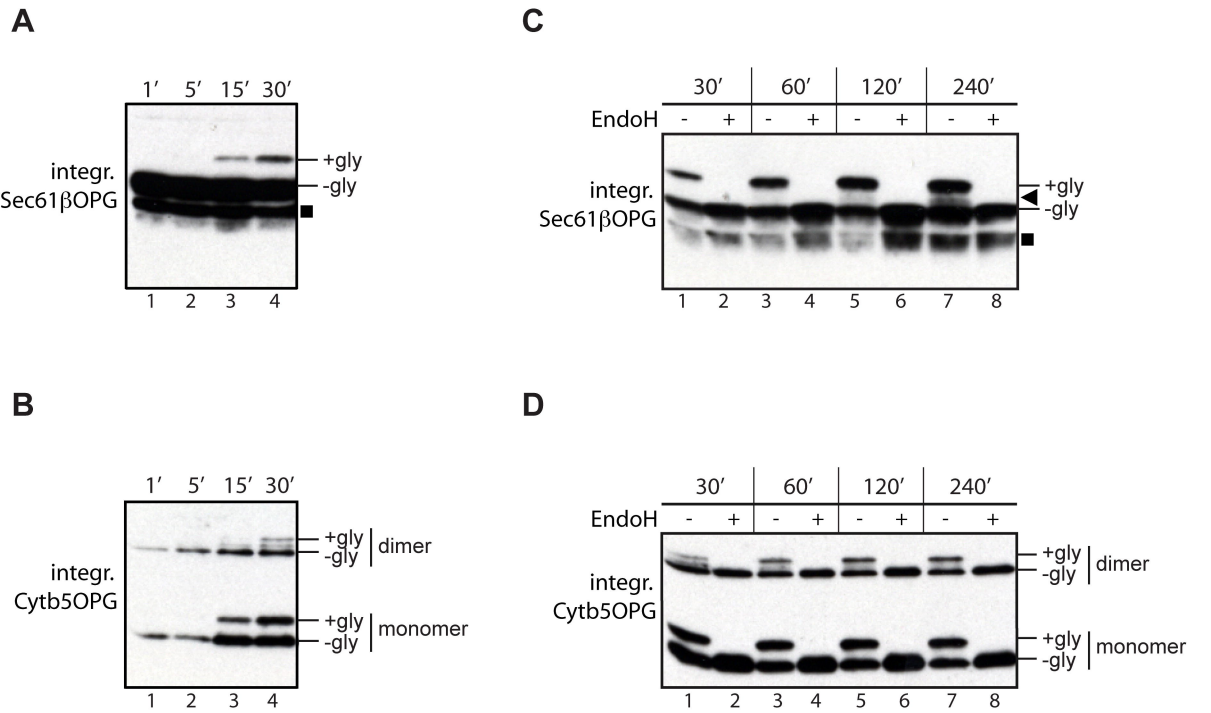
A
1′ 5′ 15′ 30′
integr.
Sec61βOPG
+gly
-gly
1 2 3 4
B
1′ 5′ 15′ 30′
integr.
Cytb5OPG
+gly
-gly
dimer
+gly
-gly
monomer
1 2 3 4
C
30′ 60′ 120′ 240′
EndoH - + - + - + - +
integr.
Sec61βOPG
+gly
-gly
1 2 3 4 5 6 7 8
D
30′ 60′ 120′ 240′
EndoH - + - + - + - +
integr.
Cytb5OPG
+gly
-gly
dimer
+gly
-gly
monomer
1 2 3 4 5 6 7 8

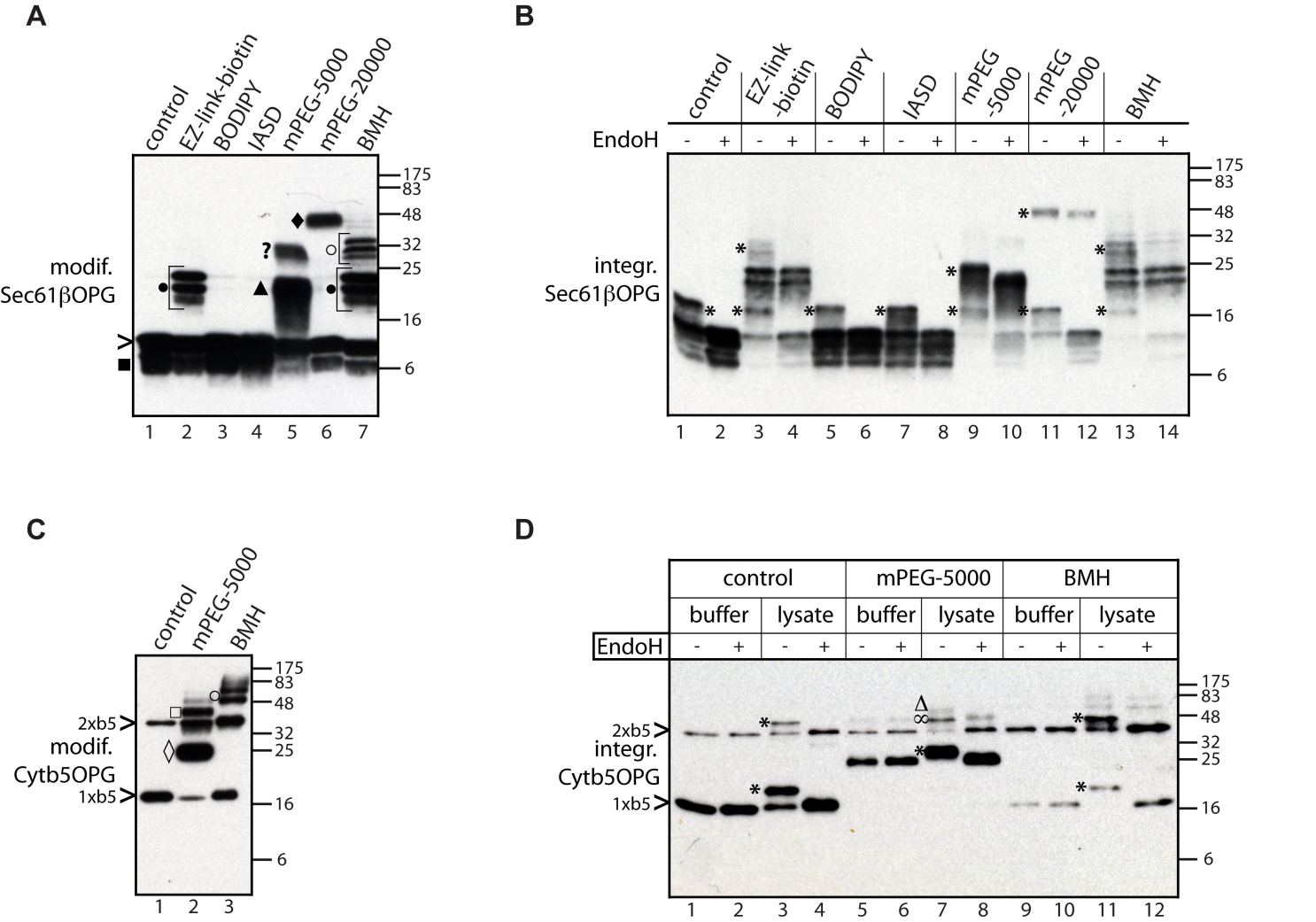
A
control
EZ-link-biotin
BODIPY
IASD
mPEG-5000
mPEG-20000
BMH
modif.
Sec61βOPG
175
83
48
32
25
16
6
1 2 3 4 5 6 7
B
control
EZ-link
-biotin
BODIPY
IASD
mPEG
-5000
mPEG
-20000
BMH
EndoH
- + - + - + - + - + - + - +
integr.
Sec61βOPG
175
83
48
32
25
16
6
1 2 3 4 5 6 7 8 9 10 11 12 13 14
C
control
mPEG-5000
BMH
2xb5
modif.
Cytb5OPG
1xb5
175
83
48
32
25
16
6
1 2 3
D
control
mPEG-5000
BMH
buffer
lysate
buffer
lysate
buffer
lysate
EndoH
- + - + - + - + - + - +
2xb5
integr.
Cytb5OPG
1xb5
175
83
48
32
25
16
6
1 2 3 4 5 6 7 8 9 10 11 12

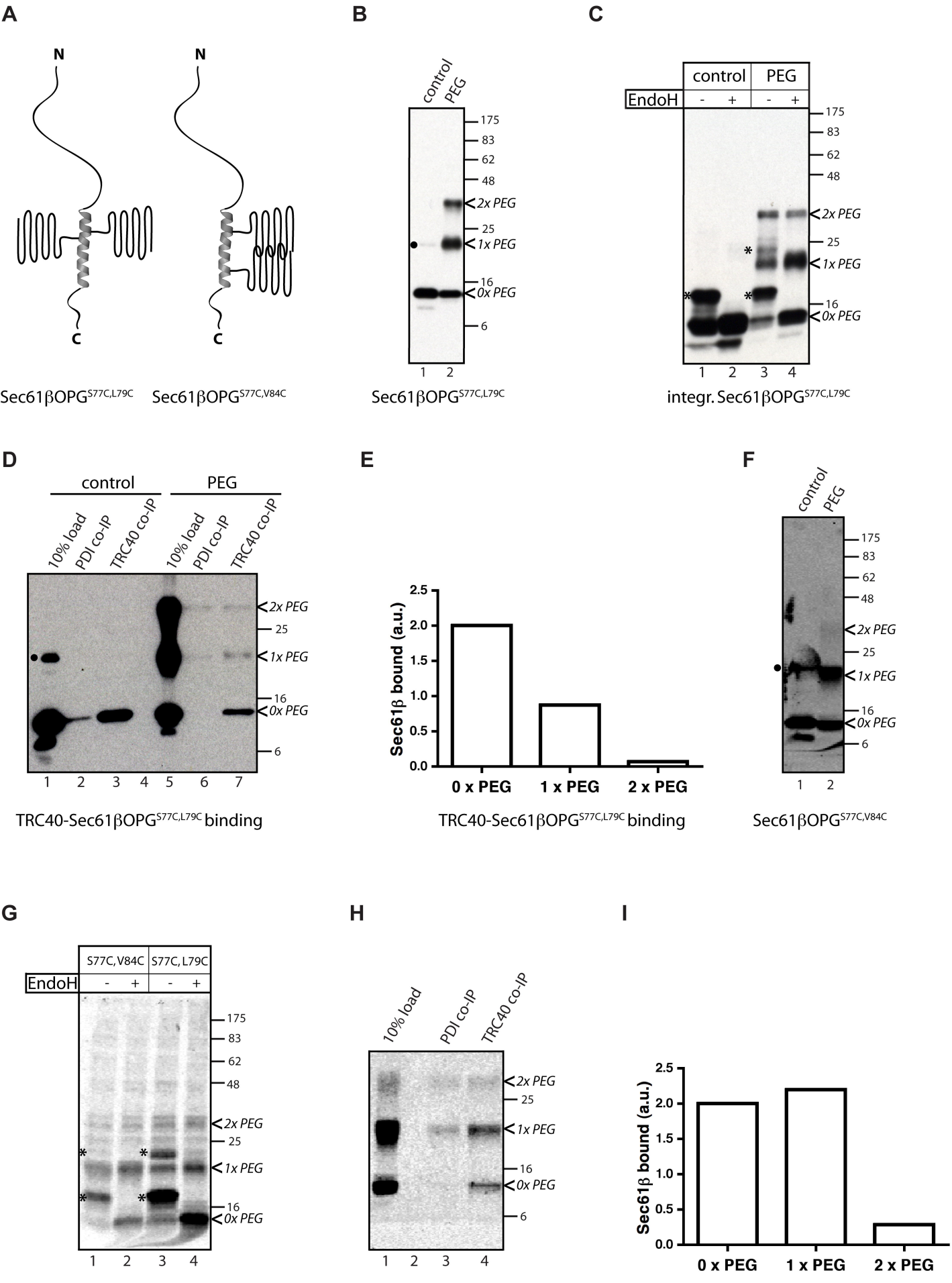
A
N
C
N
C
Sec61βOPG^S77C,L79C
Sec61βOPG^S77C,V84C
B
control
PEG
175
83
62
48
2x PEG
25
1x PEG
16
0x PEG
6
1 2
Sec61βOPG^S77C,L79C
C
control
PEG
EndoH
- + - +
175
83
62
48
2x PEG
25
1x PEG
16
0x PEG
1 2 3 4
integr. Sec61βOPG^S77C,L79C
D
control
PEG
10% load
PDI co-IP
TRC40 co-IP
10% load
PDI co-IP
TRC40 co-IP
2x PEG
25
1x PEG
16
0x PEG
6
1 2 3 4 5 6 7
TRC40-Sec61βOPG^S77C,L79C binding
E
Sec61β bound (a.u.)
2.5
2.0
1.5
1.0
0.5
0.0
0 x PEG
1 x PEG
2 x PEG
TRC40-Sec61βOPG^S77C,L79C binding
F
control
PEG
175
83
62
48
2x PEG
25
1x PEG
16
0x PEG
6
1 2
Sec61βOPG^S77C,V84C
G
S77C, V84C
S77C, L79C
EndoH
- + - +
175
83
62
48
2x PEG
25
1x PEG
16
0x PEG
1 2 3 4
integr. Sec61βOPG
H
10% load
PDI co-IP
TRC40 co-IP
2x PEG
25
1x PEG
16
0x PEG
6
1 2 3 4
TRC40-Sec61βOPG^S77C,V84C binding
I
Sec61β bound (a.u.)
2.5
2.0
1.5
1.0
0.5
0.0
0 x PEG
1 x PEG
2 x PEG
TRC40-Sec61βOPG^S77C,V84C binding

A

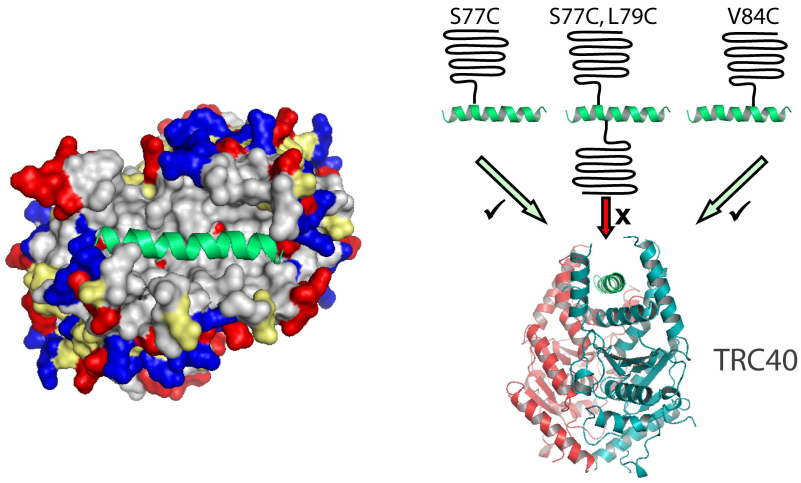
S77C
S77C, L79C
V84C
TRC40

B

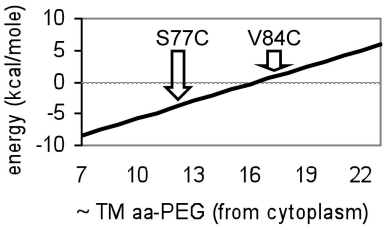
energy (kcal/mole)
10
5
0
-5
-10
S77C
V84C
7
10
13
16
19
22
~ TM aa-PEG (from cytoplasm)

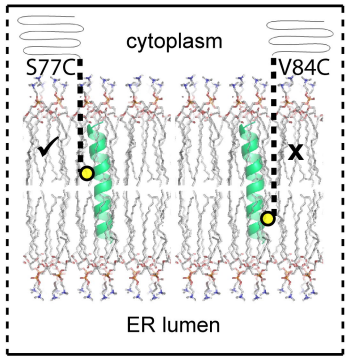
cytoplasm
S77C
V84C
ER lumen

C

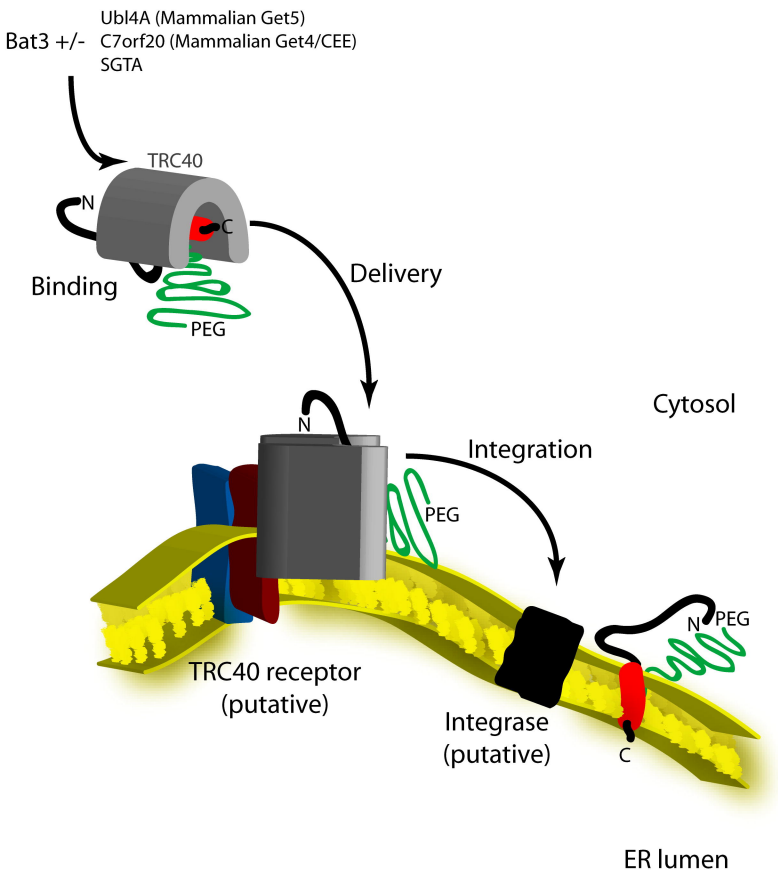
Bat3 +/-
Ubl4A (Mammalian Get5)
C7orf20 (Mammalian Get4/CEE)
SGTA
TRC40
N
C
Binding
PEG
Delivery
Cytosol
N
Integration
PEG
TRC40 receptor
(putative)
Integrase
(putative)
C
N
PEG
ER lumen

SUPPLEMENTARY DATA

Calculations of the energetic cost for membrane integration of PEGylated Sec61βOPG.

Boundaries of the TMS of Sec61βOPG were determined using a prediction algorithm for changes in free energy, ΔG, upon Sec61 translocon mediated protein integration into a lipid bilayer (Hessa et al., 2007). The transfer energy for the predicted 23 amino acid segment (see Table S1) was calculated based on the water-octanol partition scale (Wimley et al., 1996) and a value of -11.5 kcal/mol was obtained.

LogP values of atom fragments of the maleimide-PEG moiety were computed by best fit to a training set of 2473 compounds (Meylan and Howard, 2000), and the sum obtained (-5.0 to -5.3) was in good agreement with the data available for the logP of PEG-400 derived from water-hexane partitioning (-4.824), assuming that PEG-400 is composed of on average 8 to 9 x CH_2CH_2O repeats, and taking into account any potential discrepancy between water-hexane and water-octanol systems. Making equivalent calculations for a 35 Å stretch of PEG, corresponding to the length of the predicted transmembrane region, and converting the results to ΔG, the cost of transferring the PEG polymer into a lipid bilayer in a conformation that spans both leaflets was estimated as approximately +3.6 kcal/mol.

A rotameric entropy loss for an extended PEG chain was estimated based on a comparison with studies of aliphatic side chain conformers in proteins (Bougouffa and Warwicker, 2008) and the role of ligand rigidification in modulating binding affinities (Hanson et al., 2007). Hence, the entropy was calculated from the equation $S = -R\sum(plnp)$, where R is the universal gas constant, p the probability for each rotamer, and the sum is taken over all rotamers. For a torsional system with 3 stable rotamers, assuming a transition between equal probabilities for each, and just one (extended chain) rotamer, a free energy contribution of +0.6 kcal/mol at T = 300 K for each torsion was

obtained. Over the 35 Å TMS length, this amounts to +17.0 kcal/mol for a fully extended chain.

A contribution of the maleimide-PEG linker region to the energetic cost of inserting PEGylated Sec61βOPG into a lipid bilayer was estimated making an assumption, based on the manufacturer's data, that in the experimental conditions used the maleimide-linker ring remains intact. Taking into account the nature of the maleimide-linker components and their bond rotamer status, the following parameters were calculated: length in the extended conformation, 10 Å; ΔG for octanol partitioning of -0.5 kcal/mol (calculated from logP); rotamer entropy loss in extended conformation contributing +3.6 kcal/mol, i.e. a net value of +3.1 kcal/mol.

The estimated contribution of each component to the overall energetic cost for the membrane integration of the PEGylated forms of Sec61β^{S77C} and Sec61β^{V84C} is presented in Table S2. Whilst the ΔG values shown for the lipid partitioning of PEG attached to these two distinct sites are estimates and absolute values may differ, our calculations clearly indicate that the integration of PEGylated Sec61β^{S77C} is energetically more favourable than that of Sec61β^{V84C}. It should be noted that in all calculations presented above an extended conformation of the maleimide-PEG moiety, parallel to the TMS of Sec61β, was assumed. This conformation minimises occlusion of the PEG chain from solvent and provides a defined conformer for calculations. Whilst other conformations are theoretically possible, these would most likely require higher energy for their membrane integration, due to increased number of the PEG repeats that would have to be accommodated by the lipid bilayer.

Protein (species)	Sequence
Sec61βOPG^{S77C} *(human)*	GSPGPTPSGTNVGSSGRSPSKAVAARAAGSTVRQRKNASSGTRS AGRTTSAGTGGMWRFYTEDSPGLKVGPVPVLVMCLLFIASVFM LHIWGKYTRSGPNFYVPFSNKTG
Sec61βOPG^{S77C,L79C} *(human)*	GSPGPTPSGTNVGSSGRSPSKAVAARAAGSTVRQRKNASSGTRS AGRTTSAGTGGMWRFYTEDSPGLKVGPVPVLVMCLCFIASVFM LHIWGKYTRSGPNFYVPFSNKTG
Sec61βOPG^{S77C,V84C} *(human)*	GSPGPTPSGTNVGSSGRSPSKAVAARAAGSTVRQRKNASSGTRS AGRTTSAGTGGMWRFYTEDSPGLKVGPVPVLVMCLLFIASCFM LHIWGKYTRSGPNFYVPFSNKTG
Cytb5OPG^{S119C} *(human)*	GSAEQSDEAVKYYTLEEIQKHNHSKSTWLILHHKVYDLTKFLE EHPGGEEVLREQAGGDATENFEDVGHSTDAREMSKTFIIGELHP DDRPKLNKPPETLITTIDSSSSWWTNWVIPAICAVAVALMYRLY MAEDGPNFYVPFSNKTG
RAMP4OPG (mouse)	GSVAKQRIRMANEKHSKNITQRGNVAKTSRNAPEEKASVGPWL LALFIFVVCGSAIFQIIQSIRMGMGPNFYVPFSNKTG
Syb2OPG (rat)	GSSATAATVPPAAPAGEGGPPAPPPNLTSNRRLQQTQAQVDEV VDIMRVNVDKVLERDQKLSELDDRADALQAGASQFETSAAKL KRKYWWKNLKMMIILGVICAIILIIIIVYFSTGPNFYVPFSNKTG

Table S1. Sequence of TA-proteins used in the study.

Sequences of TA-proteins used in the current study are presented with the predicted transmembrane segments being highlighted in yellow and the opsin-derived, C-terminal tag underlined. Mutations introduced into the amino acid sequences are indicated in red font. Amino acid numbering reflects that of the wild-type proteins, however the recombinant versions lack an initiator methonine and have instead a GlySer dipeptide (highlighted in green) resulting from the thrombin-mediated cleavage of the N-terminal HisTrx tag.

PEG link	TM contribution	maleimide-linker	PEG distance (Å)	PEG contribution	Sum
S77C	-11.5	3.1	7.5	4.4	-4.0
V84C	-11.5	3.1	16	9.4	1.0

Table S2. Contribution of different factors to the energetic cost of membrane integration of the PEGylated variants of Sec61β (see also Supplementary Data). All values are in kcal/mol unless stated otherwise.

SUPPLEMENTARY FIGURE LEGENDS

Figure S1. Both monomers of TA-protein dimers are authentically integrated into the ER membrane.

Dimers of Sec61βOPG were generated by cross-linking the single cysteine mutant S77C (see Table S1) with 1 mM of the indicated thiol-reactive reagents having a spacer length of 8-13Å. The reactions were incubated for 10 min at 25°C, quenched with 15 mM 2-ME and the modified proteins were used in a membrane integration assay (see Materials and Methods). The membrane-associated fraction was isolated by centrifugation, treated with Endoglycosidase H where indicated and products analysed by immunoblotting (A). Glycosylated monomers and dimers are indicated (1x glyc. and 2x glyc., respectively). BMH cross-linked single cysteine mutants of Sec61βOPG (B) and Cytb5OPG (C) were used in a membrane integration reaction (see Materials and Methods) and the isolated membrane fraction subjected to partial digestion with Endoglycosidase H (0.21 U/µl). At the indicated times, aliquots were mixed directly with Laemmli sample buffer, and products subsequently analysed by immunoblotting (B and C). Migration of Sec61βOPG and Cytb5OPG dimers is indicated, and various N-glycosylated species of both proteins are shown (*). The doublet corresponding to the Sec61βOPG dimer results from a truncated form of the recombinant protein (see main text, Figures 2 and 5), leading to a population of mixed dimers. These species are also responsible for the additional N-glycosylated protein species identified by EndoH treatment (B).

SUPPLEMENTARY REFERENCES

Bougouffa, S. and Warwicker, J. (2008). Volume-based solvation models out-perform area-based models in combined studies of wild-type and mutated protein-protein interfaces. *BMC Bioinformatics* **9**, 448.

Hanson, W. M., Domek, G. J., Horvath, M. P. and Goldenberg, D. P. (2007). Rigidification of a flexible protease inhibitor variant upon binding to trypsin. *J Mol Biol* **366**, 230-43.

Hessa, T., Meindl-Beinker, N. M., Bernsel, A., Kim, H., Sato, Y., Lerch-Bader, M., Nilsson, I., White, S. H. and von Heijne, G. (2007). Molecular code for transmembrane-helix recognition by the Sec61 translocon. *Nature* **450**, 1026-30.

Meylan, W. M. and Howard, P. H. (2000). Estimating log P with atom/fragments and water solubility with log P. *Perspect Drug Discov* **19**, 67-84.

Wimley, W. C., Creamer, T. P. and White, S. H. (1996). Solvation energies of amino acid side chains and backbone in a family of host-guest pentapeptides. *Biochemistry* **35**, 5109-24.

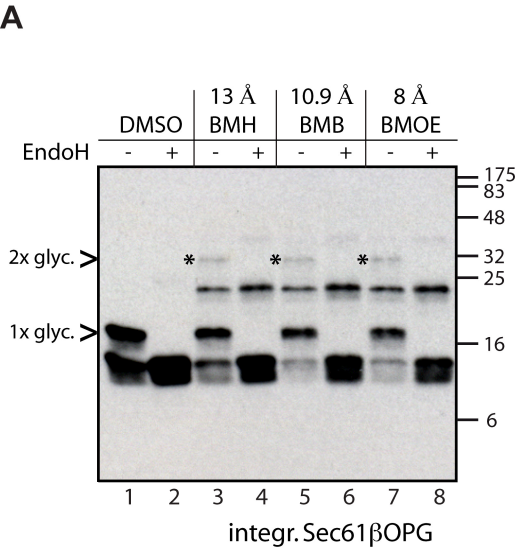
A
DMSO
13 Å BMH
10.9 Å BMB
8 Å BMOE
EndoH
- + - + - + - +
2x glyc.
1x glyc.
175
83
48
32
25
16
6
1 2 3 4 5 6 7 8
integr. Sec61βOPG

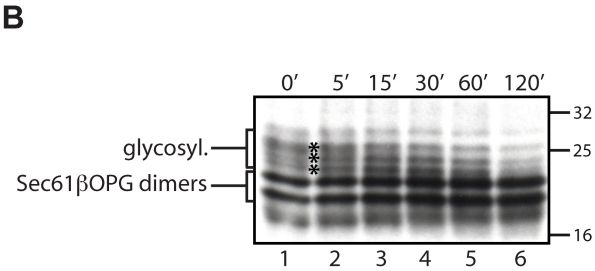
B
0′ 5′ 15′ 30′ 60′ 120′
glycosyl.
Sec61βOPG dimers
32
25
16
1 2 3 4 5 6

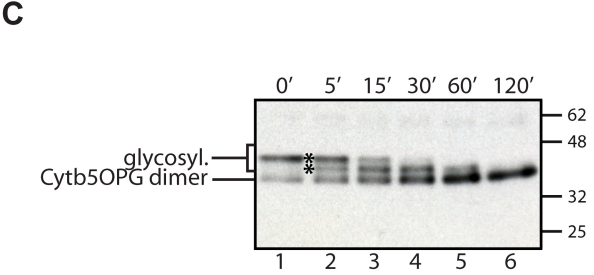
C
0′ 5′ 15′ 30′ 60′ 120′
glycosyl.
Cytb5OPG dimer
62
48
32
25
1 2 3 4 5 6

CHAPTER 2.2

A role for cytosolic and membrane-bound factors during cytochrome b5 biogenesis

(preliminary data in the form of a manuscript intended for submission to the Journal of Cell Science)

A role for cytosolic and membrane-bound factors during cytochrome b5 biogenesis

Pawel Leznicki[1], Peter U. Mayerhofer[2], Stephen Rigby[1], Arthur E. Johnson[2] and Stephen High[1]*

[1]Faculty of Life Sciences, University of Manchester, Oxford Road, Manchester, M13 9PT, UK.
[2]Department of Molecular and Cellular Medicine, Texas A&M Health Science Center, College Station, Texas 77843-1114, USA.

*To whom correspondence should be addressed: stephen.high@manchester.ac.uk

Page heading title: *Cytochrome b5 biogenesis*

Key words: Cytochrome b5, endoplasmic reticulum, fluorescence, PEGylation, Sec61β

SUMMARY

The physicochemical properties of the transmembrane segment (TMS) of a tail-anchored protein define its preferred pathway for post-translational integration at the endoplasmic reticulum (ER). Low TMS hydrophobicity, exemplified by cytochrome b5 (Cytb5), dictates that the protein is delivered to the ER via a pathway that is either "unassisted" and/or facilitated by Hsp70/Hsp40 chaperones. To further characterise its biogenesis, we investigated the requirements for the membrane integration of purified, recombinant, Cytb5. In the absence of cytosolic components, Cytb5 associated with ER-derived membranes and its C-terminus was protected from protease digestion. However, an N-glycosylation assay suggested that fully authentic membrane integration occurred only in the presence of cytosol. Complimentary biophysical studies suggested that the binding of cytosolic factors to the Cytb5 TMS prevents the protein from aggregating and maintains it in an integration-competent state compatible with accurate membrane integration. Preliminary studies of the accessibility of cysteine residues present in membrane-integrated recombinant polypeptides suggest that both soluble and membrane-bound components influence the conformation or environment of Cytb5 within the lipid bilayer. Based on our results, we speculate that the authentic membrane integration of Cytb5 results from the cooperative action of cytosolic and membrane-associated proteins.

INTRODUCTION

Tail anchored (TA) proteins constitute a group of integral membrane polypeptides characterised by a C-terminal stretch of hydrophobic amino acids that acts as both a targeting signal and a membrane anchor (Borgese et al., 2003; Kutay et al., 1993; Rabu et al., 2009). This localisation of the single transmembrane segment (TMS) of a TA-protein prevents its co-translational recognition by the signal recognition particle (SRP) and ensures that TA-proteins are delivered to target membranes after their synthesis at the ribosome has been terminated (Borgese et al., 2003; Kutay et al., 1995; Rabu et al., 2009).

Following release from the ribosome, TA-proteins can directly insert into the endoplasmic reticulum (ER), the mitochondrial outer membrane and, in plants, the chloroplast outer envelope (Borgese et al., 2003; Rabu et al., 2009). As for the bulk of secretory and membrane proteins that rely on the canonical, co-translation, route for translocation across and integration into the ER membrane; TA-proteins destined for compartments of the secretory pathway or the plasma membrane must pass through the ER before they are transported to their target membrane by vesicular trafficking (Kutay et al., 1995; Linstedt et al., 1995). To date, distinct routes for TA-protein delivery to the ER membrane have been reported and pathway choice seems to be determined primarily by the relative hydrophobicity of a TA-protein TMS (Brambillasca et al., 2006; Rabu et al., 2009; Rabu et al., 2008). Hence, most TA-proteins have a moderately hydrophobic membrane-spanning region (Kalbfleisch et al., 2007), and their biogenesis relies on a specialised targeting factor, known as TRC40 in mammalian cells and Get3 in yeast (Favaloro et al., 2008; Favaloro et al., 2010; Schuldiner et al., 2005; Schuldiner et al., 2008; Stefanovic and Hegde, 2007), together with additional upstream components (Jonikas et al., 2009; Leznicki et al., 2010; Mariappan et al., 2010). TA-proteins with a more hydrophobic TMS can be cross-linked to the SRP54 subunit, indicative of a novel, post-translational function for SRP in TA-protein biogenesis (Abell et al., 2004). Importantly, TA-proteins utilising either TRC40/Get3- or SRP-dependent routes rely on a proteinaceous component(s) at the ER membrane (Abell et al., 2004; Kim et al., 1997; Kutay et al., 1995; Schuldiner et al., 2008; Stefanovic and Hegde, 2007), which for the yeast GET pathway has been identified as the Get1/Get2 complex (Schuldiner et al., 2008). The

identity of the putative receptors for the mammalian TRC40-mediated route and the SRP-dependent pathway is, however, either unknown or controversial (Abell et al., 2004; Rabu et al., 2009).

Another distinct route for delivery to the ER membrane is exploited by a subset of TA-proteins that are characterised by a TMS of comparatively low hydrophobicity, with cytochrome b5 (Cytb5) being by far the most extensively studied example (Brambillasca et al., 2006; Brambillasca et al., 2005; Colombo et al., 2009; Rabu et al., 2009; Rabu et al., 2008). This pathway is often referred to as the "unassisted" or spontaneous route for TA-protein integration, owing to the apparent lack of any membrane-bound component that is required for insertion into the lipid bilayer. Hence, protease-protection experiments suggested that C-terminally tagged variants of Cytb5 and protein tyrosine phosphatase 1B (PTP1B) are capable of inserting into both protease-treated microsomes and protein-free liposomes (Brambillasca et al., 2005; Colombo et al., 2009; Stefanovic and Hegde, 2007). Whilst it is widely accepted that membrane proteins seem dispensable for the membrane insertion of Cytb5 *in vitro*, the cytosolic requirements for its targeting to the ER are less clear. For example, inhibition of Hsp/Hsc70 chaperones with selective small molecules resulted in a decrease in the membrane integration of TA-proteins exploiting the "unassisted" pathway, but not of the clients of the TRC40- or SRP-mediated routes (Rabu et al., 2008). This observation is consistent with Cytb5 integration being ATP-dependent, although surprisingly only nanomolar concentrations of the nucleotide are required (Brambillasca et al., 2006; Favaloro et al., 2008; Yabal et al., 2003). On the other hand, recent studies using recombinant Cytb5 indicated that neither cytosolic proteins nor nucleotides are required for the membrane integration of this TA-protein (Colombo et al., 2009; Favaloro et al., 2010). Furthermore, although the binding of Cytb5 to soluble factors was observed (Colombo et al., 2009), it was speculated that these components do not play any role in the delivery and membrane integration steps. Rather, it was postulated that Cytb5 self-associates into oligomers that remain in dynamic equilibrium with a monomer that is capable of spontaneous insertion into the ER membrane (Colombo et al., 2009). Whether such oligomers exist *in vivo* is currently unknown.

In order to better understand the role for cytosolic and membrane-associated components during Cytb5 membrane integration, we tested the requirements of the purified recombinant protein for its insertion into the ER membrane. We found that cytosolic factors maintain Cytb5 in what can be described as an integration-competent state, and also appear to stimulate its integration into biological membranes. By analysing the availability of novel cysteine residues to a thiol-reactive probe, we showed that both soluble and membrane-bound proteins affect the conformation or environment of Cytb5 within the lipid bilayer. Our results indicate that the membrane integration of Cytb5 is a complex process relying on cooperation between cytosolic and membrane-associated factors, and indicate that current views of this process (Colombo et al., 2009) may be over-simplistic.

RESULTS

Cytochrome b5 associates with a lipid bilayer in the absence of cytosolic factors.

In order to establish a role for cytosolic proteins during the membrane integration of cytochrome b5 (Cytb5), we expressed a variant of this protein bearing a single cysteine residue near the middle of the predicted transmembrane segment (TMS) (cf. Figure 1A) in *E. coli*, and purified this recombinant polypeptide by chromatographic means. Cytb5 was tagged at the C-terminus with a short extension, derived from bovine opsin (OPG) and containing an N-glycosylation site, and modification of this tag by the ER lumen-oriented oligosaccharyltransferase complex was used to identify "authentic" membrane-integrated material – with its C-terminus fully translocated into the ER lumen (Abell et al., 2007; Brambillasca et al., 2005; Favaloro et al., 2008; Favaloro et al., 2010; Leznicki et al., 2010; Rabu et al., 2008).

Recombinant Cytb5OPG was mixed with ER-derived microsomes in the presence of cytosol or buffer, and the glycosylation status of the protein and its protease sensitivity were then tested (Figure 1B). In agreement with a previous study (Colombo et al., 2009), protease-resistant fragments of Cytb5OPG were observed when either buffer or cell lysate were present during the membrane integration reaction (Figure 1B, lanes 2 and 5). Since these protein species were recognised by an antibody recognising the opsin epitope tag, it could be concluded that in both cases the C-terminal part of the polypeptide was most likely translocated across the ER membrane. Interestingly, the protease-protected fragment generated after proteinase K treatment of the Cytb5OPG integrated in the presence of cytosol appeared to migrate more slowly upon SDS-PAGE than the fragment obtained after digestion of the material integrated in the presence of buffer alone (Figure 1B, cf. lanes 2 and 5). This apparent difference in the electrophoretic mobility of the protease-inaccessible fragments obtained under these two experimental conditions may reflect a cytosol-dependent post-translational modification of the protected fragment or a subtle difference in the molecular mass of these two Cytb5OPG-derived species (see below).

Strikingly, N-glycosylated Cytb5OPG could only be detected when the membrane integration reaction was carried out in the presence of cell lysate (Figure 1B, cf. lanes 1, 2, 4 and 5), even though experimental evidence strongly suggests that cytosolic

proteins are not required for the N-glycosylation reaction (Bozkurt et al., 2009; Favaloro et al., 2010; Leznicki et al., 2010). Whilst a Cytb5OPG fragment representing an N-glycosylated, protease-protected peptide derived from the protein monomer was detected (Figure 1B, lane 5, marked by an asterisk), no species corresponding to a protease-resistant dimer-derived fragment was identified. This suggests that Cytb5OPG dimerises via its proteinase K-accessible cytosolic domain (Figure 1B, lanes 2 and 5).

Cytosolic factors stimulate Cytb5 membrane integration and keep the recombinant polypeptide in an integration-competent state.

Previous analysis of Cytb5 insertion into protein-free liposomes (Colombo et al., 2009) suggested that the formation of a protease-resistant, and hence presumably membrane-integrated, protein species proceeds with equivalent kinetics in the presence or absence of cell lysate, suggesting that cytosolic proteins do not participate in the membrane integration of Cytb5. In order to address the role of cytosolic components during the membrane integration of Cytb5 by a different assay, we labelled a single cysteine residue located near the middle of the TMS using an environmentally-sensitive fluorescent probe, 7-nitrobenz-2-oxa-1,3-diazole-4-yl (NBD), and monitored changes in its fluorescence during membrane integration. Typically, an increase in the hydrophobicity of the local environment, such as that occurring upon integration into a lipid bilayer, results in an increase in NBD emission and a "blue" shift of the fluorescence maximum towards shorter wavelengths (Jittikoon et al., 2007; Mayerhofer et al., 2009).

NBD-labelled Cytb5OPG was thus mixed with buffer or cytosol, in the form of heme-free rabbit reticulocyte lysate (see Materials and Methods), ER-derived membranes were added when indicated, and changes in NBD fluorescence were monitored (Figure 2A). In both cases, the addition of microsomes resulted in an increase in NBD fluorescence; however, the increase in fluorescence was more rapid in the presence of cytosol with half maximal fluorescence ($F_{1/2}$) reached in ~ 450 seconds compared with ~ 600 seconds with buffer alone (Figure 2A). The corresponding average rates of increase in fluorescence at $F_{1/2}$ were estimated as ~ 14 au/sec in the presence of cytosol and ~ 6 au/sec with buffer alone. Emission spectra taken after completion of the incubations confirmed the differences in absolute fluorescence emission levels for

the proteins integrated in the presence of buffer or cytosol, and revealed that the fluorescence maximum for Cytb5OPG integrated in the presence of lysate was slightly blue-shifted (525 nm vs 527 nm) (Figure 2B).

NBD-labelled Cytb5OPG in buffer was next mixed with an equal volume of buffer or cytosol and the fluorescence emission was monitored until it reached equilibrium after approximately 30 min (Figure 2C). Cytb5OPG was incubated for additional 60 min in the dark, and after ensuring that NBD fluorescence did not change, ER-derived membranes were added and the fluorescence was further monitored (Figure 2C). Whilst the dilution of NBD-labelled Cytb5OPG with buffer results in a decrease in fluorescence, the addition of cell lysate causes a marked increase in the dye's fluorescence intensity when corrected for the dilution effect (see Figure 2C, cf. respective signals at 5400 seconds, see also Figure 2D, buffer spectrum (dashed red) and cytosol spectrum (solid red)). Furthermore, whilst the addition of ER-derived membranes to Cytb5OPG incubated with cytosol led to a ~ 10500 au increase in NBD fluorescence, for Cytb5OPG incubated in buffer this was only ~ 6000 au (Figure 2D, cf. samples with and without membranes). Assuming that NBD fluorescence provides a direct indication of environment, these data suggest that in the presence of cytosol either more Cytb5OPG becomes membrane associated/integrated or that the probe has access to a different environment than when membranes are added in the presence of buffer alone. The emission spectra recorded after each incubation described also provide support for the view that the TA region, including the NBD probe, may associate with one or more factors in the lysate (see Figure 2D).

Importantly, the attachment of NBD to the TMS of Cytb5OPG did not block the membrane integration step, and the fluorescently-labelled protein was efficiently N-glycosylated when the integration reaction was carried out in the presence of cell lysate (Figure 2E) consistent with the ability of TA-proteins to tolerate a range of modifications to their TMS (Leznicki, Warwicker and High, manuscript submitted). A strong correlation between the amount of NBD-labelled Cytb5OPG undergoing N-glycosylation and the relative volume of cytosol in the reaction was observed (Figure 2E), further supporting the hypothesis that authentic membrane integration depends on the action of cytosolic factors. This is also consistent with the NBD probe attached

to Cytb5OPG inhabiting distinct environments following membrane integration in the presence of cytosol or buffer (cf. Figure 2B).

As an alternative strategy to determine the ability of the TMS of Cytb5 to bind cytosolic components, the recombinant TA-protein was modified with a spin-label, MTSSL, and the status of this probe monitored by electron paramagnetic resonance (EPR) (Figure 3). The significant decrease in the levels of detectable MTSSL signal upon transferring Cytb5OPG from a solution containing 0.1 % (w/v) LDAO detergent to one with only a very modest level of detergent (~ 0.01 % w/v), suggests that whilst soluble in the presence of detergent, labelled Cytb5OPG forms high molecular weight complexes in its absence (Figure 3, cf. traces I and II) consistent with previous reports (Colombo et al., 2009; Leto and Holloway, 1979; Spatz and Strittmatter, 1971). Tellingly, the incubation of Cytb5OPG with either heme-free (hf) or "full" rabbit reticulocyte lysates resulted in almost identical EPR spectra that bore a clear resemblance to that obtained in the presence of detergent (Figure 3, cf. traces I, III and IV). This analysis suggests that cytosolic components can, at least partially, substitute for detergent to keep Cytb5OPG in a largely soluble form (Figure 3). The slight shift to the left for the 3498 Gauss peak seen with detergent (Figure 3, trace I, see *) suggests that in the presence of cytosol the MTSSL probe is located in a less hydrophobic environment (Figure 3).

Cytosolic and membrane-bound proteins affect the apparent conformation of membrane-integrated Cytb5.

Differences in both the electrophoretic mobility of protease protected fragments (Figure 1B, cf. lanes 2 and 5) and NBD probe fluorescence (Figures 2B and 2D) obtained following incubation of recombinant Cytb5OPG with ER-derived membranes in the presence of buffer or cytosol suggest that differences in the specific membrane-associated environment of the TA-protein may occur under different conditions. To address this possibility we engineered additional single cysteine variants of Cytb5OPG where cysteine residues were placed adjacent to the predicted TMS or at the extreme C-terminus of the polypeptide chain (Figure 4A). A membrane integration reaction of each of these Cytb5OPG derivatives, together with the original S119C variant (cf. Figure 4A), was carried out in the presence of buffer or cell lysate. The accessibility of the various cysteine residues to a membrane-impermeable

reagent, mPEG-5000, was then established (Le Gall et al., 2004). A similar strategy has been used to determine the boundaries of several transmembrane regions including the bacterial aerotaxis receptor (Amin et al., 2006) and a yeast vacuolar ATPase subunit (Wang et al., 2008).

Cysteine 107 is located on the cytoplasmic side of the Cytb5OPG predicted TMS and the membrane-associated form could be efficiently modified with PEG-5000 following incubation in the presence of buffer (Figure 4B, cf. lanes 1 and 2, ●) although no N-glycosylation of the lumenal tail was observed. In contrast, when the same analysis was carried out using recombinant Cytb5OPG incubated with membranes in the presence of cytosol, the C-terminus was efficiently N-glycosylated but the protein was no longer efficiently PEGylated (Figure 4B, cf. lanes 3 and 4). Hence, the presence of lysate during membrane integration appears to affect the accessibility of a novel cysteine introduced at residue 107 of the Cytb5 coding region. When the accessibility of cysteines located within the TMS, or to its C-terminus, were investigated (Figure 4A), very inefficient labelling of residues 119 and 147 was observed for the membrane-associated material generated in the presence of buffer (Figure 4B, lane 6, upper panel; Figure 4C, lane 6, ●). No PEGylation of these residues was apparent when the membrane integration reaction was performed in the presence of cytosol, although N-glycosylation was now readily apparent (Figures 4B and 4C). Treatment of the membrane-associated samples with 4 M urea prior to PEG labelling resulted in a modest increase in the modification of S119C (Figure 4B, lane 6, lower panel, ●) but otherwise did not alter the behaviour of the recombinant proteins. Hence, the lack of Cytb5OPG^{S107C} modification with mPEG-5000 after the cytosol-stimulated membrane integration seems unlikely to result from the binding of cytosolic proteins to this region (Figure 4B, see relevant panels). Likewise, the lack of reactivity of cysteines located at residues 119, 132 and 147 seems unlikely to reflect a loose association with soluble components. Taken together, these data suggest that the C-terminus of Cytb5OPG is located in the ER lumen following incubation with microsomes and buffer or cytosol, but that N-glycosylation is only detected in the latter case.

The potential involvement of membrane-associated factors in defining the conformation of membrane-integrated Cytb5OPG, and hence the potential reactivity of Cys^{107}, was investigated by subjecting ER-derived membranes to biochemical treatments affecting their composition, and following both the N-glycosylation status and mPEG-5000 accessibility of $Cytb5OPG^{S107C}$ after integration into these microsomes in the presence of cytosol. When ER-derived membranes were washed with high salt or EDTA to deplete loosely associated proteins and ribosomes (Walter and Blobel, 1983), membrane integration of $Cytb5OPG^{S107C}$ was detected under conditions where the protein was N-glycosylated and its cysteine residue only marginally accessible to mPEG-5000 (Figure 5A, lanes 1-16, ♦). Likewise, partial depletion of both peripheral membrane proteins and the lumenal content of the vesicles by incubation with pH 9.5 buffer (Nicchitta and Blobel, 1993) did not affect membrane integration of $Cytb5OPG^{S107C}$ by these criteria (Figure 5A, cf. lanes 5, 6, 17 and 18). However, by increasing the pH of the alkaline extraction buffer to 11.3 (Fujiki et al., 1982), the resulting ER-derived membranes behaved as though incubated with buffer even in the presence of lysate. Hence, $Cytb5OPG^{S107C}$ is no longer N-glycosylated but the cysteine residue is now available for mPEG-5000 labelling (Figure 5A, cf. lanes 5, 6, 19 and 20, ●). Given that in these conditions a functional cytosol is present, we conclude that the previously observed lack of mPEG-5000 modification of $Cytb5OPG^{S107C}$ integrated into untreated microsomes in the presence of cell lysate is unlikely to result from any cytosol-mediated inhibition of labelling or post-translational modification of the cysteine residue.

The treatment of ER-derived microsomes with alkaline buffer of pH higher than 11.0 typically removes most peripherally-bound membrane proteins and the lumenal content (Miller et al., 1995; Nicchitta and Blobel, 1993), suggesting that such components may influence Cytb5 membrane integration. This hypothesis was strengthened by the finding that N-ethylmaleimide (NEM) treatment of the ER-derived microsomes or prior extraction with 4 M urea both led to a rescue of the ability to PEGylate $Cytb5OPG^{S107C}$ in the presence of cytosol, consistent with a role for peripheral membrane proteins in generating a conformation that is refractive to PEG modification (Figure 4B, cf. lanes 2, 4, 6 and 8, ●).

In order to establish the general functionality of the variously treated microsome preparations their ability to N-glycosylate a second model TA-protein, Sec61βOPG, was compared to the behaviour of Cytb5OPG. The integration of Sec61βOPG relies on the TRC40 pathway (see Introduction and (Favaloro et al., 2010; Leznicki et al., 2010; Stefanovic and Hegde, 2007)), a process sensitive to protease or NEM treatment of ER-derived microsomes ((Stefanovic and Hegde, 2007) and unpublished data). Since we find that the membrane integration of recombinant Sec61βOPG is significantly slower than that of Cytb5OPG (Leznicki, Warwicker and High, manuscript submitted), membrane integration reactions were carried out for 4 hours to ensure completion. The N-glycosylation status of both TA-proteins was then determined by quantitative immunoblotting (see Figure 5C). This analysis showed that treatment of microsomal membranes with alkaline sodium carbonate buffer at pH 11.3 prevents any authentic N-glycosylation of both Cytb5OPG and Sec61βOPG, presumably by affecting the function of the oligosaccharyltransferase complex (Figure 5C, cf. lanes 4 and 5, 9 and 10). In contrast, washing the ER-derived membranes with 4 M urea results in a ~ 40 % decrease in the amount of correctly N-glycosylated Sec61βOPG but an 80 % decrease in authentic N-glycosylation of Cytb5OPG (Figure 5C, cf. lanes 1-3 and 6-8). Hence, the effect of treating microsomes with 4 M urea is less pronounced for a TRC40-dependent TA-protein substrate than for Cytb5OPG. Interestingly, a Cytb5OPG species of currently unknown origin was observed when urea- and alkaline pH-treated microsomes were used for the membrane integration reaction (Figure 5C, lanes 3 and 5, ■). When the effects of these membrane treatments on both the PEGylation of cysteine 107 and the N-glycosylation of the C-terminal extension of Cytb5OPG are considered together, one might reasonably speculate that 4 M urea removes proteinaceous factors that facilitate Cytb5 biogenesis and/or N-glycosylation but are of lesser importance for Sec61β biosynthesis.

DISCUSSION

In the present study we have addressed the role of cytosolic and membrane-associated proteins during the integration of Cytb5 into the ER. To this end, we used purified recombinant proteins and combined biochemical tools with biophysical methodology. We showed that regardless of the presence of cell lysate, the opsin epitope tagged C-terminus of Cytb5 is protease-inaccessible after incubation with ER-derived membranes. Furthermore, a cysteine residue located at the extreme C-terminus of the polypeptide chain cannot be efficiently modified by a PEGylation reagent in either case. The simplest explanation of this observation is that cytosolic components are not essential for the translocation of the C-terminal tag on Cytb5 across the ER membrane and into the lumen. However, in the absence of cytosol this C-terminal tag is not N-glycosylated and other scenarios are also possible. For example, in the absence of cytosol the C-terminus of Cytb5 may remain on the cytosolic face of the ER membrane but be buried in the headgroup region of the lipid bilayer, making it refractive to proteinase K digestion and modification by hydrophilic thiol-reactive probes such as mPEG-5000 (Dailey and Strittmatter, 1981; Enoch et al., 1979). An important task for the near future will be to perform control reactions to establish whether all of the cysteine residues introduced into Cytb5OPG (cf. Figure 4A) can react with sulfhydryl-specific probes in the absence of ER-derived membranes. This analysis should clarify whether the apparent lack of reactivity of Cys^{147} results from inaccessibility such as that resulting from its translocation into the ER lumen, or simply reflects an intrinsic lack of reactivity. The location of the presumptive Cytb5 ER lumenal domain can also be further investigated by alternative approaches. Hence, the use of fluorescently-labelled derivatives of single cysteine variants of Cytb5OPG would allow for so-called "iodide quenching" experiments to be performed with integrated polypeptides. In such experiments, fluorescent probes located in the ER lumen can only be effectively quenched after the membranes are permeabilised using toxins such as streptolysin O or melittin (Crowley et al., 1994; Haigh and Johnson, 2002; Hamman et al., 1997). Similarly, the location of different cysteine residues present in membrane-associated Cytb5OPG generated in the presence of buffer or cytosol could be tested by using alternative thiol-specific reagents differing in reactivity towards exposed and membrane-embedded cysteine residues, and having

distinct capacities to cross the lipid bilayer (Fujita et al., 2010; Kim et al., 2004; Le Gall et al., 2004; Wang et al., 2008).

Regardless of the precise transmembrane topology of the Cytb5 C-terminus, we observe a clear difference in the reactivity of a cysteine residue introduced at position 107 when a membrane integration reaction is carried out in the presence or absence of cytosolic components. In the absence of cytosol Cytb5 associates with the lipid bilayer in a conformation that allows for Cys^{107} to be efficiently modified with a thiol-reactive probe, whilst cytosolic factors result in a C-terminally N-glycosylated form of Cytb5 where Cys^{107} appears inaccessible. This lack of Cys^{107} labelling with mPEG-5000 does not seem to result from the binding of soluble proteins to the cytosolic region of Cytb5 (cf. Figure 4B), nor can it be readily attributed to the post-translational modification of the protein (cf. Figures 5A and 5B). One potential explanation is that Cytb5 inserts "deeper" into the lipid bilayer when cytosolic components are present (Figure 6), consistent with formation of a slightly slower migrating, protease-resistant fragment of Cytb5 after cytosol-stimulated membrane integration (cf. Figure 1B). In this model, the C-terminal N-glycosylation tag would only be sufficiently far enough from the ER membrane to be modified when integration takes place in the presence of cytosol ((Nilsson and von Heijne, 1993) and cf. Figure 6, pathway C1-C2).

This potential variability in Cytb5 membrane insertion also appears to depend on membrane-associated proteins, hence the treatment of ER microsomes with high pH, 4 M urea or N-ethylmaleimide, all result in Cytb5OPG becoming membrane-associated in a form where Cys^{107} is accessible (cf. Figures 5A and 5B). Of particular note is the observation that urea-washed microsomes are still capable of N-glycosylating substantial amounts of the TRC40-dependent TA-protein, Sec61β, but are much less competent for facilitating Cytb5 integration, even after an extended incubation period. We speculate that the urea treatment removes peripheral membrane proteins that can assist Cytb5 integration. In contrast, the effect on Sec61β suggests that either these components are less important, or, in our view more likely, a distinct protein(s) of relevance to the TRC40 pathway is perturbed by the urea treatment.

The data outlined above can be used to formulate a working hypothesis that cytosolic and membrane-associated proteins cooperate during the integration of Cytb5 into the ER membrane, and ensure that the C-terminus is fully translocated to the ER lumen whilst the amino acid at position 107 is shielded by the lipid bilayer (Figure 6, routes C1 and C2). In the absence of cytosolic and/or membrane-bound factors Cytb5 fails to integrate in this conformation and inserts with the residue 107 exposed to the cytosol (Figure 6, routes B1 and B2; C1 and C2'). Interestingly, recent work from the von Heijne group indicates that particular transmembrane segments in oligomeric membrane protein subunits can significantly alter their positions relative to the lipid bilayer during protein folding (Kauko et al., 2010), whilst the integration of some marginally hydrophobic transmembrane helices into the ER membrane may involve extensive post-translational rearrangements within these segments (Hedin et al., 2010). Hence, it is possible that the precise conformation/environment of Cytb5 can be influenced by the presence of cytosolic and/or membrane-bound proteins. Although it is unlikely that the urea treatment used would remove components such as palmitoylated cytochrome c or integral membrane protein sugar transporters, we cannot formally exclude that previously reported interactions of Cytb5 with such components might contribute to the different environments of Cys^{107} that we report (Fan et al., 2009; Mauk et al., 1995).

The hypothesis that cytosolic factors may influence the conformation of the Cytb5 TMS is also supported by the finding that certain viral proteins assume a dual topology at the ER membrane by post-translationally translocating segments of their polypeptide chain across the lipid bilayer. For NS4B of the hepatitis C virus it was shown that such translocation of the N-terminus across the ER membrane is influenced by another viral protein, NS5A, that binds to this region and prevents it from crossing the lipid bilayer (Lundin et al., 2006). Similarly, cytosolic interacting partners can affect the transmembrane topology of factors involved in regulating apoptosis such as Bcl-2 and Bax. Hence, the binding of BH3-only proteins can displace the C-terminal membrane anchor of Bcl-w and Bax from an intramolecular binding groove enabling protein integration into the mitochondrial outer membrane (Suzuki et al., 2000; Wilson-Annan et al., 2003).

Time-resolved analysis of the membrane integration of fluorescently-labelled Cytb5 provided further evidence that soluble proteins participate in the integration of Cytb5, and indicated that cytosolic components can stimulate association of Cytb5 with the ER membrane (cf. Figure 2). A clear difference in the kinetics of membrane insertion, as judged by changes in NBD fluorescence, was observed dependent on whether Cytb5 was pre-incubated with buffer or cytosol prior to the addition of ER-derived membranes. This suggests that components of cell lysate bind Cytb5 and maintain the protein in an integration-competent state (cf. (Rabu et al., 2009; Rabu et al., 2008)). An association of cytosolic proteins with the transmembrane region of Cytb5 was confirmed by changes in both NBD fluorescence and the EPR signal in the presence of lysate, and we speculate that the cytosol can partially substitute for detergent to prevent Cytb5 aggregation (cf. Figures 2 and 3). It should be noted that a recent study addressing the kinetics of membrane integration of *in vitro* translated and recombinant Cytb5 variants suggested that cytosolic proteins do not have any stimulatory function during Cytb5 membrane insertion (Colombo et al., 2009). However, Colombo et al. (2009) used protein-free liposomes to assay these kinetics, providing a potential explanation for the apparent similarity of Cytb5 integration in the presence and absence of cell lysate if our speculation that peripheral membrane proteins can facilitate this process proves to be correct (see above). To our knowledge this is the first use of fluorescence- and EPR-based methodology to study the biogenesis of a TA-protein, and we believe that this strategy will ultimately provide novel insights into the biogenesis of both Cytb5 and TA-proteins synthesised via alternative routes.

Although preliminary in nature, our current study indicates that the biogenesis of Cytb5 at the ER membrane could be significantly more complex than previously anticipated, and may require a sophisticated collaboration between cytosolic and membrane-bound factors. Clearly, the identification of the putative cytosolic holdase and membrane-bound “receptor” will be the main goal of our future research.

MATERIALS AND METHODS

Materials. Bacterial expression vector, pHisTrx, was a kind gift from Dr Richard Kammerer (University of Manchester) whilst the monoclonal anti-opsin epitope tag antibody was provided by Paul Hargrave (Department of Ophthalmology, University of Florida, USA). *N*,*N*'-dimethyl-*N*-(iodoacetyl)-*N*'-(7-nitrobenz-2-oxa-1,3-diazol-4-yl)ethylenediamine (IANBD amide) was purchased from Molecular Probes, (1-Oxyl-2,2,5,5-tetramethylpyrroline-3-methyl) methanethiosulfonate (MTSSL) was supplied by Alexis Biochemicals and polyethylene glycol 5000 maleimide (mPEG-5000) was obtained from Nektar. Nuclease-treated rabbit reticulocyte lysate was from Promega, whilst the untreated rabbit reticulocyte lysate used in the EPR experiments was from Green Hectares.

Protein expression, purification and labelling with NBD or MTSSL. Cytb5OPG variants and Sec61βOPG were purified as described previously (Leznicki et al., 2010) but an additional ion exchange chromatography step was included during purification of Cytb5OPG in order to remove any contaminating DnaK. Hence, protein eluted from NiNTA agarose beads by thrombin cleavage was desalted, buffer exchanged to buffer D (50 mM HEPES-KOH, pH 7.9, 50 mM KOAc, 10 % (v/v) glycerol, 0.1 % (w/v) LDAO), and the resulting protein solution incubated with Q-Sepharose resin for 2 hours at 4ºC. Beads were then washed with buffer D and Cytb5OPG, essentially free of contaminating DnaK, was eluted in buffer D supplemented with 200 mM NaCl.

Labelling of Cytb5OPG with NBD or MTSSL was carried out by incubating the NiNTA-purified protein with 1 mM thiol-reactive probe overnight at 4ºC, followed by quenching of the unreacted probes with 10 mM DTT (NBD) or 20 mM cysteine (MTSSL) for 2 hours at 4ºC. Excess probes were removed by gel filtration, and the resulting protein solutions exchanged into buffer D. Labelled Cytb5OPG was then subjected to ion exchange chromatography as described above. The protein concentrations and extent of NBD labelling were calculated from the extinction coefficients for Cytb5OPG (ε_{280} = 30,940 M^{-1} cm^{-1}) and NBD conjugate (ε_{478} = 25,000 M^{-1} cm^{-1}), respectively.

Membrane integration reaction and protease protection assay. Cytb5OPG (final concentration of ~ 0.36 μM) was mixed with 50 μl rabbit reticulocyte lysate (Promega) or buffer R (50 mM HEPES-KOH, pH 7.5, 40 mM KOAc, 5 mM $MgCl_2$) and 6 μl sheep rough microsomes (final concentration of ~ 2.2 OD_{280} per ml), and the reaction was incubated for 1 hour at 30ºC. Membranes were then isolated by centrifugation (120,000 x g, 10 min, 4ºC) through an HSC cushion (750 mM sucrose; 500 mM KOAc; 5 mM $Mg(OAc)_2$; 50 mM HEPES-KOH, pH 7.9), resuspended in LSC buffer (250 mM sucrose; 100 mM KOAc; 5 mM $Mg(OAc)_2$; 50 mM HEPES-KOH, pH 7.9) and either directly solubilised in a Laemmli buffer or further treated as described.

To check the protease sensitivity of membrane-integrated Cytb5OPG, three membrane integration reactions were combined, microsomes isolated as described above and resuspended in 68 μl of LSC buffer. The suspension was then split in three and each 20 μl aliquot received 2 μl of water, 2 μl of proteinase K (2.5 mg/ml) or 2 μl of proteinase K (2.5 mg/ml) and 2.2 μl of 10 % (v/v) Triton X-100. Digestion was carried out on ice for 30 min and proteinase K was inactivated by the addition of 2.5 mM PMSF and further incubating on ice for 10 min. Laemmli buffer was then added and the samples immediately heated to ~ 95ºC for 10 min.

Membrane treatments and cysteine accessibility to mPEG-5000. Sheep rough microsomes isolated by centrifugation (120,000 x g, 10 min, 4ºC) through an 0.5 M sucrose cushion in RM(-) buffer (50 mM HEPES-KOH, pH 7.9, 50 mM KOAC, 2 mM $Mg(OAc)_2$, 1 mM DTT) were resuspended to the starting volume in RM buffer (50 mM HEPES-KOH, pH 7.9, 250 mM sucrose, 50 mM KOAC, 2 mM $Mg(OAc)_2$, 1 mM DTT) supplemented with 0.2 – 1 M KOAc, 10 – 25 mM EDTA or in sodium carbonate solution of pH 9.5 or pH 11.3, as indicated. Membranes were incubated for 15-20 min on ice, isolated through 0.5 M sucrose cushion in RM(-) buffer and resuspended in RM buffer to the starting volume. For urea treatment of microsomes the isolated membranes were incubated for 15-20 min on ice in 2 or 4 M urea solution. Following 2-fold dilution in RM buffer microsomes were isolated by centrifugation (120,000 x g, 10 min, 4ºC) through HSC cushion, washed with RM buffer to remove any remaining urea, and after re-isolation through HSC cushion,

were resuspended to the starting volume in RM buffer. NEM modification of membranes was performed by treating microsomes isolated through an HSC cushion with 2 mM NEM for 30 min at 25ºC, followed by quenching of the unreacted NEM with 20 mM of DTT for 10 min at 25ºC. Microsomes were then re-isolated through the HSC cushion and resuspended in RM buffer to the starting volume.

Accessibility of the cysteine residues of Cytb5OPG variants to mPEG-5000 was addressed by carrying out the membrane integration reactions as described above (see "Membrane integration reaction and protease protection assay"), resuspending the membrane pellet after centrifugation in 33 µl LSC buffer and splitting the reaction in two. Each aliquot (15 µl) was then mixed with water or mPEG-5000 (pre-quenched with a ~4.5-fold molar excess of glycine), to a final concentration of 1mM. The reactions were incubated for 10 min at 25ºC and then unreacted mPEG-5000 quenched with 20 mM DTT for 10 min at 25ºC.

To compare integration of Cytb5OPG and Sec61βOPG into the variously treated microsomes, 0.26 µM of Cytb5OPG and 1.9 µM of Sec61βOPG were incubated with 25 µl of rabbit reticulocyte lysate (Promega) and 5 µl sheep microsomes (~ 3.5 OD_{280} per ml before treatment) for 4 hours at 30ºC. Membranes were isolated by centrifugation (120,000 x g, 10 min, 4ºC) through HSC cushion, solubilised in Laemmli buffer and samples were resolved by SDS-PAGE followed by quantitative immunoblotting (LiCor) using anti-opsin epitope tag antibody.

Fluorescence measurements. NBD-labelled Cytb5OPG was mixed with buffer R or heme-free rabbit reticulocyte lysate prepared as described (Wahlman et al., 2007) to a final concentration and volume as indicated in the figure legend. An energy generating system (0.9-1.5 mM ATP, 0.9-1.5 mM GTP, 6.8-12 mM creatine phosphate and 6.8 x 10^{-3}-12 x 10^{-3} U/µl creatine phosphokinase) was also included in the reactions and membranes were added to a final concentration of ~ 0.35 OD_{280} per ml. NBD fluorescence was measured using the SLM 8100 photon-counting spectrofluorimeter and an excitation wavelength of 468 nm. Kinetics of membrane integration of NBD-labelled Cytb5OPG were monitored at 530 nm, whilst emission spectra were recorded from 510 nm to 560 nm in triplicate and average values used.

The background fluorescence obtained by carrying out parallel reactions with the unlabelled derivative of Cytb5OPG was subtracted from corresponding results for the NBD-labelled protein.

To estimate the N-glycosylation of the NBD-labelled Cytb5OPG used for the fluorescence measurements, after the analysis was complete, the microsomes were recovered by centrifugation through an HSC cushion and resuspended in Laemmli buffer. Samples were resolved by SDS-PAGE and the in-gel fluorescence detected using the Pharos FX system.

EPR spectroscopy. Cytb5OPG (final concentration of ~ 1 μM) labelled with MTSSL was incubated for 10 min at 30ºC with buffer D, buffer R, untreated rabbit reticulocyte lysate (Green Hectares) or its heme-free variant, all supplemented with an energy generating system (1 mM ATP, 100 μM GTP, 10 mM creatine phosphate and 100 μg/ml creatine phosphokinase). EPR spectra were then recorded using Bruker ELEXSYS E500/E580 EPR spectrometer (Bruker GmbH, Rheinstetten, Germany). Twenty repeats were then averaged and background values, obtained when unlabelled Cytb5OPG was used, were subtracted from the corresponding spectra of MTSSL-modified Cytb5OPG.

REFERENCES

Abell, B. M., Pool, M. R., Schlenker, O., Sinning, I. and High, S. (2004). Signal recognition particle mediates post-translational targeting in eukaryotes. *Embo J* **23**, 2755-64.

Abell, B. M., Rabu, C., Leznicki, P., Young, J. C. and High, S. (2007). Post-translational integration of tail-anchored proteins is facilitated by defined molecular chaperones. *J Cell Sci* **120**, 1743-51.

Amin, D. N., Taylor, B. L. and Johnson, M. S. (2006). Topology and boundaries of the aerotaxis receptor Aer in the membrane of Escherichia coli. *J Bacteriol* **188**, 894-901.

Borgese, N., Colombo, S. and Pedrazzini, E. (2003). The tale of tail-anchored proteins: coming from the cytosol and looking for a membrane. *J Cell Biol* **161**, 1013-9.

Bozkurt, G., Stjepanovic, G., Vilardi, F., Amlacher, S., Wild, K., Bange, G., Favaloro, V., Rippe, K., Hurt, E., Dobberstein, B. et al. (2009). Structural insights into tail-anchored protein binding and membrane insertion by Get3. *Proc Natl Acad Sci U S A* **106**, 21131-6.

Brambillasca, S., Yabal, M., Makarow, M. and Borgese, N. (2006). Unassisted translocation of large polypeptide domains across phospholipid bilayers. *J Cell Biol* **175**, 767-77.

Brambillasca, S., Yabal, M., Soffientini, P., Stefanovic, S., Makarow, M., Hegde, R. S. and Borgese, N. (2005). Transmembrane topogenesis of a tail-anchored protein is modulated by membrane lipid composition. *Embo J* **24**, 2533-42.

Colombo, S. F., Longhi, R. and Borgese, N. (2009). The role of cytosolic proteins in the insertion of tail-anchored proteins into phospholipid bilayers. *J Cell Sci* **122**, 2383-92.

Crowley, K. S., Liao, S., Worrell, V. E., Reinhart, G. D. and Johnson, A. E. (1994). Secretory proteins move through the endoplasmic reticulum membrane via an aqueous, gated pore. *Cell* **78**, 461-71.

Dailey, H. A. and Strittmatter, P. (1981). Orientation of the carboxyl and NH2 termini of the membrane-binding segment of cytochrome b5 on the same side of phospholipid bilayers. *J Biol Chem* **256**, 3951-5.

Enoch, H. G., Fleming, P. J. and Strittmatter, P. (1979). The binding of cytochrome b5 to phospholipid vesicles and biological membranes. Effect of orientation on intermembrane transfer and digestion by carboxypeptidase Y. *J Biol Chem* **254**, 6483-8.

Fan, R. C., Peng, C. C., Xu, Y. H., Wang, X. F., Li, Y., Shang, Y., Du, S. Y., Zhao, R., Zhang, X. Y., Zhang, L. Y. et al. (2009). Apple sucrose transporter SUT1 and sorbitol transporter SOT6 interact with cytochrome b5 to regulate their affinity for substrate sugars. *Plant Physiol* **150**, 1880-901.

Favaloro, V., Spasic, M., Schwappach, B. and Dobberstein, B. (2008). Distinct targeting pathways for the membrane insertion of tail-anchored (TA) proteins. *J Cell Sci* **121**, 1832-40.

Favaloro, V., Vilardi, F., Schlecht, R., Mayer, M. P. and Dobberstein, B. (2010). Asna1/TRC40-mediated membrane insertion of tail-anchored proteins. *J Cell Sci* **123**, 1522-30.

Fujiki, Y., Hubbard, A. L., Fowler, S. and Lazarow, P. B. (1982). Isolation of intracellular membranes by means of sodium carbonate treatment: application to endoplasmic reticulum. *J Cell Biol* **93**, 97-102.

Fujita, H., Kida, Y., Hagiwara, M., Morimoto, F. and Sakaguchi, M. (2010). Positive charges of translocating polypeptide chain retrieve an upstream marginal hydrophobic segment from the endoplasmic reticulum lumen to the translocon. *Mol Biol Cell* **21**, 2045-56.

Haigh, N. G. and Johnson, A. E. (2002). A new role for BiP: closing the aqueous translocon pore during protein integration into the ER membrane. *J Cell Biol* **156**, 261-70.

Hamman, B. D., Chen, J. C., Johnson, E. E. and Johnson, A. E. (1997). The aqueous pore through the translocon has a diameter of 40-60 A during cotranslational protein translocation at the ER membrane. *Cell* **89**, 535-44.

Hedin, L. E., Ojemalm, K., Bernsel, A., Hennerdal, A., Illergard, K., Enquist, K., Kauko, A., Cristobal, S., von Heijne, G., Lerch-Bader, M. et al. (2010). Membrane insertion of marginally hydrophobic transmembrane helices depends on sequence context. *J Mol Biol* **396**, 221-9.

Jittikoon, J., East, J. M. and Lee, A. G. (2007). A fluorescence method to define transmembrane alpha-helices in membrane proteins: studies with bacterial diacylglycerol kinase. *Biochemistry* **46**, 10950-9.

Jonikas, M. C., Collins, S. R., Denic, V., Oh, E., Quan, E. M., Schmid, V., Weibezahn, J., Schwappach, B., Walter, P., Weissman, J. S. et al. (2009). Comprehensive characterization of genes required for protein folding in the endoplasmic reticulum. *Science* **323**, 1693-7.

Kalbfleisch, T., Cambon, A. and Wattenberg, B. W. (2007). A bioinformatics approach to identifying tail-anchored proteins in the human genome. *Traffic* **8**, 1687-94.

Kauko, A., Hedin, L. E., Thebaud, E., Cristobal, S., Elofsson, A. and von Heijne, G. (2010). Repositioning of transmembrane alpha-helices during membrane protein folding. *J Mol Biol* **397**, 190-201.

Kim, P. K., Annis, M. G., Dlugosz, P. J., Leber, B. and Andrews, D. W. (2004). During apoptosis bcl-2 changes membrane topology at both the endoplasmic reticulum and mitochondria. *Mol Cell* **14**, 523-9.

Kim, P. K., Janiak-Spens, F., Trimble, W. S., Leber, B. and Andrews, D. W. (1997). Evidence for multiple mechanisms for membrane binding and integration via carboxyl-terminal insertion sequences. *Biochemistry* **36**, 8873-82.

Kutay, U., Ahnert-Hilger, G., Hartmann, E., Wiedenmann, B. and Rapoport, T. A. (1995). Transport route for synaptobrevin via a novel pathway of insertion into the endoplasmic reticulum membrane. *Embo J* **14**, 217-23.

Kutay, U., Hartmann, E. and Rapoport, T. A. (1993). A class of membrane proteins with a C-terminal anchor. *Trends Cell Biol* **3**, 72-5.

Le Gall, S., Neuhof, A. and Rapoport, T. (2004). The endoplasmic reticulum membrane is permeable to small molecules. *Mol Biol Cell* **15**, 447-55.

Leto, T. L. and Holloway, P. W. (1979). Mechanism of cytochrome b5 binding to phosphatidylcholine vesicles. *J Biol Chem* **254**, 5015-9.

Leznicki, P., Clancy, A., Schwappach, B. and High, S. (2010). Bat3 promotes the membrane integration of tail-anchored proteins. *J Cell Sci* **123**, 2170-8.

Linstedt, A. D., Foguet, M., Renz, M., Seelig, H. P., Glick, B. S. and Hauri, H. P. (1995). A C-terminally-anchored Golgi protein is inserted into the endoplasmic reticulum and then transported to the Golgi apparatus. *Proc Natl Acad Sci U S A* **92**, 5102-5.

Lundin, M., Lindstrom, H., Gronwall, C. and Persson, M. A. (2006). Dual topology of the processed hepatitis C virus protein NS4B is influenced by the NS5A protein. *J Gen Virol* **87**, 3263-72.

Mariappan, M., Li, X., Stefanovic, S., Sharma, A., Mateja, A., Keenan, R. J. and Hegde, R. S. (2010). A ribosome-associating factor chaperones tail-anchored membrane proteins. *Nature*.

Mauk, A. G., Mauk, M. R., Moore, G. R. and Northrup, S. H. (1995). Experimental and theoretical analysis of the interaction between cytochrome c and cytochrome b5. *J Bioenerg Biomembr* **27**, 311-30.

Mayerhofer, P. U., Cook, J. P., Wahlman, J., Pinheiro, T. T., Moore, K. A., Lord, J. M., Johnson, A. E. and Roberts, L. M. (2009). Ricin A chain insertion into endoplasmic reticulum membranes is triggered by a temperature increase to 37 {degrees}C. *J Biol Chem* **284**, 10232-42.

Miller, J. D., Tajima, S., Lauffer, L. and Walter, P. (1995). The beta subunit of the signal recognition particle receptor is a transmembrane GTPase that anchors the alpha subunit, a peripheral membrane GTPase, to the endoplasmic reticulum membrane. *J Cell Biol* **128**, 273-82.

Nicchitta, C. V. and Blobel, G. (1993). Lumenal proteins of the mammalian endoplasmic reticulum are required to complete protein translocation. *Cell* **73**, 989-98.

Nilsson, I. M. and von Heijne, G. (1993). Determination of the distance between the oligosaccharyltransferase active site and the endoplasmic reticulum membrane. *J Biol Chem* **268**, 5798-801.

Rabu, C., Schmid, V., Schwappach, B. and High, S. (2009). Biogenesis of tail-anchored proteins: the beginning for the end? *J Cell Sci* **122**, 3605-12.

Rabu, C., Wipf, P., Brodsky, J. L. and High, S. (2008). A precursor-specific role for Hsp40/Hsc70 during tail-anchored protein integration at the endoplasmic reticulum. *J Biol Chem* **283**, 27504-13.

Schuldiner, M., Collins, S. R., Thompson, N. J., Denic, V., Bhamidipati, A., Punna, T., Ihmels, J., Andrews, B., Boone, C., Greenblatt, J. F. et al. (2005). Exploration of the function and organization of the yeast early secretory pathway through an epistatic miniarray profile. *Cell* **123**, 507-19.

Schuldiner, M., Metz, J., Schmid, V., Denic, V., Rakwalska, M., Schmitt, H. D., Schwappach, B. and Weissman, J. S. (2008). The GET complex mediates insertion of tail-anchored proteins into the ER membrane. *Cell* **134**, 634-45.

Spatz, L. and Strittmatter, P. (1971). A form of cytochrome b5 that contains an additional hydrophobic sequence of 40 amino acid residues. *Proc Natl Acad Sci U S A* **68**, 1042-6.

Stefanovic, S. and Hegde, R. S. (2007). Identification of a targeting factor for posttranslational membrane protein insertion into the ER. *Cell* **128**, 1147-59.

Suzuki, M., Youle, R. J. and Tjandra, N. (2000). Structure of Bax: coregulation of dimer formation and intracellular localization. *Cell* **103**, 645-54.

Wahlman, J., DeMartino, G. N., Skach, W. R., Bulleid, N. J., Brodsky, J. L. and Johnson, A. E. (2007). Real-time fluorescence detection of ERAD substrate retrotranslocation in a mammalian in vitro system. *Cell* **129**, 943-55.

Walter, P. and Blobel, G. (1983). Preparation of microsomal membranes for cotranslational protein translocation. *Methods Enzymol* **96**, 84-93.

Wang, Y., Toei, M. and Forgac, M. (2008). Analysis of the membrane topology of transmembrane segments in the C-terminal hydrophobic domain of the yeast vacuolar ATPase subunit a (Vph1p) by chemical modification. *J Biol Chem* **283**, 20696-702.

Wilson-Annan, J., O'Reilly, L. A., Crawford, S. A., Hausmann, G., Beaumont, J. G., Parma, L. P., Chen, L., Lackmann, M., Lithgow, T., Hinds, M. G. et al. (2003). Proapoptotic BH3-only proteins trigger membrane integration of prosurvival Bcl-w and neutralize its activity. *J Cell Biol* **162**, 877-87.

Yabal, M., Brambillasca, S., Soffientini, P., Pedrazzini, E., Borgese, N. and Makarow, M. (2003). Translocation of the C terminus of a tail-anchored protein across the endoplasmic reticulum membrane in yeast mutants defective in signal peptide-driven translocation. *J Biol Chem* **278**, 3489-96.

FIGURE LEGENDS

Figure 1. Cytb5OPG associates with the ER membrane in the absence of cytosolic components.

A) A schematic representation of the Cytb5OPG variant used for the protease-protection assay and biophysical studies. Serine 119 located near the middle of the predicted transmembrane segment (TMS) was mutated to a cysteine and a short extension derived from bovine opsin (OPG) was added to the C-terminus of the polypeptide. The N-glycosylation site within the opsin epitope tag is also indicated. B) Cytb5OPG was incubated with ER-derived microsomes in the presence of buffer (buffer) or rabbit reticulocyte lysate (cytosol), membranes were isolated and proteinase K (PK) digestion of the exposed segments of the protein carried out. Samples were resolved on a 16 % Tricine SDS-PAGE gel, and products visualised by immunoblotting with the anti-opsin epitope tag antibody. The migrations of protease-protected fragments (b5 PF), and full-length monomeric (1xb5) and dimeric (2xb5) forms of Cytb5OPG are indicated. Glycosylated variants of the Cytb5OPG monomer and dimer are marked, as is the presumptive glycosylated form of the protected fragment (*). TX – Triton X-100.

Figure 2. Cytosolic proteins maintain Cytb5OPG in an integration-competent state and stimulate its membrane integration.

A) NBD-labelled Cytb5OPG (final concentration ~ 93 nM) was mixed with 250 µl of buffer (Buf.) or heme-free rabbit reticulocyte lysate (Cyt.), both supplemented with an energy generating system. After recording the initial fluorescence, ER-derived microsomes (membr.) were added and NBD fluorescence was further monitored. Half-maximal values of the fluorescence intensity ($F_{1/2}$) are indicated. B) Upon completion of the kinetic analysis presented in panel A, fluorescence emission scans of NBD-labelled Cytb5OPG were taken. C) NBD-labelled Cytb5OPG (5.55 µl of 9.3 µM solution) was mixed with 250 µl of buffer and at the time indicated 250 µl of buffer (Buf.) or heme-free rabbit reticulocyte lysate (Cyt.) was added, and the NBD fluorescence was monitored until it reached equilibrium (~1800 sec). Shutters were then closed and reactions incubated in the dark for approximately one hour. The NBD fluorescence was recorded again, ER-derived microsomes (membr.) were added and

changes in NBD fluorescence then followed. D) For each combination used during the kinetic analysis shown in panel C, fluorescence emission spectra were also taken. The fluorescence of NBD-labelled Cytb5OPG after addition of equal volume of buffer (+ Buf.) is indicated by a dashed red line and of cell lysate (+ Cyt.) by a solid red line. Spectra recorded after mixing reactions containing buffer (+ Buf. + Membr.) or cytosol (+ Cyt. + Membr.) with ER-derived membranes are shown in dashed blue and solid blue lines, respectively. E) A kinetic analysis of the membrane integration of fluorescently-labelled Cytb5OPG was performed as for panel A in the presence of buffer or an increasing amount of heme-free rabbit reticulocyte lysate (cyt.) as indicated. The membrane-associated fractions were isolated, resolved by SDS-PAGE and the in-gel NBD fluorescence detected. Lanes 1 and 4 correspond to the reactions presented in panel A.

Figure 3. Cytosolic components can substitute for detergent and prevent Cytb5OPG from aggregating.

Cytb5OPG was modified with a spin label, MTSSL, and electron paramagnetic resonance (EPR) spectra were recorded in the presence of buffer supplemented with 0.1 % (w/v) LDAO (detergent, trace I) or buffer containing only a trace amount of detergent resulting from dilution of Cytb5OPG preparation (buffer, trace II). EPR spectra were also taken for MTSSL-labelled Cytb5OPG diluted into heme-free (hf lysate, trace III) and untreated (full lysate, trace IV) lysates. A line corresponding to 3498 Gauss that marks spectral peaks shifted between detergent and cytosol samples is indicated (*).

Figure 4. Cytosolic components affect the conformation of membrane-integrated Cytb5OPG.

A) A schematic representation of the single cysteine variants of Cytb5OPG used in the current study. Predicted transmembrane segment (TMS) and the opsin-derived epitope tag (OPG) are indicated together with the N-glycosylation site located within the tag. B) Membrane integration reactions of the indicated Cytb5OPG derivatives were carried out in the presence of buffer (buf.) or rabbit reticulocyte lysate (RRL), microsomes were isolated, resuspended in LSC buffer or 4 M urea and the accessibility of cysteine residues to mPEG-5000 was tested (see Materials and Methods). The PEGylated Cytb5OPG species are shown (●). C) The membrane-

associated Cytb5OPG variants indicated were labelled with mPEG-5000 as in panel B after resuspending isolated microsomes in LSC buffer. The PEG-5000 modified Cytb5OPG species is indicated (●).

Figure 5. Membrane-associated factors influence Cytb5OPG conformation within the lipid bilayer.

A) ER-derived microsomes treated with solutions of the indicated composition or pH were used for a membrane integration reaction of Cytb5OPG^{S107C} carried out in the presence of rabbit reticulocyte lysate. The labelling of the cysteine residue with mPEG-5000 was determined using reactions carried out with untreated membranes in the presence of rabbit reticulocyte lysate (lysate) or buffer (buffer) as a negative and positive control, respectively. Efficient modification of Cytb5OPG with PEG-5000 is indicated (●) whilst a marginal labelling is marked as (♦). B) ER-derived membranes were treated with 2 mM NEM or 4 M urea and used together with untreated membranes (contr.) for a membrane integration reaction of Cytb5OPG^{S107C}. The modification of the cysteine residue with mPEG-5000 was established using Cytb5OPG^{S107C} integrated into untreated microsomes in the presence of buffer (buffer) for comparison. PEGylated Cytb5OPG species are indicated (●). C) Microsomes incubated with solutions of the indicated urea concentrations or with 100 mM sodium carbonate, pH 11.3, were used in the membrane integration reactions of recombinant Cytb5OPG and Sec61βOPG. After a four-hour incubation at 30ºC, membranes were isolated and samples resolved by SDS-PAGE followed by a quantitative immunoblotting with the primary anti-opsin epitope tag antibody and a secondary fluorescently labelled anti-mouse antibody. The level of N-glycosylation of TA-proteins relative to that obtained with control-treated membranes is shown (% N-glyc.). A novel Cytb5OPG species detected when membrane integration was carried out with microsomes washed with 4 M urea or sodium carbonate, pH 11.3, is indicated (■).

Figure 6. A schematic representation of Cytb5 integration into the ER membrane.

Cytb5 released from the ribosome is bound by cytosolic factors that prevent the protein from aggregating and maintain it in an integration-competent state (C1). Cytb5 is next targeted to a peripherally-associated component(s) of the ER membrane (C2) and its integration results in residue 107 (blue triangle) being buried within the lipid bilayer and the Asn residue (black dot) of the opsin epitope tag becoming N-glycosylated. In the absence of the putative peripheral membrane proteins, Cytb5 is released by the cytosolic factors into the lipid bilayer such that residue 107 is exposed to the cytosol whilst the potential N-glycosylation site is too close to the membrane surface to allow for its efficient modification (C2'). Lack of cytosolic factors (B1) also results in Cytb5 inserting into untreated membranes (B2), and presumably membranes lacking peripheral proteins (B2'), in a conformation where residue 107 is exposed and the opsin epitope tag cannot be N-glycosylated.

A

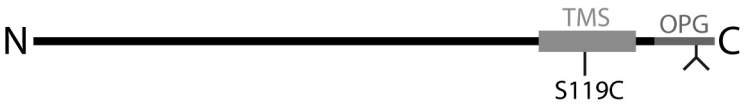
N
TMS
OPG
C
S119C

B

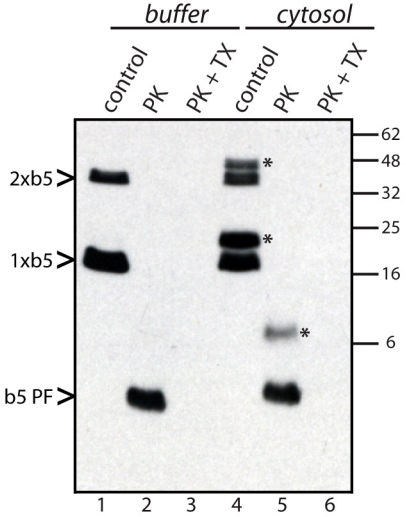
buffer
cytosol
control
PK
PK + TX
control
PK
PK + TX
2xb5
1xb5
b5 PF
62
48
32
25
16
6
*
*
*
1
2
3
4
5
6

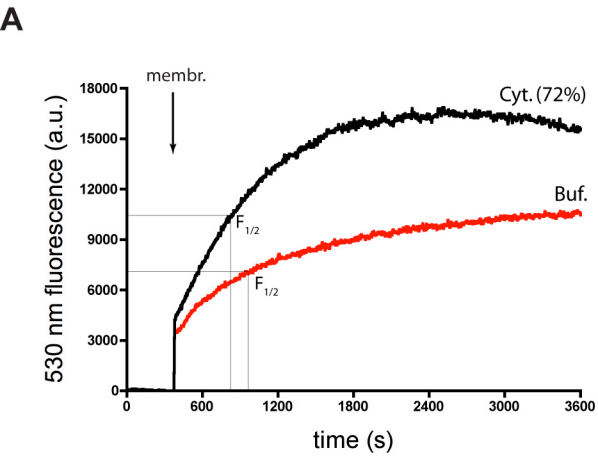
A
membr.
Cyt. (72%)
Buf.
$F_{1/2}$
$F_{1/2}$
530 nm fluorescence (a.u.)
time (s)

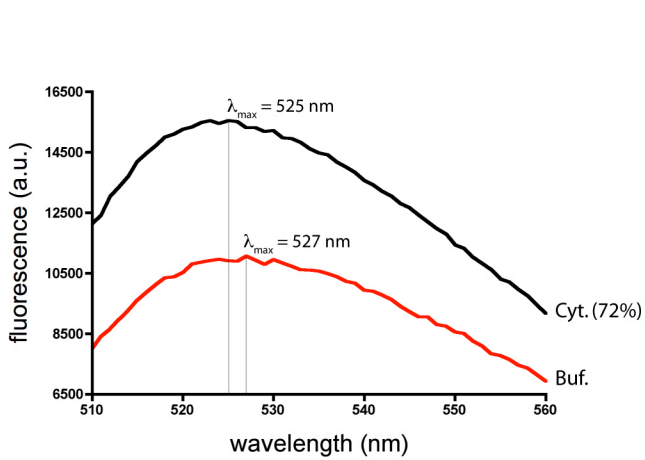
B
λ_{max} = 525 nm
λ_{max} = 527 nm
Cyt. (72%)
Buf.
fluorescence (a.u.)
wavelength (nm)

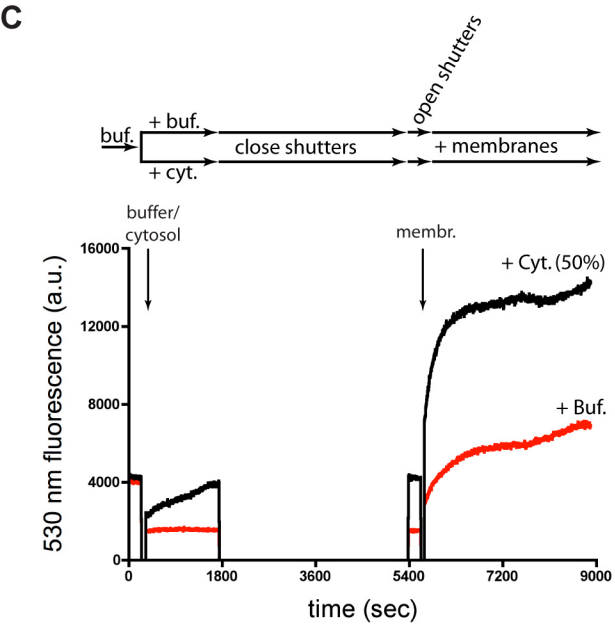
C
buf.
+ buf.
+ cyt.
close shutters
open shutters
+ membranes
buffer/
cytosol
membr.
+ Cyt. (50%)
+ Buf.
530 nm fluorescence (a.u.)
time (sec)

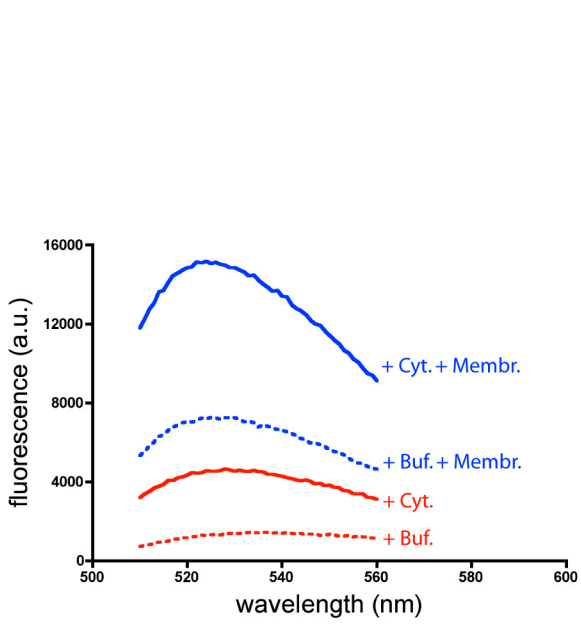
D
+ Cyt. + Membr.
+ Buf. + Membr.
+ Cyt.
+ Buf.
fluorescence (a.u.)
wavelength (nm)

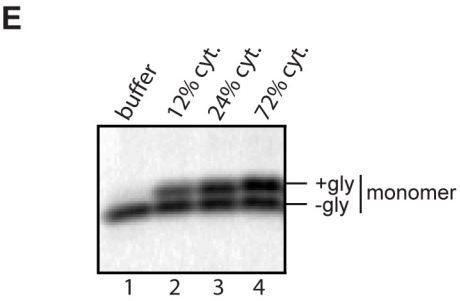
E
buffer
12% cyt.
24% cyt.
72% cyt.
+gly
-gly
monomer
1
2
3
4

Figure 3

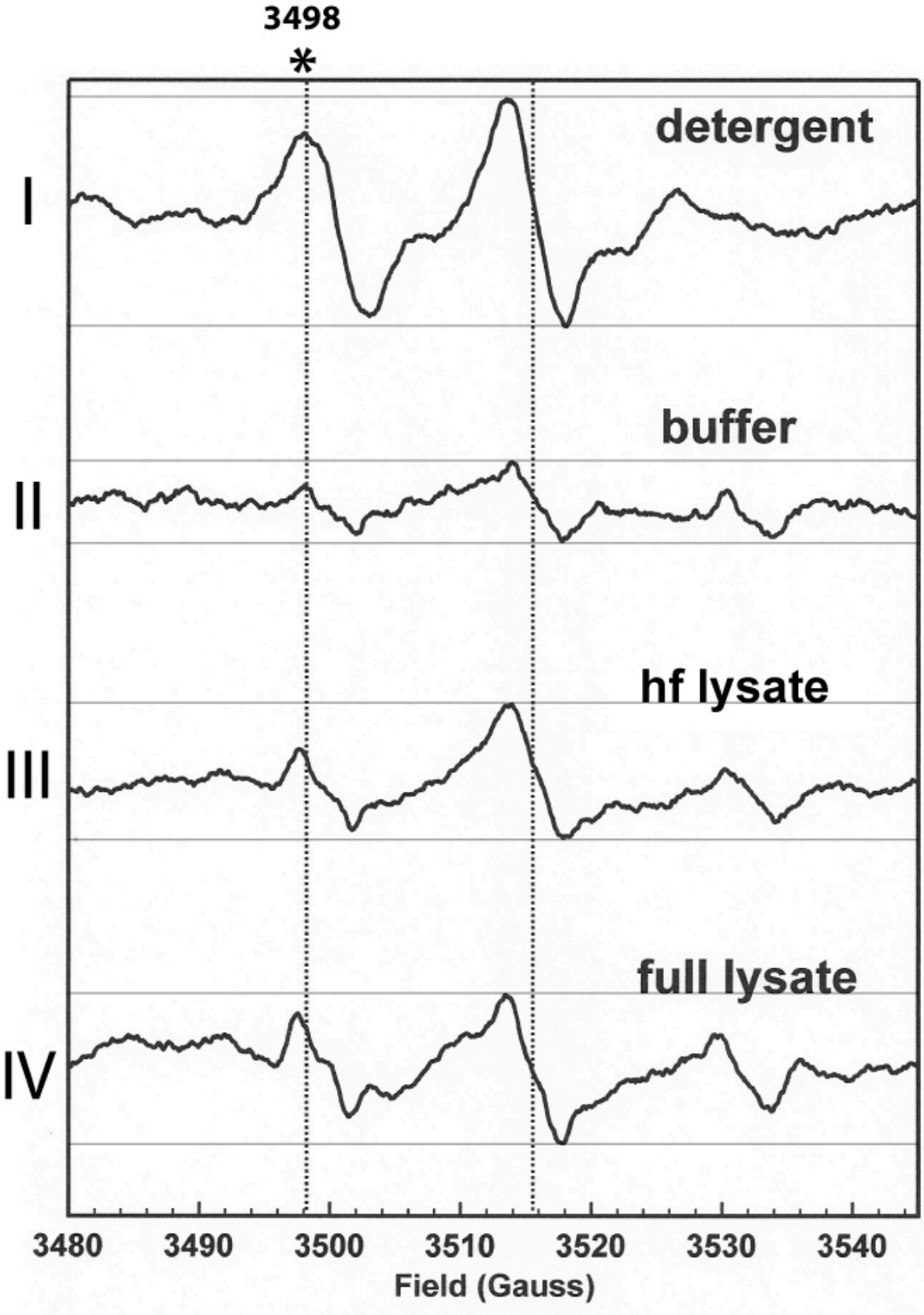
3498
detergent
I
buffer
II
hf lysate
III
full lysate
IV
3480
3490
3500
3510
3520
3530
3540
Field (Gauss)

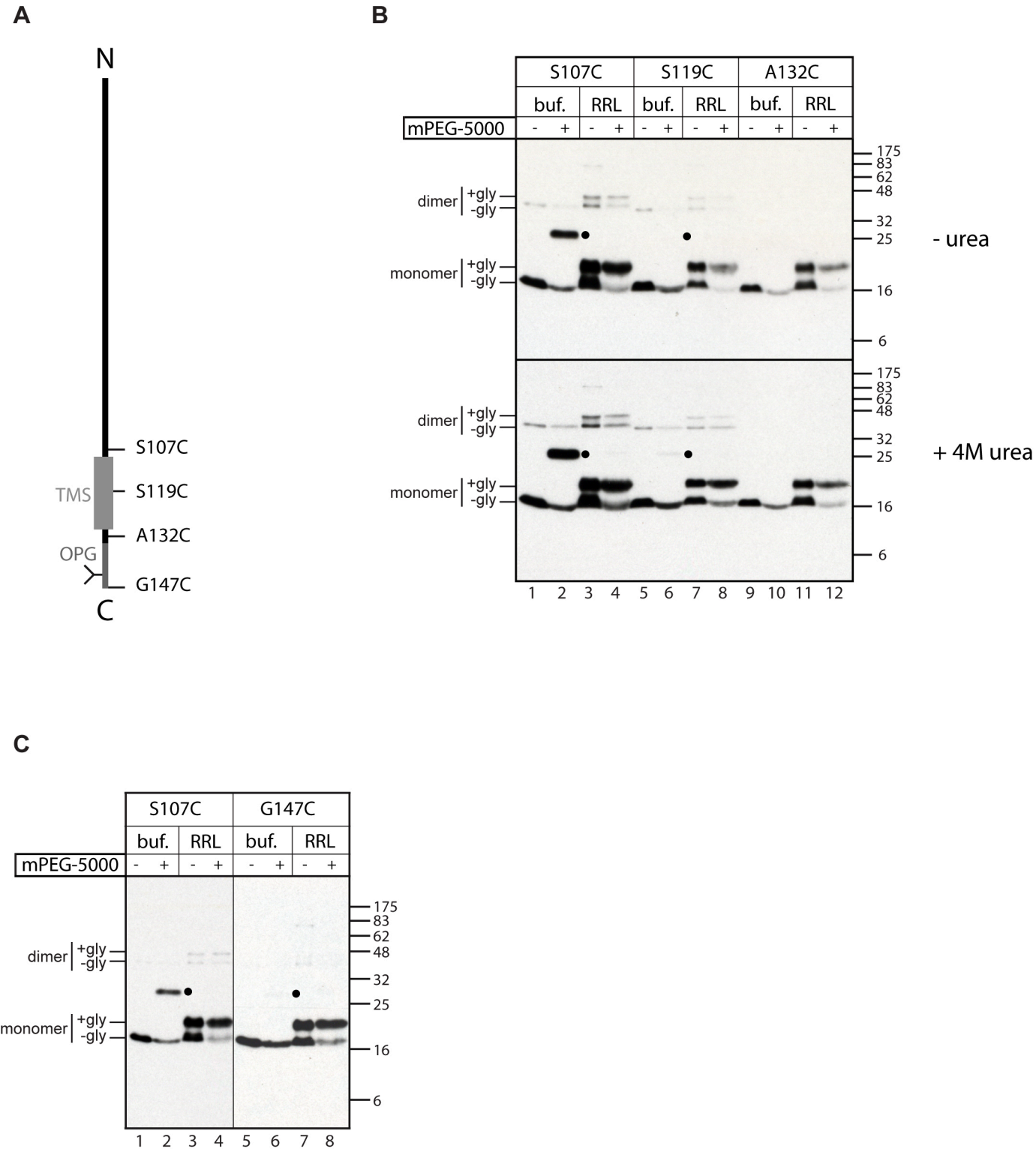
A
N
S107C
TMS
S119C
A132C
OPG
G147C
C
B
S107C
S119C
A132C
buf.
RRL
mPEG-5000
- urea
+ 4M urea
dimer
monomer
+gly
-gly
175
83
62
48
32
25
16
6
1 2 3 4 5 6 7 8 9 10 11 12
C
S107C
G147C
1 2 3 4 5 6 7 8

A

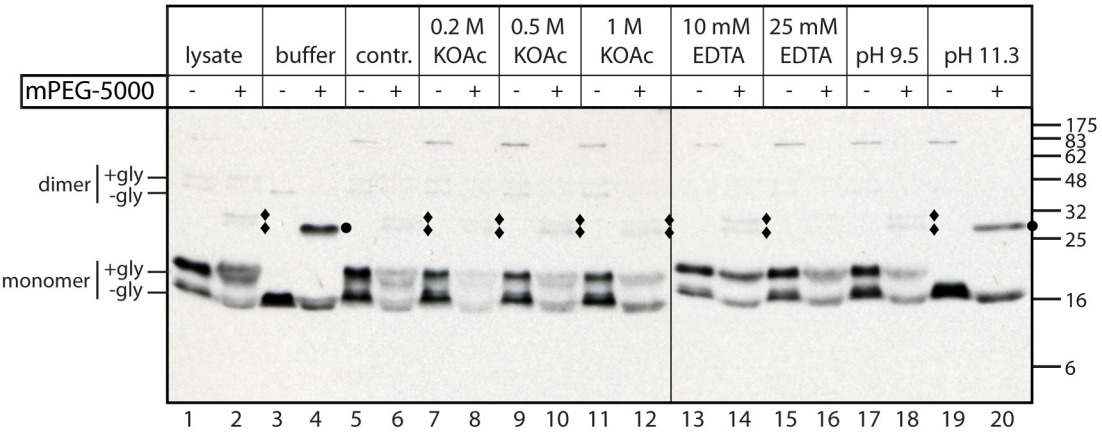
lysate
buffer
contr.
0.2 M KOAc
0.5 M KOAc
1 M KOAc
10 mM EDTA
25 mM EDTA
pH 9.5
pH 11.3
mPEG-5000
- + - + - + - + - + - + - + - + - + - +
dimer +gly -gly
monomer +gly -gly
175
83
62
48
32
25
16
6
1 2 3 4 5 6 7 8 9 10 11 12 13 14 15 16 17 18 19 20

B

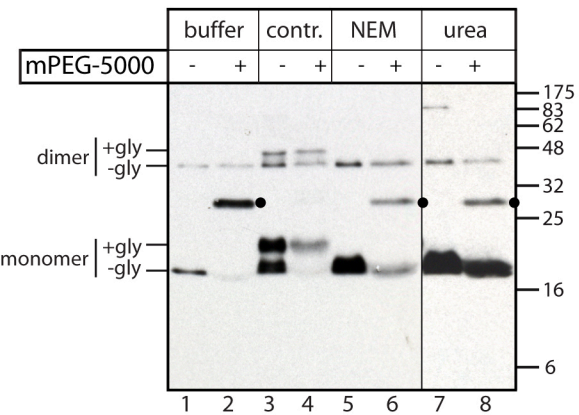
buffer
contr.
NEM
urea
mPEG-5000
- + - + - + - +
dimer +gly -gly
monomer +gly -gly
175
83
62
48
32
25
16
6
1 2 3 4 5 6 7 8

C

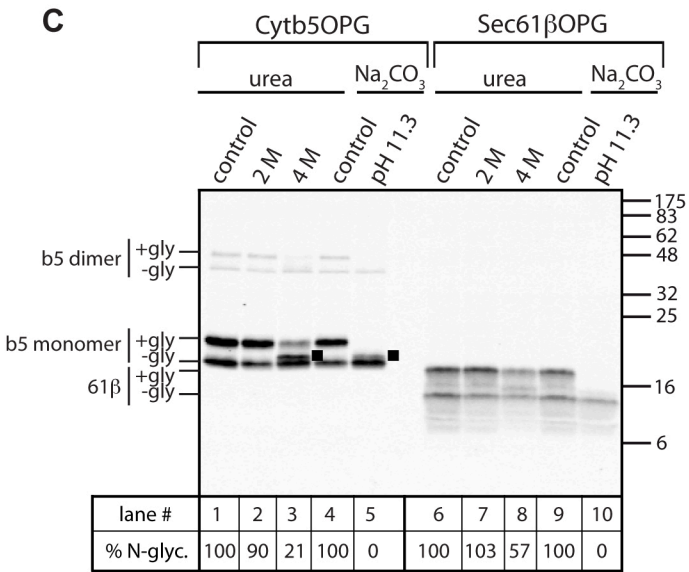
Cytb5OPG
Sec61βOPG
urea
Na2CO3
urea
Na2CO3
control
2 M
4 M
control
pH 11.3
control
2 M
4 M
control
pH 11.3
b5 dimer +gly -gly
b5 monomer +gly -gly
61β +gly -gly
175
83
62
48
32
25
16
6
lane # 1 2 3 4 5 6 7 8 9 10
% N-glyc. 100 90 21 100 0 100 103 57 100 0

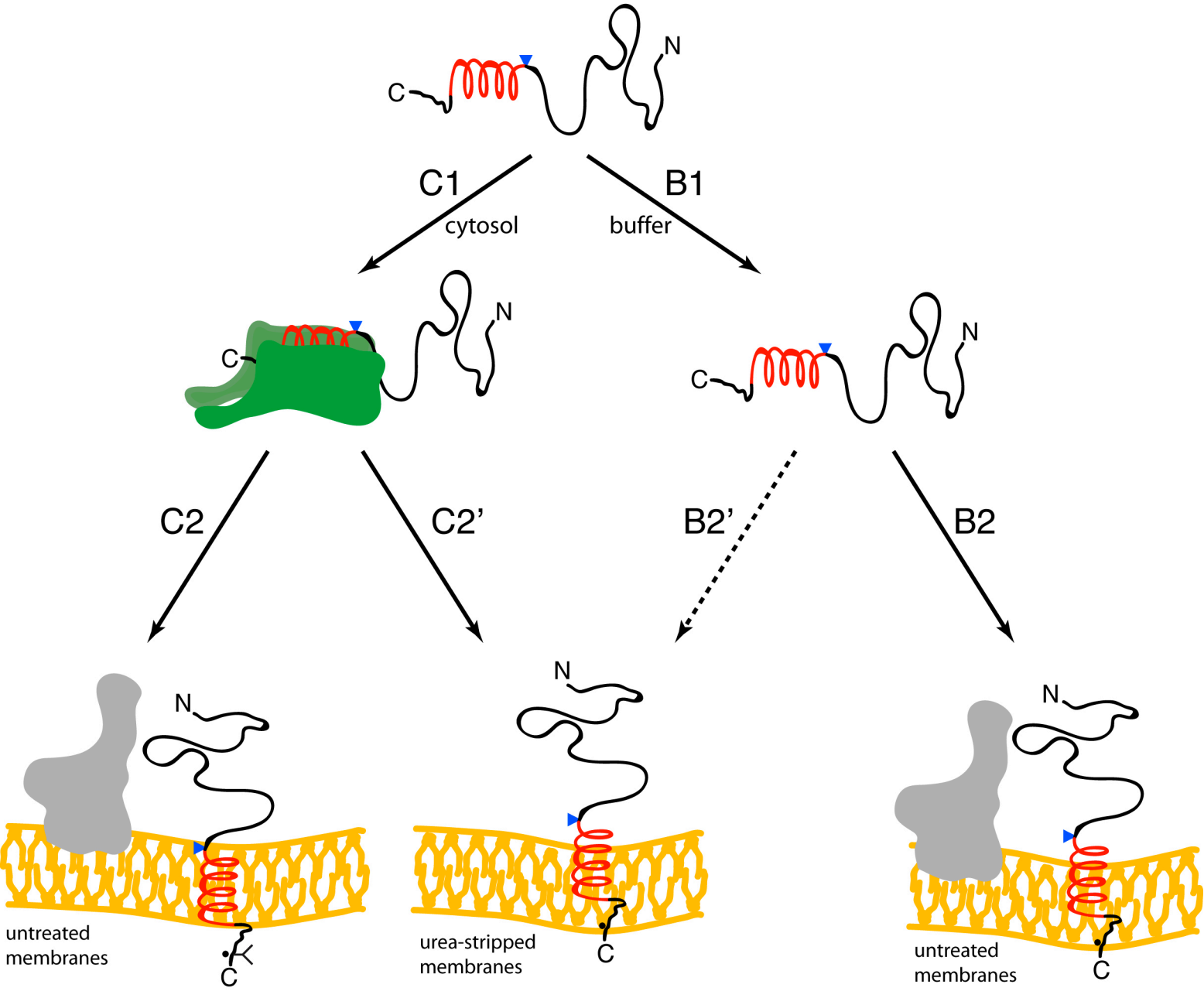
C
N
C1
cytosol
B1
buffer
C
N
C
N
C2
C2'
B2'
B2
N
N
N
untreated
membranes
urea-stripped
membranes
untreated
membranes
C
C
C

CHAPTER 2.3

Bat3 promotes the membrane integration of tail-anchored proteins

(article published in the Journal of Cell Science (2010) 123, 2170-8)

Bat3 promotes the membrane integration of tail-anchored proteins

Pawel Leznicki, Anne Clancy, Blanche Schwappach and Stephen High*

Faculty of Life Sciences, University of Manchester, Oxford Road, Manchester, M13 9PT, UK

*Author for correspondence (stephen.high@manchester.ac.uk)

Accepted 6 April 2010
Journal of Cell Science 123, 2170-2178

doi:10.1242/jcs.066738

Summary

The membrane integration of tail-anchored proteins at the endoplasmic reticulum (ER) is post-translational, with different tail-anchored proteins exploiting distinct cytosolic factors. For example, mammalian TRC40 has a well-defined role during delivery of tail-anchored proteins to the ER. Although its *Saccharomyces cerevisiae* equivalent, Get3, is known to function in concert with at least four other components, Get1, Get2, Get4 and Get5 (Mdy2), the role of additional mammalian proteins during tail-anchored protein biogenesis is unclear. To this end, we analysed the cytosolic binding partners of Sec61β, a well-defined substrate of TRC40, and identified Bat3 as a previously unknown interacting partner. Depletion of Bat3 inhibits the membrane integration of Sec61β, but not of a second, TRC40-independent, tail-anchored protein, cytochrome b5. Thus, Bat3 influences the in vitro membrane integration of tail-anchored proteins using the TRC40 pathway. When expressed in *Saccharomyces cerevisiae* lacking a functional GET pathway for tail-anchored protein biogenesis, Bat3 associates with the resulting cytosolic pool of non-targeted chains and diverts it to the nucleus. This Bat3-mediated mislocalisation is not dependent upon Sgt2, a recently identified component of the yeast GET pathway, and we propose that Bat3 either modulates the TRC40 pathway in higher eukaryotes or provides an alternative fate for newly synthesised tail-anchored proteins.

Key words: Asna-1, SGTA, Get3, Sec61β, TRC40

Introduction

Tail-anchored proteins are a distinct class of integral membrane proteins, distinguished by the presence of a single C-terminal transmembrane region that targets the polypeptide for membrane integration and anchors the protein in the lipid bilayer (Borgese et al., 2007; Kutay et al., 1993; Rabu et al., 2009). Tail-anchored proteins destined for locations within the eukaryotic secretory pathway are all synthesised at the endoplasmic reticulum (ER) and can then be retained or sorted to various subcellular compartments (Behrens et al., 1996; Borgese et al., 2007; Kutay et al., 1995; Linstedt et al., 1995). The biogenesis of tail-anchored (TA) proteins at the ER has been of particular interest because the process is post-translational, and hence quite distinct from the classical signal recognition particle dependent, co-translational, pathway associated with protein synthesised at this location (Cross et al., 2009). In vitro systems have revealed several different pathways that can deliver TA proteins to the mammalian ER, with different TA protein substrates preferentially using distinct cytosolic factors to assist their biogenesis (for reviews, see Borgese et al., 2007; Rabu et al., 2009). Pathway selection is influenced by the relative hydrophobicity of the tail-anchor region, presumably by mediating the recruitment of specific cytosolic factors (Rabu et al., 2008; Rabu et al., 2009). Several recent studies have focussed on the role of mammalian TRC40 (Asna-1), and its *Saccharomyces cerevisiae* equivalent, Get3, during the post-translational targeting of TA proteins to the ER (Favaloro et al., 2008; Schuldiner et al., 2008; Stefanovic and Hegde, 2007). TRC40 was shown to promote the membrane integration of a number of model TA proteins with comparatively hydrophobic tail-anchor regions, including Sec61β and RAMP4 (Favaloro et al., 2008; Stefanovic and Hegde, 2007). By contrast, perturbation of the TRC40 pathway appears to have little or no effect on cytochrome b5 (Cytb5) integration at the ER membrane, as judged by in vitro assays (Colombo et al., 2009; Stefanovic and Hegde, 2007). This correlates with data suggesting that the cytosolic molecular chaperones Hsc70 and Hsp40 can facilitate the ER integration of proteins with moderately hydrophobic tail-anchor regions, including Cytb5 (Rabu et al., 2008). Alternatively, the lack of TRC40 dependency for Cytb5 integration might reflect a role for new cytosolic components, or even an unassisted mechanism (Colombo et al., 2009).

TRC40 and Get3 are conserved ATPases, which mediate ATP-dependent TA-protein integration at the ER membrane (Favaloro et al., 2008; Favaloro et al., 2010; Rabu et al., 2009; Schuldiner et al., 2008; Stefanovic and Hegde, 2007). Furthermore, several recent studies of Get3 provide structural insights into the mechanisms that underlie its substrate binding and release, and provide models for how ATP binding and hydrolysis might influence these steps (Bozkurt et al., 2009; Hu et al., 2009; Mateja et al., 2009; Suloway et al., 2009). Studies of *S. cerevisiae* have shown that several components function in concert with Get3: Get1 and Get2 are ER-localised membrane receptors for the GET pathway of TA-protein delivery (Schuldiner et al., 2008), whereas Get4 and Get5 are cytosolic components that appear to act in concert with Get3 before membrane delivery (Jonikas et al., 2009; Rabu et al., 2009). It is assumed that higher eukaryotes possess functional equivalents of these additional components (Rabu et al., 2009), and indeed TRC40 appears to be part of a larger cytosolic complex (Stefanovic and Hegde, 2007). To address the identity of other components that might contribute to this pathway, we analysed the cytosolic binding partners of Sec61β – a well-defined TRC40 substrate (Stefanovic and Hegde, 2007).

We identified Bat3 (Kabbage and Dickman, 2008) as a new interacting component that binds to both Sec61β and RAMP4, but not to a version of Sec61β that lacks the hydrophobic TA region.

Strikingly, Bat3 depletion from reticulocyte lysate inhibited the membrane integration of recombinant Sec61β but did not affect Cytb5 insertion, specifically implicating Bat3 in the TRC40 pathway. When biosynthetic intermediates were analysed, the Sec61β chains that co-fractionated with Bat3 appeared distinct from the integration-competent population associated with TRC40. When expressed in *S. cerevisiae* lacking a functional GET pathway, mammalian Bat3 associated with the resulting cytosolic pool of non-targeted TA proteins and diverted it to the nucleus. Sgt2 has recently been identified, both biochemically and genetically, as an additional component of the yeast GET pathway (Chang et al., 2010; Costanzo et al., 2010). Its mammalian equivalent, SGTA is known to associate with Bat3 (Winnefeld et al., 2006), suggesting that these components function in concert during TA-protein biogenesis. We found that SGTA was preferentially associated with tail-anchor regions in a similar fashion to Bat3. However, the Bat3-dependent relocalisation of TA proteins occurs in the absence of Sgt2, confirming a role for Sgt2 in the GET pathway but ruling out any requirement for this component to enable Bat3 to redirect non-targeted TA proteins to the nucleus in yeast. *S. cerevisiae* lack an obvious Bat3 equivalent, and we propose that Bat3 either modulates the TRC40 pathway in higher eukaryotes, or provides an alternative fate for newly synthesised TA proteins that complements the role of the TRC40 complex.

Results

Recombinant Sec61β requires cytosolic factors and ATP for membrane integration

Previous studies of TA-protein biogenesis have successfully analysed the behaviour and binding partners of in vitro synthesised polypeptides to identify key components and to understand the pathways that mediate TA-protein delivery to the ER membrane (for a review, see Rabu et al., 2009). As an alternative strategy, we have now exploited recombinant polypeptides expressed in *Escherichia coli* to identify novel cytosolic factors that bind the TA region of Sec61β and contribute to its membrane integration. To this end, we expressed human Sec61β, with a short C-terminal extension bearing an N-glycosylation site (Abell et al., 2007; Colombo et al., 2009; Kutay et al., 1995; Rabu et al., 2008), as a polyhistidine-tagged fusion protein in *E. coli* (supplementary material Fig. S1A). The recombinant polypeptide was purified by nickel affinity chromatography and released from the affinity tag by proteolysis (Colombo et al., 2009), generating full-length recombinant Sec61β and a small amount of truncated material, which probably lacks a few residues at the N-terminus (supplementary material Fig. S1B).

To ensure that our recombinant Sec61β was capable of binding relevant cytosolic factors, we confirmed that the protein was efficiently integrated into ER-derived microsomes as judged by a well-established N-glycosylation assay (Abell et al., 2007; Kutay et al., 1995; Rabu et al., 2008) (supplementary material Fig. S1C). Efficient membrane integration of recombinant Sec61β requires the addition of cytosol (Fig. 1A), and membrane insertion is enhanced when the proportion of lysate is increased (Fig. 1B). As expected from previous studies (Abell et al., 2007; Favaloro et al., 2008; Stefanovic and Hegde, 2007), the membrane integration of recombinant Sec61β was also exquisitely sensitive to the presence of nucleotide triphosphate (Fig. 1C). Hence, the requirements for the membrane integration of recombinant Sec61β appear to be identical to those previously defined using in vitro synthesised polypeptides. Thus, the recombinant protein provides a viable tool for the biochemical analysis of the cytosolic factors that promote membrane integration (Colombo et al., 2009).

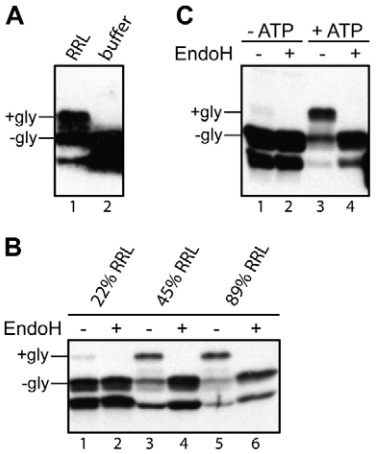

Fig. 1. Sec61β-OPG membrane integration requires cytosol and nucleotide triphosphates. (**A**) A membrane-integration reaction of recombinant Sec61βOPG was performed in the presence of sheep microsomes and either rabbit reticulocyte lysate (RRL) or a buffer control. The membrane fraction was isolated and analysed by immunoblotting with a monoclonal antibody recognising the OPG tag. N-glycosylated (+gly) and non-glycosylated (–gly) forms of Sec61βOPG are labelled. The lower product is a truncated version of Sec61βOPG (supplementary material Fig. S1B,C). (**B**) Three 50 µl membrane-integration reactions containing ~1.1 µM Sec61β-OPG and ~2.1 OD_{280}/ml sheep pancreatic microsomes supplemented with increasing amounts of rabbit reticulocyte lysate (% of total reaction volume shown) were performed and analysed by EndoH treatment and immunoblotting. (**C**) A standard membrane-integration reaction carried out with untreated rabbit reticulocyte lysate in the presence or absence of an energy regenerating system, as indicated.

The tail-anchor of Sec61β recruits several cytosolic factors

To identify novel cytosolic components that might contribute to the biogenesis of TA proteins, we looked for proteins that bound preferentially to recombinant polypeptides with an intact tail-anchor region (supplementary material Fig. S1A). To this end, recombinant opsin-epitope-tagged versions of Sec61β (Sec61β-OPG) with and without the tail-anchor region were coupled to an Ultralink resin and then used as bait for binding to components present in reticulocyte lysate. Upon analysis of the bound material, we noted that the binding of several proteins was substantially enhanced by the presence of the tail anchor (Fig. 2A). Strikingly, when a second recombinant protein with an intact tail-anchor region, RAMP4-OPG, was immobilised, an almost identical pattern of binding partners was detected (Fig. 2A). The behaviour of these components was consistent with a role in TA-protein biogenesis (Favaloro et al., 2008; Stefanovic and Hegde, 2007) and we investigated their identity using a combination of mass spectrometry and immunoblotting. In the case of cytosolic factors previously implicated in TA-protein biogenesis, we found that the recovery of SRP54, TRC40, Hsp/Hsc70 and Hsp40 were all enhanced by the presence of the hydrophobic tail-anchor regions of Sec61β and RAMP4 (Fig. 2B). The binding of an additional component of ~175 kDa was only apparent when the tail anchor was present (Fig. 2A, lanes 2 and 3, see asterisk). We were able to identify this protein as Bat3 by mass spectrometry, and confirmed its preferential binding to recombinant proteins with an

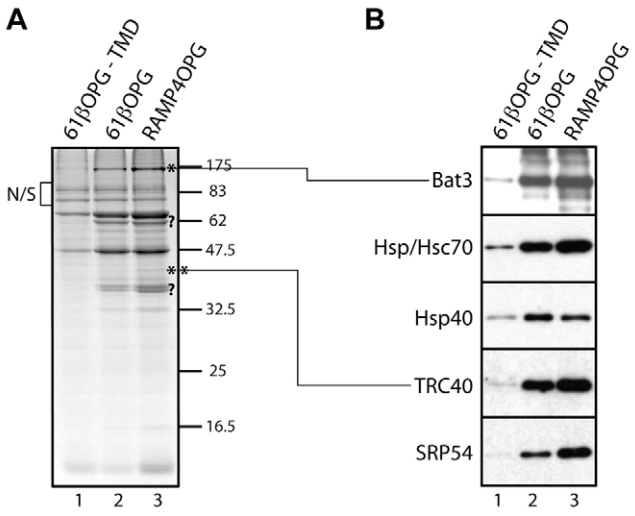

Fig. 2. Identification of tail-anchor-specific cytosolic factors. (**A**) Comparable amounts of opsin epitope-tagged versions (OPG) of a Sec61β variant lacking the transmembrane domain (–TMD), full-length Sec61β and RAMP4 (supplementary material Fig. S1A) were immobilised on UltraLink Biosupport, incubated with rabbit reticulocyte lysate and binding partners eluted with 0.1% (v/v) Triton X-100 after extensive washing. Following SDS-PAGE and Coomassie Blue staining, components strongly enriched in lanes 2 and 3 were further characterised. Relevant proteins successfully identified by mass spectrometry are shown (*, **), other candidates (?) remain uncharacterised. (**B**) Eluted material was analysed by immunoblotting for specific components, as indicated.

intact tail-anchor region by immunoblotting (Fig. 2B). Bat3 (HLA-B associated transcript 3, also known as Scythe and Bag6) has no obvious homology with TRC40 and is involved in a variety of biological processes (see Discussion).

Depletion of Bat3 specifically inhibits membrane integration of Sec61β

Since the membrane integration of recombinant Sec61β is entirely dependent upon the addition of cytosol in the form of reticulocyte lysate (Fig. 1A,B), we reasoned that if Bat3 contributed to Sec61β integration, its removal would inhibit this process. We therefore used an immunodepletion approach previously exploited to establish the dependence of TA-protein integration upon TRC40 (Colombo et al., 2009). The efficiency of Bat3 immunodepletion from reticulocyte lysate reflected the amount of primary antibody used, whereas significant levels remained in the paired controls (Fig. 3A). When the resulting lysates were analysed for their ability to stimulate Sec61β membrane insertion, integration was substantially reduced when Bat3 levels had been efficiently depleted (Fig. 3A, integ. Sec61β-OPG). To address whether Bat3 depletion simply removed other known components, we analysed various cytosolic factors implicated in Sec61β integration. No obvious differences in the levels of TRC40, Hsp/Hsc70 or SRP54 were apparent (Fig. 3A, TRC40 and Hsp/Hsc70 plus SRP54 panels). Strikingly, the reduction in Sec61β integration observed upon our most efficient Bat3 immunodepletion (Fig. 3A, integ. Sec61β-OPG) was comparable with that seen upon TRC40 depletion (Fig. 3B, integ. Sec61β-OPG). In this case, although depletion of TRC40 was effective, any reduction in Bat3 levels was extremely modest (Fig. 3B) and inconsistent with any defect in Sec61β-OPG membrane integration (Fig. 3A).

The biogenesis of the TA-protein cytochrome b5 (Cytb5) is not dependent upon the canonical TRC40-mediated pathway (Favaloro et al., 2008; Favaloro et al., 2010; Rabu et al., 2008; Stefanovic and Hegde, 2007), and its membrane insertion is unaffected by the immunodepletion of this component (Colombo et al., 2009). In contrast to the clear reduction in Sec61β insertion, depletion of Bat3 had no effect upon the membrane integration of Cytb5 (Fig. 3C). Likewise, TRC40 immunodepletion had no effect on Cytb5 integration (Fig. 3C). This assay confirms that Bat3 depletion does not affect N-glycosylation per se. More importantly, the substrate specificity of Bat3 depletion for inhibiting the integration of Sec61β, but not Cytb5 (Fig. 3), combined with the tail-anchor-dependent association of Bat3 with Sec61β and RAMP4 (Fig. 2), suggests that Bat3 influences the TRC40 mediated route for TA-protein integration (Rabu et al., 2009).

A Bat3-enriched fraction rescues Sec61β membrane integration

As an alternative approach for identifying cytosolic factors that facilitate TA-protein biogenesis, we developed a strategy to selectively deplete candidate components on the basis of their differential binding to various resins (Gorlich et al., 1994). After an empirical screening of a range of matrices, Cibacron Blue agarose was identified as a resin that substantially reduces the levels of Bat3 and SRP54 present in reticulocyte lysate, whilst leaving both TRC40 and Hsp/Hsc70 unaffected (Fig. 4A). When Cibacron-treated lysate was tested in a membrane-integration assay, its ability to promote the membrane integration of Sec61β was substantially impaired, although comparable treatments with other resins did not perturb this process (Fig. 4B). Thus, we found a correlation between Bat3 levels and the ability of reticulocyte lysate to promote Sec61β integration. We detected a substantial amount of Bat3 in the mixture of proteins that could be eluted from the Cibacron resin using a high-salt wash (Fig. 4C; supplementary material Fig. S2). Furthermore, when this eluted material was added back to the previously depleted reticulocyte lysate, Sec61β membrane integration was restored (Fig. 4D). Additional fractionation using nickel-NTA agarose reiterated a clear correlation between the presence of Bat3 and the ability of an eluted fraction to promote membrane integration (supplementary material Fig. S2). In summary, although TRC40 remains in reticulocyte lysate following either Bat3 immunodepletion (Fig. 3A) or Cibacron Blue agarose treatment (Fig. 4A), efficient Sec61β integration is only observed when Bat3 and TRC40 are both present in the lysate (Fig. 3A,B; Fig. 4).

Bat3 and TRC40 associate with distinct populations of Sec61β polypeptides

TRC40/Get3 forms a stable association with newly synthesised TA proteins (Favaloro et al., 2008; Stefanovic and Hegde, 2007), and functions at a late stage of the ER-delivery process (Bozkurt et al., 2009). We investigated the relationship of Bat3 with newly synthesised Sec61β-OPG chains generated by cell-free translation. Radiolabelled Sec61β chains were generated using a reticulocyte-lysate translation system and then fractionated by centrifugation through a sucrose gradient (Favaloro et al., 2008; Stefanovic and Hegde, 2007). Each fraction was analysed for the presence of both radiolabelled Sec61β polypeptides and a variety of cytosolic factors including Bat3 and TRC40 (Fig. 5A). In parallel, equivalent samples were analysed for their capacity to support

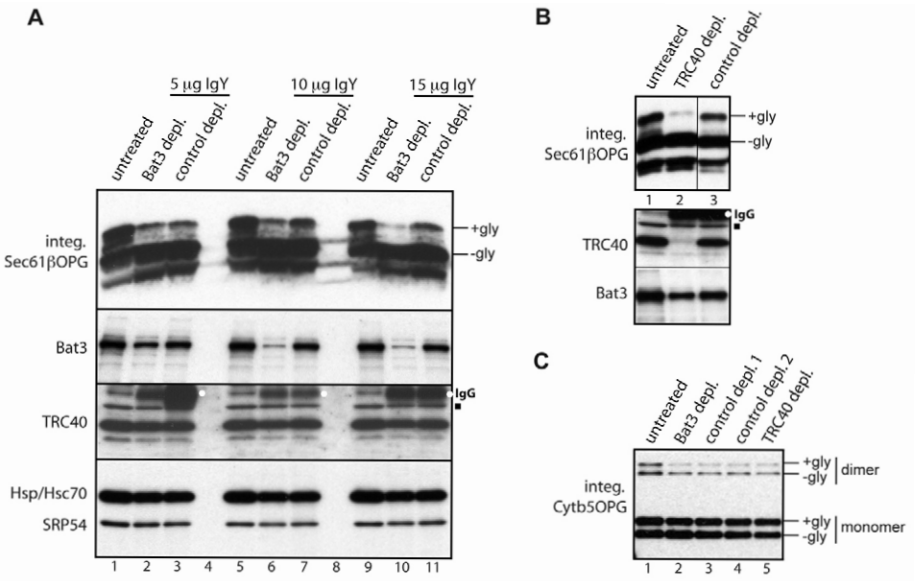

Fig. 3. Bat3 is required for Sec61β-OPG membrane integration. Samples of rabbit reticulocyte lysate were immunodepleted of Bat3 or TRC40, subjected to a parallel control immunodepletion using appropriate chicken or rabbit antibodies, or left completely untreated, as indicated. (**A**) Upper panel, the ability of different reticulocyte lysate preparations to support the membrane integration of Sec61β-OPG was assessed via N-glycosylation (+gly and –gly) following immunoblotting with the anti-opsin monoclonal antibody. Lower panels, reticulocyte lysate was left untreated or treated with increasing amounts of a chicken anti-Bat3 IgY or a control chicken IgY as indicated, and samples immunodepleted using a secondary antibody. The resulting levels of Bat3, TRC40, Hsp/Hsc70 and SRP54 were determined by immunoblotting as indicated. Individual boxes show scans from one exposure of a single piece of film. (**B**) Upper panel, the ability of different lysate preparations to support the membrane integration of Sec61β-OPG was determined as described in A. This panel shows the scan from a single piece of film with two irrelevant lanes separating the TRC40 depletion (lane 2) and the parallel control sample (lane 3) removed for simplicity, as indicated by the vertical line. Lower panel, the levels of TRC40 and Bat3 were determined as for A. (**C**) The ability of different lysate preparations to support the membrane integration of Cytb5-OPG was determined as for A. A small amount of SDS-resistant Cytb5-OPG dimer was observed. In some cases, samples subjected to immunodepletion contained residual immunoglobulin heavy chain (labelled IgG) that crossreacted with the secondary antibody (see A and B, TRC40 immunoblot, white dots). A minor species observed with the TRC40 serum is also indicated (B and C, TRC40 panel, filled square).

the membrane integration of the radiolabelled Sec61βOPG chains present in the fraction, using N-glycosylation as the readout (Fig. 5B). These experiments show that the bulk of TRC40 co-migrates with the peak of integration competent Sec61β chains (~80% of total N-glycosylation) found in fractions 5 to 8 of the gradient (Fig. 5A,B).

The distribution of Bat3 is clearly distinct from that of TRC40, showing a partial overlap but peaking at a lower part of the gradient from fractions 7 to 11 (Fig. 5A). In particular, we noted that although fraction 9 contains the strongest Bat3 signal, it supports rather low levels of Sec61β membrane integration (Fig. 5A,B; ~4% of total N-glycosylated material). Hence, although fraction 9 contains levels of Sec61β chains comparable with fractions 7 and 8 (Fig. 5A), the population of TA proteins found in the same fraction as the peak of Bat3 appears far less competent for membrane integration (Fig. 5B, compare fraction 7 with fraction 9).

Bat3 can influence the fate of a tail-anchored protein in *S. cerevisiae*

We found no evidence to suggest that a stable complex is formed between the bulk of Bat3 and TRC40 present in reticulocyte lysate (Figs 3-5); therefore, to gain further insight into the role of Bat3 during TA-protein biogenesis, we exploited an experimental system originally designed to characterise components of the equivalent GET pathway in *S. cerevisiae*. This assay relies on the observation that the deletion of components of the GET pathway inhibits the ER integration of a model TA protein, GFP-Sed5 (Weinberger et al., 2005), reducing its trafficking to the Golgi and concomitantly increasing the level of cytosolic GFP-Sed5 that has failed to become membrane integrated (Jonikas et al., 2009; Schuldiner et al., 2008).

Although quite clearly distinct, mammalian Bat3 and yeast Mdy2 (Get5) both contain a ubiquitin-like domain (Hu et al., 2006; Kabbage and Dickman, 2008) and we tested the hypothesis that Bat3 is a functional equivalent of one of the two novel cytosolic components, Get4 and Mdy2 (Get5), which have been recently identified in *S. cerevisiae* (Jonikas et al., 2009) and are presumed to have mammalian homologues (Rabu et al., 2009). Full-length human Bat3 could be expressed in both wild-type and *Δmdy2* (*Δget5*) deletion strains (Fig. 6A,B), and immunofluorescence microscopy showed that Bat3 was readily detected in the nucleus of both strains (Fig. 6C and supplementary material Fig. S3A). This is consistent with studies in cultured mammalian cells where populations of Bat3 in both the nucleus and the cytosol can be observed (Desmots et al., 2008). Bat3 expression had no effect on the location of GFP-Sed5 in wild-type cells, where numerous punctae were seen, consistent with efficient membrane integration and Golgi localization (Fig. 6D,E and supplementary material Fig. S3C, wild-type panels) (Jonikas et al., 2009; Schuldiner et al., 2008; Weinberger et al., 2005). By contrast, the cytosolic accumulation of GFP-Sed5 that was apparent upon the loss of Mdy2 (Get5) (Jonikas et al., 2009) was reduced by expression of full-length Bat3, with GFP-Sed5 being redirected to the nucleus (Fig. 6D,E and supplementary material Fig. S3C, *Δget5* panels). This reduction in cytosolic fluorescence and nuclear localisation of GFP-Sed5 required the full-length Bat3 protein with an intact nuclear

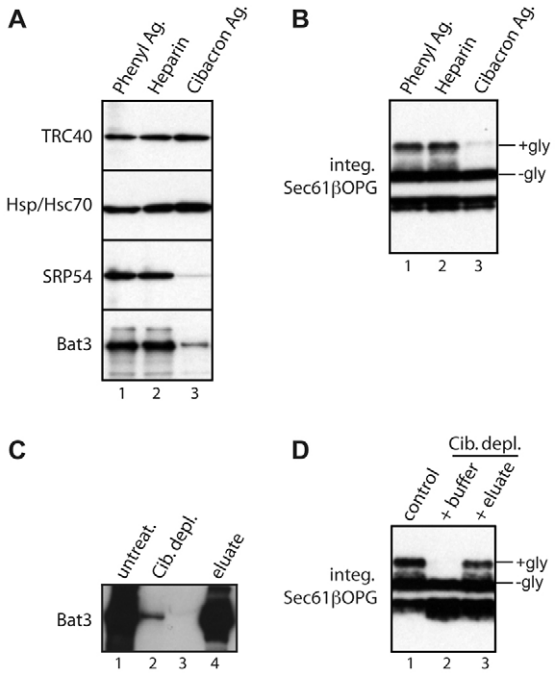

Fig. 4. A Bat3-containing fraction restores Sec61β-OPG membrane integration. (**A**) Reticulocyte lysate was incubated with different resins and the depletion of various cytosolic factors determined by immunoblotting, as indicated. (**B**) The resin-depleted lysate preparations were used to stimulate the membrane integration of recombinant Sec61βOPG. (**C**) Material bound to Cibacron Blue agarose was recovered and analysed for Bat3 content by immunoblotting and comparison with equivalent amounts of untreated lysate and Cibacron-depleted lysate as indicated. Lane 3 is empty. (**D**) The membrane integration of recombinant Sec61β-OPG was determined in the presence of untreated lysate (lane 1), Cibacron-depleted lysate supplemented with buffer (lane 2), or Cibacron-depleted lysate supplemented with the eluate from the Cibacron resin (lane 3). Individual boxes all represent a single exposure, as described for Fig. 3.

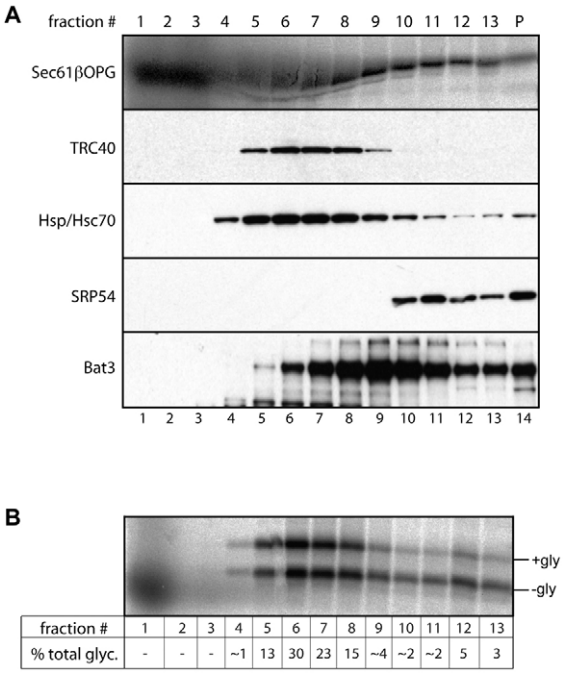

Fig. 5. Bat3 and TRC40 are associated with distinct populations of Sec61β-OPG polypeptides. (**A**) To recapitulate biosynthetic associations, Sec61β-OPG was translated in rabbit reticulocyte lysate, the material subjected to centrifugation through a 5-25% sucrose gradient, and 13 fractions plus the pellet recovered (fraction 1=top, p=pellet). Following SDS-PAGE, the location of Sec61βOPG chains was determined by phosphorimaging of the radiolabelled chains (upper panel), whereas the migration of various cytosolic factors was established by immunoblotting (as labelled). The distortion of the radiolabelled Sec61βOPG samples seen in fractions 4-8 results from the presence of large quantities of unlabelled globin chains present in the lysate used for in vitro translation. (**B**) A portion of each sucrose gradient fraction was incubated with canine pancreatic microsomes, the membranes recovered and the glycosylation status of Sec61β-OPG determined by phosphorimaging. The proportion of the total N-glycosylated material resulting from each individual fraction (% total glyc.) was estimated to provide a comparative measure of membrane integration.

localisation signal (NLS). Hence, although an N-terminal fragment of Bat3 and a full-length version with the NLS rendered non-functional were both efficiently expressed (Fig. 6A,B and supplementary material Fig. S3E), neither Bat3 variant supported the nuclear relocalisation of GFP-Sed5 (Fig. 6F). Immunofluorescence microscopy confirmed the cytosolic localisation of the two Bat3 mutants (supplementary material Fig. S3B,D), and we conclude that full-length Bat3 associates with GFP-Sed5 and redirects this TA protein to the nucleus by virtue of its previously defined NLS (Manchen and Hubberstey, 2001).

Although the expression of full-length Bat3 did not restore a wild-type phenotype for GFP-Sed5 localisation in the *mdy2*-deletion strains, the protein had a clear effect on the fate of the TA substrate. To establish whether this effect simply resulted from some perturbation of the remaining cytosolic GET complex, we looked at the outcome of Bat3 expression in yeast strains lacking other components of the GET pathway. A strikingly similar effect, namely a reduction in cytosolic labelling and the appearance of a nuclear GFP-Sed5 signal, was also observed in strains lacking either Get3 or Get4 (Fig. 6G,H). Clearly Bat3 is not compensating for the loss of a specific component of the GET pathway in yeast, but rather providing a non-physiological alternative under conditions where the GET pathway is perturbed. This conclusion was further supported by the lack of any apparent perturbation of GFP-Sed5 localisation following Bat3 expression in wild-type cells (Fig. 6E). Since Bat3 is able to redirect GFP-Sed5 to the nucleus in all three of the GET-pathway mutants tested, the association of Bat3 with a TA protein does not require Get3, Get4 or Mdy2 (Get5).

Yeast Sgt2 has recently been implicated in the GET pathway for TA-protein biogenesis (Chang et al., 2010; Costanzo et al., 2010) and its mammalian equivalent, SGTA (SGT), is a known interacting partner of Bat3 and Hsp/Hsc70 in mammalian cells (Winnefeld et al., 2006). We therefore addressed the possibility that any role for Bat3 during TA-protein biogenesis might also involve SGTA and/or its yeast equivalent. When the mammalian cytosolic components that bind tail-anchor regions were re-analysed by immunoblotting, we found that SGTA was enriched in fractions eluted from full-length TA proteins (Fig. 7A), consistent with a potential role in TA-protein biogenesis (Fig. 2). However, the ability of Bat3 to relocalise GFP-Sed5 to the nucleus of a *Δget5* strain was not dependent upon the presence of Sgt2 (Fig. 7B). Furthermore, the loss of Sgt2 alone proved sufficient to enable Bat3-mediated

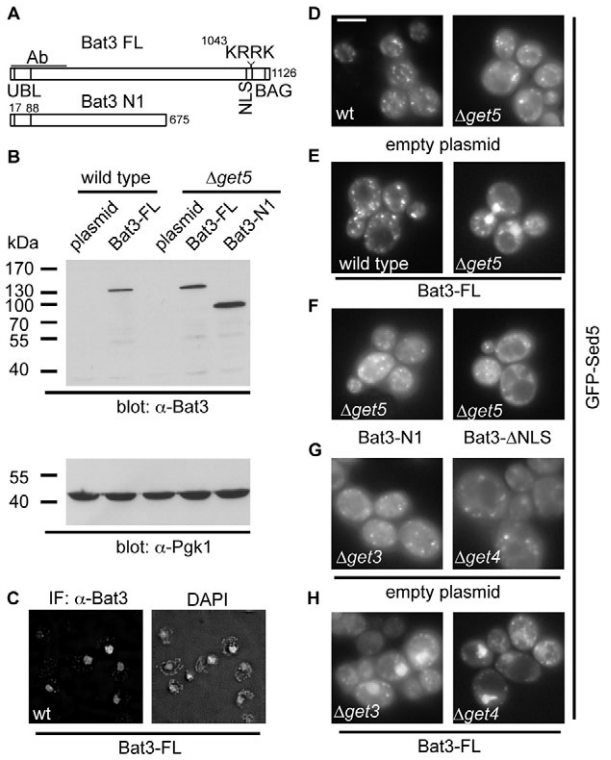

Fig. 6. Bat3 relocalises GFP-Sed5 in *S. cerevisiae GET* mutants. (**A**) Outline of full-length Bat3 (isoform 2), and the N-terminal fragment used in this study. The locations of the ubiquitin-like domain, NLS and BAG domains and the antibody-binding region are indicated. In the ΔNLS mutant, the KRRK motif shown is altered to KRSL to disrupt nuclear targeting of Bat3 (Manchen and Hubberstey, 2001). (**B**) Immunoblot showing Bat3 and phosphoglycerate kinase 1 (Pgk1) levels in wild-type or *Δmdy2* (*Δ*get5)-transformed *S. cerevisiae* cells. (**C**) Subcellular localisation of full-length Bat3 expressed in wild-type *S. cerevisiae* and DAPI staining of nuclei visualised by immunofluorescence microscopy. (**D-H**) The effect of Bat3 expression upon the subcellular localisation of GFP-Sed5 was determined by live-cell imaging in wild-type, *Δget3*, *Δget4* or *Δmdy2* (*Δget5*) cells, as indicated. Full-length Bat3, an N-terminal fragment or the ΔNLS mutant, were used as indicated. See also supplementary material Fig. S2C for fixed and immunostained cells of the same genotype demonstrating co-localisation of Bat3 and GFP-Sed5 immunoreactivity with DAPI staining of the nucleus in *Δmdy2* (*Δget5*) cells. Scale bar: 5 µm.

relocalisation (Fig. 7B). Thus, Bat3 can associate with TA proteins in the absence of any of the known soluble proteins of the yeast GET pathway, including Sgt2.

Discussion

To better understand the pathways and components responsible for the biogenesis of TA proteins we used an affinity-binding approach to identify candidate cytosolic factors. A number of proteins preferentially associate with both Sec61β- and RAMP4-bearing intact tail-anchors, including all of the cytosolic factors previously implicated in TA-protein biogenesis (Abell et al., 2004; Abell et al., 2007; Favaloro et al., 2008; Rabu et al., 2008; Stefanovic and Hegde, 2007). We found an additional component of ~175 kDa that was substantially enriched in the presence of a tail anchor, and this protein was identified as Bat3. Bat3 has been implicated in a variety of biological processes, including the regulation of apoptosis (Desmots et al., 2008), Hsp70 stability (Corduan et al., 2009; Sasaki et al., 2008) and function of natural killer cells (Simhadri et al., 2008). Bat3 has no clear homology with TRC40, and its most obvious features are an N-terminal ubiquitin-like domain, a nuclear-localisation signal (NLS) and a C-terminal BAG domain (Kabbage and Dickman, 2008).

Strikingly, Bat3 depletion results in a substantial inhibition of the reticulocyte-lysate-dependent membrane integration of Sec61β, indicating that this component can influence the biogenesis of TA protein. Whether Bat3 removal also depletes other, as yet unidentified, cytosolic components that are important for TA-protein biogenesis remains to be established. However, the removal of Bat3 does not substantially alter TRC40 levels, nor is the integration of the TRC40-independent substrate Cytb5 affected by Bat3 removal. We conclude that the role of Bat3 is most likely restricted to TA proteins that are TRC40 clients (Colombo et al., 2009; Rabu et al., 2009; Rabu et al., 2008; Stefanovic and Hegde, 2007). Although the peak of integration-competent Sec61β chains co-migrate with the bulk of TRC40, strongly supporting a role in promoting membrane integration (Bozkurt et al., 2009; Favaloro et al., 2008; Stefanovic and Hegde, 2007), the bulk of Bat3 co-migrates with a pool of Sec61β chains that are poorly membrane integrated. Thus, although Bat3 can influence the fate of TA-protein substrates of the TRC40 pathway, its function might be spatially and temporally distinct from the TRC40-mediated delivery step that precedes membrane integration (Bozkurt et al., 2009; Favaloro et al., 2010). Interestingly, a recent proteomic analysis that used the ubiquitin-like-domain-containing protein UBL4A as bait identified a protein network containing both Bat3 and TRC40 (Asna-1), together with SGTA and C7orf20 [see table S4 in Sowa et al. (Sowa et al., 2009)]. Hence, Bat3 and TRC40 might associate transiently or share common interacting partners.

To place the role of Bat3 into a cellular context, we exploited *S. cerevisiae* mutants lacking various components of the GET pathway that is functionally equivalent to the mammalian TRC40 pathway, but is at present far better defined (Jonikas et al., 2009; Rabu et al., 2009; Schuldiner et al., 2008). The very clear outcome of this approach is that the expression of Bat3 in a variety of GET-pathway mutants results in the relocalisation of a model GET-pathway substrate, GFP-Sed5, to the nucleus. We show that the ability of Bat3 to redirect GFP-Sed5 to the nucleus relies on a previously defined nuclear-localisation signal present in Bat3, which is known to be functional in mammalian cells (Desmots et al., 2008; Manchen and Hubberstey, 2001). These data are reminiscent of the PEX19-mediated nuclear relocalisation of several peroxisomal membrane protein substrates, in this instance elicited by the introduction of an artificial NLS motif into PEX19, which was used to help identify class 1 peroxisomal-membrane proteins (Jones et al., 2004). The effect of Bat3 expression in *S. cerevisiae* strongly supports a model where the association of TA proteins with Bat3 influences their subsequent fate in vivo.

We found that the effect of Bat3 is comparable in the absence of any of known cytosolic and/or peripheral-ER-membrane components of the GET pathway (Get3, Get4 and Get5) (Jonikas et al., 2009; Rabu et al., 2009; Schuldiner et al., 2008). The simplest explanation of these data is that full-length Bat3 can associate with GFP-Sed5 independently of Get3, Get4 or Get5, with the resulting complex entering the nucleus by virtue of the NLS present in Bat3, thereby reducing the level of cytosolic GFP-Sed5 when the GET pathway is non-functional. This hypothesis is in good agreement with a ‘high-confidence’ interaction identified

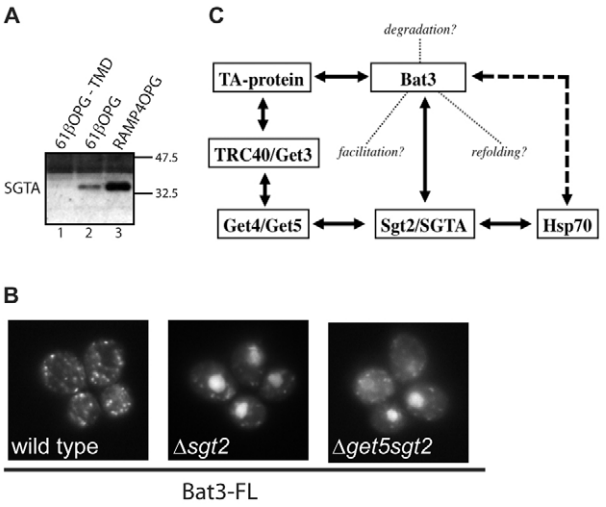

Fig. 7. Bat3 relocalisation of GFP-Sed5 is independent of Sgt2. (**A**) Reticulocyte-lysate components eluted from recombinant TA proteins with or without a TA segment (see Fig. 2) were analysed for the presence of SGTA by immunoblotting. (**B**) Live-cell imaging of GFP-Sed5 in wild-type, *Δsgt2 and Δmdy2sgt2 S. cerevisiae* expressing full-length human Bat3. (**C**) Summary of potential interactions between TA proteins, Bat3, SGTA/Sgt2, Hsp70 and components of the TRC40/GET pathway (see Chang et al., 2010; Corduan et al., 2009; Costanzo et al., 2010; Favaloro et al., 2008; Jonikas et al., 2009; Sasaki et al., 2008; Schuldiner et al., 2008; Stefanovic and Hegde, 2007; Stelzl et al., 2005; Winnefeld et al., 2006). Solid lines indicate known or presumed physical interactions, the dashed line, a regulatory interaction and the dotted lines indicate possible contributions of Bat3 to TA-protein biogenesis.

between Bat3 and syntaxin 5A, the human homologue of Sed5, using a yeast two-hybrid approach (Stelzl et al., 2005). Two recent publications identify the yeast protein Sgt2 as a component of the GET pathway for TA-protein biogenesis (Chang et al., 2010; Costanzo et al., 2010), providing an alternative model for our observations when Bat3 is expressed in yeast. Specifically, Bat3 interacts with the mammalian equivalent of Sgt2, SGTA (Winnefeld et al., 2006), providing a potential intermediary between the TRC40/GET pathway and Bat3 (Fig. 7C). Although we found that mammalian SGTA preferentially associates with hydrophobic TA segments, the Bat3-dependent relocalisation of TA proteins in yeast does not require Sgt2, and in fact the loss of Sgt2 alone is sufficient to enable Bat3-mediated relocalisation to occur. These data strongly support a role for Sgt2 in the yeast GET pathway (Chang et al., 2010; Costanzo et al., 2010), and indicate that SGTA might have a similar role in higher eukaryotes (Fig. 5A; Fig. 7C). However, the association of Bat3 with GFP-Sed5 in yeast, and its redirection to the nucleus does not require Sgt2. We conclude that either the association of Bat3 with TA proteins observed in yeast is direct, as previously suggested (Stelzl et al., 2005), or that the process involves some other functionally conserved component associated with or regulated by Bat3, for example Hsp/Hsc70 (Corduan et al., 2009; Sasaki et al., 2008).

Although we can only speculate about the precise role(s) of Bat3 during TA-protein biogenesis, the following scenarios provide a basis for further experimentation. Our current results suggest that Bat3 is not stably associated with other components of the TRC40 pathway (Fig. 5A; Fig. 7C); however, Bat3 might modulate or enhance particular steps in the TRC40 cycle for TA-protein delivery to the ER (Rabu et al., 2009). Hence, Bat3 could facilitate the formation of a productive TRC40-substrate ER-delivery complex (Rabu et al., 2009), or promote the interaction of the assembled complex with the ER membrane. If so, then the role of Bat3 can be circumvented by the co-expression of TRC40/Get3 and a TA-protein substrate in *E. coli*, because this results in a functional ER-delivery complex (Bozkurt et al., 2009; Favaloro et al., 2010). Alternatively, Bat3 could contribute to the recycling of the TRC40 complex by facilitating its release from the, as yet unidentified, mammalian ER-membrane receptor after delivery of TA protein has occurred (Rabu et al., 2009). Equally, the association of selected TA proteins with Bat3 might in fact represent an alternative and complementary fate to TRC40 binding. In this scenario, association with Bat3 could provide aberrant or misfolded TA proteins with an opportunity for refolding and return to the TRC40 pathway (Fig. 7C), most likely via the actions of Hsp/Hsc70 chaperones (Corduan et al., 2009; Sasaki et al., 2008). Removal of Bat3 from our *in vitro* system could cause the TRC40 pool to be titrated out by binding aberrant TA proteins to form complexes that are incapable of authentic ER delivery. Bat3 might also regulate the entry of aggregated or terminally misfolded TA proteins into a degradative pathway (Fig. 7C) (Auld et al., 2006), which is consistent with the presence of its N-terminal ubiquitin-like domain (Kabbage and Dickman, 2008).

Whatever the precise role of Bat3 during TA-protein biogenesis, the presence of a C-terminal BAG domain provides an opportunity for its regulation via several cellular components, including Hsp70 (Kabbage and Dickman, 2008). Intriguingly, the so-called BAG domain, found in various proteins, including Bat3, was first identified via its interaction with Bcl-2, a TA protein (Janiak et al., 1994) implicated in the regulation of apoptosis (Heath-Engel et al., 2008). Hence, one could speculate that the modulation of apoptosis and proliferation ascribed to Bat3 (Scythe) (Desmots et al., 2005) might reflect a BAG-domain-dependent interaction with TA proteins such as Bcl-2. Interestingly, our previous studies suggest that, similarly to Cytb5, Bcl2 is not an obligatory client of the generic TRC40-mediated pathway (Rabu et al., 2008), and on this basis it seems unlikely that Bat3 will influence the membrane integration of Bcl2 in a similar fashion to Sec61β. It is becoming increasingly apparent that the biogenesis of TA proteins is a remarkably complex and multifaceted process. Defining the precise function of Bat3 during this process and understanding this in the context of its various other cellular roles will be a major focus of our future efforts.

Materials and Methods

Materials

Bacterial expression vector, pHisTrx, was a gift from Richard Kammerer (University of Manchester, Manchester, UK). Rabbit polyclonal antisera recognising TRC40 (Asna-1) was a gift from Bernhard Dobberstein (ZMBH, Heidelberg, Germany) and the monoclonal anti-opsin tag antibody (Adamus et al., 1991) was provided by Paul Hargrave (Department of Ophthalmology, University of Florida, FL). Commercial antibodies were used to detect Hsp/Hsc70 and Hsp40 (Stressgen), SRP54 (BD Biosciences), Bat3 (Abcam), yeast Pgk1 (Invitrogen) and GFP (ab290, Abcam). Nuclease-treated rabbit reticulocyte lysate for in vitro translation was from Promega, rabbit reticulocyte untreated lysate was from Green Hectares.

Protein expression and purification

cDNAs encoding single cysteine variants of Sec61β, Sec61β lacking the tail anchor, RAMP4 and cytochrome b5, in each case including an in-frame opsin tag at the 3′ end (see supplementary material Fig. S1A), were subcloned into the pHisTrx expression vector and all constructs confirmed by DNA sequencing. The proteins were expressed in *Escherichia coli* strain BLR (DE3) pLysS cells by IPTG induction, and after harvesting cells were lysed in buffer A [50 mM Tris-HCl, pH 7.4, 300 mM

NaCl, 10 mM $MgCl_2$, 10 mM imidazole, 5 mM 2-ME, 1 mM PMSF, 10 % (v/v) glycerol] supplemented with 0.2 mg/ml lysozyme, 15 U/ml DNase I, complete protease inhibitor cocktail (Roche) and 1% (w/v) dodecyl-β-D-maltopyranoside (DDM) for 1 hour at room temperature followed by three passes through a 25-gauge needle. Insoluble material was pelleted (30 min; 10,000 ***g*** at 4°C) and the His-tagged recombinant proteins isolated by binding to nickel-NTA resin and extensive washing with buffer B [50 mM Tris-HCl, pH 7.4, 300 mM NaCl, 10 mM imidazole, 10% (v/v) glycerol] supplemented with 0.1% (w/v) DDM. For the purification of recombinant RAMP4OPG, subsequent buffers contained 0.1% (w/v) DDM throughout the subsequent procedures. For Sec61βOPG and Cytb5OPG, the detergent was exchanged to 0.75% (w/v) octyl-β-D-glucopyranoside or 0.1% n-dodecyl-N,N-dimethylamine-N-oxide respectively, by extensive washing of the beads using buffer B supplemented with the appropriate detergent. For the Sec61βOPG variant lacking the tail anchor, Triton X-100 was used in place of DDM through out the procedure [1% (w/v) during cell lysis and 0.1% (w/v) during subsequent steps].

To release the recombinant proteins from the resin, beads resuspended in buffer B supplemented with the appropriate detergent were incubated with 15 U thrombin per ml of suspension overnight at room temperature. The resin was then isolated by centrifugation, and the thrombin either inactivated by the addition of PMSF or removed by incubating the supernatant with Benzamidine Sepharose (1 hour, 4°C). The resulting solution was then centrifuged at 100,000 ***g*** for 1 hour at 4°C to remove any aggregates. Protein concentration was estimated by absorbance at 280 nm and/or Coomassie Brilliant Blue staining of SDS-PAGE gels using lysozyme as a standard. Proteins were aliquoted, frozen in liquid N_2 and stored at –80°C.

Membrane-integration reaction

Integration reactions comprised of 1.9 µM Sec61β-OPG, or 0.5 µM Cytb5-OPG, 5 µl sheep pancreatic microsomes (final concentration of ~3.5 OD_{280} per ml) (Kaderbhai et al., 1995) and rabbit reticulocyte lysate (Promega) made up to 30 µl, unless stated otherwise. The reactions were incubated at 30°C for 4 hours and then the membrane fraction recovered by centrifugation through a 140 µl HSC cushion (750 mM sucrose, 500 mM potassium acetate, 5 mM magnesium acetate, 50 mM HEPES-KOH, pH 7.9) for 10 minutes at 120,000 ***g*** and 4°C. Where appropriate, the membrane fraction was resuspended in 32 µl LSC buffer (250 mM sucrose, 100 mM potassium acetate, 5 mM magnesium acetate, 50 mM HEPES-KOH, pH 7.9), split in two and one half treated with Endoglycosidase H (New England Biolabs) as described by the supplier. All samples were solubilised in Laemmli buffer and resolved by SDS-PAGE before detection by immunoblotting.

Identification of cytosolic factors interacting with TA proteins

Recombinant proteins were immobilized via amino groups on 10 mg of UltraLink Biosupport (Pierce) according to manufacturer's instruction. The estimated concentration of bound proteins was: Sec61β-OPG, 0.9 mg/ml; Sec61β-OPG-TMD, 1.67 mg/ml; RAMP4-OPG, 0.99 mg/ml. Beads were stored in 800 µl buffer R (50 mM HEPES-KOH, pH 7.5, 40 mM potassium acetate, 5 mM $MgCl_2$) with 0.1% (v/v) Triton X-100. For the pull-down experiment one third of the beads (about 25 µl volume) was washed with buffer R alone to remove detergent, then incubated with 800 µl of untreated rabbit reticulocyte lysate (Green Hectares, Oregon) supplemented with an energy regeneration system (1 mM ATP, 100 µM GTP, 10 mM creatine phosphate and 100 µg/ml creatine phosphokinase) for 2 hours at 4°C. The beads were washed three times with 1 ml buffer R and the remaining proteins eluted with 128 µl buffer R supplemented with 0.1% (v/v) Triton X-100. Eluted material was TCA precipitated, solubilised in Laemmli buffer and resolved by SDS-PAGE followed by Coomassie Brilliant Blue staining. Proteins that appeared to interact specifically with full-length TA proteins were excised and analysed by mass spectrometry following in-gel trypsin digestion.

Immunodepletion of cytosolic factors from rabbit reticulocyte lysate

20 µl (bead volume) of Protein-A-Sepharose was mixed with 120 µg rabbit anti-chicken antibody and incubated for 1 hour at 4°C. The beads were then washed with buffer R to remove any unbound antibody and 120 µl rabbit reticulocyte lysate (Promega), pre-incubated for 1 hour at 4°C with 5, 10 or 15 µg of chicken anti-Bat3 or chicken anti-SSBP1 control antibody was added as indicated. The beads and lysates were further incubated for 1 hour at 4°C, the Protein-A-Sepharose pelleted by centrifugation and the resulting immunodepleted lysates used in the membrane integration reaction as previously described. TRC40 (Asna-1) was similarly depleted by a 1 hour incubation of 120 µl rabbit reticulocyte lysate with 20 µl (bead volume) Protein-A-Sepharose-coated with anti-TRC40 antibody. Beads coated with an equivalent amount of non-related rabbit serum were used for control reactions.

Depletion of cytosolic factors from rabbit reticulocyte lysate by resin treatment

75 µl rabbit reticulocyte lysate (Promega) was incubated for 2 hours at 4°C with 30 µl of the indicated resins [50% (v/v) suspensions] previously equilibrated with buffer R. Unbound material was collected and analysed for cytosolic components of interest by immunoblotting or tested for function in a membrane-integration assay using recombinant Sec61β-OPG. For add-back experiments, 100 µl Cibacron Blue agarose [50% (v/v) suspension] was incubated with 250 µl of rabbit reticulocyte lysate (Promega) for 2 hours at 4°C, the beads were then washed three times in buffer R and bound material eluted with 100 µl buffer R supplemented with 1.5 M NaCl. After desalting 5 µl of the eluate or equivalent buffer control was mixed with 20 µl of the Cibacron-treated rabbit reticulocyte lysate, and a membrane integration-assay performed.

Sucrose-gradient centrifugation

Sec61β-OPG was synthesised in a 100 µl reaction volume in vitro, as previously described (Rabu et al., 2008) and the material fractionated by centrifugation through a sucrose gradient using a modified version of the procedure described (Stefanovic and Hegde, 2007). Thirteen individual fractions were collected from the gradient (1=top, 13=bottom) whereas pelleted material (P) was resuspended directly into the Laemmli buffer. A portion of fraction was mixed with the Laemmli buffer and, after SDS-PAGE, the location of distinct cytosolic factors was determined by immunoblotting and the distribution of the radiolabelled Sec61β-OPG visualised by phosphorimaging. In a parallel experiment, 50 µl of each fraction was mixed with canine pancreas microsomes (final concentration of 2.0 OD_{280} per ml), incubated for 50 minutes at 30°C and the membrane fraction isolated as described for membrane integration reaction. Following SDS PAGE and quantitative phosphorimaging, the relative proportion of the total N-glycosylated material in each fraction was determined to provide a measure of the capacity for membrane integration for the Sec61β-OPG chains present in each fraction.

Bat3 expression and analysis in *S. cerevisiae*

The full-length version of Bat3, isoform 2, was obtained from Origene and cloned into the yeast expression vector p416Met25 (Mumberg et al., 1994) via the *Xba*I and *Xho*I restriction sites. For the Bat3-N1 fragment that lacked the C-terminus, a stop codon was introduced in place of residue 676 of the wild-type sequence. The Bat3 ΔNLS mutant was generated as previously described (Manchen and Hubberstey, 2001). GFP-Sed5 was expressed from plasmid pRS315 (Weinberger et al., 2005). All yeast strains used were derived from BY4741 (MATa *his3Δ1 leu2Δ0 met15Δ0 ura3Δ0*) (Brachmann et al., 1998). The respective deletion strains for *GET3* (*Δget3::Kan*^{R}), *GET4* (*Δget4::Kan*^{R}), *GET5/MDY2* (*Δget5/mdy2::Kan*^{R}) and *SGT2* (*Δsgt2::Kan*^{R}) were obtained from Euroscarf (Winzeler et al., 1999). A *Δsgt2::Kan*^{R} *Δget5/mdy2::Nat*^{R} double deletion was created using standard PCR-based replacement methods with plasmid pAG25 (Goldstein and McCusker, 1999).Yeast transformation and growth in synthetic complete medium lacking uracil and/or leucine followed well-established protocols (Ausubel et al., 1997), whereas total cell lysates for western blotting analysis were prepared as described (Yaffe and Schatz, 1984). Anti-Bat3 chicken antibody was used at 1:5000 and anti-Pgk1 mouse monoclonal at 1:2000; anti-chicken and anti-mouse horseradish-peroxidase conjugated secondary antibodies were used at 1:2500 and 1:5000, respectively. Immunofluorescence followed the method described (Roberts et al., 1991), except that cells were fixed for 1 hour in 4% formaldehyde. Attached spheroblasts were then incubated in ice-cold methanol for 6 minutes, followed by ice-cold acetone for 30 seconds. Anti-GFP and anti-Bat3 primary antibodies were diluted 1:1000, the respective anti-rabbit (Alexa Fluor 488, Invitrogen) and anti-chicken (Alexa Fluor 594, Invitrogen) secondary antibodies 1:500. Stained spheroplasts were mounted in SlowFade Gold antifade reagent containing DAPI (Invitrogen). Live-cell imaging of yeast cells was performed at room temperature in synthetic complete medium employing a DeltaVison restoration microscope equipped with a 100×, 0.35-1.5 Uplan Apo objective and a GFP filter set (Chroma 86006). The images were collected with a Coolsnap HQ camera (Photometrics). The same set-up was used to image immunostained spheroplasts for which stacks with Z optical spacing of 0.3 µm were acquired. Raw images were deconvolved using the additive algorithm of Softworx software.

This work was supported by a PhD studentship (P.L.) and Senior Fellowship (B.S.) from the Wellcome Trust. Mass spectrometry was performed by the biomolecular analysis core facility and microscopy in the bioimaging facility at the Faculty of Life Sciences. We thank Richard Kammerer for guidance regarding *E. coli* expression systems, Quentin Roebuck for technical assistance, Martin Pool, Lisa Swanton and Phil Woodman for their comments during manuscript preparation, and all of our colleagues who provided reagents and advice. Deposited in PMC for release after 6 months.

Note added in proof

A recent phylogenetic analysis (Borgese and Righi, 2010) suggests that the membrane insertion of TA proteins in prokaryotes either occurs through an unassisted pathway or is mediated by Hsp40 and Hsp70s.

Supplementary material available online at
http://jcs.biologists.org/cgi/content/full/123/13/2170/DC1

References

Abell, B. M., Pool, M. R., Schlenker, O., Sinning, I. and High, S. (2004). Signal recognition particle mediates post-translational targeting in eukaryotes. *EMBO J.* **23**, 2755-2764.

Abell, B. M., Rabu, C., Leznicki, P., Young, J. C. and High, S. (2007). Post-translational integration of tail-anchored proteins is facilitated by defined molecular chaperones. *J. Cell Sci.* **120**, 1743-1751.

Adamus, G., Zam, Z. S., Arendt, A., Palczewski, K., McDowell, J. H. and Hargrave, P. A. (1991). Anti-rhodopsin monoclonal antibodies of defined specificity: characterization and application. *Vision Res.* **31**, 17-31.

Auld, K. L., Hitchcock, A. L., Doherty, H. K., Frietze, S., Huang, L. S. and Silver, P. A. (2006). The conserved ATPase Get3/Arr4 modulates the activity of membrane-associated proteins in Saccharomyces cerevisiae. *Genetics* **174**, 215-227.

Ausubel, F. M., Brent, R., Kingston, R. E., Moore, D. D., Seidman, J. G., Smith, J. A. and Struhl, K. (1997). *Current Protocols in Molecular Biology*. New York: Greene Publishing Associates and Wiley-Interscience.

Behrens, T. W., Kearns, G. M., Rivard, J. J., Bernstein, H. D., Yewdell, J. W. and Staudt, L. M. (1996). Carboxyl-terminal targeting and novel post-translational processing of JAW1, a lymphoid protein of the endoplasmic reticulum. *J. Biol. Chem.* **271**, 23528-23534.

Borgese, N., Brambillasca, S. and Colombo, S. (2007). How tails guide tail-anchored proteins to their destinations. *Curr. Opin. Cell Biol.* **19**, 368-375.

Borgese, N. and Righi, R. (2010). Remote origins of tail-anchored proteins. *Traffic* [Epub ahead of print] doi: 10.1111/j.1600-0854.2010.01068.x.

Bozkurt, G., Stjepanovic, G., Vilardi, F., Amlacher, S., Wild, K., Bange, G., Favaloro, V., Rippe, K., Hurt, E., Dobberstein, B. et al. (2009). Structural insights into tail-anchored protein binding and membrane insertion by Get3. *Proc. Natl. Acad. Sci. USA* **106**, 21131-21136.

Brachmann, C. B., Davies, A., Cost, G. J., Caputo, E., Li, J., Hieter, P. and Boeke, J. D. (1998). Designer deletion strains derived from Saccharomyces cerevisiae S288C: a useful set of strains and plasmids for PCR-mediated gene disruption and other applications. *Yeast* **14**, 115-132.

Chang, Y. W., Chuang, Y. C., Ho, Y. C., Cheng, M. Y., Sun, Y. J., Hsiao, C. D. and Wang, C. (2010). Crystal structure of Get4/Get5 complex and its interactions with Sgt2, Get3 and Ydj1. *J. Biol. Chem.* **285**, 9962-9970.

Colombo, S. F., Longhi, R. and Borgese, N. (2009). The role of cytosolic proteins in the insertion of tail-anchored proteins into phospholipid bilayers. *J. Cell Sci.* **122**, 2383-2392.

Corduan, A., Lecomte, S., Martin, C., Michel, D. and Desmots, F. (2009). Sequential interplay between BAG6 and HSP70 upon heat shock. *Cell. Mol. Life Sci.* **66**, 1998-2004.

Costanzo, M., Baryshnikova, A., Bellay, J., Kim, Y., Spear, E. D., Sevier, C. S., Ding, H., Koh, J. L., Toufighi, K., Mostafavi, S. et al. (2010). The genetic landscape of a cell. *Science* **327**, 425-431.

Cross, B. C., Sinning, I., Luirink, J. and High, S. (2009). Delivering proteins for export from the cytosol. *Nat. Rev. Mol. Cell Biol.* **10**, 255-264.

Desmots, F., Russell, H. R., Lee, Y., Boyd, K. and McKinnon, P. J. (2005). The reaper-binding protein scythe modulates apoptosis and proliferation during mammalian development. *Mol. Cell. Biol.* **25**, 10329-10337.

Desmots, F., Russell, H. R., Michel, D. and McKinnon, P. J. (2008). Scythe regulates apoptosis-inducing factor stability during endoplasmic reticulum stress-induced apoptosis. *J. Biol. Chem.* **283**, 3264-3271.

Favaloro, V., Spasic, M., Schwappach, B. and Dobberstein, B. (2008). Distinct targeting pathways for the membrane insertion of tail-anchored (TA) proteins. *J. Cell Sci.* **121**, 1832-1840.

Favaloro, V., Vilardi, F., Schlecht, R., Mayer, M. P. and Dobberstein, B. (2010). Asna1/TRC40-mediated membrane insertion of tail-anchored proteins. *J. Cell Sci.* **123**, 1522-1530.

Goldstein, A. L. and McCusker, J. H. (1999). Three new dominant drug resistance cassettes for gene disruption in Saccharomyces cerevisiae. *Yeast* **15**, 1541-1553.

Gorlich, D., Prehn, S., Laskey, R. A. and Hartmann, E. (1994). Isolation of a protein that is essential for the first step of nuclear protein import. *Cell* **79**, 767-778.

Heath-Engel, H. M., Chang, N. C. and Shore, G. C. (2008). The endoplasmic reticulum in apoptosis and autophagy: role of the BCL-2 protein family. *Oncogene* **27**, 6419-6433.

Hu, J., Li, J., Qian, X., Denic, V. and Sha, B. (2009). The crystal structures of yeast Get3 suggest a mechanism for tail-anchored protein membrane insertion. *PLoS One* **4**, e8061.

Hu, Z., Potthoff, B., Hollenberg, C. P. and Ramezani-Rad, M. (2006). Mdy2, a ubiquitin-like (UBL)-domain protein, is required for efficient mating in Saccharomyces cerevisiae. *J. Cell Sci.* **119**, 326-338.

Janiak, F., Leber, B. and Andrews, D. W. (1994). Assembly of Bcl-2 into microsomal and outer mitochondrial membranes. *J. Biol. Chem.* **269**, 9842-9849.

Jones, J. M., Morrell, J. C. and Gould, S. J. (2004). PEX19 is a predominantly cytosolic chaperone and import receptor for class 1 peroxisomal membrane proteins. *J. Cell Biol.* **164**, 57-67.

Jonikas, M. C., Collins, S. R., Denic, V., Oh, E., Quan, E. M., Schmid, V., Weibezahn, J., Schwappach, B., Walter, P., Weissman, J. S. et al. (2009). Comprehensive characterization of genes required for protein folding in the endoplasmic reticulum. *Science* **323**, 1693-1697.

Kabbage, M. and Dickman, M. B. (2008). The BAG proteins: a ubiquitous family of chaperone regulators. *Cell Mol. Life Sci.* **65**, 1390-1402.

Kaderbhai, M. A., Harding, V. J., Karim, A., Austen, B. M. and Kaderbhai, N. N. (1995). Sheep pancreatic microsomes as an alternative to the dog source for studying protein translocation. *Biochem. J.* **306**, 57-61.

Kutay, U., Hartmann, E. and Rapoport, T. A. (1993). A class of membrane proteins with a C-terminal anchor. *Trends Cell Biol.* **3**, 72-75.

Kutay, U., Ahnert-Hilger, G., Hartmann, E., Wiedenmann, B. and Rapoport, T. A. (1995). Transport route for synaptobrevin via a novel pathway of insertion into the endoplasmic reticulum membrane. *EMBO J.* **14**, 217-223.

Linstedt, A. D., Foguet, M., Renz, M., Seelig, H. P., Glick, B. S. and Hauri, H. P. (1995). A C-terminally-anchored Golgi protein is inserted into the endoplasmic reticulum and then transported to the Golgi apparatus. *Proc. Natl. Acad. Sci. USA* **92**, 5102-5105.

Manchen, S. T. and Hubberstey, A. V. (2001). Human Scythe contains a functional nuclear localization sequence and remains in the nucleus during staurosporine-induced apoptosis. *Biochem. Biophys. Res. Commun.* **287**, 1075-1082.

Mateja, A., Szlachcic, A., Downing, M. E., Dobosz, M., Mariappan, M., Hegde, R. S. and Keenan, R. J. (2009). The structural basis of tail-anchored membrane protein recognition by Get3. *Nature* **461**, 361-366.

Mumberg, D., Muller, R. and Funk, M. (1994). Regulatable promoters of Saccharomyces cerevisiae: comparison of transcriptional activity and their use for heterologous expression. *Nucleic Acids Res.* **22**, 5767-5768.

Rabu, C., Wipf, P., Brodsky, J. L. and High, S. (2008). A Precursor-specific Role for Hsp40/Hsc70 during Tail-anchored Protein Integration at the Endoplasmic Reticulum. *J. Biol. Chem.* **283**, 27504-27513.

Rabu, C., Schmid, V., Schwappach, B. and High, S. (2009). Biogenesis of tail-anchored proteins: the beginning for the end? *J. Cell Sci.* **122**, 3605-3612.

Roberts, C. J., Raymond, C. K., Yamashiro, C. T. and Stevens, T. H. (1991). Methods for studying the yeast vacuole. *Methods Enzymol.* **194**, 644-661.

Sasaki, T., Marcon, E., McQuire, T., Arai, Y., Moens, P. B. and Okada, H. (2008). Bat3 deficiency accelerates the degradation of Hsp70-2/HspA2 during spermatogenesis. *J. Cell Biol.* **182**, 449-458.

Schuldiner, M., Metz, J., Schmid, V., Denic, V., Rakwalska, M., Schmitt, H. D., Schwappach, B. and Weissman, J. S. (2008). The GET complex mediates insertion of tail-anchored proteins into the ER membrane. *Cell* **134**, 634-645.

Simhadri, V. R., Reiners, K. S., Hansen, H. P., Topolar, D., Simhadri, V. L., Nohroudi, K., Kufer, T. A., Engert, A. and Pogge von Strandmann, E. (2008). Dendritic cells release HLA-B-associated transcript-3 positive exosomes to regulate natural killer function. *PLoS One* **3**, e3377.

Sowa, M. E., Bennett, E. J., Gygi, S. P. and Harper, J. W. (2009). Defining the human deubiquitinating enzyme interaction landscape. *Cell* **138**, 389-403.

Stefanovic, S. and Hegde, R. S. (2007). Identification of a targeting factor for posttranslational membrane protein insertion into the ER. *Cell* **128**, 1147-1159.

Stelzl, U., Worm, U., Lalowski, M., Haenig, C., Brembeck, F. H., Goehler, H., Stroedicke, M., Zenkner, M., Schoenherr, A., Koeppen, S. et al. (2005). A human protein-protein interaction network: a resource for annotating the proteome. *Cell* **122**, 957-968.

Suloway, C. J., Chartron, J. W., Zaslaver, M. and Clemons, W. M., Jr (2009). Model for eukaryotic tail-anchored protein binding based on the structure of Get3. *Proc. Natl. Acad. Sci. USA* **106**, 14849-14854.

Weinberger, A., Kamena, F., Kama, R., Spang, A. and Gerst, J. E. (2005). Control of Golgi morphology and function by Sed5 t-SNARE phosphorylation. *Mol. Biol. Cell* **16**, 4918-4930.

Winnefeld, M., Grewenig, A., Schnolzer, M., Spring, H., Knoch, T. A., Gan, E. C., Rommelaere, J. and Cziepluch, C. (2006). Human SGT interacts with Bag-6/Bat-3/Scythe and cells with reduced levels of either protein display persistence of few misaligned chromosomes and mitotic arrest. *Exp. Cell Res.* **312**, 2500-2514.

Winzeler, E. A., Shoemaker, D. D., Astromoff, A., Liang, H., Anderson, K., Andre, B., Bangham, R., Benito, R., Boeke, J. D., Bussey, H. et al. (1999). Functional characterization of the S. cerevisiae genome by gene deletion and parallel analysis. *Science* **285**, 901-906.

Yaffe, M. P. and Schatz, G. (1984). Two nuclear mutations that block mitochondrial protein import in yeast. *Proc. Natl. Acad. Sci. USA* **81**, 4819-4823.

Bat3 promotes the membrane integration of tail-anchored proteins

*Pawel Leznicki, Anne Clancy, Blanche Schwappach and Stephen High**

Supplementary Figure Legends

Figure S1. Expression and purification of recombinant Sec61βOPG.

A) Sequences of tail-anchored protein derivatives used in this study. Predicated transmembrane domains are highlighted in yellow and the opsin N-glycosylation tag derived from bovine opsin (OPG) is in green font. For Sec61βOPG, an endogenous cysteine at residue 39 was mutated to a serine and an endogenous serine at residue 77 was replaced with a cysteine whilst for cytochrome b5 (Cytb5) serine 119 was altered to a cysteine (all changes shown in red font). B) Sec61βOPG in pHisTrx vector was expressed in *E.coli* and the resulting fusion protein purified on NiNTA agarose before removal of the HisTrx tag using thrombin. The purified protein was resolved on SDS-PAGE and stained with Coomassie Brilliant Blue, full-length and N-terminally truncated forms of Sec61βOPG are indicated. A minor contaminant corresponding to *E. coli* DnaK is also identified (•), the removal of this component by an additional step of ion exchange chromatography did not alter the membrane integration properties of the resulting recombinant protein preparation (our unpublished data). C) The ability of recombinant Sec61βOPG to integrate into sheep pancreatic microsomes in the presence of rabbit reticulocyte lysate was determined using N-glycosylation of the C-terminal OPG tag. N-glycosylation was confirmed by EndoH digestion, and the N-glycosylated (+gly), non-glycosylated (-gly) and truncated forms (trunc.) of Sec61βOPG are shown.

Figure S2. NiNTA agarose binding profile of the Cibacron-eluted material.

Cibacron Blue Agarose (600 µl) was incubated with 5 ml of rabbit reticulocyte lysate for 2 hours at 4°C, the beads were then extensively washed and the bound proteins eluted with 1.5 M NaCl (480 µl). The eluate was desalted, concentration of imidazole adjusted to 5 mM and the resulting protein solution incubated with NiNTA agarose (100 µl bead volume). The unbound fraction was collected, beads washed and the bound proteins eluted using a step-wise gradient of increasing imidazole concentrations from 10 mM to 500 mM. After desalting, 5 µl of lysates and 10 µl from each fraction were run on an SDS-PAGE gel that was later stained with Coomassie Brilliant Blue (panel A). In parallel, 2 µl from each fraction were used for immunoblotting with anti-Bat3 antibody (panel B). The capacity of each fraction to restore the integration competence of the Cibacron-treated lysate was tested (see panel C) by adding 5 µl of buffer R as a control (lane 2), or 5 µl from each of the fractions indicated (lanes 3 to 10), to 20 µl of the Cibacron-treated lysate and then

carrying out a Sec61βOPG integration reaction and visualising the results by immunobloting with anti-opsin antibody (cf. Figures 3 and 4 of main text).

Figure S3. Immunofluorescence analysis of Bat3 and GFP-Sed5 in S. cerevisiae

The subcellular localisation of full-length Bat3 (panel A) and an N-terminal fragment of Bat3 (panel B) (cf. Figure 6A) was determined by immunofluorescence microscopy in *Δmdy2* (*Δget5*) strain and compared to a DAPI staining of the nucleus. C) The subcellular localisations of full-length Bat3 and GFP-Sed5 were determined by immunofluorescence microscopy in wild-type and *Δmdy2* (*Δget5*) cells that were also stained with DAPI to reveal the nucleus. D) The subcellular localisation of a Bat3 ΔNLS mutant was determined as described for panels A and B. E) Immunoblot confirming efficient expression of the Bat3 ΔNLS mutant in *Δmdy2* (*Δget5*) *S. cerevisiae* cells.

A

Protein (species)	Sequence
Sec61βOPG full length (human)	GSPGPTPSGTNVGSSGRSPSKAVAARAAGSTVRQRKNASSGT RSAGRTTSAGTGGMWRFYTEDSPGLKVGPVPVLVMCLLFIAS VFMLHIWGKYTRSGPNFYVPFSNKTG
Sec61βOPG no TMD (human)	GSPGPTPSGTNVGSSGRSPSKAVAARAAGSTVRQRKNASSGT RSAGRTTSAGTGGMWRFYTEDSPGLKVGPGPNFYVPFSNKTG
RAMP4OPG (mouse)	GSVAKQRIRMANEKHSKNITQRGNVAKTSRNAPEEKASVGPW LLALFIFVVCGSAIFQIIQSIRMGMGPNFYVPFSNKTG
Cytb5OPG (human)	GSAEQSDEAVKYYTLEEIQKHNHSKSTWLILHHKVYDLTKFL EEHPGGEEVLREQAGGDATENFEDVGHSTDAREMSKTFIIGE LHPDDRPKLNKPPETLITTIDSSSSWWTNWVIPAICAVAVAL MYRLYMAEDGPNFYVPFSNKTG

B

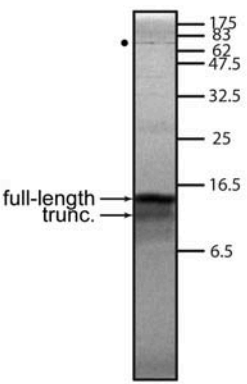

C

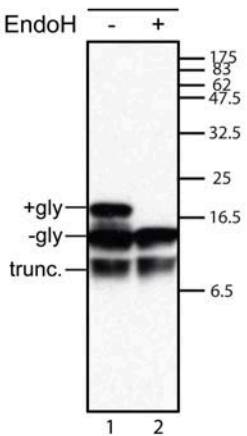

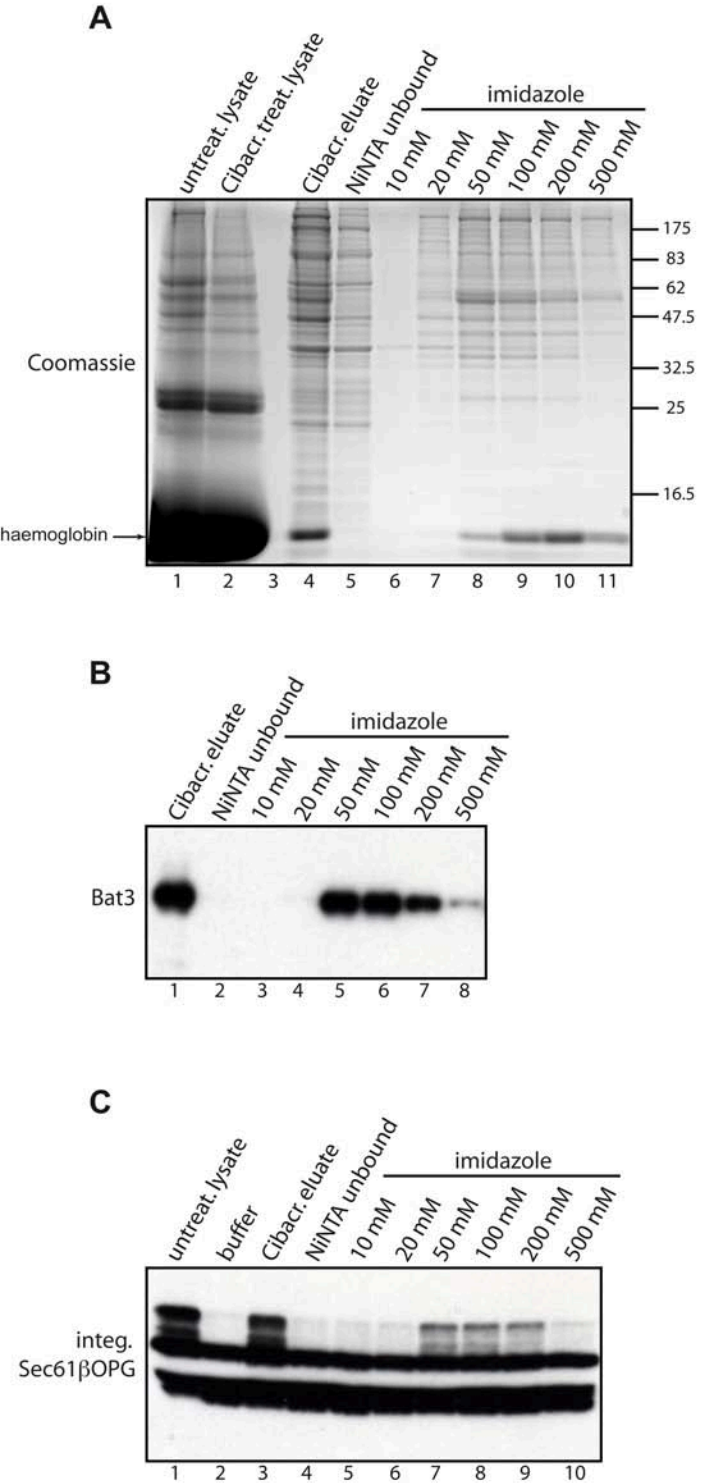
A
untreat. lysate
Cibacr. treat. lysate
Cibacr. eluate
NiNTA unbound
imidazole
10 mM
20 mM
50 mM
100 mM
200 mM
500 mM
175
83
62
47.5
32.5
25
16.5
Coomassie
haemoglobin
1 2 3 4 5 6 7 8 9 10 11
B
Cibacr. eluate
NiNTA unbound
imidazole
10 mM
20 mM
50 mM
100 mM
200 mM
500 mM
Bat3
1 2 3 4 5 6 7 8
C
untreat. lysate
buffer
Cibacr. eluate
NiNTA unbound
imidazole
10 mM
20 mM
50 mM
100 mM
200 mM
500 mM
integ.
Sec61βOPG
1 2 3 4 5 6 7 8 9 10

Figure S3

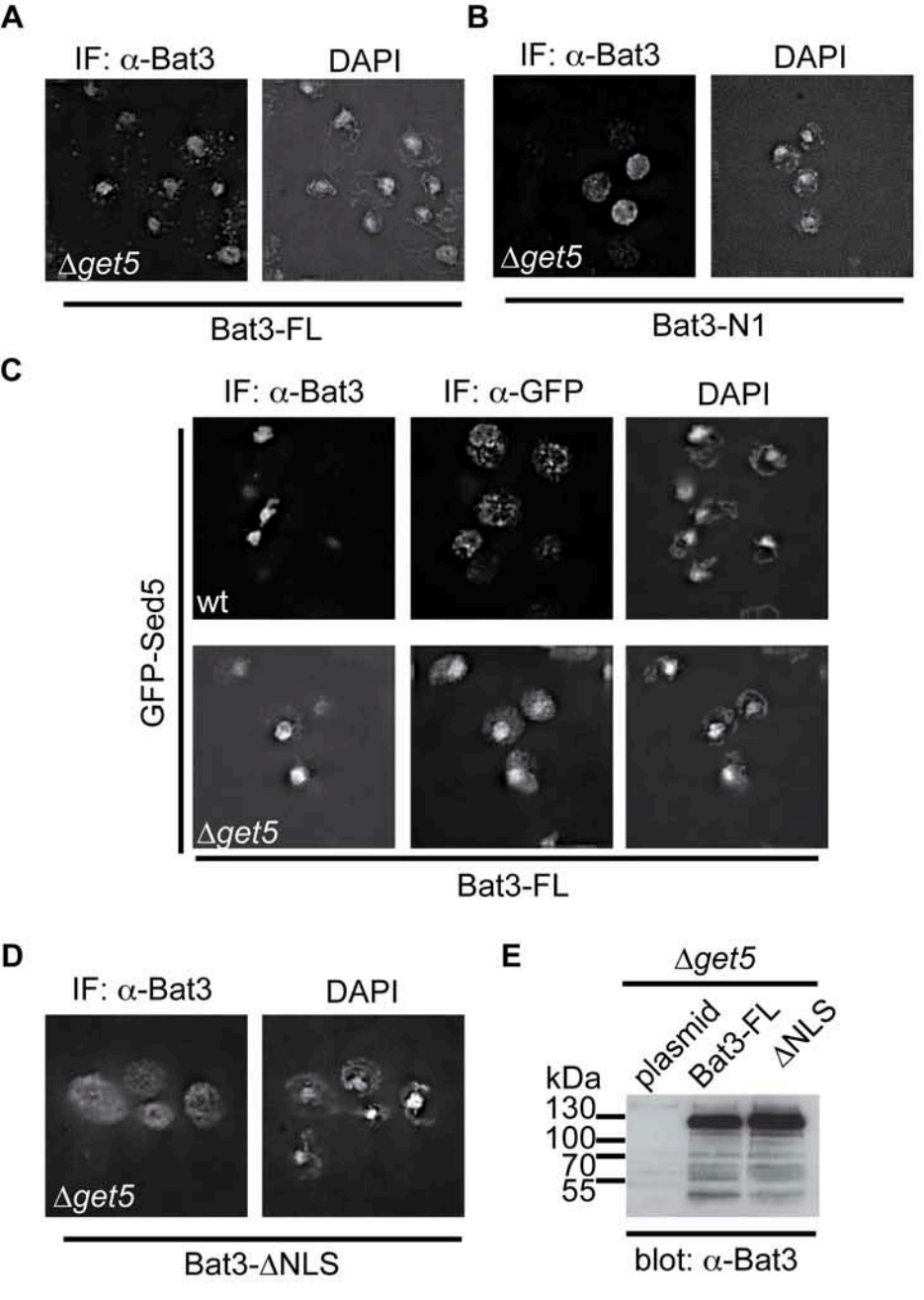
A
IF: α-Bat3
DAPI
Δget5
Bat3-FL
B
IF: α-Bat3
DAPI
Δget5
Bat3-N1
C
IF: α-Bat3
IF: α-GFP
DAPI
GFP-Sed5
wt
Δget5
Bat3-FL
D
IF: α-Bat3
DAPI
Δget5
Bat3-ΔNLS
E
Δget5
plasmid
Bat3-FL
ΔNLS
kDa
130
100
70
55
blot: α-Bat3

CHAPTER 2.4

Mass spectrometric analysis of the cytosolic interacting partners of tail-anchored proteins – Appendix to Chapter 2.3

In order to more comprehensively analyse the cytosolic interacting partners of TA-proteins, additional pull-down experiments using immobilised recombinant polypeptides were carried out as previously described (Chapter 2.3 and (Leznicki et al., 2010)). Full-length RAMP4OPG and Sec61βOPG were chosen as well-defined substrates of the TRC40-dependent pathway (Favaloro et al., 2008; Favaloro et al., 2010; Stefanovic and Hegde, 2007) whereas Sec61βOPG lacking the transmembrane and lumenal domains served as a negative control. Factors bound to immobilised TA-proteins were eluted sequentially, first with a high salt buffer, then with buffer supplemented with detergent, and finally with 6 M urea. When the resulting samples were resolved by SDS-PAGE a number of proteins appeared to preferentially associate with the two full-length TA-proteins as judged by the relative intensities of the Coomassie-stained products (see Figure 1). The identities of the most clearly enriched components were analysed by mass spectrometry (see Table 1 at the end of this chapter). This approach resulted in the identification of several components previously implicated in the biogenesis of TA-proteins such as TRC40 (Asna-1) and SRP (see Chapter 2.3). A number of other proteins that appeared to bind in a transmembrane segment (TMS)-dependent manner were also identified and these included, among others, Bat3, SGTA, DNAJC7, ubiquilin-1, Pex19 and TTC1 (Table 1 and see below).

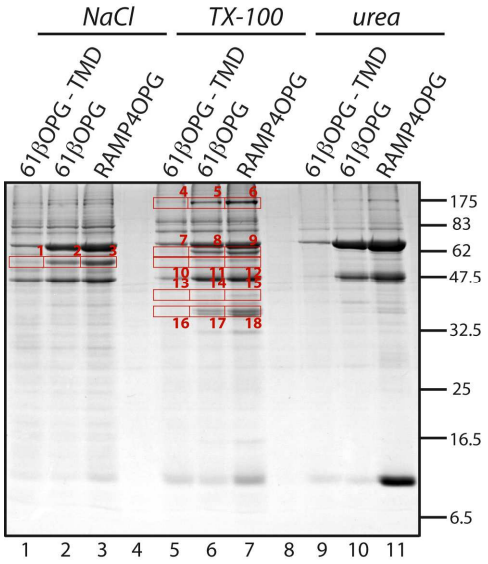

Figure 1. Cytosolic binding partners of TA-proteins that utilise the TRC40-dependent pathway.
Recombinant TA-proteins as indicated were coupled to UltraLink Biosupport via free amino groups and the beads then incubated with untreated rabbit reticulocyte lysate as previously described (Chapter 2.3 and (Leznicki et al., 2010)). Bound proteins were eluted in 64 µl of buffer R (50 mM HEPES-KOH, pH 7.5, 40 mM KOAc, 5 mM $MgCl_2$) containing 1 M NaCl, followed by elution with buffer R supplemented with 0.1% (v/v) Triton X-100 (TX-100) and, finally, with 6 M urea. The eluted proteins were TCA precipitated, resolved by SDS-PAGE and proteins preferentially bound to full-length TA-proteins were analysed by mass spectrometry. The bands that were excised and subjected to in-gel trypsin digestion and mass spectrometry are shown. The numbering of the bands corresponds to that used in Table 1.

To determine whether these components interacted specifically with TRC40 clients, pull-down experiments were also carried out using immobilised variants of Cytb5OPG (Figure 2A) and Syb2OPG (Figure 2B), two TA-proteins relying predominantly on the "unassisted"/chaperone-facilitated and SRP-mediated pathways, respectively (see Introduction and (Rabu et al., 2009)). Bound proteins were eluted as described above and components whose binding appeared to be enhanced in the presence of the TMS were again analysed by mass spectrometry (see Tables 2 and 3). Strikingly, evidence for an interaction of Cytb5OPG with Bat3 and SGTA could be detected (Table 2) even though our previous analysis (Chapter 2.3 and (Leznicki et al., 2010)) indicated that the depletion of Bat3 does not detectably affect Cytb5 membrane integration (see also below). A component that appeared to bind preferentially to full-length Cytb5OPG but was only marginally associated with other immobilised full-length TA-proteins was identified as DNAJB4 (Tables 2 and 3). This interaction with DNAJB4 was not further investigated due to the unavailability of suitable antibodies.

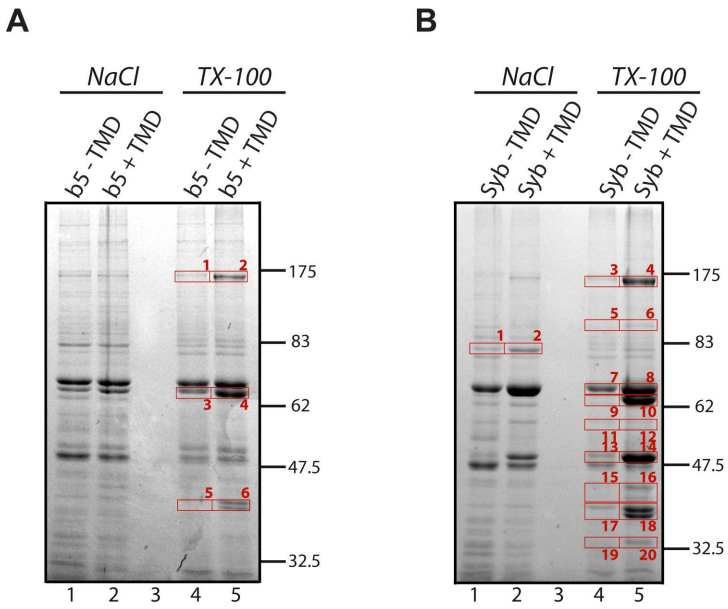

Figure 2. Cytosolic interactions of TA-proteins relying on alternative pathways for ER delivery. Binding of cytosolic factors to Cytb5OPG (A) and Syb2OPG (B) variants was investigated as described for Figure 1. The products that appeared to interact in a transmembrane segment-dependent manner were identified by mass spectrometry. The bands indicated were excised and analysed; the numbering corresponds to that used in Table 2 for Cytb5OPG and Table 3 for Syb2OPG.

A similar analysis of Syb2OPG interacting partners led to the identification of a number of proteins that were presumed to associate in a TMS-dependent manner (Figure 2B and Table 3). Many of these components were common for Syb2OPG, RAMP4OPG and Sec61βOPG, suggesting that Syb2 can use the TRC40-dependent pathway for its delivery to the ER membrane, as indicated by a previous study that defined an ATP-dependent route for its membrane integration (Kutay et al., 1995); and consistent with the hypothesis that different pathways for TA-protein membrane integration may be functionally redundant (Rabu et al., 2009). The ability of Syb2 to use the TRC40-dependent route is also further supported by the identification of the mammalian Get4 homologue, C7orf20, as an interacting partner of Syb2OPG (Table 3) (Chartron et al., 2010; Mariappan et al., 2010). However, an enrichment of SRP54, a subunit of the signal recognition particle, was also suggested when the pull-down assay was carried out using full-length Syb2OPG (see Table 3) consistent with the suggestion that Syb2 can also utilise a novel, post-translational function of SRP for its targeting to the ER (Abell et al., 2004). It is likely that the immobilised recombinant TA-proteins used for these pull-down assays are present in a significant excess over their cytosolic interacting partners. Under these circumstances, components of all potential delivery pathways available to these precursors may be isolated in such binding experiments. Whilst several of the components identified by mass spectrometry have been confirmed to associate preferentially with a polypeptide bearing a TMS ((Leznicki et al., 2010); see also Chapter 2.3 and below), the results described above and shown in Tables 1-3 should be treated as qualitative data only. Any estimations of the relative affinities of individual components for specific TA-proteins will require further investigation using additional techniques.

Based on published data, several proteins identified as TA-protein interacting partners deserve special consideration. Among these, Bat3, SGTA and C7orf20 were all shown to form a protein network with TRC40 (Sowa et al., 2009), suggesting their involvement in TA-protein delivery to the ER membrane via the TRC40-dependent route. This is also supported by the fact that C7orf20 is believed to be the mammalian equivalent of yeast Get4 (Chartron et al., 2010; Mariappan et al., 2010), whilst the yeast homologue of SGTA, Sgt2, was shown to be part of the GET pathway by several groups (Battle et al., 2010; Chang et al., 2010; Costanzo et al., 2010; Leznicki

et al., 2010). Our analysis of the role for Bat3 in TA-protein biogenesis (Chapter 2.3 and (Leznicki et al., 2010)) also suggests that at least some of the other components identified above may also participate in TA-protein delivery to the ER membrane.

A number of co-chaperones known to regulate the function of members of the Hsp70 and Hsp90 families were also identified in our mass spectrometric analysis. For example, SGTA, DNAJC7 and TTC1 all contain tetratricopeptide repeat (TPR) motifs that can mediate their interactions with Hsp70s and Hsp90s (Brychzy et al., 2003; Liou and Wang, 2005; Liu et al., 1999; Lotz et al., 2008). Moreover, DNAJC7 and other members of the DnaJ family (≈ Hsp40s) have a so-called J-domain that stimulates the ATPase activity of Hsp70s, and thus stabilises the binding of substrate to this major cellular chaperone (Brychzy et al., 2003; Hageman et al., 2010; Moffatt et al., 2008). Intriguingly, our analysis also identified both Pex19, a key component for the post-translational delivery of peroxisomal membrane proteins (Fujiki et al., 2006; Jones et al., 2004; Rottensteiner et al., 2004), and ubiquilin-1, a component previously implicated in protein degradation (Lim et al., 2009; Wang and Monteiro, 2007), as interacting partners of immobilised full-length TA-proteins (Tables 1-3).

The specificity of the binding of several of these cytosolic factors was addressed by repeating the pull-down experiments with a selection of the immobilised TA-protein variants, and analysing their interactions with specific proteins by immunoblotting (Figure 3, see also Figure 2 in Chapter 2.3 and (Leznicki et al., 2010)). It should be noted that these binding studies relied on the availability of antibodies that would recognise the rabbit homologues of the proteins identified since rabbit reticulocyte lysate was used as a readily available source of cytosol. Most of the proteins analysed by immunoblotting were found to bind specifically to substrates of the TRC40-mediated pathway but were not detectably associated with Cytb5 that depends on an alternative route for its delivery to the ER (Figure 3; see also Introduction). Bat3 was the only protein that efficiently associated with immobilised Cytb5OPG, although this interaction does not seem to be required for its membrane integration, at least when tested *in vitro* (cf. Chapter 2.3 and (Leznicki et al., 2010)). Strikingly, the levels of both TRC40 and SGTA associated with RAMP4OPG appeared significantly higher than with Sec61βOPG although similar amounts of the two TA-proteins were present

(Figure 3, lanes 6 and 7, compare relevant panels). The qualitatively similar association of other factors with these two TA-proteins (Figure 3, cf. lanes 2, 3, 6 and 7, see Pex19 and DNAJC7 panels) confirms that this difference is unlikely to be the result of variations in the levels of the immobilised TA-proteins. Taken together, these data suggest that the transmembrane regions of RAMP4 and Sec61β differ in their ability to recruit SGTA and TRC40, although the basis for this potential difference is currently unclear. Interestingly, the potential interaction of Cytb5OPG with SGTA previously suggested by mass spectrometry (cf. Table 2) could not be convincingly confirmed by the immunoblotting analysis. This may be attributed to the comparatively inefficient recognition of rabbit SGTA by the chicken antibody used, since we observed the same effect when immobilised Sec61βOPG was used as a bait (Figure 3, cf. lanes 6-8, SGTA panel; see also Figure 7 in Chapter 2.3 and (Leznicki et al., 2010)).

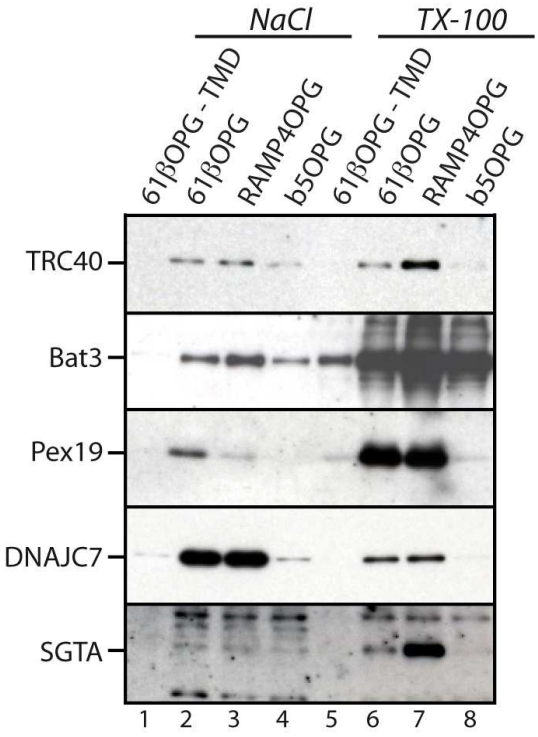

Figure 3. Substrate specificity of TA-protein interacting partners.
Pull-down experiments were carried out as described for Figure 1 using immobilised TA-proteins as shown. After elution, samples were mixed with Laemmli buffer, resolved by SDS-PAGE, and the binding of various cytosolic proteins determined by immunoblotting as indicated.

In order to investigate possible interactions between the various components identified in the pull-down experiments outlined above, I immunoprecipitated some of these cytosolic factors and determined their association with other soluble proteins by

Western blotting (Figure 4). Again, my analysis was limited by the availability of suitable antibodies that could be used for immunoprecipitation and immunoblotting. Based on the literature, Bat3 and TRC40 may be part of the same complex (Sowa et al., 2009) and I tested whether such a complex exists in rabbit reticulocyte lysate, and if its formation was dependent on the presence of a TA-protein substrate. To this end, immunoprecipitation of either TRC40 (Figure 4A) or Bat3 (Figure 4B) was carried out in the presence or absence of added recombinant Sec61βOPG, and the association of specific soluble proteins then monitored by Western blotting. When an anti-TRC40 antibody was used for immunoisolation, a significant amount of TRC40-associated Bat3 could be detected upon elution with Triton X-100 (Figure 4A, Bat3 panel, lane 3). In contrast, only background levels of Bat3 were detected when a control anti-PDI serum was used (Figure 4A, Bat3 panel, lane 4). Qualitatively similar Bat3 binding was observed regardless of the presence or absence of Sec61βOPG (Figure 4A, Bat3 panel, cf. lanes 3 and 5). Likewise, a Bat3-TRC40 interaction was also detected when anti-Bat3 antibody was used to isolate the putative Bat3-TRC40 complex, although in this case substantially more TRC40 was co-immunoprecipitated when recombinant Sec61βOPG was present (Figure 4B, TRC40 panel, cf. lanes 3 and 5). This suggests that any Bat3-TRC40 interaction may be transient and can be stabilised by the presence of a TA-protein substrate. In this scenario, the efficient co-immunoisolation of Bat3 observed in the absence of recombinant Sec61βOPG when using the anti-TRC40 antibody (cf. Figure 4A, Bat3 panel, lane 3) may result from an antibody-induced stabilisation of Bat3-TRC40 complex. Hence, binding of the anti-TRC40 antibody would mimic the presence of a TA-protein, perhaps by "locking" TRC40 in a conformation competent for stable binding to Bat3, somewhat reminiscent of the action of certain human anti-SRP54 autoantibodies that recognise the native protein (Romisch et al., 2006). Notably, no binding of TRC40 to a control anti-SSBP1 antibody could be detected (Figure 4B), and no stable interaction of Pex19 with either TRC40 or Bat3 was observed (Figures 4A and 4B, Pex19 panels).

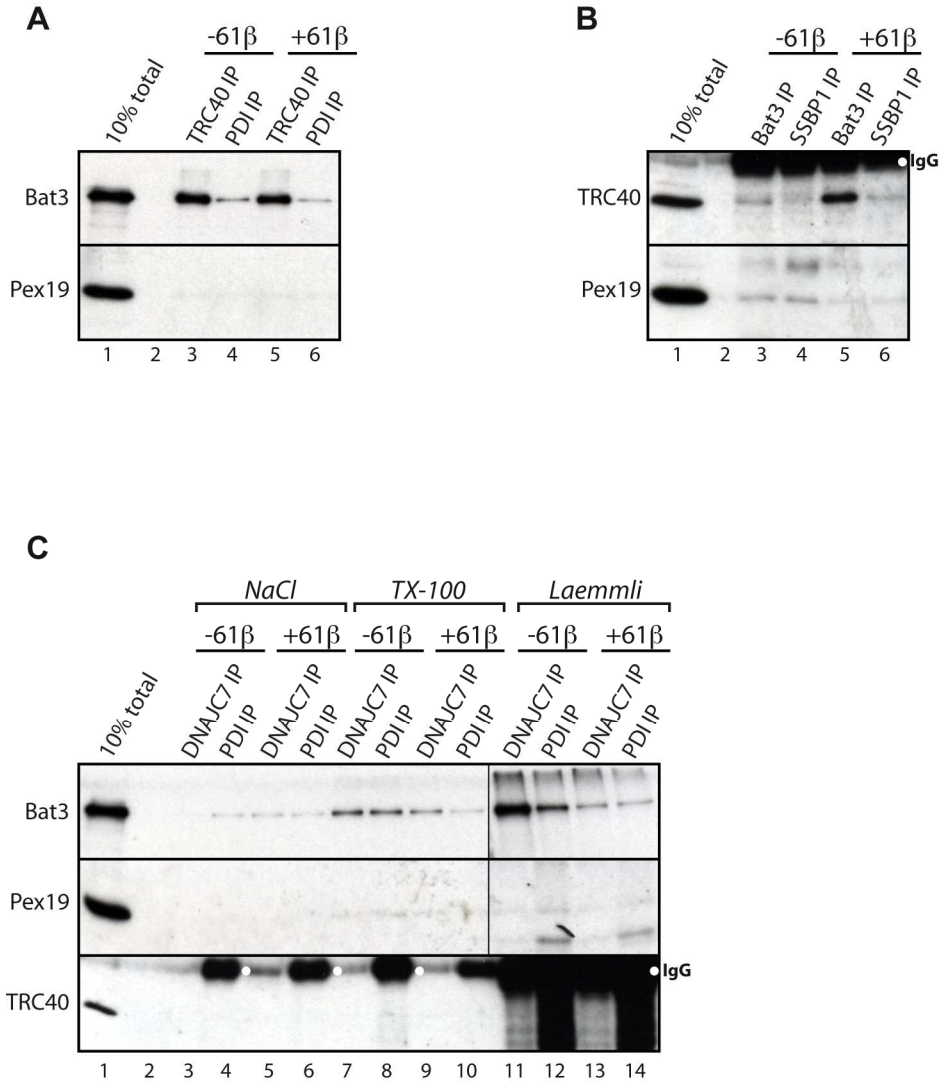

Figure 4. Cytosolic binding partners of TA-proteins form complexes.
Interactions between cytosolic components interacting with TA-proteins (Figures 1-3 and Tables 1-3) were addressed by co-immunoprecipitation. A) 7.5 µl of rabbit anti-TRC40 antibody or anti-PDI control serum was mixed with 20 µl of Protein A Sepharose (50 % slurry), incubated for 1 h at 4ºC and washed with 1 ml of buffer R. 60 µl of rabbit reticulocyte lysate pre-incubated with ~ 2.4 µM Sec61βOPG or buffer control for 30 min at 30ºC was then added, and reactions were further incubated for 1 h at 4ºC. Non-specifically bound proteins were removed by washing the beads three times with 1 ml of buffer R supplemented with 0.5 M NaCl. The remaining proteins were eluted with buffer R containing 0.5 % (v/v) Triton X-100, samples were resolved by SDS-PAGE and immunoblotted for the indicated components. B) 60 µl of rabbit reticulocyte lysate was incubated with ~ 2.4 µM Sec61βOPG or buffer control for 30 min at 30ºC, chicken anti-Bat3 antibody or anti-SSBP1 control serum was then added, and reactions were further incubated for 1 h at 4ºC. This pre-treated lysate was mixed with rabbit anti-chicken antibody immobilised on Protein A Sepharose, and binding of cytosolic proteins was addressed as described for A). C) Cytosolic proteins were isolated using rabbit anti-DNAJC7 antibody and anti-PDI control serum as described for A). Non-specifically associated proteins were removed by washing the beads three times with 1 ml of buffer R and elution was carried out first with buffer R supplemented with 1 M NaCl, then with buffer R containing 0.5 % (v/v) Triton X-100, and finally with the Laemmli buffer. Samples were processed as described for A) and B). Cross-reactive bands corresponding to IgG used for immunoprecipitation are indicated by white dots.

The interactions of DNAJC7 with other cytosolic components were also investigated using a similar strategy. In this case, the binding of DNAJC7 to immobilised TA-proteins was known to be salt-sensitive (Figure 1, cf. lanes 1-3, and Figure 3, DNAJC7 panel, cf. lanes 2 and 3), consistent with the indirect binding of its TPR domain(s) to another soluble protein that binds the TA-protein. Hence, for this analysis a more extensive elution protocol was used (see legend to Figure 4). An obvious association of DNAJC7 with Bat3 was only observed in the absence of Sec61βOPG, and this binding could only be disrupted by SDS (Figure 4C, Bat3 panel, cf. lanes 11 and 12). Since the levels of DNAJC7 that could be directly immunoisolated in the presence and absence of recombinant Sec61βOPG appear qualitatively comparable (data not shown), this TA-protein-dependent difference in the binding of Bat3 to DNAJC7 could not be attributed to any variability in the recovery of DNAJC7. A similar analysis failed to identify any evidence for the binding of either Pex19 or TRC40 to DNAJC7 (Figure 4C, see Pex19 and TRC40 panels).

Finally, I also addressed the possibility of using *in vitro* translated substrates as a platform for future research efforts to characterise the interacting partners of the cytosolic components identified above. Hence, cDNAs coding for the human versions of four cytosolic proteins identified as potential TA-protein interacting partners were cloned into an *in vitro* expression vector, synthesised in a rabbit reticulocyte lysate system and the interactions of the resulting radiolabelled proteins with other cytosolic factors investigated by cross-linking (see Figure 5). One advantage of this approach is the covalent stabilisation of protein-protein interactions, allowing for the detection of transiently associated components. A number of putative interacting partners were observed when cross-linking of SGTA and Pex19 was carried out and in both cases the various adducts were immunoprecipitated by antibodies recognising the radiolabelled protein (Figures 5B and 5D). The most prominent cross-linking product obtained with SGTA most likely corresponds to an oligomeric form of the protein (Figure 5B, lanes 8, 10 and 12, see ●) (Liou and Wang, 2005). Strikingly, cross-linking of DNAJC7 (Figure 5A, cf. lanes 8, 9, 12 and 13), SGTA (Figure 5B, cf. lanes 8, 9, 12 and 13) and Pex19 (Figure 5D, cf. lanes 6-13) all resulted in very high-molecular weight products (*) that may possibly represent adducts with Bat3.

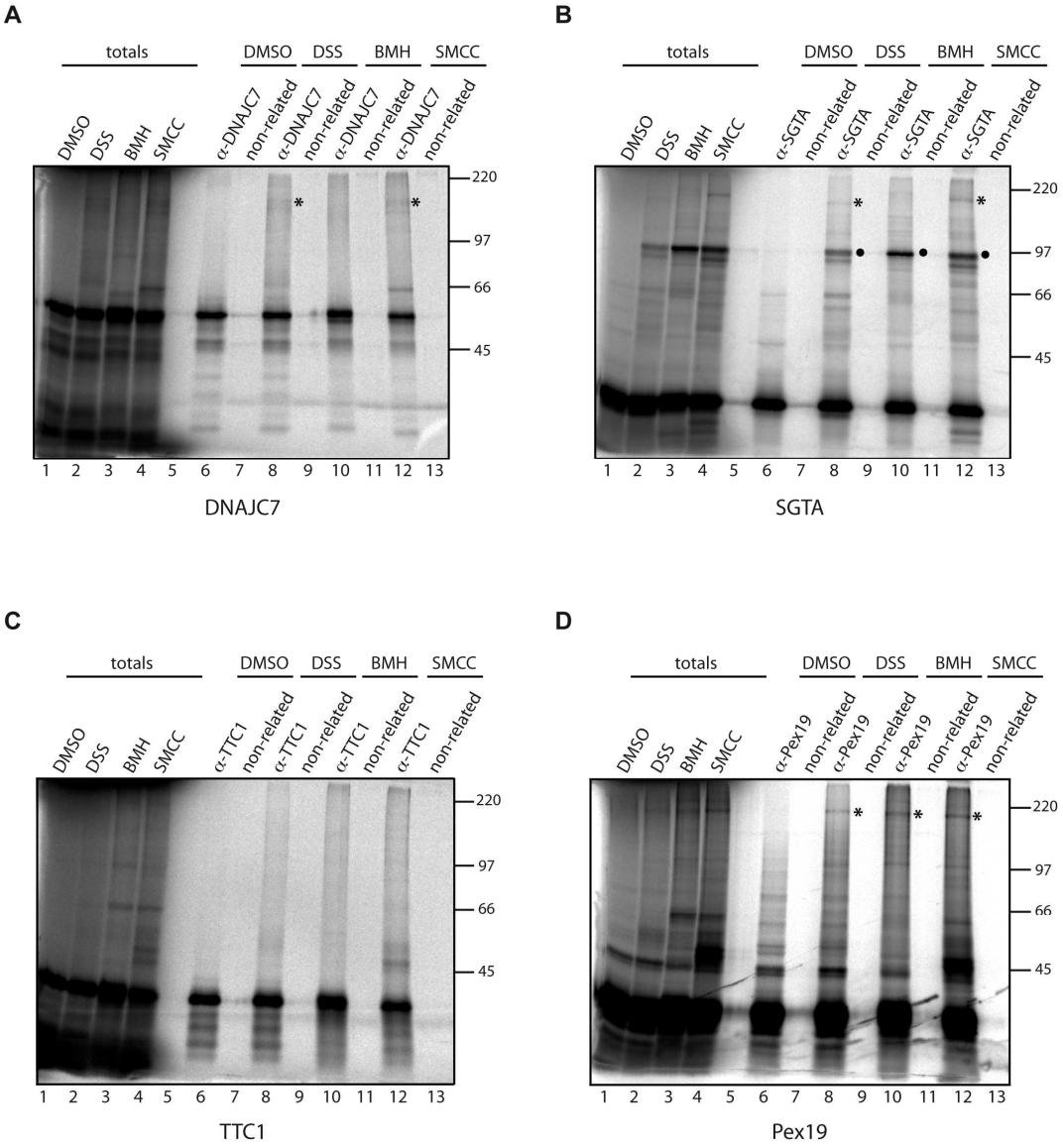

Figure 5. Cytosolic binding partners of TA-proteins interact with other soluble components in a cell-free system.

The cytosolic proteins indicated were synthesised *in vitro* using a rabbit reticulocyte lysate system containing ^{35}S Met/Cys for 45 min at 30ºC, the reactions were treated with 1 mM puromycin for 10 min at 30ºC, and then equal volumes (33 µl) mixed with 1 mM cross-linking reagents as shown or a DMSO control. After 10 min incubation at 30ºC unreacted cross-linkers were quenched by the addition of 50 mM glycine (DSS), 10 mM 2-mercaptoethanol (BMH) or both (SMCC), and the reactions digested with RNaseA (~0.27 mg/ml) for 5 min at 37ºC. 10 µl of the total reaction products was then mixed with 45 µl of 2x concentrated Laemmli buffer (totals) and the remaining samples mixed with 220 µl Triton IP buffer (1 % (v/v) Triton X-100, 140 mM NaCl, 1 mM EDTA, 10 mM Tris-HCl, pH 7.5), 6 µl cold Cys/Met mix, 3 µl 100 mM PMSF and 15 µl pansorbin suspension (50% v/v). Reactions were incubated for 1 h at 4ºC and 120 µl of the soluble fraction was incubated overnight at 4ºC with 1 µl of anti-cytosolic factor antibody or a non-related serum. 1 µl of rabbit anti-mouse or anti-chicken antibody was then added where appropriate, the reactions incubated for 2 h at 4ºC and 25 µl of Protein A Sepharose (50 % slurry) was added. Following 2 h incubation at 4ºC, the beads were washed 3 times with 1 ml of Triton IP buffer and bound proteins were released by the addition of 45 µl of 2x concentrated Laemmli buffer and heating to 70ºC for 10 min. 20 µl from each sample was resolved on a 10 % SDS-PAGE gel and the radiolabelled products were visualised by phosphorimaging. High-molecular weight products potentially corresponding to a Bat3-containing adduct were observed after cross-linking of DNAJC7, SGTA and Pex19 (*), whilst the potential oligomerisation of SGTA was also detected (●) (Liou and Wang, 2005).

However, the unequivocal identification of these interacting partners will require extensive additional immunoprecipitation analysis. Nonetheless, the number of discrete adducts observed with SGTA and Pex19 show that this methodology is a viable option for obtaining a better understanding of the protein-protein interaction network for the various factors involved in TA-protein biogenesis (cf. (Oliver et al., 1999)).

		TMS	-	+	+	-	+	+
Identified Proteins (28)	Accession Number	Mol. Weight	band 1	band 2	band 3	band 4	band 5	band 6
Large proline-rich protein BAT3 OS=Mus musculus	BAT3_MOUSE	121 kDa				2	20	22
Ubiquilin-1 OS=Homo sapiens GN=UBQLN1	UBQL1_HUMAN (+1)	63 kDa						
DnaJ homolog subfamily C member 7 OS=Homo sapiens	DNJC7_HUMAN (+1)	56 kDa		12	17			
Small glutamine-rich tetratricopeptide repeat-containing protein alpha OS=Bos taurus	SGTA_BOVIN (+1)	34 kDa						
Trypsin OS=Sus scrofa	TRYP_PIG	24 kDa	1	2	2	2	3	2
Nucleosome assembly protein 1-like 1 OS=Homo sapiens	NP1L1_HUMAN (+1)	45 kDa		7	7	1	1	
Heat shock cognate 71 kDa protein OS=Bos taurus	HSP7C_BOVIN (+5)	71 kDa						2
T-complex protein 1 subunit gamma OS=Mus musculus	TCPG_MOUSE (+1)	61 kDa						
Small glutamine-rich tetratricopeptide repeat-containing protein alpha OS=Mus musculus	SGTA_MOUSE (+1)	34 kDa						
Glyceraldehyde-3-phosphate dehydrogenase OS=Bos taurus	G3P_BOVIN (+3)	36 kDa						
Peroxisomal biogenesis factor 19 OS=Bos taurus	PEX19_BOVIN	33 kDa						
ATPase ASNA1 OS=Bos taurus	ASNA_BOVIN (+2)	39 kDa						
Tetratricopeptide repeat protein 1 OS=Bos taurus	TTC1_BOVIN (+1)	34 kDa						
Elongation factor 1-alpha, somatic form OS=Xenopus laevis	EF1A0_XENLA (+31)	50 kDa						
Keratin, type II cytoskeletal 1 OS=Homo sapiens	K2C1_HUMAN (+1)	66 kDa						
DnaJ homolog subfamily B member 1 OS=Bos taurus	DNJB1_BOVIN	38 kDa						
Arachidonate 12-lipoxygenase, 12S-type OS=Oryctolagus cuniculus	LOX12_RABIT (+1)	75 kDa						
DnaJ homolog subfamily A member 4 OS=Mus musculus	DNJA4_MOUSE	45 kDa						
Heat shock 70 kDa protein 1A OS=Mus musculus	HS71A_MOUSE (+2)	70 kDa						
Large proline-rich protein BAT3 OS=Homo sapiens	BAT3_HUMAN	119 kDa						3
Hsc70-interacting protein OS=Mus musculus	F10A1_MOUSE	42 kDa						
Stress-induced-phosphoprotein 1 OS=Bos taurus	STIP1_BOVIN (+3)	62 kDa						
Keratin, type I cytoskeletal 9 OS=Homo sapiens	K1C9_HUMAN	62 kDa						
Tubulin beta-2C chain OS=Bos taurus	TBB2C_BOVIN (+7)	50 kDa						
T-complex protein 1 subunit alpha OS=Bos taurus	TCPA_BOVIN (+6)	60 kDa						
Nucleosome assembly protein 1-like 4 OS=Bos taurus	NP1L4_BOVIN (+2)	44 kDa			2			
Signal recognition particle 54 kDa protein OS=Bos taurus	SRP54_BOVIN (+6)	56 kDa						
Poly(rC)-binding protein 1 OS=Bos taurus	PCBP1_BOVIN (+3)	37 kDa						

Table 1. Cytosolic binding partners of TA-proteins utilising the TRC40-mediated pathway for delivery to the ER membrane. Interacting partners of Sec61βOPG and RAMP4OPG variants were investigated as described for Figure 1, the indicated bands were excised and proteins identified by mass spectrometry. Band numbering corresponds to that shown in Figure 1. Proteins preferentially interacting with full-length TA-proteins that were previously implicated in TA-protein delivery to the ER, and those of possible importance for TA-protein biogenesis based on the available literature, are highlighted in orange. Proteins with an unknown relationship to TA-protein biogenesis are marked in yellow, whilst those likely to represent non-specific binding are indicated in green.

		TMS	-	+	+	-	+	+
Identified Proteins (28)	**Accession Number**	**Mol. Weight**	**band 7**	**band 8**	**band 9**	**band 10**	**band 11**	**band 12**
Large proline-rich protein BAT3 OS=Mus musculus	**BAT3_MOUSE**	**121 kDa**	**7**					
Ubiquilin-1 OS=Homo sapiens GN=UBQLN1	**UBQL1_HUMAN (+1)**	**63 kDa**		**8**	**7**	**1**		**1**
DnaJ homolog subfamily C member 7 OS=Homo sapiens	**DNJC7_HUMAN (+1)**	**56 kDa**					**2**	**8**
Small glutamine-rich tetratricopeptide repeat-containing protein alpha OS=Bos taurus	**SGTA_BOVIN (+1)**	**34 kDa**						
Trypsin OS=Sus scrofa	TRYP_PIG	24 kDa	1	2	2	2	2	2
Nucleosome assembly protein 1-like 1 OS=Homo sapiens	NP1L1_HUMAN (+1)	45 kDa					2	2
Heat shock cognate 71 kDa protein OS=Bos taurus	HSP7C_BOVIN (+5)	71 kDa			17			
T-complex protein 1 subunit gamma OS=Mus musculus	**TCPG_MOUSE (+1)**	**61 kDa**		**6**				**9**
Small glutamine-rich tetratricopeptide repeat-containing protein alpha OS=Mus musculus	**SGTA_MOUSE (+1)**	**34 kDa**						
Glyceraldehyde-3-phosphate dehydrogenase OS=Bos taurus	G3P_BOVIN (+3)	36 kDa						
Peroxisomal biogenesis factor 19 OS=Bos taurus	**PEX19_BOVIN**	**33 kDa**						
ATPase ASNA1 OS=Bos taurus	**ASNA_BOVIN (+2)**	**39 kDa**						
Tetratricopeptide repeat protein 1 OS=Bos taurus	**TTC1_BOVIN (+1)**	**34 kDa**						**1**
Elongation factor 1-alpha, somatic form OS=Xenopus laevis	EF1A0_XENLA (+31)	50 kDa				2		
Keratin, type II cytoskeletal 1 OS=Homo sapiens	K2C1_HUMAN (+1)	66 kDa			1			1
DnaJ homolog subfamily B member 1 OS=Bos taurus	**DNJB1_BOVIN**	**38 kDa**						
Arachidonate 12-lipoxygenase, 12S-type OS=Oryctolagus cuniculus	LOX12_RABIT (+1)	75 kDa		1	3			
DnaJ homolog subfamily A member 4 OS=Mus musculus	DNJA4_MOUSE	45 kDa					2	2
Heat shock 70 kDa protein 1A OS=Mus musculus	HS71A_MOUSE (+2)	70 kDa			4			
Large proline-rich protein BAT3 OS=Homo sapiens	**BAT3_HUMAN**	**119 kDa**						
Hsc70-interacting protein OS=Mus musculus	F10A1_MOUSE	42 kDa					1	3
Stress-induced-phosphoprotein 1 OS=Bos taurus	STIP1_BOVIN (+3)	62 kDa		2				1
Keratin, type I cytoskeletal 9 OS=Homo sapiens	K1C9_HUMAN	62 kDa			1			
Tubulin beta-2C chain OS=Bos taurus	TBB2C_BOVIN (+7)	50 kDa				3		
T-complex protein 1 subunit alpha OS=Bos taurus	TCPA_BOVIN (+6)	60 kDa						2
Nucleosome assembly protein 1-like 4 OS=Bos taurus	NP1L4_BOVIN (+2)	44 kDa						
Signal recognition particle 54 kDa protein OS=Bos taurus	**SRP54_BOVIN (+6)**	**56 kDa**						**2**
Poly(rC)-binding protein 1 OS=Bos taurus	PCBP1_BOVIN (+3)	37 kDa						

Table 1. continued

		TMS	-	+	+	-	+	+
Identified Proteins (28)	**Accession Number**	**Mol. Weight**	**band 13**	**band 14**	**band 15**	**band 16**	**band 17**	**band 18**
Large proline-rich protein BAT3 OS=Mus musculus	**BAT3_MOUSE**	**121 kDa**						
Ubiquilin-1 OS=Homo sapiens GN=UBQLN1	**UBQL1_HUMAN (+1)**	**63 kDa**						
DnaJ homolog subfamily C member 7 OS=Homo sapiens	**DNJC7_HUMAN (+1)**	**56 kDa**						
Small glutamine-rich tetratricopeptide repeat-containing protein alpha OS=Bos taurus	**SGTA_BOVIN (+1)**	**34 kDa**		**1**	**5**	**1**	**6**	**6**
Trypsin OS=Sus scrofa	TRYP_PIG	24 kDa	1	1	2	1	2	1
Nucleosome assembly protein 1-like 1 OS=Homo sapiens	NP1L1_HUMAN (+1)	45 kDa						
Heat shock cognate 71 kDa protein OS=Bos taurus	HSP7C_BOVIN (+5)	71 kDa						
T-complex protein 1 subunit gamma OS=Mus musculus	**TCPG_MOUSE (+1)**	**61 kDa**						
Small glutamine-rich tetratricopeptide repeat-containing protein alpha OS=Mus musculus	**SGTA_MOUSE (+1)**	**34 kDa**			**2**		**2**	**2**
Glyceraldehyde-3-phosphate dehydrogenase OS=Bos taurus	G3P_BOVIN (+3)	36 kDa					3	5
Peroxisomal biogenesis factor 19 OS=Bos taurus	**PEX19_BOVIN**	**33 kDa**					**4**	**3**
ATPase ASNA1 OS=Bos taurus	**ASNA_BOVIN (+2)**	**39 kDa**		**4**	**5**			
Tetratricopeptide repeat protein 1 OS=Bos taurus	**TTC1_BOVIN (+1)**	**34 kDa**		**3**	**4**			
Elongation factor 1-alpha, somatic form OS=Xenopus laevis	EF1A0_XENLA (+31)	50 kDa						
Keratin, type II cytoskeletal 1 OS=Homo sapiens	K2C1_HUMAN (+1)	66 kDa				5		
DnaJ homolog subfamily B member 1 OS=Bos taurus	**DNJB1_BOVIN**	**38 kDa**		**5**	**2**			
Arachidonate 12-lipoxygenase, 12S-type OS=Oryctolagus cuniculus	LOX12_RABIT (+1)	75 kDa						
DnaJ homolog subfamily A member 4 OS=Mus musculus	DNJA4_MOUSE	45 kDa						
Heat shock 70 kDa protein 1A OS=Mus musculus	HS71A_MOUSE (+2)	70 kDa						
Large proline-rich protein BAT3 OS=Homo sapiens	**BAT3_HUMAN**	**119 kDa**						
Hsc70-interacting protein OS=Mus musculus	F10A1_MOUSE	42 kDa						
Stress-induced-phosphoprotein 1 OS=Bos taurus	STIP1_BOVIN (+3)	62 kDa						
Keratin, type I cytoskeletal 9 OS=Homo sapiens	K1C9_HUMAN	62 kDa				2		
Tubulin beta-2C chain OS=Bos taurus	TBB2C_BOVIN (+7)	50 kDa						
T-complex protein 1 subunit alpha OS=Bos taurus	TCPA_BOVIN (+6)	60 kDa						
Nucleosome assembly protein 1-like 4 OS=Bos taurus	NP1L4_BOVIN (+2)	44 kDa						
Signal recognition particle 54 kDa protein OS=Bos taurus	**SRP54_BOVIN (+6)**	**56 kDa**						
Poly(rC)-binding protein 1 OS=Bos taurus	PCBP1_BOVIN (+3)	37 kDa			2			

Table 1. continued

		TMS	-	+	-	+	-	+
Identified Proteins (30)	**Accession Number**	**Mol. Weight**	**band 1**	**band 2**	**band 3**	**band 4**	**band 5**	**band 6**
Keratin, type II cuticular Hb6 OS=Homo sapiens	KRT86_HUMAN	53 kDa				18	14	3
Arachidonate 15-lipoxygenase OS=Oryctolagus cuniculus	LOX15_RABIT	75 kDa	3	6	11	8	3	3
Keratin, type I cuticular Ha1 OS=Homo sapiens	K1H1_HUMAN (+1)	47 kDa				14	15	3
Large proline-rich protein BAT3 OS=Homo sapiens	**BAT3_HUMAN**	**119 kDa**	**5**	**17**				
Clathrin heavy chain 1 OS=Bos taurus	CLH1_BOVIN (+1)	192 kDa	14	7				
Heat shock cognate 71 kDa protein OS=Bos taurus	HSP7C_BOVIN (+6)	71 kDa	2	2	10	1		
Keratin, type I cuticular Ha4 OS=Homo sapiens	KRT34_HUMAN	49 kDa				3	3	
Ubiquilin-1 OS=Homo sapiens GN=UBQLN1	**UBQL1_HUMAN (+1)**	**63 kDa**				**5**	**1**	**1**
Keratin, type II cuticular Hb5 OS=Homo sapiens	KRT85_HUMAN	56 kDa				6	4	
DnaJ homolog subfamily B member 1 OS=Homo sapiens	**DNJB1_HUMAN (+1)**	**38 kDa**					**4**	**7**
Small glutamine-rich tetratricopeptide repeat-containing protein alpha OS=Bos taurus	**SGTA_BOVIN (+1)**	**34 kDa**					**1**	**4**
Keratin, type I cuticular Ha3-I OS=Homo sapiens	KT33A_HUMAN	46 kDa				4	3	
Elongation factor 1-delta OS=Oryctolagus cuniculus	EF1D_RABIT	31 kDa					2	4
Stress-induced-phosphoprotein 1 OS=Macaca fascicularis	STIP1_MACFA	63 kDa			6			
DnaJ homolog subfamily B member 4 OS=Bos taurus	**DNJB4_BOVIN (+2)**	**38 kDa**					**1**	**4**
Eukaryotic translation initiation factor 2 subunit 1 OS=Bos taurus	IF2A_BOVIN (+2)	36 kDa					2	4
Coatomer subunit alpha OS=Homo sapiens	COPA_HUMAN	138 kDa	3	1				
Elongation factor 1-delta OS=Rattus norvegicus	EF1D_RAT	31 kDa					1	2
Hemoglobin subunit beta OS=Callithrix argentata	HBB_CALAR (+13)	16 kDa		2				1
Keratin-associated protein 11-1 OS=Homo sapiens	KR111_HUMAN	17 kDa				3		
Eukaryotic translation initiation factor 3 subunit A OS=Homo sapiens	EIF3A_HUMAN (+2)	167 kDa	2					
Poly(rC)-binding protein 1 OS=Bos taurus	PCBP1_BOVIN (+3)	37 kDa					1	2
60S acidic ribosomal protein P0-like OS=Homo sapiens	RLA0L_HUMAN (+6)	34 kDa					1	2
Ran GTPase-activating protein 1 OS=Mus musculus	RAGP1_MOUSE	64 kDa			3			
Small glutamine-rich tetratricopeptide repeat-containing protein alpha OS=Mus musculus	**SGTA_MOUSE (+1)**	**34 kDa**						**3**
Keratin, type I cytoskeletal 9 OS=Homo sapiens	K1C9_HUMAN	62 kDa	2					
Cytochrome b5 OS=Bos taurus	CYB5_BOVIN (+5)	15 kDa						2
Eukaryotic translation initiation factor 3 subunit M OS=Bos taurus	EIF3M_BOVIN (+3)	42 kDa						2
Keratin-associated protein 3-1 OS=Homo sapiens	KRA31_HUMAN	11 kDa					2	
26S proteasome non-ATPase regulatory subunit 13 OS=Gallus gallus	PSD13_CHICK (+3)	43 kDa						2

Table 2. Cytosolic binding partners of Cytb5OPG. Interacting partners of Cytb5OPG variants were identified by mass spectrometry following their isolation as described for Figure 2. The same colour-coding as described for Table 1 was used. Band numbering corresponds to that of Figure 2A.

		TMS	-	+	-	+	-	+
Identified Proteins (66)	**Accession Number**	**Mol. Weight**	**band 1**	**band 2**	**band 3**	**band 4**	**band 5**	**band 6**
Heat shock cognate 71 kDa protein OS=Bos taurus	HSP7C_BOVIN (+3)	71 kDa	9	15	6	6	3	14
Ubiquilin-1 OS=Homo sapiens GN=UBQLN1	**UBQL1_HUMAN**	**63 kDa**				**1**		**1**
Large proline-rich protein BAT3 OS=Homo sapiens	**BAT3_HUMAN**	**119 kDa**			**12**	**21**	**4**	**2**
Hsc70-interacting protein OS=Mus musculus	F10A1_MOUSE	42 kDa			1	2		1
Heat shock protein HSP 90-beta OS=Equus caballus	**HS90B_HORSE (+4)**	**83 kDa**	**13**	**18**				
Serotransferrin OS=Oryctolagus cuniculus	TRFE_RABIT	77 kDa	20	10				
Arachidonate 15-lipoxygenase OS=Oryctolagus cuniculus	LOX15_RABIT	75 kDa	3		1	2		1
Small glutamine-rich tetratricopeptide repeat-containing protein alpha OS=Bos taurus	**SGTA_BOVIN (+1)**	**34 kDa**	**1**					**1**
UDP-N-acetylglucosamine--peptide N-acetylglucosaminyltransferase 110 kDa subunit OS=Homo	OGT1_HUMAN	117 kDa				1	4	20
Elongation factor 1-alpha, somatic form OS=Xenopus laevis	EF1A0_XENLA (+12)	50 kDa	3	1	1		2	1
Heat shock protein HSP 90-alpha OS=Bos taurus	**HS90A_BOVIN (+4)**	**85 kDa**	**7**	**9**				
Creatine kinase M-type OS=Oryctolagus cuniculus	KCRM_RABIT	43 kDa						
Stress-induced-phosphoprotein 1 OS=Homo sapiens	STIP1_HUMAN (+1)	63 kDa						
DnaJ homolog subfamily B member 1 OS=Mus musculus	DNJB1_MOUSE	38 kDa						
Ubiquitin OS=Bos taurus	UBIQ_BOVIN (+26)	9 kDa				3		2
RuvB-like 2 OS=Mus musculus	RUVB2_MOUSE	51 kDa						
C-1-tetrahydrofolate synthase, cytoplasmic	C1TC_PONAB	101 kDa					9	5
DnaJ homolog subfamily C member 7	**DNJC7_HUMAN (+2)**	**56 kDa**						
Eukaryotic translation initiation factor 3 subunit F OS=Homo sapiens	EIF3F_HUMAN (+3)	38 kDa						
Poly(rC)-binding protein 1 OS=Bos taurus	PCBP1_BOVIN (+3)	37 kDa						
Elongation factor 1-delta OS=Oryctolagus cuniculus	EF1D_RABIT	31 kDa						
Trypsin OS=Sus scrofa	TRYP_PIG	24 kDa	1	1	1	2		1
ATPase ASNA1 OS=Bos taurus	**ASNA_BOVIN (+1)**	**39 kDa**						
Hemoglobin subunit alpha-1/2 OS=Oryctolagus cuniculus	HBA_RABIT	16 kDa	1	2			1	1
UPF0363 protein C7orf20 homolog OS=Bos taurus	**CG020_BOVIN (+2)**	**36 kDa**						
Eukaryotic translation initiation factor 3 subunit M OS=Bos taurus	EIF3M_BOVIN (+3)	42 kDa						
Tetratricopeptide repeat protein 1 OS=Bos taurus	**TTC1_BOVIN**	**34 kDa**						
Hemoglobin subunit beta-1/2 OS=Oryctolagus cuniculus	HBB_RABIT	16 kDa	1	2				2
T-complex protein 1 subunit gamma OS=Mus musculus	TCPG_MOUSE (+1)	61 kDa						
DnaJ homolog subfamily A member 2 OS=Bos taurus	DNJA2_BOVIN (+3)	46 kDa						
Ubiquilin-4 OS=Homo sapiens	**UBQL4_HUMAN**	**64 kDa**						
Heat shock 70 kDa protein 1A OS=Bos taurus	HS71A_BOVIN (+5)	70 kDa						
Actin-1/3 OS=Caenorhabditis elegans	ACT1_CAEEL (+53)	42 kDa						
T-complex protein 1 subunit delta OS=Rattus norvegicus	TCPD_RAT	58 kDa						
T-complex protein 1 subunit eta OS=Homo sapiens	TCPH_HUMAN (+1)	59 kDa						
Keratin, type I cuticular Ha1 OS=Homo sapiens	K1H1_HUMAN (+3)	47 kDa	2	1	1			
DnaJ homolog subfamily A member 4 OS=Mus musculus	DNJA4_MOUSE	45 kDa						
AP-2 complex subunit alpha-2 OS=Mus musculus	AP2A2_MOUSE (+1)	104 kDa					1	5
Protein argonaute-2 OS=Homo sapiens	AGO2_HUMAN (+3)	97 kDa	4					
Large proline-rich protein BAT3 OS=Rattus norvegicus	**BAT3_RAT**	**115 kDa**				**2**	**1**	
Isocitrate dehydrogenase [NADP], mitochondrial OS=Homo sapiens	IDHP_HUMAN (+1)	51 kDa						
DnaJ homolog subfamily B member 4 OS=Bos taurus	DNJB4_BOVIN (+2)	38 kDa						
ATP-binding cassette sub-family E member 1 OS=Homo sapiens	ABCE1_HUMAN (+1)	67 kDa						
Clathrin heavy chain 1 OS=Bos taurus	CLH1_BOVIN (+1)	192 kDa			6			
Large proline-rich protein BAT3 OS=Mus musculus	**BAT3_MOUSE**	**121 kDa**			**2**	**2**		
Transferrin receptor protein 1 OS=Mus musculus	TFR1_MOUSE	86 kDa	2	1				
Ubiquilin-2 OS=Homo sapiens	**UBQL2_HUMAN**	**66 kDa**						
Elongation factor 1-gamma OS=Oryctolagus cuniculus	EF1G_RABIT	50 kDa						
40S ribosomal protein S3a-A OS=Xenopus laevis	RS3AA_XENLA (+11)	30 kDa						
Peroxisomal biogenesis factor 19 OS=Bos taurus	**PEX19_BOVIN**	**33 kDa**						
40S ribosomal protein SA OS=Bos taurus	RSSA_BOVIN (+9)	33 kDa						
Hepatocyte growth factor-regulated tyrosine kinase substrate OS=Mus musculus	HGS_MOUSE (+1)	86 kDa					1	2
26S proteasome non-ATPase regulatory subunit 12 OS=Homo sapiens	PSD12_HUMAN (+1)	53 kDa						
Signal recognition particle 54 kDa protein OS=Bos taurus	**SRP54_BOVIN (+5)**	**56 kDa**						
Phosphatidylinositol transfer protein beta isoform OS=Bos taurus	PIPNB_BOVIN (+4)	32 kDa						
60S acidic ribosomal protein P0-like OS=Homo sapiens	RLA0L_HUMAN (+5)	34 kDa						
Ferrochelatase, mitochondrial OS=Bos taurus	HEMH_BOVIN	47 kDa						
Eukaryotic translation initiation factor 2 subunit 3 OS=Gallus gallus	IF2G_CHICK (+3)	51 kDa						
26S proteasome non-ATPase regulatory subunit 6 OS=Bos taurus	PSMD6_BOVIN (+2)	46 kDa						
Eukaryotic translation initiation factor 2 subunit 1 OS=Bos taurus	IF2A_BOVIN (+7)	36 kDa						
UPF0027 protein C22orf28 homolog OS=Mus musculus	CV028_MOUSE (+1)	55 kDa						
Importin subunit beta-1 OS=Homo sapiens	IMB1_HUMAN (+2)	97 kDa	2					
Syntaxin-4 OS=Bos taurus	STX4_BOVIN (+3)	34 kDa						
Cysteinyl-tRNA synthetase, cytoplasmic OS=Homo sapiens	SYCC_HUMAN (+1)	85 kDa	2					
Phenylalanyl-tRNA synthetase beta chain OS=Mus musculus	SYFB_MOUSE	66 kDa						
WD repeat and FYVE domain-containing protein 1 OS=Homo sapiens	WDFY1_HUMAN	46 kDa						

Table 3. Cytosolic binding partners of Syb2OPG. Interacting partners of Syb2OPG variants were identified by mass spectrometry following their isolation as described for Figure 2. The same colour-coding as described for Table 1 was used. Band numbering corresponds to that of Figure 2B.

		TMS	-	+	-	+	-	+
Identified Proteins (66)	**Accession Number**	**Mol. Weight**	**band 7**	**band 8**	**band 9**	**band 10**	**band 11**	**band 12**
Heat shock cognate 71 kDa protein OS=Bos taurus	HSP7C_BOVIN (+3)	71 kDa	26	21	12	7		
Ubiquilin-1 OS=Homo sapiens GN=UBQLN1	**UBQL1_HUMAN**	**63 kDa**	**2**	**5**	**1**	**11**	**8**	**2**
Large proline-rich protein BAT3 OS=Homo sapiens	**BAT3_HUMAN**	**119 kDa**						
Hsc70-interacting protein OS=Mus musculus	F10A1_MOUSE	42 kDa				4		1
Heat shock protein HSP 90-beta OS=Equus caballus	**HS90B_HORSE (+4)**	**83 kDa**						
Serotransferrin OS=Oryctolagus cuniculus	TRFE_RABIT	77 kDa						
Arachidonate 15-lipoxygenase OS=Oryctolagus cuniculus	LOX15_RABIT	75 kDa	7	3	2	11	1	
Small glutamine-rich tetratricopeptide repeat-containing protein alpha OS=Bos taurus	**SGTA_BOVIN (+1)**	**34 kDa**						
UDP-N-acetylglucosamine--peptide N-acetylglucosaminyltransferase 110 kDa subunit OS=Homo	OGT1_HUMAN	117 kDa						
Elongation factor 1-alpha, somatic form OS=Xenopus laevis	EF1A0_XENLA (+12)	50 kDa	1		2	1	1	1
Heat shock protein HSP 90-alpha OS=Bos taurus	**HS90A_BOVIN (+4)**	**85 kDa**						
Creatine kinase M-type OS=Oryctolagus cuniculus	KCRM_RABIT	43 kDa						1
Stress-induced-phosphoprotein 1 OS=Homo sapiens	STIP1_HUMAN (+1)	63 kDa			10	8		
DnaJ homolog subfamily B member 1 OS=Mus musculus	DNJB1_MOUSE	38 kDa						
Ubiquitin OS=Bos taurus	UBIQ_BOVIN (+26)	9 kDa		1		2		1
RuvB-like 2 OS=Mus musculus	RUVB2_MOUSE	51 kDa						
C-1-tetrahydrofolate synthase, cytoplasmic	C1TC_PONAB	101 kDa						
DnaJ homolog subfamily C member 7	**DNJC7_HUMAN (+2)**	**56 kDa**					**3**	**4**
Eukaryotic translation initiation factor 3 subunit F OS=Homo sapiens	EIF3F_HUMAN (+3)	38 kDa						
Poly(rC)-binding protein 1 OS=Bos taurus	PCBP1_BOVIN (+3)	37 kDa						
Elongation factor 1-delta OS=Oryctolagus cuniculus	EF1D_RABIT	31 kDa						
Trypsin OS=Sus scrofa	TRYP_PIG	24 kDa	1			1		
ATPase ASNA1 OS=Bos taurus	**ASNA_BOVIN (+1)**	**39 kDa**						
Hemoglobin subunit alpha-1/2 OS=Oryctolagus cuniculus	HBA_RABIT	16 kDa			1	1		1
UPF0363 protein C7orf20 homolog OS=Bos taurus	**CG020_BOVIN (+2)**	**36 kDa**						
Eukaryotic translation initiation factor 3 subunit M OS=Bos taurus	EIF3M_BOVIN (+3)	42 kDa						
Tetratricopeptide repeat protein 1 OS=Bos taurus	**TTC1_BOVIN**	**34 kDa**						
Hemoglobin subunit beta-1/2 OS=Oryctolagus cuniculus	HBB_RABIT	16 kDa				1		1
T-complex protein 1 subunit gamma OS=Mus musculus	TCPG_MOUSE (+1)	61 kDa				8		
DnaJ homolog subfamily A member 2 OS=Bos taurus	DNJA2_BOVIN (+3)	46 kDa						
Ubiquilin-4 OS=Homo sapiens	**UBQL4_HUMAN**	**64 kDa**		**5**				
Heat shock 70 kDa protein 1A OS=Bos taurus	HS71A_BOVIN (+5)	70 kDa	2	1		2		
Actin-1/3 OS=Caenorhabditis elegans	ACT1_CAEEL (+53)	42 kDa						
T-complex protein 1 subunit delta OS=Rattus norvegicus	TCPD_RAT	58 kDa						4
T-complex protein 1 subunit eta OS=Homo sapiens	TCPH_HUMAN (+1)	59 kDa						6
Keratin, type I cuticular Ha1 OS=Homo sapiens	K1H1_HUMAN (+3)	47 kDa						
DnaJ homolog subfamily A member 4 OS=Mus musculus	DNJA4_MOUSE	45 kDa						
AP-2 complex subunit alpha-2 OS=Mus musculus	AP2A2_MOUSE (+1)	104 kDa						
Protein argonaute-2 OS=Homo sapiens	AGO2_HUMAN (+3)	97 kDa						
Large proline-rich protein BAT3 OS=Rattus norvegicus	**BAT3_RAT**	**115 kDa**						
Isocitrate dehydrogenase [NADP], mitochondrial OS=Homo sapiens	IDHP_HUMAN (+1)	51 kDa						
DnaJ homolog subfamily B member 4 OS=Bos taurus	DNJB4_BOVIN (+2)	38 kDa						
ATP-binding cassette sub-family E member 1 OS=Homo sapiens	ABCE1_HUMAN (+1)	67 kDa			3	1		
Clathrin heavy chain 1 OS=Bos taurus	CLH1_BOVIN (+1)	192 kDa						
Large proline-rich protein BAT3 OS=Mus musculus	**BAT3_MOUSE**	**121 kDa**						
Transferrin receptor protein 1 OS=Mus musculus	TFR1_MOUSE	86 kDa						
Ubiquilin-2 OS=Homo sapiens	**UBQL2_HUMAN**	**66 kDa**		**3**				
Elongation factor 1-gamma OS=Oryctolagus cuniculus	EF1G_RABIT	50 kDa						
40S ribosomal protein S3a-A OS=Xenopus laevis	RS3AA_XENLA (+11)	30 kDa						
Peroxisomal biogenesis factor 19 OS=Bos taurus	**PEX19_BOVIN**	**33 kDa**						
40S ribosomal protein SA OS=Bos taurus	RSSA_BOVIN (+9)	33 kDa						
Hepatocyte growth factor-regulated tyrosine kinase substrate OS=Mus musculus	HGS_MOUSE (+1)	86 kDa						
26S proteasome non-ATPase regulatory subunit 12 OS=Homo sapiens	PSD12_HUMAN (+1)	53 kDa						
Signal recognition particle 54 kDa protein OS=Bos taurus	**SRP54_BOVIN (+5)**	**56 kDa**						**3**
Phosphatidylinositol transfer protein beta isoform OS=Bos taurus	PIPNB_BOVIN (+4)	32 kDa						
60S acidic ribosomal protein P0-like OS=Homo sapiens	RLA0L_HUMAN (+5)	34 kDa						
Ferrochelatase, mitochondrial OS=Bos taurus	HEMH_BOVIN	47 kDa						
Eukaryotic translation initiation factor 2 subunit 3 OS=Gallus gallus	IF2G_CHICK (+3)	51 kDa						
26S proteasome non-ATPase regulatory subunit 6 OS=Bos taurus	PSMD6_BOVIN (+2)	46 kDa						
Eukaryotic translation initiation factor 2 subunit 1 OS=Bos taurus	IF2A_BOVIN (+7)	36 kDa						
UPF0027 protein C22orf28 homolog OS=Mus musculus	CV028_MOUSE (+1)	55 kDa					2	
Importin subunit beta-1 OS=Homo sapiens	IMB1_HUMAN (+2)	97 kDa						
Syntaxin-4 OS=Bos taurus	STX4_BOVIN (+3)	34 kDa						
Cysteinyl-tRNA synthetase, cytoplasmic OS=Homo sapiens	SYCC_HUMAN (+1)	85 kDa						
Phenylalanyl-tRNA synthetase beta chain OS=Mus musculus	SYFB_MOUSE	66 kDa	2					
WD repeat and FYVE domain-containing protein 1 OS=Homo sapiens	WDFY1_HUMAN	46 kDa						

Table 3. continued

		TMS	-	+	-	+	-	+	-	+
Identified Proteins (66)	**Accession Number**	**Mol. Weight**	**band 13**	**band 14**	**band 15**	**band 16**	**band 17**	**band 18**	**band 19**	**band 20**
Heat shock cognate 71 kDa protein OS=Bos taurus	HSP7C_BOVIN (+3)	71 kDa								
Ubiquilin-1 OS=Homo sapiens GN=UBQLN1	**UBQL1_HUMAN**	**63 kDa**	**1**		**1**					
Large proline-rich protein BAT3 OS=Homo sapiens	**BAT3_HUMAN**	**119 kDa**								
Hsc70-interacting protein OS=Mus musculus	F10A1_MOUSE	42 kDa	5	7	6					
Heat shock protein HSP 90-beta OS=Equus caballus	**HS90B_HORSE (+4)**	**83 kDa**								
Serotransferrin OS=Oryctolagus cuniculus	TRFE_RABIT	77 kDa								
Arachidonate 15-lipoxygenase OS=Oryctolagus cuniculus	LOX15_RABIT	75 kDa								
Small glutamine-rich tetratricopeptide repeat-containing protein alpha OS=Bos taurus	**SGTA_BOVIN (+1)**	**34 kDa**				**4**	**4**	**7**	**3**	**1**
UDP-N-acetylglucosamine--peptide N-acetylglucosaminyltransferase 110 kDa subunit OS=Homo	OGT1_HUMAN	117 kDa								
Elongation factor 1-alpha, somatic form OS=Xenopus laevis	EF1A0_XENLA (+12)	50 kDa	5	2	1				1	
Heat shock protein HSP 90-alpha OS=Bos taurus	**HS90A_BOVIN (+4)**	**85 kDa**								
Creatine kinase M-type OS=Oryctolagus cuniculus	KCRM_RABIT	43 kDa			5	8	4			
Stress-induced-phosphoprotein 1 OS=Homo sapiens	STIP1_HUMAN (+1)	63 kDa								
DnaJ homolog subfamily B member 1 OS=Mus musculus	DNJB1_MOUSE	38 kDa			1		9	3		
Ubiquitin OS=Bos taurus	UBIQ_BOVIN (+26)	9 kDa				2				1
RuvB-like 2 OS=Mus musculus	RUVB2_MOUSE	51 kDa	5	10						
C-1-tetrahydrofolate synthase, cytoplasmic	C1TC_PONAB	101 kDa								
DnaJ homolog subfamily C member 7	**DNJC7_HUMAN (+2)**	**56 kDa**								
Eukaryotic translation initiation factor 3 subunit F OS=Homo sapiens	EIF3F_HUMAN (+3)	38 kDa	2	5	1					
Poly(rC)-binding protein 1 OS=Bos taurus	PCBP1_BOVIN (+3)	37 kDa			6	6				
Elongation factor 1-delta OS=Oryctolagus cuniculus	EF1D_RABIT	31 kDa					7	4		
Trypsin OS=Sus scrofa	TRYP_PIG	24 kDa	1	2		2				
ATPase ASNA1 OS=Bos taurus	**ASNA_BOVIN (+1)**	**39 kDa**			**2**	**4**	**2**	**2**		
Hemoglobin subunit alpha-1/2 OS=Oryctolagus cuniculus	HBA_RABIT	16 kDa				1				
UPF0363 protein C7orf20 homolog OS=Bos taurus	**CG020_BOVIN (+2)**	**36 kDa**						**1**	**3**	**5**
Eukaryotic translation initiation factor 3 subunit M OS=Bos taurus	EIF3M_BOVIN (+3)	42 kDa				6				
Tetratricopeptide repeat protein 1 OS=Bos taurus	**TTC1_BOVIN**	**34 kDa**			**1**	**6**	**1**	**1**		
Hemoglobin subunit beta-1/2 OS=Oryctolagus cuniculus	HBB_RABIT	16 kDa				1				
T-complex protein 1 subunit gamma OS=Mus musculus	TCPG_MOUSE (+1)	61 kDa								
DnaJ homolog subfamily A member 2 OS=Bos taurus	DNJA2_BOVIN (+3)	46 kDa	4	3						
Ubiquilin-4 OS=Homo sapiens	**UBQL4_HUMAN**	**64 kDa**								
Heat shock 70 kDa protein 1A OS=Bos taurus	HS71A_BOVIN (+5)	70 kDa								
Actin-1/3 OS=Caenorhabditis elegans	ACT1_CAEEL (+53)	42 kDa			2	5				
T-complex protein 1 subunit delta OS=Rattus norvegicus	TCPD_RAT	58 kDa								
T-complex protein 1 subunit eta OS=Homo sapiens	TCPH_HUMAN (+1)	59 kDa								
Keratin, type I cuticular Ha1 OS=Homo sapiens	K1H1_HUMAN (+3)	47 kDa								
DnaJ homolog subfamily A member 4 OS=Mus musculus	DNJA4_MOUSE	45 kDa	3	3						
AP-2 complex subunit alpha-2 OS=Mus musculus	AP2A2_MOUSE (+1)	104 kDa								
Protein argonaute-2 OS=Homo sapiens	AGO2_HUMAN (+3)	97 kDa								
Large proline-rich protein BAT3 OS=Rattus norvegicus	**BAT3_RAT**	**115 kDa**								
Isocitrate dehydrogenase [NADP], mitochondrial OS=Homo sapiens	IDHP_HUMAN (+1)	51 kDa			2	1				
DnaJ homolog subfamily B member 4 OS=Bos taurus	DNJB4_BOVIN (+2)	38 kDa					4	1		
ATP-binding cassette sub-family E member 1 OS=Homo sapiens	ABCE1_HUMAN (+1)	67 kDa								
Clathrin heavy chain 1 OS=Bos taurus	CLH1_BOVIN (+1)	192 kDa								
Large proline-rich protein BAT3 OS=Mus musculus	**BAT3_MOUSE**	**121 kDa**								
Transferrin receptor protein 1 OS=Mus musculus	TFR1_MOUSE	86 kDa								
Ubiquilin-2 OS=Homo sapiens	**UBQL2_HUMAN**	**66 kDa**								
Elongation factor 1-gamma OS=Oryctolagus cuniculus	EF1G_RABIT	50 kDa	4							
40S ribosomal protein S3a-A OS=Xenopus laevis	RS3AA_XENLA (+11)	30 kDa							4	
Peroxisomal biogenesis factor 19 OS=Bos taurus	**PEX19_BOVIN**	**33 kDa**						**3**		
40S ribosomal protein SA OS=Bos taurus	RSSA_BOVIN (+9)	33 kDa			1	2				
Hepatocyte growth factor-regulated tyrosine kinase substrate OS=Mus musculus	HGS_MOUSE (+1)	86 kDa								
26S proteasome non-ATPase regulatory subunit 12 OS=Homo sapiens	PSD12_HUMAN (+1)	53 kDa	1	3						
Signal recognition particle 54 kDa protein OS=Bos taurus	**SRP54_BOVIN (+5)**	**56 kDa**								
Phosphatidylinositol transfer protein beta isoform OS=Bos taurus	PIPNB_BOVIN (+4)	32 kDa								3
60S acidic ribosomal protein P0-like OS=Homo sapiens	RLA0L_HUMAN (+5)	34 kDa					3			
Ferrochelatase, mitochondrial OS=Bos taurus	HEMH_BOVIN	47 kDa				2				
Eukaryotic translation initiation factor 2 subunit 3 OS=Gallus gallus	IF2G_CHICK (+3)	51 kDa	3							
26S proteasome non-ATPase regulatory subunit 6 OS=Bos taurus	PSMD6_BOVIN (+2)	46 kDa				3				
Eukaryotic translation initiation factor 2 subunit 1 OS=Bos taurus	IF2A_BOVIN (+7)	36 kDa					2			
UPF0027 protein C22orf28 homolog OS=Mus musculus	CV028_MOUSE (+1)	55 kDa								
Importin subunit beta-1 OS=Homo sapiens	IMB1_HUMAN (+2)	97 kDa								
Syntaxin-4 OS=Bos taurus	STX4_BOVIN (+3)	34 kDa								2
Cysteinyl-tRNA synthetase, cytoplasmic OS=Homo sapiens	SYCC_HUMAN (+1)	85 kDa								
Phenylalanyl-tRNA synthetase beta chain OS=Mus musculus	SYFB_MOUSE	66 kDa								
WD repeat and FYVE domain-containing protein 1 OS=Homo sapiens	WDFY1_HUMAN	46 kDa				2				

Table 3. continued

CHAPTER THREE

Discussion

The main focus of my study was to address the role of cytosolic factors during tail-anchored (TA) protein biogenesis at the endoplasmic reticulum (ER). Whilst a requirement for soluble components during targeting to the ER membrane was well-established for most TA-proteins (Favaloro et al., 2008; Favaloro et al., 2010; Leznicki et al., 2010; Rabu et al., 2009; Rabu et al., 2008; Stefanovic and Hegde, 2007), a small subset of substrates appeared to be capable of integrating into a lipid bilayer in the absence of cytosol (Colombo et al., 2009). Furthermore, many of the details of the ER delivery of TA-proteins relying on the TRC40 targeting factor (see Introduction) were unclear at the beginning of my work (Stefanovic and Hegde, 2007). In particular, studies of the homologous pathway in yeast indicated that additional mammalian cytosolic proteins may well be involved in the biogenesis of this group of TA-proteins (Battle et al., 2010; Costanzo et al., 2010; Jonikas et al., 2009).

I. Validity of the unassisted pathway for Cytb5 integration.

In order to address the role of cytosolic components during TA-protein delivery to the mammalian ER, I exploited bacterially expressed and chromatographically-purified recombinant TA-proteins. This allowed me to separate protein synthesis from their membrane targeting and insertion. Hence, the composition of "integration reactions" could be modulated so as to investigate the role of individual components in TA-protein delivery. I found that substrates of the TRC40-dependent pathway, such as Sec61β, and TA-proteins postulated to exploit a "spontaneous" and/or chaperone-mediated route(s), as exemplified by cytochrome b5 (Cytb5), both required the presence of cytosol for efficient membrane integration when an N-glycosylation assay was used as a read-out (Chapters 2.1 – 2.3). This observation supports the idea that even if some TA-proteins can spontaneously partition into the lipid bilayer without the involvement of any membrane-bound protein receptor (Borgese et al., 2007; Brambillasca et al., 2006; Brambillasca et al., 2005; Colombo et al., 2009), these substrates would still require a soluble component(s) for delivery to their target membrane. Chaperones of the Hsp70 family could potentially perform this role, since their inhibition by small molecules causes a selective decrease in the membrane integration of TA-proteins previously classified as substrates of the "unassisted" pathway (Rabu et al., 2008).

Further evidence that substrates of the "unassisted" and/or chaperone-mediated pathway(s) can exploit soluble components during targeting to the ER membrane was obtained from biophysical studies of recombinant Cytb5 modified within its transmembrane segment (TMS) with fluorescent or spin probes (Chapter 2.2). Hence, cytosolic proteins seem to prevent Cytb5 from aggregating and maintain it in a so-called "integration-competent" form that could later be efficiently inserted into the lipid bilayer. This observation again supports the possible involvement of the Hsp70 chaperones that were previously shown to maintain the secretory protein pre-pro-alpha-factor in an unfolded state and facilitate its post-translational translocation across the yeast ER membrane (Ngosuwan et al., 2003). On this basis, I would argue that the Cytb5 delivery step is best described as "chaperone-facilitated". Hence, it seems reasonable to conclude that the previously postulated "lack of assistance" defined for Cytb5 biogenesis (Brambillasca et al., 2006; Brambillasca et al., 2005; Colombo et al., 2009) should refer only to the membrane-integration step of the process, if at all (see below).

II. Plasticity of TA-protein biogenesis.

Regardless of the precise identity of the targeting factors involved, I have shown that components of both the TRC40- and chaperone-facilitated pathways are surprisingly flexible, and can accommodate TMSs that have been extensively modified by chemical means (Chapter 2.1). The physiological significance of this binding remains to be fully established but, as already speculated (Chapter 2.1), such plasticity could be exploited for the membrane delivery of soluble proteins, such as SNAP-25, that can associate with a newly synthesised TA-protein prior to the membrane targeting of the resulting complex (Vogel et al., 2000). Another interesting aspect of the flexibility of these targeting factors is the possibility of their binding to ubiquitinated substrates. In this case, the same soluble components might have a dual role and mediate either membrane delivery or protein degradation (see below). This could be especially important in the case of TA-proteins, which may be particularly prone to misfolding and/or aggregation due to the post-translational nature of their membrane integration. Interestingly, links between the ubiquitin-proteasome system and the yeast homologue of TRC40, Get3, have already been reported (Auld et al., 2006), whilst Hsp70 chaperones are known to communicate with the proteasome via co-factors such as CHIP (C-terminus of Hsc70 interacting protein) (McDonough and Patterson, 2003).

These results are also consistent with the finding that the TMSs of integral membrane proteins can undergo post-translational modifications prior to integration (Caballero et al., 1998; Ochsenbauer-Jambor et al., 2001; Ryan et al., 2010).

III. Membrane integration step during TA-protein biogenesis.

Although not the primary intention, my analysis of TA-protein biogenesis at the ER also provided some insights into the membrane integration step of this process. The insertion of PEGylated Sec61β into ER-derived microsomes shows a very strong correlation with estimates for the changes in free energy that would be associated with TMS partitioning into a lipid bilayer (Chapter 2.1). If this model proves correct, then one might speculate that cytosolic proteins would be required both to protect TA substrates from aggregating and to promote their targeting to the ER. Any membrane-bound factors would act to bring TA-proteins to the ER membrane surface, and perhaps facilitate their release from soluble components. In this model a specialised integrase would not be essential since the membrane insertion step would be driven by the laws of thermodynamics. It is worth noting that conceptually similar scenarios, based on the energetic effects of partitioning into a lipid bilayer, were previously proposed for the membrane integration of phage components, such as M13 and Pf3 coat proteins (Kiefer and Kuhn, 1999; Soekarjo et al., 1996). Interestingly, subsequent analysis revealed that whilst thermodynamically-favourable *per se*, the insertion of these proteins is actually mediated by a distinct prokaryotic integrase, YidC (Dalbey and Kuhn, 2004; Kuhn et al., 2003; Samuelson et al., 2000). Hence, although in agreement with my experimental data, a pathway for the membrane integration of TA-proteins driven solely by thermodynamics is just one of several possibilities, and further studies will be required to either validate or disprove this hypothesis.

IV. Positioning of Cytb5 within the lipid bilayer.

Although preliminary in nature, the accessibility of various cysteine residues introduced into Cytb5 indicates that its membrane integration may not necessarily be driven exclusively by a "hydrophobic effect" as previously postulated (Borgese et al., 2007; Brambillasca et al., 2006; Colombo et al., 2009); but may in fact be influenced by cytosolic components and perhaps also peripheral membrane proteins (Chapter 2.2). When the sequence of the C-terminal portion of Cytb5 is analysed using

experimentally-determined scales for amino acid partitioning into the interfacial and hydrocarbon core regions of a lipid bilayer (White and Wimley, 1999; Wimley et al., 1996; Wimley and White, 1996), it seems that the predicted TMS of Cytb5 would indeed favour a membrane environment (Figure 3.1A). However, for unassisted TMS partitioning into a lipid bilayer additional factors have to be considered, with the known preference for aromatic residues to be located at the interfacial regions being the most significant (White and Wimley, 1994; White and Wimley, 1999; Yau et al., 1998). Hence, if the membrane integration of Cytb5 was defined solely by such underlying thermodynamic effect, then the three Trp residues located towards the N-terminus of the predicted TMS (cf. Figure 3.1A) would all cluster in the lipid headgroup phase (interfacial region) (Figure 3.1B, II). Since the interfacial regions of the ER membrane appear relatively thin (Crowley et al., 1994; Lewis and Engelman, 1983), this arrangement would most likely place four N-terminal serines (residues 105-108) in the cytosol with the C-terminal opsin-derived tag (OPG) (cf. Chapters 2.1-2.3) at least partially located within the interfacial region on the lumenal side of the ER membrane (Figure 3.1B, II). As a consequence, the resulting proximity of Asn residue 144 to the ER lumenal membrane surface would preclude its efficient modification by the oligosaccharyltransferase complex (Nilsson and von Heijne, 1993) (Figure 3.1B, II).

These theoretical considerations are in good agreement with data obtained studying the membrane integration of Cytb5 in the absence of cytosolic proteins, and using microsomes stripped of peripheral membrane components, but are inconsistent with experiments performed using cytosol and untreated membranes. In the first case, residue 107, mutated from serine to cysteine, can be efficiently labelled with the membrane-impermeable probe mPEG-5000, whilst the microsome-associated protein is not N-glycosylated (Chapter 2.2). On the other hand, Cytb5 integrated into untreated ER membranes in the presence of cytosol is efficiently modified by the oligosaccharyltransferase complex, but cysteine 107 is protected from mPEG-5000 labelling (Chapter 2.2). This suggests that co-operation between cytosolic and membrane-bound components might enable an alternative conformation of the Cytb5 TMS and its flanking regions (Figure 3.1B, I). In this conformation the relevant Trp residues would probably reside within the hydrocarbon core, consistent with their capacity to partition into an octanol phase (Wimley et al., 1996), whilst the negatively

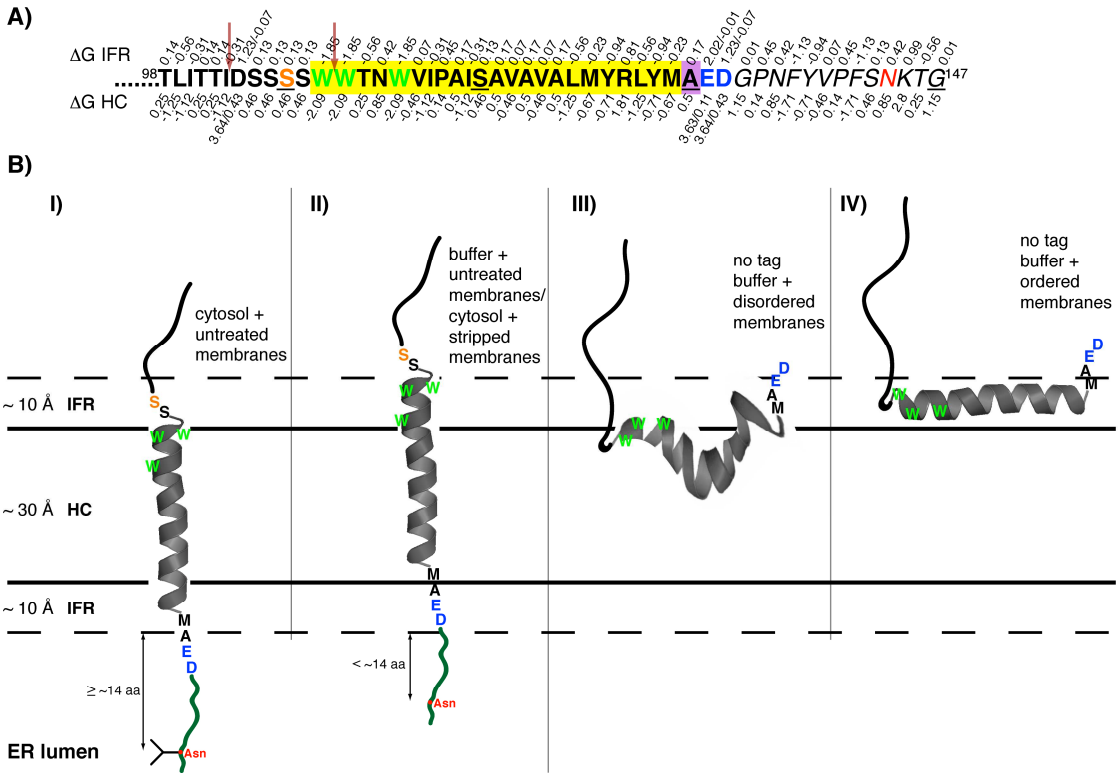

Figure 3.1 Possible conformations of cytochrome b5 within the lipid bilayer. A) Amino acid sequence of the C-terminal region of cytochrome b5 (Cytb5) is shown with the free energy cost of partitioning each residue into the interfacial region (IFR) and hydrocarbon core (HC) of the lipid bilayer indicated (White and Wimley, 1999; Wimley et al., 1996; Wimley and White, 1996). Depending on the protonation state of acidic residues, different values for the energetic cost of their partitioning into the lipid bilayer are given, with the deprotonated form partitioning being more thermodynamically-unfavourable. The predicted transmembrane segment (TMS) is highlighted in yellow, with Ala132, whose classification as belonging to the TMS depends on the prediction software used, being highlighted in purple. Trp residues (W) expected to preferentially localise to the IFR are indicated in light green with the acidic amino acids of the original Cytb5 C-terminus shown in blue. Residues mutated to cysteines in the study presented (Chapter 2.2) are underlined, with the residue 107, modified by mPEG-5000 after membrane integration of Cytb5 in the absence of cytosol, indicated in orange. The opsin-derived epitope tag is in italics with the N-glycosylated Asn marked in red. Predicted proteinase K cleavage sites to the N-terminus of the TMS are indicated by arrows. **B)** Depending on the environment and the length of Cytb5 polypeptide, different protein conformations within a lipid bilayer can be proposed. In the presence of cytosol and untreated membranes Cytb5 inserts with residue 107 localising to the IFR, tryptophans in the HC region and C-terminal charged amino acids in the ER lumen (I). This conformation allows for efficient N-glycosylation of the opsin-derived epitope tag. Lack of cytosolic and/or peripheral membrane proteins results in a cytoplasmic location of residue 107, tryptophans within the IFR and charged C-terminal amino acids occluded by the lumenal IFR (II). Due to its location relative to the oligosaccharyltransferase complex, the Asn residue of the opsin-derived epitope tag cannot be efficiently modified (Nilsson and von Heijne, 1993). Based on early reports carried out using proteins lacking any C-terminal extension, two additional conformations of Cytb5 integrated into a lipid bilayer in the absence of cytosolic factors are suggested (Arinc et al., 1987; Chester et al., 1992; Dailey and Strittmatter, 1981a; Dailey and Strittmatter, 1981b; Enoch et al., 1979; Holloway et al., 1982; Rzepecki et al., 1986). The addition of Cytb5 to "disordered" lipid bilayers, such as biological membranes and dimyristyl phosphatidylcholine vesicles, may result in a hairpin-loop conformation with both the N- and C-termini facing the cytosol (III). More ordered lipid bilayers, exemplified by phosphatidylcholine vesicles, could favour Cytb5 partitioning only into the IFR region resulting in a protein species that is easily exchanged between different vesicle populations (see Introduction and (Enoch et al., 1979; Holloway et al., 1982)). Colour coding used is the same as in panel A but with the opsin-derived epitope tag also indicated in dark green.

charged acidic residues of the original Cytb5 C-terminus would be located to the lumenal side. This arrangement is in good agreement with an *in situ* study that confirmed the translocation of a Cytb5 C-terminal peptide into the ER lumen (Kuroda et al., 1996) (Figure 3.1B, I). This topology also places the Asn residue of the opsin-derived tag at a distance from the membrane predicted to be sufficient to allow for its efficient N-glycosylation. The postulated difference in conformations of Cytb5 integrated into the ER membrane in the presence or absence of cytosol would also account for the apparently distinct electrophoretic mobility of the resulting proteinase K-protected fragments (Figure 3.1A, see arrows).

Whether the putative collaborative action of cytosolic and membrane-associated factors drives Cytb5 integration into a lipid bilayer by an active mechanism, or passively enables the postulated "deeper" insertion is unclear. A possible mode of action for cytosolic proteins would be to stimulate the formation of an α-helix-like conformation within TMS, thereby ensuring the intramolecular hydrogen bonding essential for efficient membrane integration as exemplified by insertion of the pHLIP peptide into a lipid bilayer (Andreev et al., 2010; White and Wimley, 1999; Wimley et al., 1996; Wimley and White, 1996). In the absence of cytosolic components, the folding of Cytb5 would have to occur in the interfacial regions of a lipid bilayer leading to a distinct protein conformation. Once within the lipid bilayer and in a stable conformation, any perpendicular movement of the presumed α-helical membrane-spanning region would most likely be restricted by the preference of the charged C-terminal residues for an aqueous environment at the lumenal side (Figure 3.1B, I) and of the tryptophan cluster for the interfacial region at the cytosolic leaflet of the ER membrane (Figure 3.1B, II). The importance of both the tryptophan cluster and C-terminal acidic residues for Cytb5 binding to a lipid bilayer is reflected by their evolutionary conservation, and the finding that their substitutions or modifications result in an altered association of Cytb5 with membranes (Dailey and Strittmatter, 1981b; Ladokhin et al., 1992; Tretyachenko-Ladokhina et al., 1993).

It is worth noting that the C-terminus of membrane-integrated Cytb5 lacking the opsin epitope tag and generated in the absence of cytosolic or peripheral membrane proteins may remain in the membrane environment (cf. Figure 3.1B, II). Alternatively, since

the partitioning of such "uncapped" polypeptides is thermodynamically highly unfavourable (Ben-Tal et al., 1996; Hristova and White, 2005), the untagged protein may assume a quite distinct membrane-associated conformation, as suggested by earlier studies (Arinc et al., 1987; Chester et al., 1992; Dailey and Strittmatter, 1981a; Dailey and Strittmatter, 1981b; Rzepecki et al., 1986). Hence, in the case of "disordered" lipid bilayers, such as biological membranes and dimyristyl phosphatidylcholine vesicles, Cytb5 can bind in a so-called hairpin-loop topology with both the N- and C-termini located in the cytosol (Arinc et al., 1987; Chester et al., 1992; Dailey and Strittmatter, 1981a; Dailey and Strittmatter, 1981b; Rzepecki et al., 1986) and consistent with theoretical considerations (Engelman and Steitz, 1981) (Figure 3.1B, III). More ordered lipid bilayers, exemplified by phosphatidylcholine vesicles, may accept Cytb5 only into their interfacial region, resulting in a protein species that can be easily transferred between different vesicle populations (see Introduction and (Ben-Tal et al., 1996; Enoch et al., 1979; Holloway et al., 1982; White and Wimley, 1994)) (Figure 3.1B, IV).

A number of experiments can be designed to test the model presented above. As previously discussed (Chapter 2.2, see Discussion), fluorescently labelled variants of Cytb5OPG could be used to carry out "iodide quenching" experiments and establish the location of specific labelled cysteines relative to the lipid bilayer. Similarly, modification of these residues with thiol-reactive probes could provide complementary information about the conformation of membrane-associated Cytb5. By monitoring the N-glycosylation of a Cytb5 variant bearing a longer C-terminal extension, directly comparable to that used by Colombo et al. (2009), it should also be possible to verify whether a lack of cytosolic and/or peripheral membrane proteins results in a distinct positioning of the membrane-embedded region (cf. Figure 3.1B). Lastly, the potential effect of the C-terminal tag on the conformation of membrane-bound Cytb5 could be addressed by using a recombinant protein without this extension, and subjecting it to the fluorescence quenching and/or modification-based studies already described.

V. Candidates for Cytb5-specific cytosolic components.

Clearly the identification of a putative holdase and a membrane-bound receptor/integrase for Cytb5 will be the main aim of our future research. Members of

the Hsp70 family constitute good candidates for soluble components involved in the biogenesis of Cytb5, as indicated by a previous study (Rabu et al., 2008). At the same time, my pull-down analysis identified an Hsp40 protein, DNAJB4 (mammalian Hlj1), as a potential Cytb5-specific binding partner (Chapter 2.4). It is unclear whether DNAJB4 could function in isolation as a TA-protein binding partner that facilitates delivery to the ER membrane, or rather as a modulator of Hsp70 chaperones. Notably, DNAJB4 was previously shown to bind to the transmembrane segment-containing C-terminal tail of the human mu opioid receptor (Ancevska-Taneva et al., 2006), consistent with a recent finding that some DNAJ proteins can act independently of any Hsp70 partners (Hageman et al., 2010). However, the fact that DNAJ proteins also define the functional specificity of Hsp70 chaperones (Kampinga and Craig, 2010) makes both modes of action for DNAJB4 plausible. Future *in vitro* immunodepletion and *in vivo* siRNA experiments can be performed to address the potential role of DNAJB4 during Cytb5 biogenesis. Of particular note is the fact that Hsp70s support the integration of the M13 procoat protein into ER-derived microsomes, and their action cannot be substituted by other molecular chaperones involved in protein folding (Wiech et al., 1993). This suggests a more specific function for Hsp70s, possibly related to their interaction with a membrane-bound component(s), analogous to the cooperation observed between cytosolic and ER-associated proteins during Cytb5 membrane integration (see Chapter 2.2).

VI. Identity and function of novel components of the TRC40 pathway.

Mass spectrometric analysis of the cytosolic interacting partners of TA-proteins, followed by complementary functional studies, provided insights into the complexity of the TRC40-mediated route for TA-protein biogenesis at the ER membrane (Chapters 2.3 and 2.4). We identified a novel functional component of this pathway, Bat3 (HLA-B-associated transcript 3, also known as Bag-6 or Scythe). Based on our results we concluded that Bat3 acts upstream of TRC40 and speculated that it may assist the loading of TA-proteins onto TRC40 (Chapter 2.3). A subsequent publication is in close agreement with our findings, additionally showing that Bat3 together with two other components, Ubl4a and C7orf20 (TRC35), is recruited by ribosomes actively translating a TA polypeptide (Mariappan et al., 2010). The authors conclude that this "Bat3 complex" transfers TA-protein substrates to TRC40 (Mariappan et al., 2010). A previous mass spectrometric analysis had identified Bat3 as part of a protein

network that also included TRC40, Ubl4a, C7orf20 and SGTA (small glutamine-rich tetratricopeptide repeat-containing protein) (Sowa et al., 2009). Interestingly, both C7orf20 and SGTA interact with immobilised TA-proteins in our pull-down assay (Chapter 2.4), and SGTA binding to TRC40-dependent substrates was confirmed by immunoblotting (Chapters 2.3 and 2.4). Whilst TRC40 (Get3), C7orf20 (Get4), Ubl4a (Get5) and SGTA (Sgt2) all have clear yeast homologues (in parenthesis) that have been shown to participate in the GET pathway (Battle et al., 2010; Chang et al., 2010; Chartron et al., 2010; Costanzo et al., 2010; Jonikas et al., 2009; Schuldiner et al., 2005), Bat3 appears to be specific for multicellular eukaryotes perhaps suggesting a regulatory function.

Based on our own results, and current published data, it is possible to draw a hypothetical protein-protein interaction network illustrating how Bat3 might communicate with a number of other cytosolic components (Figure 3.2). Hence, an interaction of Bat3 with SGTA has been convincingly established by independent yeast two-hybrid and mass spectrometric analyses (Lehner et al., 2004; Rual et al., 2005; Sowa et al., 2009). Co-immunoprecipitation experiments determined that the C-terminal, glutamine-rich domain of SGTA is dispensable for binding to Bat3 (Winnefeld et al., 2006), whereas the N-terminal 96 residues of Bat3, containing the ubiquitin-like domain (UBL), were sufficient to interact with SGTA in a yeast two-hybrid screen (Figure 3.2) (Lehner et al., 2004). These data are also consistent with a different yeast two-hybrid screen where the Bat3 fragments used all lacked >250 residues of the N-terminus and no interaction with SGTA was detected (Stelzl et al., 2005). This Bat3-SGTA interaction is reminiscent of that established between Sgt2 (yeast homologue of SGTA) and Get5 that was mapped to the N-terminal part of Sgt2 and the UBL domain of Get5 (Chang et al., 2010; Chartron et al., 2010; Liou et al., 2007). By analogy, SGTA might bind to the UBL region of Ubl4a (mammalian homologue of Get5), and the oligomerisation of SGTA (Liou and Wang, 2005) would allow for its simultaneous interaction with both Bat3 and Ubl4a (Figure 3.2).

By further extrapolating structural information and genetic data obtained for components of the yeast GET pathway (Battle et al., 2010; Bozkurt et al., 2010; Chang et al., 2010; Chartron et al., 2010; Costanzo et al., 2010; Jonikas et al., 2009), one can speculate that Ubl4a (mammalian Get5) and C7orf20 (mammalian

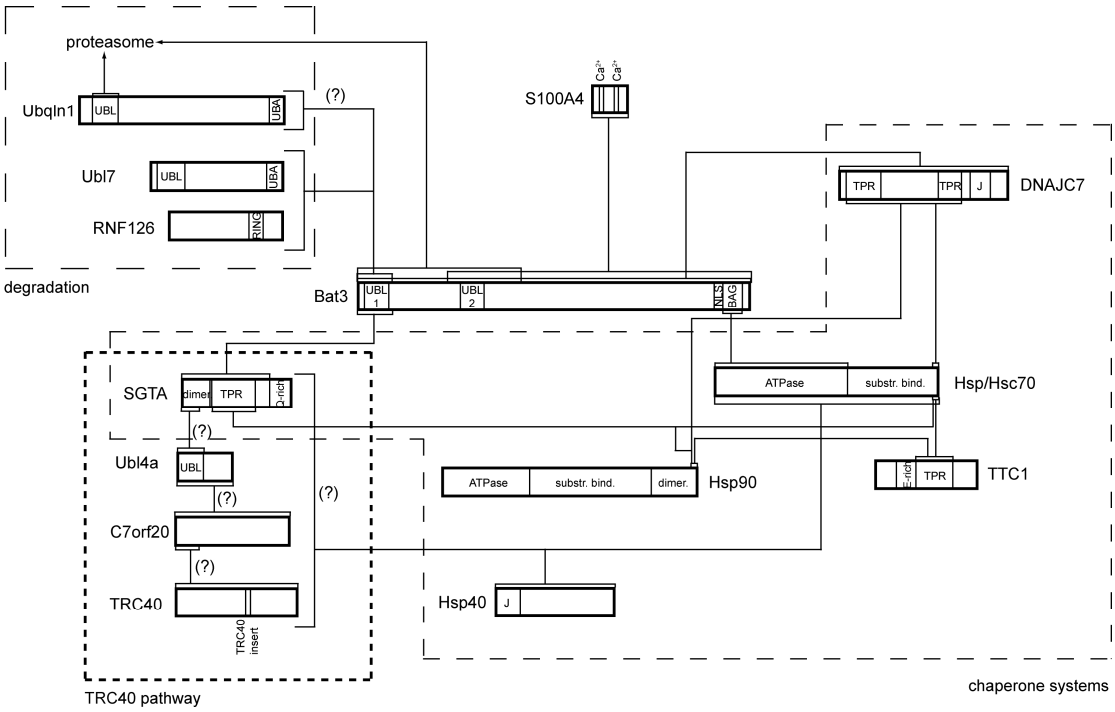

Figure 3.2 Hypothetical protein-protein interaction network for cytosolic TA-protein binding partners. Interactions of mammalian cytosolic proteins that associate preferentially with the full-length variants of immobilised recombinant TA-proteins are presented, based on experimental results and published data (see text). Coding region length, domain organisation and regions mediating protein-protein interactions are drawn to scale where possible. Hypothetical interactions based on analogy to the yeast system, or a comparison with other known binding partners, are indicated (?). Dimer – dimerisation domain; Ca^{2+} – putative calcium binding site; E-rich – glutamate-rich domain; J – J domain; NLS – nuclear localisation signal; Q-rich – glutamine-rich domain; TRC40 insert – sequence specific to archeal and eukaryotic TRC40 homologues; UBA – ubiquitin-associated domain; UBL – ubiquitin-like domain.

homologue of Get4) interact with each other directly, consistent with a mass spectrometric analysis of selected human protein networks (Sowa et al., 2009). However, the precise domains involved in any such interaction are unclear since the N-terminal region of Get5, implicated in binding to Get4, is fungi-specific and not conserved in mammalian Ubl4a (Chang et al., 2010; Chartron et al., 2010). At the same time, the N-terminal portion of Get4 that mediates its binding to Get3 is conserved, suggesting that the homologous region of C7orf20 will interact with TRC40 (Figure 3.2).

This conjecture, together with recent reports of a role for Bat3 during TA-protein biogenesis ((Leznicki et al., 2010; Mariappan et al., 2010) and Chapter 2.3), enable the construction of a working model describing a unified view of how individual components contribute to TA-protein biogenesis (Figure 3.3). Hence, a ribosome

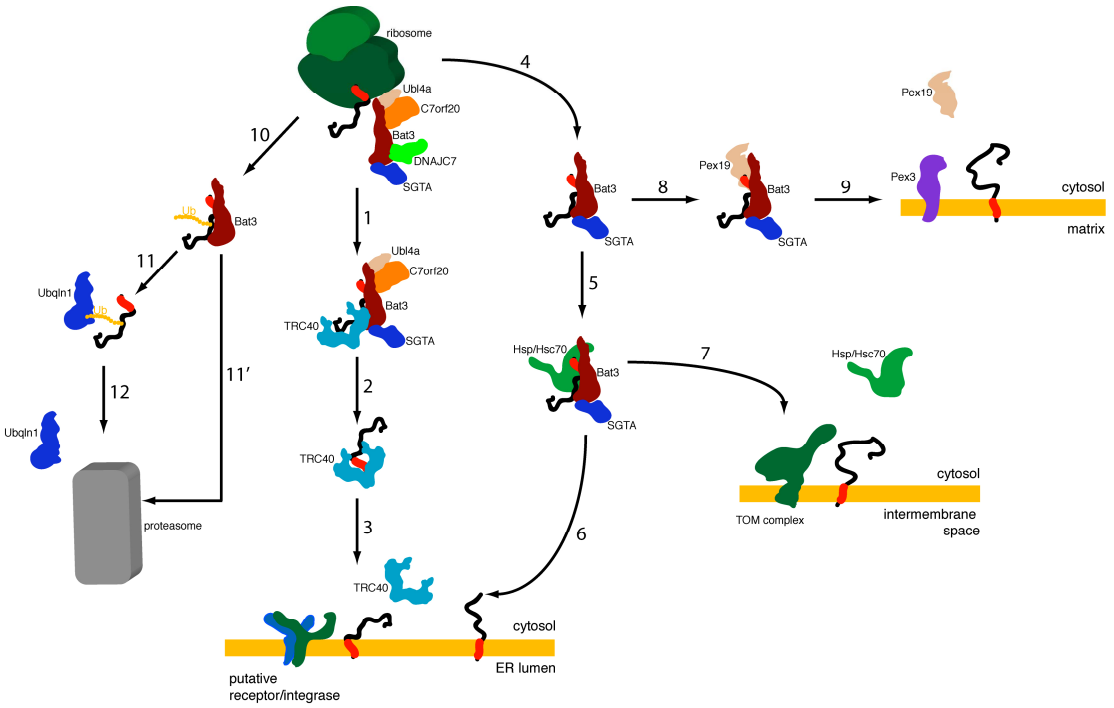

Figure 3.3 Schematic representation of hypothetical pathways for tail-anchored protein biogenesis. Synthesis of a TA-protein results in the ribosomal recruitment of Bat3, Ubl4a and C7orf20 ("Bat3 complex") while the transmembrane segment (TMS) is still buried inside the ribosomal exit tunnel. Bat3 is also complexed with DNAJC7 to ensure its cytoplasmic localisation, and SGTA also interacts with Bat3 and may even cooperate with the "Bat3 complex". Upon translation termination, the newly synthesised TA-protein is bound by the "Bat3 complex" (1), followed by its transfer to TRC40 (2) and subsequent integration into the ER membrane (3). TA-proteins of a relatively low TMS hydrophobicity and/or those destined for other intracellular compartments may be bound by the Bat3-SGTA complex alone (4) and then transferred to Hsp/Hsc70 chaperones (5), that would facilitate integration into the ER (6) or mitochondrial outer membranes (7). Discrimination between these two possible destinations could be regulated by additional cytosolic components (such as Hsp90) and/or membrane-bound receptors. Membrane proteins destined for peroxisomes could be transferred from the Bat3-SGTA complex to Pex19 (8) and later inserted into the peroxisomal membrane (9). The misfolding of a TA-protein and/or cellular perturbations that affect its biogenesis could lead to ubiquitination (10) and transfer from Bat3 to ubiquilin 1 (Ubqln1) (11) followed by proteasomal degradation (12). Alternatively, Bat3 could directly associate with the proteasome and promote TA-protein degradation (11'). To ensure clarity, the potential role of DNAJC7 in retaining Bat3 in the cytosol is not indicated in most cases, and the various components shown are not drawn to scale.

synthesising a TA polypeptide would recruit Bat3, Ubl4a and C7orf20 whilst the TMS is still buried inside the ribosomal exit tunnel (Mariappan et al., 2010), facilitating the binding of this "Bat3 complex" to a tail-anchor region upon termination of translation (Figure 3.3, step 1). Subsequent interaction with TRC40 would result in a transfer of the TA-protein to this targeting factor, that would in turn enable the membrane integration step via its association with a putative membrane-bound receptor/integrase (Figure 3.3, steps 2 and 3). The precise role of SGTA is

unclear; however, given its evolutionary conservation and the fact that its yeast homologue constitutes an integral part of the GET pathway that functions before Get4/Get5 (see (Battle et al., 2010; Chang et al., 2010; Costanzo et al., 2010; Leznicki et al., 2010) and Introduction), it seems likely that SGTA contributes to substrate transfer from the ribosome to the "Bat3 complex" and/or TRC40.

Interestingly, even though Bat3 and SGTA interact with each other, it seems that both can also bind directly to a TA-protein substrate. This idea is supported by the finding that both components are recovered in a detergent-sensitive fraction when a pull-down assay with immobilised recombinant TA-proteins is performed, indicating an association mediated by hydrophobic forces (see (Leznicki et al., 2010) and Chapters 2.3 and 2.4). Furthermore, Bat3 expressed in yeast can bind to a model TA-protein in the absence of Sgt2 (see (Leznicki et al., 2010) and Chapter 2.3), whilst a yeast two-hybrid analysis suggested an interaction of Bat3 with a number of proteins containing hydrophobic membrane-spanning segments or signal peptides (Stelzl et al., 2005). Similarly, SGTA binds to several integral membrane proteins including type I glucose transporter (Liou and Wang, 2005), the Vpu protein of human HIV-1 virus (Dutta and Tan, 2008) and synaptotagmin-4 (Rual et al., 2005), as well as associates with the signal peptide of myostatin (Wang et al., 2003).

VII. Co-ordination of TA-protein delivery pathways.

Both Bat3 and SGTA can interact with Hsp70 chaperones and inhibit their ATPase and/or refolding activities (Angeletti et al., 2002; Thress et al., 2001). Whilst in the case of Bat3 this interaction occurs between its C-terminal BAG domain and the ATPase domain of Hsp70 (Doong et al., 2002; Kabbage and Dickman, 2008; Thress et al., 2001), for SGTA it is a consequence of the binding of the TPR domain of SGTA to a C-terminal EEVD motif of Hsp70 (Angeletti et al., 2002; Liou and Wang, 2005; Liu et al., 1999) (Figure 3.2). A Bat3 and/or SGTA-mediated inhibition of its chaperone activity might function to prevent Hsp70 binding to a TA-protein emerging from the ribosomal exit tunnel, thereby initially promoting substrate entry into the TRC40-dependent delivery route. From this perspective it is intriguing that our mass spectrometric analysis suggests that both SGTA and Bat3 associate with immobilised recombinant Cytb5 (Chapter 2.4), a TA-protein relying on a chaperone-facilitated route (see Introduction and above). Hence, whilst no association of the "Bat3

complex" could be observed with Cytb5 synthesised *in vitro* (Mariappan et al., 2010), and Bat3 immunodepletion does not affect Cytb5 membrane integration (see (Leznicki et al., 2010) and Chapter 2.3), its binding could be confirmed by immunoblotting (see Chapter 2.4). Whether the association of Bat3 and SGTA with Cytb5 that we observe reflects a true physiological interaction will require further detailed investigation. However, if Bat3 and SGTA really bind to newly synthesised TA-proteins exploiting the chaperone-dependent route *in vivo*, then additional regulatory mechanisms for discriminating between substrates of the TRC40- and chaperone-mediated pathways would be required, and these could well involve Ubl4a and C7orf20 (cf. Figure 3.3, steps 4-6).

Although distinct pathways for TA-protein delivery to the ER membrane are often portrayed as being independent of one another, there is in fact good evidence for some degree of overlap or interplay between them (see also (Rabu et al., 2009)). As detailed above, Bat3 and SGTA participate in delivering TRC40 clients to the ER, yet at the same time they modulate the activities of Hsp70 chaperones (Angeletti et al., 2002; Liou and Wang, 2005; Liu et al., 1999; Thress et al., 2001). Furthermore, yeast components of the GET pathway were shown to interact with Ydj1, a major cellular Hsp40 co-chaperone that regulates the function of Hsp70s (Chang et al., 2010; Liou et al., 2007). It seems plausible that a similar interaction also occurs in higher eukaryotes, providing another link between the TRC40 pathway and the chaperone-mediated route (Figure 3.2). Further evidence for redundancy between these two pathways is the observation that the deletion of components of the yeast GET pathway causes no obvious phenotype in the absence of additional stress (Auld et al., 2006; Cherry et al., 1998; Schuldiner et al., 2005; Schuldiner et al., 2008), whilst the siRNA-mediated depletion of TRC40 in mammalian cells has no obvious effect on TA-protein biogenesis at the ER (data not shown).

The mass spectrometric investigation of the cytosolic interacting partners of immobilised TRC40-dependent TA-proteins identified two further Hsp70 co-chaperones (Chapter 2.4). These proteins, TTC1 (TPR1) and DNAJC7 (TPR2), both contain repeated tetratricopeptide motifs that mediate their interactions with Hsp70s and Hsp90s (Brychzy et al., 2003; Liu et al., 1999; Lotz et al., 2008; Moffatt et al., 2008; Murthy et al., 1996). DNAJC7 also has a J-domain that typically stimulates the

ATPase activity of Hsp70s and increases their affinity for substrates (Brychzy et al., 2003). In the case of glucocorticoid receptor activation, it has been suggested that DNAJC7 mediates its retrograde transfer from Hsp90 back to Hsp70, perhaps allowing further rounds of chaperone-mediated folding to occur (Brychzy et al., 2003). Strikingly, binding of DNAJC7 to the ligand-binding domain of the constitutive androstane receptor (CAR) was reported to prevent import of the latter protein into the nucleus, and thereby ensure a cytoplasmic localisation for CAR (Kobayashi et al., 2003).

Intriguingly, Bat3 also contains a nuclear localisation signal (Manchen and Hubberstey, 2001) suggesting a potential role for DNAJC7 in regulating Bat3 intracellular localisation. Several lines of evidence support such a function. Firstly, DNAJC7 was identified in the salt-sensitive fraction of components eluted from immobilised TA-proteins, suggestive of a regulatory component rather than a direct TA-protein binding partner that would most likely associate via hydrophobic interactions (Chapter 2.4). Secondly, co-immunoprecipitation experiments suggest that DNAJC7 and Bat3 interact in the cytosol (Chapter 2.4). Finally, when co-expressed with Bat3 and a model TA-protein, Sed5, in a yeast strain with a perturbed GET pathway, DNAJC7 prevents the Bat3-dependent mislocalisation of Sed5 to the nucleus (our unpublished data; see also (Leznicki et al., 2010) and Chapter 2.3). Immunofluorescence experiments will be required to establish whether this effect results from the DNAJC7-dependent retention of Bat3 in the cytoplasm. Alternatively, though in my view less likely, DNAJC7 may bind preferentially to the TA-protein substrate and thereby outcompete Bat3 to retain Sed5 in the cytoplasm. It also remains to be established whether the overexpression of DNAJC7 in mammalian cells causes any increase in the cytosolic pool of Bat3.

It is tempting to speculate that DNAJC7 might promote the cytosolic localisation of the "Bat3 complex" that is recruited to the ribosome (Figure 3.3). Consistent with this hypothesis, both Bat3 and DNAJC7 are found in high molecular weight complexes when a pelleting assay is performed (data not shown). In this scenario, conditions such as cellular stress might stimulate DNAJC7 binding to unfolded polypeptides, either directly or via association with Hsp70s, leading to its release from Bat3, thereby allowing Bat3 translocation into the nucleus and/or enabling its apoptosis-related

functions (Desmots et al., 2005; Desmots et al., 2008; Manchen and Hubberstey, 2001). Such a model resembles the behaviour of the ER lumenal Hsp70 chaperone, BiP, in response to ER stress (Rutkowski and Kaufman, 2004).

VIII. A universal role for Bat3 in post-translational membrane protein delivery.

Strikingly, Pex19, a major targeting factor for peroxisomal membrane proteins (Fujiki et al., 2006; Jones et al., 2004; Sacksteder et al., 2000), was also identified in the pull-down assay with immobilised TRC40-dependent TA-proteins (Chapter 2.4). The binding of Pex19 to peroxisomal TA substrates was previously shown to occur via specific sequences within their targeting motifs (Delille and Schrader, 2008; Halbach et al., 2006; Rottensteiner et al., 2004), consistent with a lack of any Pex19 interaction with non-peroxisomal membrane proteins (Sacksteder et al., 2000). A detailed bioinformatic analysis of the transmembrane segments of TA-proteins delivered to the ER via the TRC40 pathway will be required to indicate whether this association may reflect authentic binding. Alternatively, Pex19 may not bind directly to TA-protein baits, but rather associate with another component that is involved in the biogenesis of several groups of membrane proteins destined for various intracellular compartments. Given the data presented above, an exciting hypothesis can be formulated where Bat3 acts as a scaffold and/or regulator of most or even all post-translational biogenesis of membrane proteins. Such a universal role is consistent with the known links between Bat3, the TRC40 pathway and the Hsp70 chaperones implicated in the biogenesis of mitochondrial membrane proteins (Endo and Yamano, 2010; Young et al., 2003). Notably, a high-confidence interaction between Bat3 and TOM20, a mitochondrial outer membrane protein, was identified in a two-hybrid analysis (Stelzl et al., 2005), whilst a recent study suggests links between the yeast GET pathway and the biogenesis of peroxisomal TA-proteins (van der Zand et al., 2010).

IX. TA-protein degradation/quality control.

Mass spectrometric analysis of the binding partners of recombinant TA-proteins also identified ubiquilin 1 (UBQLN1), a factor implicated in protein quality control via the ubiquitin-proteasome system (Lim et al., 2009; Wang and Monteiro, 2007). Although any mechanism for a ubiquilin-mediated recruitment of TA-proteins for degradation is purely hypothetical at present, some comparisons can be drawn by analysing Bat3 interacting partners. Hence, full-length Bat3 (Rual et al., 2005) and its N-terminal 96

residues (Lehner et al., 2004) were shown to interact with ubiquitin-like protein 7 (Ubl7) in a yeast two-hybrid screen. Interestingly, Ubl7 shares a common domain organisation with ubiquilin 1, having a UBL domain at its N-terminus and a ubiquitin-associated domain (UBA) at its C-terminus (Figure 3.2). In the case of ubiquilin 1, the UBL domain mediates an association with the proteasome, and the UBA region binds poly-ubiquitinated proteins (Ko et al., 2004). An interaction of Bat3 with ubiquilin would therefore provide a link between TA-protein biogenesis and their proteasomal degradation (Figure 3.3, steps 11 and 12). Other factors communicating with the ubiquitin-proteasome system, including RNF126, were also identified as Bat3 interacting partners, further supporting its potential role in directing TA-proteins for degradation (Lehner et al., 2004; Rual et al., 2005). Alternatively, Bat3 could interact with the proteasome directly as established for another member of the BAG protein family, Bag-1 (Luders et al., 2000). A recent finding that Bat3 is essential for the proteasome-mediated degradation of some newly synthesised polypeptides further highlights its involvement in protein quality control (Minami et al., 2010). Hence, when taken together, the known Bat3 interacting partners can be grouped into several distinct clusters pointing to a role as a scaffold and/or regulatory protein (Figure 3.2). It is worth noting that a calcium-binding protein, S100A4, was also identified in a yeast two-hybrid analysis as a Bat3 partner (Stelzl et al., 2005). Intriguingly, the calmodulin antagonists fluphenazine and amitriptyline also target S100 proteins (Okada et al., 2004; Okada et al., 2002), and I found that these compounds strongly inhibit the membrane integration of TA-proteins (data not shown). In short, the regulation of TA-protein biogenesis is almost certainly even more complex than suggested above.

CHAPTER FOUR

References (relevant to Chapters 1, 2.4 and 3)

REFERENCES

Abell, B. M., Jung, M., Oliver, J. D., Knight, B. C., Tyedmers, J., Zimmermann, R. and High, S. (2003). Tail-anchored and signal-anchored proteins utilize overlapping pathways during membrane insertion. *J Biol Chem* **278**, 5669-78.

Abell, B. M., Pool, M. R., Schlenker, O., Sinning, I. and High, S. (2004). Signal recognition particle mediates post-translational targeting in eukaryotes. *Embo J* **23**, 2755-64.

Abell, B. M., Rabu, C., Leznicki, P., Young, J. C. and High, S. (2007). Post-translational integration of tail-anchored proteins is facilitated by defined molecular chaperones. *J Cell Sci* **120**, 1743-51.

Ancevska-Taneva, N., Onoprishvili, I., Andria, M. L., Hiller, J. M. and Simon, E. J. (2006). A member of the heat shock protein 40 family, hlj1, binds to the carboxyl tail of the human mu opioid receptor. *Brain Res* **1081**, 28-33.

Anderson, D. J., Mostov, K. E. and Blobel, G. (1983). Mechanisms of integration of de novo-synthesized polypeptides into membranes: signal-recognition particle is required for integration into microsomal membranes of calcium ATPase and of lens MP26 but not of cytochrome b5. *Proc Natl Acad Sci U S A* **80**, 7249-53.

Andreev, O. A., Karabadzhak, A. G., Weerakkody, D., Andreev, G. O., Engelman, D. M. and Reshetnyak, Y. K. (2010). pH (low) insertion peptide (pHLIP) inserts across a lipid bilayer as a helix and exits by a different path. *Proc Natl Acad Sci U S A* **107**, 4081-6.

Angeletti, P. C., Walker, D. and Panganiban, A. T. (2002). Small glutamine-rich protein/viral protein U-binding protein is a novel cochaperone that affects heat shock protein 70 activity. *Cell Stress Chaperones* **7**, 258-68.

Arinc, E., Rzepecki, L. M. and Strittmatter, P. (1987). Topography of the C terminus of cytochrome b5 tightly bound to dimyristoylphosphatidylcholine vesicles. *J Biol Chem* **262**, 15563-7.

Auld, K. L., Hitchcock, A. L., Doherty, H. K., Frietze, S., Huang, L. S. and Silver, P. A. (2006). The conserved ATPase Get3/Arr4 modulates the activity of membrane-associated proteins in Saccharomyces cerevisiae. *Genetics* **174**, 215-27.

Battle, A., Jonikas, M. C., Walter, P., Weissman, J. S. and Koller, D. (2010). Automated identification of pathways from quantitative genetic interaction data. *Mol Syst Biol* **6**, 379.

Becker, T., Bhushan, S., Jarasch, A., Armache, J. P., Funes, S., Jossinet, F., Gumbart, J., Mielke, T., Berninghausen, O., Schulten, K. et al. (2009). Structure of monomeric yeast and mammalian Sec61 complexes interacting with the translating ribosome. *Science* **326**, 1369-73.

Ben-Tal, N., Ben-Shaul, A., Nicholls, A. and Honig, B. (1996). Free-energy determinants of alpha-helix insertion into lipid bilayers. *Biophys J* **70**, 1803-12.

Berndt, U., Oellerer, S., Zhang, Y., Johnson, A. E. and Rospert, S. (2009). A signal-anchor sequence stimulates signal recognition particle binding to ribosomes from inside the exit tunnel. *Proc Natl Acad Sci U S A* **106**, 1398-403.

Borgese, N. and Righi, M. (2010). REMOTE ORIGINS OF TAIL-ANCHORED PROTEINS. *Traffic* **11**, 877-85.

Borgese, N., Brambillasca, S. and Colombo, S. (2007). How tails guide tail-anchored proteins to their destinations. *Curr Opin Cell Biol* **19**, 368-75.

Borgese, N., Brambillasca, S., Soffientini, P., Yabal, M. and Makarow, M. (2003a). Biogenesis of tail-anchored proteins. *Biochem Soc Trans* **31**, 1238-42.

Borgese, N., Colombo, S. and Pedrazzini, E. (2003b). The tale of tail-anchored proteins: coming from the cytosol and looking for a membrane. *J Cell Biol* **161**, 1013-9.

Borgese, N., Gazzoni, I., Barberi, M., Colombo, S. and Pedrazzini, E. (2001). Targeting of a tail-anchored protein to endoplasmic reticulum and mitochondrial outer membrane by independent but competing pathways. *Mol Biol Cell* **12**, 2482-96.

Bozkurt, G., Stjepanovic, G., Vilardi, F., Amlacher, S., Wild, K., Bange, G., Favaloro, V., Rippe, K., Hurt, E., Dobberstein, B. et al. (2009). Structural insights into tail-anchored protein binding and membrane insertion by Get3. *Proc Natl Acad Sci U S A* **106**, 21131-6.

Bozkurt, G., Wild, K., Amlacher, S., Hurt, E., Dobberstein, B. and Sinning, I. (2010). The structure of Get4 reveals an alpha-solenoid fold adapted for multiple interactions in tail-anchored protein biogenesis. *FEBS Lett* **584**, 1509-14.

Brambillasca, S., Yabal, M., Makarow, M. and Borgese, N. (2006). Unassisted translocation of large polypeptide domains across phospholipid bilayers. *J Cell Biol* **175**, 767-77.

Brambillasca, S., Yabal, M., Soffientini, P., Stefanovic, S., Makarow, M., Hegde, R. S. and Borgese, N. (2005). Transmembrane topogenesis of a tail-anchored protein is modulated by membrane lipid composition. *Embo J* **24**, 2533-42.

Brychzy, A., Rein, T., Winklhofer, K. F., Hartl, F. U., Young, J. C. and Obermann, W. M. (2003). Cofactor Tpr2 combines two TPR domains and a J domain to regulate the Hsp70/Hsp90 chaperone system. *Embo J* **22**, 3613-23.

Bulbarelli, A., Sprocati, T., Barberi, M., Pedrazzini, E. and Borgese, N. (2002). Trafficking of tail-anchored proteins: transport from the endoplasmic reticulum to the plasma membrane and sorting between surface domains in polarised epithelial cells. *J Cell Sci* **115**, 1689-702.

Caballero, M., Carabana, J., Ortego, J., Fernandez-Munoz, R. and Celma, M. L. (1998). Measles virus fusion protein is palmitoylated on transmembrane-intracytoplasmic cysteine residues which participate in cell fusion. *J Virol* **72**, 8198-204.

Ceppi, P., Colombo, S., Francolini, M., Raimondo, F., Borgese, N. and Masserini, M. (2005). Two tail-anchored protein variants, differing in transmembrane domain length and intracellular sorting, interact differently with lipids. *Proc Natl Acad Sci U S A* **102**, 16269-74.

Chang, Y. W., Chuang, Y. C., Ho, Y. C., Cheng, M. Y., Sun, Y. J., Hsiao, C. D. and Wang, C. (2010). Crystal structure of Get4/Get5 complex and its interactions with Sgt2, Get3 and Ydj1. *J Biol Chem* **285**, 9962-70.

Chartron, J. W., Suloway, C. J., Zaslaver, M. and Clemons, W. M., Jr. (2010). Structural characterization of the Get4/Get5 complex and its interaction with Get3. *Proc Natl Acad Sci U S A* **107**, 12127-32.

Cherry, J. M., Adler, C., Ball, C., Chervitz, S. A., Dwight, S. S., Hester, E. T., Jia, Y., Juvik, G., Roe, T., Schroeder, M. et al. (1998). SGD: Saccharomyces Genome Database. *Nucleic Acids Res* **26**, 73-9.

Chester, D. W., Skita, V., Young, H. S., Mavromoustakos, T. and Strittmatter, P. (1992). Bilayer structure and physical dynamics of the cytochrome b5 dimyristoylphosphatidylcholine interaction. *Biophys J* **61**, 1224-43.

Colombo, S. F., Longhi, R. and Borgese, N. (2009). The role of cytosolic proteins in the insertion of tail-anchored proteins into phospholipid bilayers. *J Cell Sci* **122**, 2383-92.

Copic, A., Dorrington, M., Pagant, S., Barry, J., Lee, M. C., Singh, I., Hartman, J. L. t. and Miller, E. A. (2009). Genomewide analysis reveals novel pathways affecting endoplasmic reticulum homeostasis, protein modification and quality control. *Genetics* **182**, 757-69.

Costanzo, M., Baryshnikova, A., Bellay, J., Kim, Y., Spear, E. D., Sevier, C. S., Ding, H., Koh, J. L., Toufighi, K., Mostafavi, S. et al. (2010). The genetic landscape of a cell. *Science* **327**, 425-31.

Crowley, K. S., Liao, S., Worrell, V. E., Reinhart, G. D. and Johnson, A. E. (1994). Secretory proteins move through the endoplasmic reticulum membrane via an aqueous, gated pore. *Cell* **78**, 461-71.

Crowley, K. S., Reinhart, G. D. and Johnson, A. E. (1993). The signal sequence moves through a ribosomal tunnel into a noncytoplasmic aqueous environment at the ER membrane early in translocation. *Cell* **73**, 1101-15.

Dailey, H. A. and Strittmatter, P. (1978). Structural and functional properties of the membrane binding segment of cytochrome b5. *J Biol Chem* **253**, 8203-9.

Dailey, H. A. and Strittmatter, P. (1981a). Orientation of the carboxyl and NH2 termini of the membrane-binding segment of cytochrome b5 on the same side of phospholipid bilayers. *J Biol Chem* **256**, 3951-5.

Dailey, H. A. and Strittmatter, P. (1981b). The role of COOH-terminal anionic residues in binding cytochrome b5 to phospholipid vesicles and biological membranes. *J Biol Chem* **256**, 1677-80.

Dalbey, R. E. and Kuhn, A. (2004). YidC family members are involved in the membrane insertion, lateral integration, folding, and assembly of membrane proteins. *J Cell Biol* **166**, 769-74.

Delille, H. K. and Schrader, M. (2008). Targeting of hFis1 to peroxisomes is mediated by Pex19p. *J Biol Chem* **283**, 31107-15.

Desmots, F., Russell, H. R., Lee, Y., Boyd, K. and McKinnon, P. J. (2005). The reaper-binding protein scythe modulates apoptosis and proliferation during mammalian development. *Mol Cell Biol* **25**, 10329-37.

Desmots, F., Russell, H. R., Michel, D. and McKinnon, P. J. (2008). Scythe regulates apoptosis-inducing factor stability during endoplasmic reticulum stress-induced apoptosis. *J Biol Chem* **283**, 3264-71.

Doong, H., Vrailas, A. and Kohn, E. C. (2002). What's in the 'BAG'?--A functional domain analysis of the BAG-family proteins. *Cancer Lett* **188**, 25-32.

Dutta, S. and Tan, Y. J. (2008). Structural and functional characterization of human SGT and its interaction with Vpu of the human immunodeficiency virus type 1. *Biochemistry* **47**, 10123-31.

Endo, T. and Yamano, K. (2010). Transport of proteins across or into the mitochondrial outer membrane. *Biochim Biophys Acta* **1803**, 706-14.

Engelman, D. M. and Steitz, T. A. (1981). The spontaneous insertion of proteins into and across membranes: the helical hairpin hypothesis. *Cell* **23**, 411-22.

Enoch, H. G., Fleming, P. J. and Strittmatter, P. (1979). The binding of cytochrome b5 to phospholipid vesicles and biological membranes. Effect of orientation on intermembrane transfer and digestion by carboxypeptidase Y. *J Biol Chem* **254**, 6483-8.

Favaloro, V., Spasic, M., Schwappach, B. and Dobberstein, B. (2008). Distinct targeting pathways for the membrane insertion of tail-anchored (TA) proteins. *J Cell Sci* **121**, 1832-40.

Favaloro, V., Vilardi, F., Schlecht, R., Mayer, M. P. and Dobberstein, B. (2010). Asna1/TRC40-mediated membrane insertion of tail-anchored proteins. *J Cell Sci* **123**, 1522-30.

Fleischer, T. C., Weaver, C. M., McAfee, K. J., Jennings, J. L. and Link, A. J. (2006). Systematic identification and functional screens of uncharacterized proteins associated with eukaryotic ribosomal complexes. *Genes Dev* **20**, 1294-307.

Fleming, P. J., Koppel, D. E., Lau, A. L. and Strittmatter, P. (1979). Intramembrane position of the fluorescent tryptophanyl residue in membrane-bound cytochrome b5. *Biochemistry* **18**, 5458-64.

Fujiki, Y., Matsuzono, Y., Matsuzaki, T. and Fransen, M. (2006). Import of peroxisomal membrane proteins: the interplay of Pex3p- and Pex19p-mediated interactions. *Biochim Biophys Acta* **1763**, 1639-46.

Gilmore, R. and Blobel, G. (1985). Translocation of secretory proteins across the microsomal membrane occurs through an environment accessible to aqueous perturbants. *Cell* **42**, 497-505.

Gorlich, D. and Rapoport, T. A. (1993). Protein translocation into proteoliposomes reconstituted from purified components of the endoplasmic reticulum membrane. *Cell* **75**, 615-30.

Hageman, J., Rujano, M. A., van Waarde, M. A., Kakkar, V., Dirks, R. P., Govorukhina, N., Oosterveld-Hut, H. M., Lubsen, N. H. and Kampinga, H. H. (2010). A DNAJB chaperone subfamily with HDAC-dependent activities suppresses toxic protein aggregation. *Mol Cell* **37**, 355-69.

Haigh, N. G. and Johnson, A. E. (2002). A new role for BiP: closing the aqueous translocon pore during protein integration into the ER membrane. *J Cell Biol* **156**, 261-70.

Halbach, A., Landgraf, C., Lorenzen, S., Rosenkranz, K., Volkmer-Engert, R., Erdmann, R. and Rottensteiner, H. (2006). Targeting of the tail-anchored peroxisomal membrane proteins PEX26 and PEX15 occurs through C-terminal PEX19-binding sites. *J Cell Sci* **119**, 2508-17.

Hamman, B. D., Chen, J. C., Johnson, E. E. and Johnson, A. E. (1997). The aqueous pore through the translocon has a diameter of 40-60 A during cotranslational protein translocation at the ER membrane. *Cell* **89**, 535-44.

Hamman, B. D., Hendershot, L. M. and Johnson, A. E. (1998). BiP maintains the permeability barrier of the ER membrane by sealing the lumenal end of the translocon pore before and early in translocation. *Cell* **92**, 747-58.

High, S. and Abell, B. M. (2004). Tail-anchored protein biosynthesis at the endoplasmic reticulum: the same but different. *Biochem Soc Trans* **32**, 659-62.

High, S. and Dobberstein, B. (1992). Mechanisms that determine the transmembrane disposition of proteins. *Curr Opin Cell Biol* **4**, 581-6.

High, S., Andersen, S. S., Gorlich, D., Hartmann, E., Prehn, S., Rapoport, T. A. and Dobberstein, B. (1993). Sec61p is adjacent to nascent type I and type II signal-anchor proteins during their membrane insertion. *J Cell Biol* **121**, 743-50.

Holloway, P. W., Markello, T. C. and Leto, T. L. (1982). The Interaction of Cytochrome b(5) with Lipid Vesicles. *Biophys J* **37**, 63-4.

Honsho, M., Mitoma, J. Y. and Ito, A. (1998). Retention of cytochrome b5 in the endoplasmic reticulum is transmembrane and luminal domain-dependent. *J Biol Chem* **273**, 20860-6.

Hristova, K. and White, S. H. (2005). An experiment-based algorithm for predicting the partitioning of unfolded peptides into phosphatidylcholine bilayer interfaces. *Biochemistry* **44**, 12614-9.

Hu, J., Li, J., Qian, X., Denic, V. and Sha, B. (2009). The crystal structures of yeast Get3 suggest a mechanism for tail-anchored protein membrane insertion. *PLoS One* **4**, e8061.

Isenmann, S., Khew-Goodall, Y., Gamble, J., Vadas, M. and Wattenberg, B. W. (1998). A splice-isoform of vesicle-associated membrane protein-1 (VAMP-1) contains a mitochondrial targeting signal. *Mol Biol Cell* **9**, 1649-60.

Janda, C. Y., Li, J., Oubridge, C., Hernandez, H., Robinson, C. V. and Nagai, K. (2010). Recognition of a signal peptide by the signal recognition particle. *Nature* **465**, 507-10.

Jones, J. M., Morrell, J. C. and Gould, S. J. (2004). PEX19 is a predominantly cytosolic chaperone and import receptor for class 1 peroxisomal membrane proteins. *J Cell Biol* **164**, 57-67.

Jonikas, M. C., Collins, S. R., Denic, V., Oh, E., Quan, E. M., Schmid, V., Weibezahn, J., Schwappach, B., Walter, P., Weissman, J. S. et al. (2009). Comprehensive characterization of genes required for protein folding in the endoplasmic reticulum. *Science* **323**, 1693-7.

Kabbage, M. and Dickman, M. B. (2008). The BAG proteins: a ubiquitous family of chaperone regulators. *Cell Mol Life Sci* **65**, 1390-402.

Kalbfleisch, T., Cambon, A. and Wattenberg, B. W. (2007). A bioinformatics approach to identifying tail-anchored proteins in the human genome. *Traffic* **8**, 1687-94.

Kalies, K. U., Gorlich, D. and Rapoport, T. A. (1994). Binding of ribosomes to the rough endoplasmic reticulum mediated by the Sec61p-complex. *J Cell Biol* **126**, 925-34.

Kampinga, H. H. and Craig, E. A. (2010). The HSP70 chaperone machinery: J proteins as drivers of functional specificity. *Nat Rev Mol Cell Biol* **11**, 579-92.

Kiefer, D. and Kuhn, A. (1999). Hydrophobic forces drive spontaneous membrane insertion of the bacteriophage Pf3 coat protein without topological control. *Embo J* **18**, 6299-306.

Kim, P. K., Hollerbach, C., Trimble, W. S., Leber, B. and Andrews, D. W. (1999). Identification of the endoplasmic reticulum targeting signal in vesicle-associated membrane proteins. *J Biol Chem* **274**, 36876-82.

Kim, P. K., Janiak-Spens, F., Trimble, W. S., Leber, B. and Andrews, D. W. (1997). Evidence for multiple mechanisms for membrane binding and integration via carboxyl-terminal insertion sequences. *Biochemistry* **36**, 8873-82.

Ko, H. S., Uehara, T., Tsuruma, K. and Nomura, Y. (2004). Ubiquilin interacts with ubiquitylated proteins and proteasome through its ubiquitin-associated and ubiquitin-like domains. *FEBS Lett* **566**, 110-4.

Kobayashi, K., Sueyoshi, T., Inoue, K., Moore, R. and Negishi, M. (2003). Cytoplasmic accumulation of the nuclear receptor CAR by a tetratricopeptide repeat protein in HepG2 cells. *Mol Pharmacol* **64**, 1069-75.

Kuhn, A., Stuart, R., Henry, R. and Dalbey, R. E. (2003). The Alb3/Oxa1/YidC protein family: membrane-localized chaperones facilitating membrane protein insertion? *Trends Cell Biol* **13**, 510-6.

Kuroda, R., Kinoshita, J., Honsho, M., Mitoma, J. and Ito, A. (1996). In situ topology of cytochrome b5 in the endoplasmic reticulum membrane. *J Biochem* **120**, 828-33.

Kutay, U., Ahnert-Hilger, G., Hartmann, E., Wiedenmann, B. and Rapoport, T. A. (1995). Transport route for synaptobrevin via a novel pathway of insertion into the endoplasmic reticulum membrane. *Embo J* **14**, 217-23.

Kutay, U., Hartmann, E. and Rapoport, T. A. (1993). A class of membrane proteins with a C-terminal anchor. *Trends Cell Biol* **3**, 72-5.

Ladokhin, A. S., Tretyachenko-Ladokhina, V. G., Holloway, P. W., Wang, L. and Steggles, A. W. (1992). Biophysical studies of cytochromes B5 with amino acid substitutions in the membrane-binding domain. *Biophys J* **62**, 79-81.

Lakkaraju, A. K., Mary, C., Scherrer, A., Johnson, A. E. and Strub, K. (2008). SRP keeps polypeptides translocation-competent by slowing translation to match limiting ER-targeting sites. *Cell* **133**, 440-51.

Le Gall, S., Neuhof, A. and Rapoport, T. (2004). The endoplasmic reticulum membrane is permeable to small molecules. *Mol Biol Cell* **15**, 447-55.

Lehner, B., Semple, J. I., Brown, S. E., Counsell, D., Campbell, R. D. and Sanderson, C. M. (2004). Analysis of a high-throughput yeast two-hybrid system and its use to predict the function of intracellular proteins encoded within the human MHC class III region. *Genomics* **83**, 153-67.

Lewis, B. A. and Engelman, D. M. (1983). Lipid bilayer thickness varies linearly with acyl chain length in fluid phosphatidylcholine vesicles. *J Mol Biol* **166**, 211-7.

Leznicki, P. (2005). [Aggregation and toxicity of the proteins with polyQ repeats]. *Postepy Biochem* **51**, 215-22.

Leznicki, P., Clancy, A., Schwappach, B. and High, S. (2010). Bat3 promotes the membrane integration of tail-anchored proteins. *J Cell Sci* **123**, 2170-8.

Liao, S., Lin, J., Do, H. and Johnson, A. E. (1997). Both lumenal and cytosolic gating of the aqueous ER translocon pore are regulated from inside the ribosome during membrane protein integration. *Cell* **90**, 31-41.

Lim, P. J., Danner, R., Liang, J., Doong, H., Harman, C., Srinivasan, D., Rothenberg, C., Wang, H., Ye, Y., Fang, S. et al. (2009). Ubiquilin and p97/VCP bind erasin, forming a complex involved in ERAD. *J Cell Biol* **187**, 201-17.

Linstedt, A. D., Foguet, M., Renz, M., Seelig, H. P., Glick, B. S. and Hauri, H. P. (1995). A C-terminally-anchored Golgi protein is inserted into the endoplasmic reticulum and then transported to the Golgi apparatus. *Proc Natl Acad Sci U S A* **92**, 5102-5.

Liou, S. T. and Wang, C. (2005). Small glutamine-rich tetratricopeptide repeat-containing protein is composed of three structural units with distinct functions. *Arch Biochem Biophys* **435**, 253-63.

Liou, S. T., Cheng, M. Y. and Wang, C. (2007). SGT2 and MDY2 interact with molecular chaperone YDJ1 in Saccharomyces cerevisiae. *Cell Stress Chaperones* **12**, 59-70.

Liu, F. H., Wu, S. J., Hu, S. M., Hsiao, C. D. and Wang, C. (1999). Specific interaction of the 70-kDa heat shock cognate protein with the tetratricopeptide repeats. *J Biol Chem* **274**, 34425-32.

Lotz, G. P., Brychzy, A., Heinz, S. and Obermann, W. M. (2008). A novel HSP90 chaperone complex regulates intracellular vesicle transport. *J Cell Sci* **121**, 717-23.

Luders, J., Demand, J. and Hohfeld, J. (2000). The ubiquitin-related BAG-1 provides a link between the molecular chaperones Hsc70/Hsp70 and the proteasome. *J Biol Chem* **275**, 4613-7.

Manchen, S. T. and Hubberstey, A. V. (2001). Human Scythe contains a functional nuclear localization sequence and remains in the nucleus during staurosporine-induced apoptosis. *Biochem Biophys Res Commun* **287**, 1075-82.

Mariappan, M., Li, X., Stefanovic, S., Sharma, A., Mateja, A., Keenan, R. J. and Hegde, R. S. (2010). A ribosome-associating factor chaperones tail-anchored membrane proteins. *Nature* **466**, 1120-4.

Masaki, R., Kameyama, K. and Yamamoto, A. (2003). Post-translational targeting of a tail-anchored green fluorescent protein to the endolpasmic reticulum. *J Biochem* **134**, 415-26.

Mason, N., Ciufo, L. F. and Brown, J. D. (2000). Elongation arrest is a physiologically important function of signal recognition particle. *Embo J* **19**, 4164-74.

Mateja, A., Szlachcic, A., Downing, M. E., Dobosz, M., Mariappan, M., Hegde, R. S. and Keenan, R. J. (2009). The structural basis of tail-anchored membrane protein recognition by Get3. *Nature* **461**, 361-6.

McDonough, H. and Patterson, C. (2003). CHIP: a link between the chaperone and proteasome systems. *Cell Stress Chaperones* **8**, 303-8.

Minami, R., Hayakawa, A., Kagawa, H., Yanagi, Y., Yokosawa, H. and Kawahara, H. (2010). BAG-6 is essential for selective elimination of defective proteasomal substrates. *J Cell Biol* **190**, 637-50.

Moffatt, N. S., Bruinsma, E., Uhl, C., Obermann, W. M. and Toft, D. (2008). Role of the cochaperone Tpr2 in Hsp90 chaperoning. *Biochemistry* **47**, 8203-13.

Murthy, A. E., Bernards, A., Church, D., Wasmuth, J. and Gusella, J. F. (1996). Identification and characterization of two novel tetratricopeptide repeat-containing genes. *DNA Cell Biol* **15**, 727-35.

Ngosuwan, J., Wang, N. M., Fung, K. L. and Chirico, W. J. (2003). Roles of cytosolic Hsp70 and Hsp40 molecular chaperones in post-translational translocation of presecretory proteins into the endoplasmic reticulum. *J Biol Chem* **278**, 7034-42.

Nicchitta, C. V. and Blobel, G. (1993). Lumenal proteins of the mammalian endoplasmic reticulum are required to complete protein translocation. *Cell* **73**, 989-98.

Nilsson, I. M. and von Heijne, G. (1993). Determination of the distance between the oligosaccharyltransferase active site and the endoplasmic reticulum membrane. *J Biol Chem* **268**, 5798-801.

Ochsenbauer-Jambor, C., Miller, D. C., Roberts, C. R., Rhee, S. S. and Hunter, E. (2001). Palmitoylation of the Rous sarcoma virus transmembrane glycoprotein is required for protein stability and virus infectivity. *J Virol* **75**, 11544-54.

Okada, M., Hatakeyama, T., Itoh, H., Tokuta, N., Tokumitsu, H. and Kobayashi, R. (2004). S100A1 is a novel molecular chaperone and a member of the Hsp70/Hsp90 multichaperone complex. *J Biol Chem* **279**, 4221-33.

Okada, M., Tokumitsu, H., Kubota, Y. and Kobayashi, R. (2002). Interaction of S100 proteins with the antiallergic drugs, olopatadine, amlexanox, and cromolyn: identification of putative drug binding sites on S100A1 protein. *Biochem Biophys Res Commun* **292**, 1023-30.

Oliver, J. D., Roderick, H. L., Llewellyn, D. H. and High, S. (1999). ERp57 functions as a subunit of specific complexes formed with the ER lectins calreticulin and calnexin. *Mol Biol Cell* **10**, 2573-82.

Oliver, J., Jungnickel, B., Gorlich, D., Rapoport, T. and High, S. (1995). The Sec61 complex is essential for the insertion of proteins into the membrane of the endoplasmic reticulum. *FEBS Lett* **362**, 126-30.

Panzner, S., Dreier, L., Hartmann, E., Kostka, S. and Rapoport, T. A. (1995). Posttranslational protein transport in yeast reconstituted with a purified complex of Sec proteins and Kar2p. *Cell* **81**, 561-70.

Plath, K. and Rapoport, T. A. (2000). Spontaneous release of cytosolic proteins from posttranslational substrates before their transport into the endoplasmic reticulum. *J Cell Biol* **151**, 167-78.

Pool, M. R. (2003). Getting to the membrane: how is co-translational protein targeting to the endoplasmic reticulum regulated? *Biochem Soc Trans* **31**, 1232-7.

Pool, M. R. (2005). Signal recognition particles in chloroplasts, bacteria, yeast and mammals (review). *Mol Membr Biol* **22**, 3-15.

Rabu, C., Schmid, V., Schwappach, B. and High, S. (2009). Biogenesis of tail-anchored proteins: the beginning for the end? *J Cell Sci* **122**, 3605-12.

Rabu, C., Wipf, P., Brodsky, J. L. and High, S. (2008). A precursor-specific role for Hsp40/Hsc70 during tail-anchored protein integration at the endoplasmic reticulum. *J Biol Chem* **283**, 27504-13.

Rachubinski, R. A., Verma, D. P. and Bergeron, J. J. (1980). Synthesis of rat liver microsomal cytochrome b5 by free ribosomes. *J Cell Biol* **84**, 705-16.

Romisch, K., Miller, F. W., Dobberstein, B. and High, S. (2006). Human autoantibodies against the 54 kDa protein of the signal recognition particle block function at multiple stages. *Arthritis Res Ther* **8**, R39.

Ross, C. A. and Poirier, M. A. (2004). Protein aggregation and neurodegenerative disease. *Nat Med* **10 Suppl**, S10-7.

Rottensteiner, H., Kramer, A., Lorenzen, S., Stein, K., Landgraf, C., Volkmer-Engert, R. and Erdmann, R. (2004). Peroxisomal membrane proteins contain common Pex19p-binding sites that are an integral part of their targeting signals. *Mol Biol Cell* **15**, 3406-17.

Rual, J. F., Venkatesan, K., Hao, T., Hirozane-Kishikawa, T., Dricot, A., Li, N., Berriz, G. F., Gibbons, F. D., Dreze, M., Ayivi-Guedehoussou, N. et al. (2005). Towards a proteome-scale map of the human protein-protein interaction network. *Nature* **437**, 1173-8.

Rutkowski, D. T. and Kaufman, R. J. (2004). A trip to the ER: coping with stress. *Trends Cell Biol* **14**, 20-8.

Ryan, C. M., Souda, P., Bassilian, S., Ujwal, R., Zhang, J., Abramson, J., Ping, P., Durazo, A., Bowie, J. U., Hasan, S. S. et al. (2010). Post-translational modifications of integral membrane proteins resolved by top-down Fourier transform mass spectrometry with collisionally activated dissociation. *Mol Cell Proteomics* **9**, 791-803.

Rzepecki, L. M., Strittmatter, P. and Herbette, L. G. (1986). X-ray diffraction analysis of cytochrome b5 reconstituted in egg phosphatidylcholine vesicles. *Biophys J* **49**, 829-38.

Sacksteder, K. A., Jones, J. M., South, S. T., Li, X., Liu, Y. and Gould, S. J. (2000). PEX19 binds multiple peroxisomal membrane proteins, is predominantly cytoplasmic, and is required for peroxisome membrane synthesis. *J Cell Biol* **148**, 931-44.

Samuelson, J. C., Chen, M., Jiang, F., Moller, I., Wiedmann, M., Kuhn, A., Phillips, G. J. and Dalbey, R. E. (2000). YidC mediates membrane protein insertion in bacteria. *Nature* **406**, 637-41.

Sanz, P. and Meyer, D. I. (1988). Signal recognition particle (SRP) stabilizes the translocation-competent conformation of pre-secretory proteins. *Embo J* **7**, 3553-7.

Schuldiner, M., Collins, S. R., Thompson, N. J., Denic, V., Bhamidipati, A., Punna, T., Ihmels, J., Andrews, B., Boone, C., Greenblatt, J. F. et al. (2005). Exploration of the function and organization of the yeast early secretory pathway through an epistatic miniarray profile. *Cell* **123**, 507-19.

Schuldiner, M., Metz, J., Schmid, V., Denic, V., Rakwalska, M., Schmitt, H. D., Schwappach, B. and Weissman, J. S. (2008). The GET complex mediates insertion of tail-anchored proteins into the ER membrane. *Cell* **134**, 634-45.

Sharpe, H. J., Stevens, T. J. and Munro, S. (2010). A comprehensive comparison of transmembrane domains reveals organelle-specific properties. *Cell* **142**, 158-69.

Simon, S. M. and Blobel, G. (1991). A protein-conducting channel in the endoplasmic reticulum. *Cell* **65**, 371-80.

Soekarjo, M., Eisenhawer, M., Kuhn, A. and Vogel, H. (1996). Thermodynamics of the membrane insertion process of the M13 procoat protein, a lipid bilayer traversing protein containing a leader sequence. *Biochemistry* **35**, 1232-41.

Sowa, M. E., Bennett, E. J., Gygi, S. P. and Harper, J. W. (2009). Defining the human deubiquitinating enzyme interaction landscape. *Cell* **138**, 389-403.

Spatz, L. and Strittmatter, P. (1971). A form of cytochrome b5 that contains an additional hydrophobic sequence of 40 amino acid residues. *Proc Natl Acad Sci U S A* **68**, 1042-6.

Steel, G. J., Brownsword, J. and Stirling, C. J. (2002). Tail-anchored protein insertion into yeast ER requires a novel posttranslational mechanism which is independent of the SEC machinery. *Biochemistry* **41**, 11914-20.

Stefanovic, S. and Hegde, R. S. (2007). Identification of a targeting factor for posttranslational membrane protein insertion into the ER. *Cell* **128**, 1147-59.

Stelzl, U., Worm, U., Lalowski, M., Haenig, C., Brembeck, F. H., Goehler, H., Stroedicke, M., Zenkner, M., Schoenherr, A., Koeppen, S. et al. (2005). A human protein-protein interaction network: a resource for annotating the proteome. *Cell* **122**, 957-68.

Strittmatter, P., Rogers, M. J. and Spatz, L. (1972). The binding of cytochrome b 5 to liver microsomes. *J Biol Chem* **247**, 7188-94.

Suloway, C. J., Chartron, J. W., Zaslaver, M. and Clemons, W. M., Jr. (2009). Model for eukaryotic tail-anchored protein binding based on the structure of Get3. *Proc Natl Acad Sci U S A* **106**, 14849-54.

Thress, K., Song, J., Morimoto, R. I. and Kornbluth, S. (2001). Reversible inhibition of Hsp70 chaperone function by Scythe and Reaper. *Embo J* **20**, 1033-41.

Tretyachenko-Ladokhina, V. G., Ladokhin, A. S., Wang, L., Steggles, A. W. and Holloway, P. W. (1993). Amino acid substitutions in the membrane-binding domain of cytochrome b5 alter its membrane-binding properties. *Biochim Biophys Acta* **1153**, 163-9.

Tyedmers, J., Lerner, M., Wiedmann, M., Volkmer, J. and Zimmermann, R. (2003). Polypeptide-binding proteins mediate completion of co-translational protein translocation into the mammalian endoplasmic reticulum. *EMBO Rep* **4**, 505-10.

Van den Berg, B., Clemons, W. M., Jr., Collinson, I., Modis, Y., Hartmann, E., Harrison, S. C. and Rapoport, T. A. (2004). X-ray structure of a protein-conducting channel. *Nature* **427**, 36-44.

van der Zand, A., Braakman, I. and Tabak, H. F. (2010). Peroxisomal membrane proteins insert into the endoplasmic reticulum. *Mol Biol Cell* **21**, 2057-65.

Vogel, K., Cabaniols, J. P. and Roche, P. A. (2000). Targeting of SNAP-25 to membranes is mediated by its association with the target SNARE syntaxin. *J Biol Chem* **275**, 2959-65.

Walter, P. and Blobel, G. (1981). Translocation of proteins across the endoplasmic reticulum III. Signal recognition protein (SRP) causes signal sequence-dependent and site-specific arrest of chain elongation that is released by microsomal membranes. *J Cell Biol* **91**, 557-61.

Wang, H. and Monteiro, M. J. (2007). Ubiquilin interacts and enhances the degradation of expanded-polyglutamine proteins. *Biochem Biophys Res Commun* **360**, 423-7.

Wang, H., Zhang, Q. and Zhu, D. (2003). hSGT interacts with the N-terminal region of myostatin. *Biochem Biophys Res Commun* **311**, 877-83.

White, S. H. and Wimley, W. C. (1994). Peptides in lipid bilayers: structural and thermodynamic basis for partitioning and folding. *Curr Opin Struc Biol* **4**, 79-86.

White, S. H. and Wimley, W. C. (1999). Membrane protein folding and stability: physical principles. *Annu Rev Biophys Biomol Struct* **28**, 319-65.

Whitley, P., Grahn, E., Kutay, U., Rapoport, T. A. and von Heijne, G. (1996). A 12-residue-long polyleucine tail is sufficient to anchor synaptobrevin to the endoplasmic reticulum membrane. *J Biol Chem* **271**, 7583-6.

Wiech, H., Buchner, J., Zimmermann, M., Zimmermann, R. and Jakob, U. (1993). Hsc70, immunoglobulin heavy chain binding protein, and Hsp90 differ in their ability to stimulate transport of precursor proteins into mammalian microsomes. *J Biol Chem* **268**, 7414-21.

Wilkinson, B. M., Regnacq, M. and Stirling, C. J. (1997). Protein translocation across the membrane of the endoplasmic reticulum. *J Membr Biol* **155**, 189-97.

Wimley, W. C. and White, S. H. (1996). Experimentally determined hydrophobicity scale for proteins at membrane interfaces. *Nat Struct Biol* **3**, 842-8.

Wimley, W. C., Creamer, T. P. and White, S. H. (1996). Solvation energies of amino acid side chains and backbone in a family of host-guest pentapeptides. *Biochemistry* **35**, 5109-24.

Winnefeld, M., Grewenig, A., Schnolzer, M., Spring, H., Knoch, T. A., Gan, E. C., Rommelaere, J. and Cziepluch, C. (2006). Human SGT interacts with Bag-6/Bat-3/Scythe and cells with reduced levels of either protein display persistence of few misaligned chromosomes and mitotic arrest. *Exp Cell Res* **312**, 2500-14.

Wirth, A., Jung, M., Bies, C., Frien, M., Tyedmers, J., Zimmermann, R. and Wagner, R. (2003). The Sec61p complex is a dynamic precursor activated channel. *Mol Cell* **12**, 261-8.

Wittke, S., Dunnwald, M., Albertsen, M. and Johnsson, N. (2002). Recognition of a subset of signal sequences by Ssh1p, a Sec61p-related protein in the membrane of endoplasmic reticulum of yeast Saccharomyces cerevisiae. *Mol Biol Cell* **13**, 2223-32.

Woolhead, C. A., McCormick, P. J. and Johnson, A. E. (2004). Nascent membrane and secretory proteins differ in FRET-detected folding far inside the ribosome and in their exposure to ribosomal proteins. *Cell* **116**, 725-36.

Yabal, M., Brambillasca, S., Soffientini, P., Pedrazzini, E., Borgese, N. and Makarow, M. (2003). Translocation of the C terminus of a tail-anchored protein across the endoplasmic reticulum membrane in yeast mutants defective in signal peptide-driven translocation. *J Biol Chem* **278**, 3489-96.

Yamagata, A., Mimura, H., Sato, Y., Yamashita, M., Yoshikawa, A. and Fukai, S. (2010). Structural insight into the membrane insertion of tail-anchored proteins by Get3. *Genes Cells* **15**, 29-41.

Yau, W. M., Wimley, W. C., Gawrisch, K. and White, S. H. (1998). The preference of tryptophan for membrane interfaces. *Biochemistry* **37**, 14713-8.

Young, J. C., Hoogenraad, N. J. and Hartl, F. U. (2003). Molecular chaperones Hsp90 and Hsp70 deliver preproteins to the mitochondrial import receptor Tom70. *Cell* **112**, 41-50.

Zimmermann, R., Zimmermann, M., Wiech, H., Schlenstedt, G., Muller, G., Morel, F., Klappa, P., Jung, C. and Cobet, W. W. (1990). Ribonucleoparticle-independent transport of proteins into mammalian microsomes. *J Bioenerg Biomembr* **22**, 711-23.

CHAPTER FIVE

Appendix – additional publications

Post-translational integration of tail-anchored proteins is facilitated by defined molecular chaperones

Benjamin M. Abell[1,*], Catherine Rabu[1], Pawel Leznicki[1], Jason C. Young[2] and Stephen High[1,‡]

[1]Faculty of Life Sciences, University of Manchester, Michael Smith Building, Oxford Road, Manchester, M13 9PT, UK
[2]Department of Biochemistry, McGill University, Room 914, McIntyre Building, 3655 Promenade Sir William Osler, Montreal, QC, H3G 1Y6, Canada

*Present address: Faculty of Health and Wellbeing, Sheffield Hallam University, Howard Street, Sheffield, S1 1WB, UK
‡Author for correspondence (e-mail: stephen.high@manchester.ac.uk)

Accepted 26 March 2007
Journal of Cell Science 120, 1743-1751 Published by The Company of Biologists 2007
doi:10.1242/jcs.002410

Summary

Tail-anchored (TA) proteins provide an ideal model for studying post-translational integration at the endoplasmic reticulum (ER) of eukaryotes. There are multiple pathways for delivering TA proteins from the cytosol to the ER membrane yet, whereas an ATP-dependent route predominates, none of the cytosolic components involved had been identified. In this study we have directly addressed this issue and identify novel interactions between a model TA protein and the two cytosolic chaperones Hsp40 and Hsc70. To investigate their function, we have reconstituted the membrane integration of TA proteins using purified components. Remarkably, we find that a combination of Hsc70 and Hsp40 can completely substitute for the ATP-dependent factors present in cytosol. On the basis of this in vitro analysis, we conclude that this chaperone pair can efficiently facilitate the ATP-dependent integration of TA proteins.

Supplementary material available online at
http://jcs.biologists.org/cgi/content/full/120/10/1743/DC1

Key words: Endoplasmic reticulum, Membrane proteins, Hsc70, Hsp40, Hsp90

Introduction

The majority of proteins in higher eukaryotes are synthesised in the cytosol before being targeted to their final subcellular destination, and the presence of several distinct organelles creates a requirement for efficient and accurate targeting pathways. For the endoplasmic reticulum (ER), targeting is often co-translational and begins with the binding of the signal recognition particle (SRP) to a hydrophobic signal sequence in a nascent polypeptide chain emerging from the ribosome (Nagai et al., 2003). The resulting ribosome–nascent-chain–SRP complex is delivered to the ER membrane through interaction with the SRP receptor (Halic et al., 2006), resulting in the binding of the ribosome to the Sec61 translocon and translocation into or across the ER membrane.

Whereas the post-translational targeting of proteins to organelles, such as mitochondria, is well established, post-translational routes have also been identified for specific subsets of precursors destined for the ER. These post-translational pathways commonly depend on molecular chaperones to maintain the client polypeptide in an unfolded state, thus ensuring competency for translocation into or across the organellar membrane. In yeast, a well-defined post-translational pathway for delivering secretory proteins to the ER depends on the Hsc70-chaperone Ssa1p and the Hsp40-family co-chaperone Ydj1 (Ngosuwan et al., 2003). Hsc70 also plays an important role in protein targeting to mitochondria, with Hsc70 and Hsp90 acting cooperatively to facilitate the delivery of some precursors (Humphries et al., 2005; Young et al., 2003b). Given the pivotal role of generic chaperones such as Hsc70 in protein targeting to a variety of organelles, there must be additional factors or mechanisms that distinguish specific protein-chaperone complexes in order to ensure specificity (Reichert and Neupert, 2004; Wiedemann et al., 2004). Possible discrimination in the cytosol can be provided by factors that interact with a specific precursor-chaperone complex; thus mitochondrial targeting of some precursors is stimulated by MSF (Mihara and Omura, 1996), whereas a 14-3-3 protein binds to phosphorylated signal sequences and Hsc70 to form the guide complex implicated in chloroplast targeting (May and Soll, 2000). With the exception of a novel role for SRP (Abell et al., 2004), no specialised cytosolic factors have so far been implicated in post-translational targeting to the ER targeting.

Tail-anchored (TA) proteins are targeted to various organelles (Borgese et al., 2003), and are defined by a common C-terminal hydrophobic sequence, which functions in both targeting and membrane insertion. The location of this sequence dictates that membrane integration must occur post-translationally, because translation must terminate before the targeting sequence can emerge from the ribosomal exit tunnel (High and Abell, 2004). Thus, any direct interactions between the tail-anchor and targeting factors must also occur after translation termination. The differences in the sequences of TA proteins that are delivered to distinct subcellular organelles are often quite minor (Beilharz et al., 2003; Borgese et al., 2001) and provide no clear idea as to how specificity is achieved. Nevertheless, our previous discovery that SRP is able to target some TA proteins, such as synaptobrevin 2 (Syb2), to the ER membrane in a unique post-translational mode provides one mechanism by which specificity can be achieved (Abell et al., 2004). It was equally clear from this study that other TA proteins, including cytochrome b5 and Sec61β are targeted to

the ER in an SRP-independent manner (Abell et al., 2004; High and Abell, 2004). An ATP-dependent route for the delivery of TA proteins to the ER (Kutay et al., 1995; Yabal et al., 2003) is the prime candidate for this SRP-independent route. Whereas ATP-dependent molecular chaperones are obvious candidates for facilitating this pathway, not a single ATP-dependent factor has been identified to date (Kutay et al., 1995; Yabal et al., 2003). We therefore selected Sec61β as a model precursor to identify the cytosolic factors that mediate the ATP-dependent pathway. We show that Sec61β interacts with the molecular chaperones Hsc70 and Hsp40, and that Hsc70 binding is promoted by the presence of the TA sequence. When the integration process is reconstituted using purified components, Hsc70 stimulates membrane insertion in conjunction with Hsp40 as efficiently as complete cytosol. We conclude that Hsc70 and Hsp40 are capable of facilitating the ATP dependent delivery of TA proteins to the mammalian ER, and propose that this chaperone-mediated route is distinct from any SRP-dependent targeting.

Results

N-glycosylation of Sec61β reports membrane integration at the ER

Based on our previous study (Abell et al., 2004), we selected human Sec61β as a TA protein that can use the ATP-dependent pathway for ER integration. In order to reliably monitor its integration, we generated a version of Sec61β with a short C-terminal extension containing a site for N-glycosylation (Abell et al., 2004; Borgese et al., 2001). This polypeptide Sec61βG can only be modified if the protein is correctly inserted into the ER membrane (Fig. 1). When Sec61βG is synthesised with ER-derived microsomes (K-RM) a higher molecular-mass product is observed. This product is resistant to extraction with alkaline sodium carbonate solution and sensitive to digestion with endoglycosidase H (EndoH) (Fig. 2A, lanes 1 and 2, product 1g). We therefore conclude that it is a fully membrane integrated form of Sec61β bearing a single-N-linked glycan (Abell et al., 2004). In this case we found that 16% of the membrane-associated Sec61β was N-glycosylated. Glycosylation efficiency depends on the accessibility of the recognition sequence in the ER lumen and, for TA proteins, longer extensions generally yield higher efficiencies (see also Fig. 4B below). However, a short C-terminal extension should minimise any potential impact of the tag upon ER targeting and integration (High and Abell, 2004), although the glycosylated form of Sec61β will underestimate the total population of correctly integrated polypeptides.

Sec61β ...GLK<u>VGPVPVLVMSLLFIASVFML</u>HIWGKYTRS^{96}
Sec61β-TM ...GLKVGPMMEFAESADAALQGDPALQDAGDSSR^{96}
Sec61βG ...GLK<u>VGPVPVLVMSLLFIASVFML</u>HIWGKYTRS GGGNK*N*ITQA^{106}
Sec61βOPG ...GLK<u>VGPVPVLVMSLLFIASVFML</u>HIWGKYTRS GPNFYVPFS*N*KTG^{109}
Syb2 ...WKNLK<u>MMIILGVICAIILIIIIVYF</u>ST^{116}
Syb2G ...WKNLK<u>MMIILGVICAIILIIIIVYF</u>SS SDSGGGNGGGNK*N*ITQAPPH^{136}

Fig. 1. Model TA proteins. Sequences of the tail-anchor regions and C-terminal extensions of the polypeptides used in this study. Potential transmembrane (TM) domains are underlined, dots indicate hydrophilic domains extending beyond the sequence presented. Numbers in superscript show the total length of the polypeptides; –TM indicates replacement of the hydrophobic TM domain; G indicates a chimera with a C-terminal N-glycosylation site; OPG indicates a chimera with a C-terminal extension derived from bovine opsin including an N-glycosylation site; *N* indicates N-glycosylation-target residues.

Sec61βG integration is post-translational and requires cytosolic factors

To confirm that Sec61βG can be integrated in a strictly post-translational fashion, and to establish a role for cytosolic factors in promoting this process, the insertion of partially purified polypeptides was investigated. Hence, nascent Sec61βG chains were prepared by translating mRNA lacking a stop codon and isolating the resulting ribosome nascent chain complexes (RNCs) by centrifugation using conditions that remove loosely bound factors, such as SRP (supplementary material Fig. S1A). The isolated nascent chains were released from the ribosome by puromycin treatment and the efficiency of membrane integration was analysed under various conditions by assessing their N-glycosylation. If no cytosol is added back to the purified chains, little authentic membrane integration is seen (Fig. 2B, lanes 1-3, product 1g). By contrast, when reticulocyte lysate is present significant integration is obtained (Fig. 2B, lane 4, product 1g). The addition of EDTA abolishes integration (Fig. 2B, lane 5), but this effect is reversed by the subsequent addition of magnesium ions (Fig. 2B, lane 6). We conclude that membrane integration is stimulated by factors present in the reticulocyte lysate used for translation, and that the process is dependent upon divalent cations consistent with a role for ATP.

Efficient membrane integration of Sec61β is dependent upon ATP

The hypothesis that Sec61β integration requires ATP is supported by the inhibition of this process upon nucleotide triphosphate depletion (NTPs) (Abell et al., 2004). To establish which nucleotide(s) promote the cytosol-dependent stimulation of Sec61β integration, small molecules were depleted from lysate by gel filtration and membrane insertion reconstituted with specific nucleotide triphosphates. Increasing the relative concentration of lysate increases membrane integration consistent with stimulation by cytosolic factors (Fig. 2C, lanes 1 and 2, product 1g), whereas gel filtration causes a fourfold reduction in membrane integration (Fig. 2C, lanes 1 and 3, product 1g). This reduction is fully reversed by adding ATP to the depleted lysate (Fig. 2C, lanes 3 and 4, product 1g), whereas GTP results in a modest recovery of integration, consistent with a proportion of Sec61β being targeted via the SRP dependent pathway (Abell et al., 2004). Since only a proportion of Sec61β chains are N-glycosylated, we compared the levels of glycosylated and non-glycosylated Sec61β that remained associated with the membrane fraction after extraction with alkaline sodium carbonate solution. The relative proportion of non-glycosylated Sec61β remaining after alkaline extraction showed a trend broadly similar to that of the N-glycosylated form (Fig. 2C, quantification of 0g and 1g products). However, because we can only be certain that the N-glycosylated chains are fully membrane integrated, we focused on these glycosylated chains for the remainder of the study.

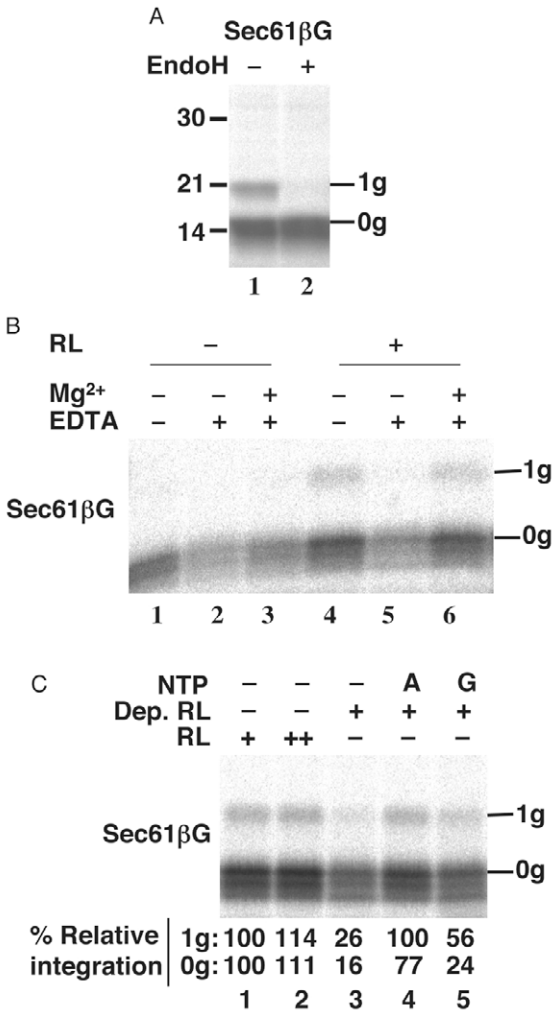

Fig. 2. N-glycosylation indicates ATP-dependent post-translational integration. (A) mRNA encoding the full-length Sec61βG polypeptide but lacking a stop codon to terminate protein synthesis (see Fig. 1) was translated for 20 minutes, and nascent-chain release synchronised by the addition of puromycin. Incubation was continued in the presence of microsomes for 30 minutes and one sample was treated with EndoH. Glycosylated and non-glycosylated Sec61β are indicated (1g and 0g respectively). Quantification showed that, in the absence of EndoH treatment, 16% of the membrane-associated chains remaining after extraction with alkaline sodium carbonate solution were N-glycosylated. Molecular mass is indicated on the left (in kDa). (B) Sec61βG was released from isolated RNCs by puromycin treatment in the presence or absence of reticulocyte lysate (RL), then treated with or without 10 mM EDTA, followed by treatment with or without 10 mM $Mg(OAc)_2$ as shown. Samples were finally incubated with microsomes for 30 minutes and membrane-associated material was isolated by extraction with alkaline sodium carbonate solution. Of the membrane-associated products recovered, 8% were N-glycosylated for the control sample (lane 4). Lower molecular weight forms of non-glycosylated Sec61β were more prevalent after RNC preparation (lanes 1-6, product 0g and below), most likely as a result of ribosome stacking (Ismail et al., 2006). We confirmed that EDTA treatment does not prevent N-glycosylation per se (data not shown), hence, a lack of glycosylated Sec61β reflects a lack of integration. (C) Sec61βG was released from isolated RNCs by puromycin treatment in the presence of buffer, reticulocyte lysate (RL) or lysate depleted of small molecules by gel filtration (Dep. RL), with additional ATP (A) or GTP (G) as shown. In one case, a double quantity of normal lysate was added (++). Samples were incubated with microsomes for 30 minutes and the membrane fraction was recovered after extraction with alkaline sodium carbonate solution as for B. The resulting material corresponding to non-glycosylated polypeptides (0g) and glycosylated polypeptides (1g) was quantified and standardised to the sample incubated with reticulocyte lysate (lane 1, relative integration=100). In this case, 6% of the membrane-associated products recovered were N-glycosylated for the control sample (lane 1).

Identification of cytosolic factors associated with Sec61β by crosslinking

To identify candidates for the ATP-dependent cytosolic factors that stimulate the membrane integration of Sec61β, we used a crosslinking approach. Nascent Sec61β chains were released from the ribosome by puromycin treatment in the presence of reticulocyte lysate. The reaction mixture was then depleted of ATP to stabilise transient interactions with components such as ATPases. Treatment with the bifunctional crosslinking reagents SMCC and BMH generated several discrete adducts, and suggested that Sec61β associates with several proteins of between 10 kDa and 90 kDa see (Fig. 3A, lanes 1-4). Using immunoprecipitation, we confirmed the identity of a 60 kDa interacting partner as the SRP54 subunit (Fig. 3B, lane 2) (Abell et al., 2004), whereas a 35 kDa partner was identified as a new adduct with Hsp40 (Fig. 3B, lane 3). Likewise a ~70 kDa interacting partner was identified as Hsc70 (Fig. 3C, lane 5). When a version of Sec61β with its tail-anchor replaced by a hydrophilic stretch of residues (Fig. 1) was analysed in the same assay, we found that Hsc70 crosslinking was clearly promoted by the presence of the tail-anchor (Fig. 3C, lanes 5 and 10). Taken together, these results show that newly synthesised Sec61β associates with defined molecular chaperones present in mammalian cytosol, and that Hsc70 binding is promoted by the presence of a tail-anchor domain.

Purified chaperones can facilitate Sec61β integration

To determine the functional role of the molecular chaperones that we had shown to be associated with Sec61β chains we reconstituted membrane insertion in the presence of different combinations of defined components in place of complete lysate (Fig. 2B,C). This approach relied on the prior depletion of stimulatory chaperones by the isolation of ribosome–nascent-chain complexes from the translation reaction by centrifugation, and we first established the efficiency of this process. This analysis showed that – in contrast to SRP, which was efficiently removed by the purification procedure – a residual amount of Hsc70 was co-purified with the RNC complexes (supplementary material Fig. S1A,B). Thus, the background level of 30% relative membrane integration (Fig. 4A, lanes 2 and 12), obtained in the absence of any exogenously added factors, may reflect the activity of such residual chaperones that remain associated with the ribosome–nascent-chain complexes during the purification process.

When the purified Sec61βG chains are supplemented with purified chaperones prior to puromycin-mediated release from the ribosome, membrane integration shows some apparent stimulation by Hsc70 alone (Fig. 4A, lanes 2 and 4). More strikingly, a combination of Hsp40 and Hsc70 together results in a level of integration equivalent to that seen with complete

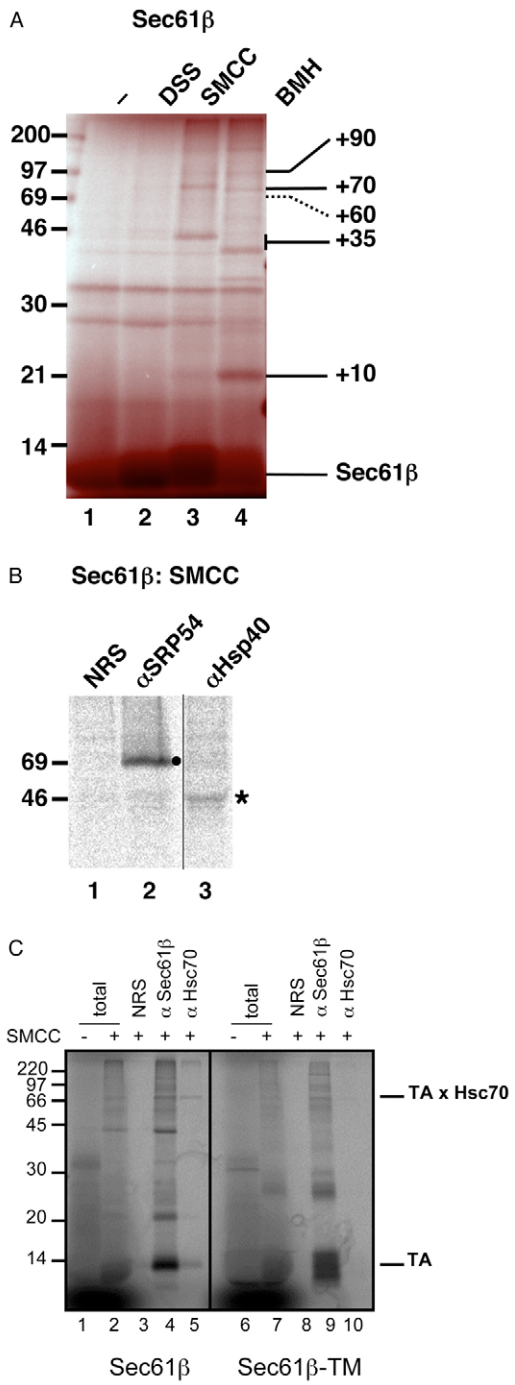

Fig. 3. Sec61β associates with cytosolic chaperones. (A) Sec61β was synthesised as in described for Fig. 2 and polypeptide chains were released from the ribosome by puromycin treatment. Samples were treated with apyrase to deplete nucleotide triphosphates, crosslinking reagents were added as shown and the resulting products resolved by SDS-PAGE. The location of Sec61β chains and the approximate molecular mass of major adducts are indicated (in kDa). (B) Products of SMCC cross-linking were subjected to immunoprecipitation with antisera recognising specific cytosolic components or a non-related serum (NRS). Adducts with SRP54 (filled circle) and Hsp40 (star) are shown. (C) Sec61β (lanes 1 to 5) or a version without the hydrophobic TM region, Sec61β-TM (lanes 6 to 10), were synthesised as for A) and total products analysed either before (lanes 1 and 6) or after (lanes 2 and 7) SMCC mediated cross-linking. Adducts were identified by immunoprecipitation carried out in the absence of prior SDS denaturation and using antisera specific for either Sec61β (lanes 4 and 9) or Hsc70 (lanes 5 and 10). A non-related serum was used as a control (lanes 3 and 8), adducts with Hsc70 are identified (filled square).

lysate (Fig. 4A, lanes 5 and 12), but only when ATP is also included in the reaction consistent with an authentic chaperone-mediated event (Fig. 4A, lanes 5 and 9). Any effect of Hsp90 is rather modest (Fig. 4A, lanes 2 and 6), and we find no indication of synergy between Hsc70-Hsp40 and Hsp90 (Fig. 4A, lanes 5 and 7). Furthermore, the purified mammalian Hsp60 complex TRiC/CCT has no effect on membrane integration (Fig. 4A, lanes 2 and 11), consistent with Hsc70-Hsp40 exerting a specific effect.

As with many reconstituted processes, we find that the purification of nascent Sec61βG chains as ribosome-bound nascent polypeptides lead to a reduction in the efficiency of N-glycosylation. In order to quantitatively and rigorously analyse the chaperone-dependent stimulation of TA protein integration, we constructed a version of Sec61 designed to be more efficiently glycosylated. We replaced the original glycosylation tag with a short section from the N-terminus of opsin that had proven well-suited to this purpose in previous studies of cytochrome b5 (Borgese et al., 2001). We found that the single site for N-glycosylation in the resulting chimera Sec61βOPG (see Fig. 1) is used very efficiently during a simple post-translational integration assay performed after puromycin release (37% of chains are N-glycosylated, see supplementary material Fig. S3A). Base-level integration of the RNC-purified Sec61βOPG chains was clearly detectable (Fig. 4B, lane 7), consistent with the co-purification of cytosolic chaperones including Hsc70 (supplementary material Fig. S1B). However, puromycin release in the presence of reticulocyte lysate, resulted in a threefold increase in membrane integration compared with control samples receiving buffer alone (Fig. 4B, lanes 6 and 7). When various combinations of purified chaperones are analysed using this second Sec61β derivative, we find that a combination of Hsp40 and Hsc70 consistently stimulates membrane integration with a high degree of statistical significance (Fig. 4B, lanes 3, 5 and 7, $P<0.01$). As previously, any stimulation by individual chaperones appears modest and the effect of combining Hsp40-Hsc70 with Hsp90 is, if anything, inhibitory. Taken together, these data suggest that Hsp40 and Hsc70 can play a major role in facilitating the ATP-dependent post-translational integration of Sec61β at the ER membrane.

To further define the significance of the Hsc70-Hsp40-mediated stimulation of TA protein membrane integration, we examined the effect of the nucleotide-exchange factor BAG1. Hsc70 activity is stimulated by BAG1 in combination with Hsp40 (Hohfeld and Jentsch, 1997) and we therefore investigated the effect of CBAG, an active fragment of BAG1 (Sondermann et al., 2001), upon the Hsc70-Hsp40-mediated membrane integration. We find that CBAG levels have a clear impact upon Hsc70-Hsp40-mediated membrane integration of Sec61βG (Fig. 4C), with maximal CBAG-dependent stimulation obtained at an estimated ratio of 1:8 (CBAG:Hsc70). This reflects a typical physiological ratio for these components (Terada and Mori, 2000), and further

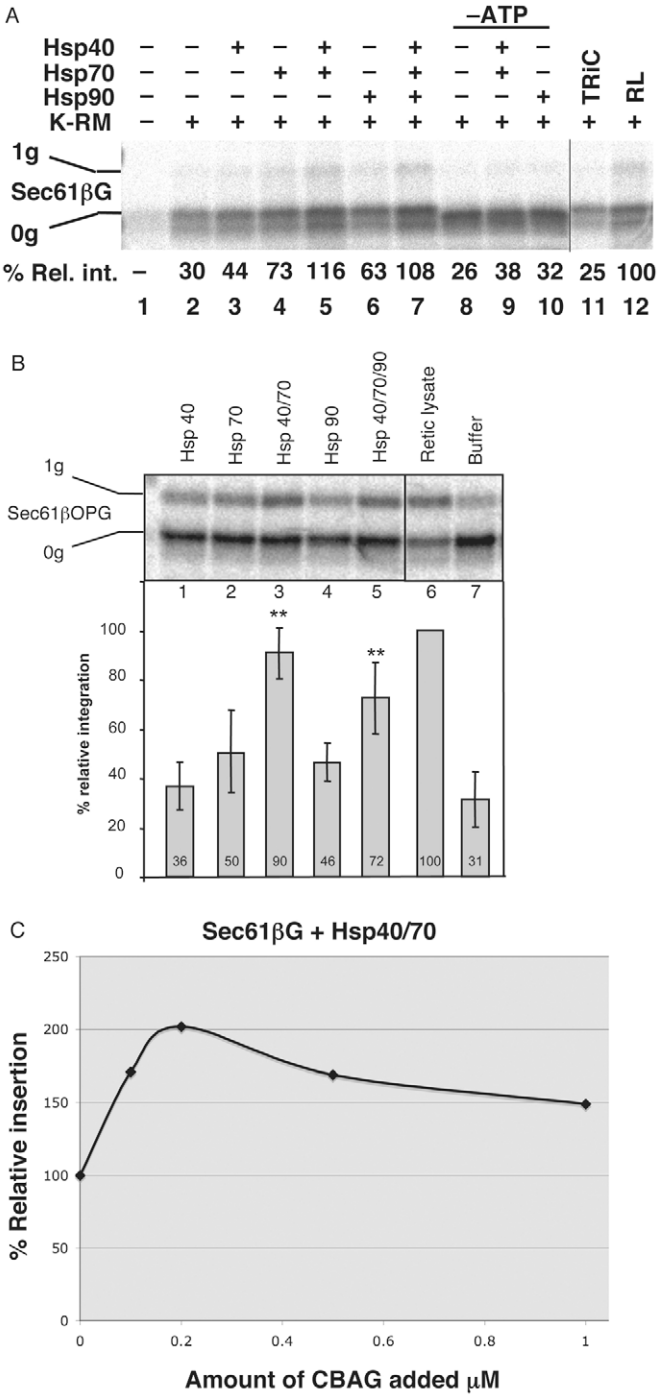

Fig. 4. Specific chaperones stimulate the membrane integration of TA proteins. (A) Sec61βG was released from isolated RNCs by puromycin treatment for 5 minutes in the presence of ATP (except for –ATP) and various molecular chaperones or reticulocyte lysate (RL) as shown. Samples were incubated with ER-derived microsomes (K-RM) for 30 minutes, and membrane-associated material was isolated as before. N-glycosylated material was quantified after extraction with alkaline sodium carbonate solution and standardised relative to the sample incubated with reticulocyte lysate (set to 100). Of the membrane associated products recovered, 10% were N-glycosylated for the control sample (lane 12). (B) Sec61βOPG was used to analyse the role of molecular chaperones as described in A. In this case, the membrane-associated material was analysed directly after the isolation of the membrane fraction through a high-salt sucrose cushion because a comparison with subsequent alkaline extraction revealed that the two procedures give similar results with this precursor (supplementary material Fig. S3B). Combinations of chaperones were added together with ATP and integration efficiency was analysed on the basis of N-glycosylation efficiency in four independent experiments. One such experiment is presented together with the average level of stimulation for the different treatments and the ±s.e.m. For the experiment shown, 42% of the membrane-associated products recovered were N-glycosylated when the sample was incubated with reticulocyte lysate (lane 6). $^{**}P<0.01$ for these chaperone combinations causing a stimulation of membrane integration when compared to the control (lane 7). (C) Sec61βG was treated as described for A, except that varying concentrations of CBAG, a C-terminal fragment of Bag1, were included. N-glycosylation was used to measure membrane integration, and the values were standardised relative to those obtained with Hsp40 and Hsc70 alone.

supports the proposal that the activity of the Hsc70-Hsp40 combination in our assay reflects an authentic biological chaperone function (see Takayama and Reed, 2001).

Different factors act at distinct stages during biosynthesis

We have previously suggested that the role of SRP during TA protein integration is largely restricted to a short period immediately after biosynthesis, whereas the factors responsible for the alternative, ATP-dependent route acted over a much longer period (Abell et al., 2004). Having now identified Hsc70-Hsp40 as one of the major cytosolic factors responsible for the ATP-dependent route in our in vitro system, we carried out a time-course analysis of Sec61βG integration in the presence of SRP, Hsc70-Hsp40 or complete lysate. This was achieved by releasing the nascent Sec61βG chains from the ribosome in the presence of the different factors for 5 minutes, followed by the addition of ER-derived microsomes and monitoring of membrane integration over a 30-minute period. The SRP-dependent integration of Sec61βG was complete within 5 minutes (Fig. 5A, ▲), consistent with our previous proposal that there is a very short window of opportunity during which SRP can target TA proteins (Abell et al., 2004). By contrast, the rate of integration achieved by Hsc70-Hsp40 was significantly slower, but the effect was sustained across the whole of the 30 minutes and ultimately surpassed the level supported by SRP (Fig. 5A, ■). The effect of complete cytosol, in the form of reticulocyte lysate, was quite distinct; hence, we observed a delay in integration of 5 minutes (Fig. 5A, ◇). However, after this delay the slopes of the curve describing membrane integration are entirely consistent with the hypothesis that, even in complete lysate, any role played by SRP is restricted to a short period after the nascent TA protein is released from the ribosome. Hence, after 10 minutes it appears that any SRP-mediated membrane integration is largely complete, and subsequent integration is presumably driven largely by Hsc70-Hsp40 (Fig. 5A, ◇ and ■).

Interplay between the SRP and chaperone pathways for TA protein integration

The time-course analysis outlined above, together with our previous work (Abell et al., 2004), suggest that the stimulation of membrane integration by SRP and Hsc70-Hsp40 are

complementary. Furthermore, whereas SRP can have a very high affinity for its substrates (Flanagan et al., 2003), it is estimated to be at least 100-fold less abundant than Hsc70 in typical mammalian cytosols (Frydman et al., 1994; Siegel and Walter, 1988), raising the possibility that its availability for the post-translational route may be limited (Abell et al., 2004). To address these issues more directly, we compared the integration of Sec61βG using nucleotide-depleted reticulocyte lysate supplemented with combinations of ATP, GTP and purified SRP. Previous studies have shown that reticulocyte lysate typically contains 5 nM endogenous SRP, and that its in vitro effects can be artificially accentuated simply by increasing its concentration (Wolin and Walter, 1989). Hence, ~12 nM purified canine SRP was added to the reaction to significantly increase the estimated SRP concentration and to establish whether this influenced TA protein integration (Wolin and Walter, 1989).

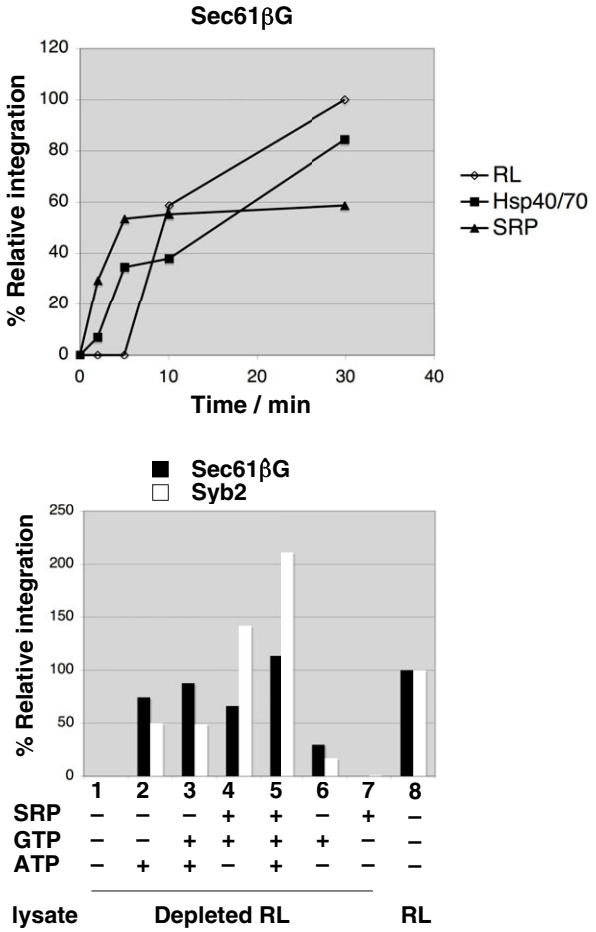

Fig. 5. Chaperone-mediated pathways operate in parallel with SRP-mediated targeting. (A) Sec61βG was released from isolated RNCs by puromycin treatment in the presence of reticulocyte lysate (◇), purified Hsp40 and Hsc70 with ATP (■) or purified SRP with GTP (▲). Samples were incubated with membranes for 0 to 30 minutes, membrane-associated material resistant to extraction with alkaline sodium carbonate solution was recovered as described above, and relative integration efficiency measured by N-glycosylation was compared with the value obtained with reticulocyte lysate after 30 minutes. (B) Sec61βG or Syb2G were isolated as RNCs and the polypeptides released from the ribosomes by puromycin treatment in the presence of reticulocyte lysate, or depleted reticulocyte lysate supplemented with SRP, ATP and GTP, as indicated. Samples were then incubated with membranes for up to 30 minutes and relative integration was measured by N-glycosylation as compared to the level obtained with reticulocyte lysate after 30 minutes.

In the case of Sec61βG, the addition of ATP resulted in a clear stimulation of membrane integration over the appropriate control (Fig. 5B, lanes 1 and 2) consistent with the use of ATP-dependent chaperones, as described above. The addition of GTP alone resulted in a more modest stimulation (Fig. 5B, lanes 1 and 6), whereas the inclusion of additional SRP enhanced this effect somewhat, consistent with SRP being limiting in this reconstituted in vitro system (Fig. 5B, lanes 4, 6 and 7). However, the effects of ATP, GTP and SRP were not additive (Fig. 5B, lanes 2, 4 and 5), suggesting that for Sec61βG there is most probably some redundancy in this in vitro system, with a fraction of chains using either the SRP-GTP-dependent, or the Hsc70-Hsp40-ATP-dependent, pathway (see Fig. 6 and Discussion).

Syb2G, a glycosylated form of Syb2 was specifically included for comparison in this analysis, because we have previously found its integration to be strongly SRP dependent (Abell et al., 2004). In this case, the ATP-mediated integration was comparatively modest, whereas the addition of SRP and GTP was almost three times more effective (Fig. 5B, combinations 1, 2 and 4). Hence, these data are consistent with a major in vitro role for SRP (Wolin and Walter, 1989) and support our previous hypothesis that the membrane integration of Syb2 is particularly SRP dependent (Abell et al., 2004). Nevertheless, the effects of ATP, GTP and SRP on membrane integration appear to be additive (Fig. 5B, combinations 2, 4 and 5), suggesting that a distinct fraction of Syb2 polypeptide chains can use the alternative, chaperone-mediated, ATP-dependent route. We conclude that the ATP- and SRP-dependent pathways for TA protein biogenesis most likely operate in parallel, and that different precursors exploit these distinct routes to varying degrees.

Discussion

The ATP-dependent stimulation of TA protein integration at the ER has been well documented but is still poorly understood (Kim et al., 1997; Kutay et al., 1995; Yabal et al., 2003). In this study, we have for the first time identified the Hsc70 chaperone system as a cytosolic factor that can facilitate this ATP-dependent pathway. Using Sec61β as a model TA precursor, we confirmed that its membrane integration is stimulated by one or more factors, present in reticulocyte lysate, that require ATP. We used a bifunctional crosslinking approach to identify candidate cytosolic factors, and confirmed our previous finding that Sec61β is a potential substrate for SRP (Abell et al., 2004). However, we now identified new interactions of Sec61β with Hsc70 (the cytosolic form of the highly conserved DnaK/Hsp70 family) and Hsp40, the cytosolic DnaJ-related co-chaperone of Hsc70. Most compelling, we show that Hsc70 functions in combination with the stimulatory co-chaperone Hsp40 to promote the ATP-dependent membrane integration of Sec61β with full efficiency when analysed in vitro. Thus, the actions of this chaperone complex conform to the established biochemical mechanisms that underlie Hsc70 functions (Mayer and Bukau, 2005; Young et al., 2004).

Early studies had implicated chaperones of the Hsp70-family in the post-translational translocation of the *S. cerevisiae* secretory protein pre-pro-α-factor into yeast microsomes (Chirico et al., 1988), and the post-translational integration of the M13 phage coat protein into canine pancreatic microsomes (Zimmermann et al., 1988). However, these studies left open the possibility that any role for Hsp70s was restricted to very specialised precursors and/or accentuated by the use of a heterologous model substrate. Our present study suggests that the Hsc70-mediated pathway is also used by TA proteins, a large class of proteins with a range of important cellular functions. For TA proteins, such as Sec61β and Syb2, although the Hsc70-Hsp40-mediated pathway appears to complement the recently described SRP-dependent post-translational pathway (Abell et al., 2004), it is mechanistically distinct.

We considered the possibility that the interactions of Sec61β with Hsc70 and its co-chaperone Hsp40 simply reflect the well-established binding of cytosolic molecular chaperones to many nascent polypeptides, both during and shortly after their synthesis (Frydman et al., 1994; Young et al., 2004). However, when a version of Sec61β that lacked its TA sequence was analysed, the binding of Hsc70 to the polypeptide was almost completely abolished. This strongly suggests that the hydrophobic TA sequence acts to continuously recruit Hsc70 onto the newly synthesised polypeptide chain, and that Hsc70 binding represents more than a transient interaction occurring during the folding of the soluble region of the newly made protein. A precedent for such a function exists in chloroplast targeting, where the binding of Hsp70 to the ferredoxin-NADP$^+$ reductase precursor has been shown to require an intact transit peptide (Rial et al., 2000). Such data support a model that in which various chaperones may play a key role during the translocation of precursor proteins into and across the membranes of a number of subcellular organelles (Young et al., 2003a).

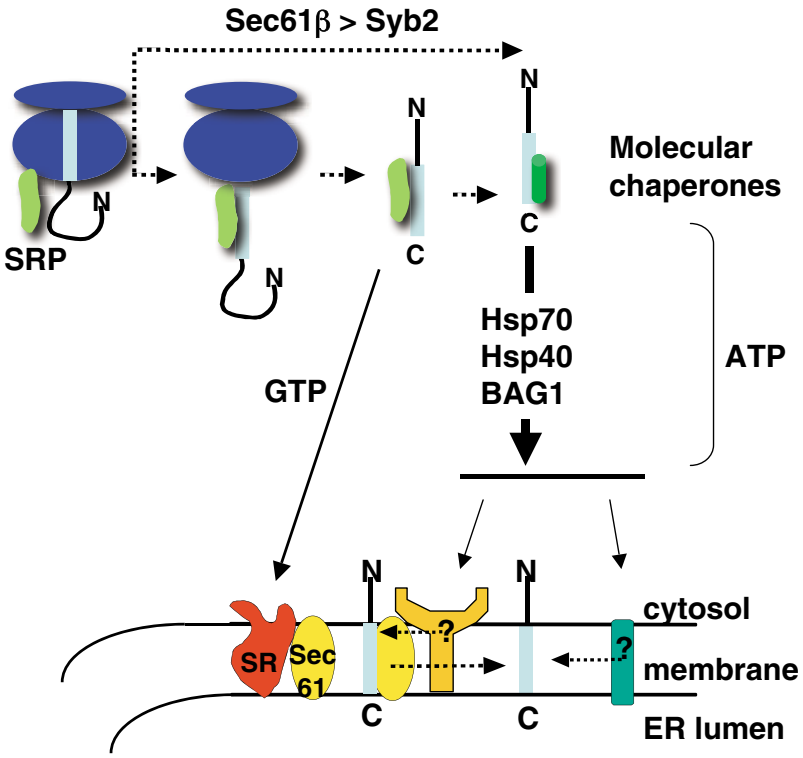

Fig. 6. A combination of SRP and molecular chaperones mediate TA protein integration. The binding of SRP to TA proteins occurs at an early stage of biosynthesis, shortly after the nascent chain is released from the ribosome. If the nascent TA protein is a poor substrate for SRP, it can use the chaperone-mediated pathway. The Hsc70-Hsp40 combination mediates the major ATP-dependent route and their activity can be modulated by co-chaperones such as BAG1. The identity of the membrane component(s) to which the molecular chaperones deliver their substrates remains unclear (High and Abell, 2004).

In order to directly address the issue of function, we purified the nascent Sec61β chains away from cytosolic factors in the reticulocyte lysate and reconstituted membrane integration using purified components. Decisively, a combination of Hsc70 and Hsp40 could efficiently substitute for complete lysate. The amount of Hsc70 used in these experiments (1.7 μM) reflects estimates of typical Hsc70 concentrations found in reticulocyte lysate (Frydman et al., 1994; Zimmermann et al., 1988). Furthermore, the Hsc70-Hsp40-mediated stimulation of membrane integration was ATP dependent and modulated by the Hsc70 co-chaperone BAG1, which acts as a nucleotide-exchange factor and functions to modulate substrate binding and release. These features confirm that Hsc70 and Hsp40 behave as authentic molecular chaperones within the context of our in vitro system (Mayer and Bukau, 2005; Young et al., 2004). By contrast, we found that the mammalian Hsp60 chaperone TRiC-CCT provides no stimulation of Sec61β integration in vitro. On this basis, we conclude that the Hsc70-Hsp40 present in the reticulocyte lysate can facilitate TA protein integration into the ER membrane (Fig. 6). Although a role for Hsp90 has been established in assisting mitochondrial import (Young et al., 2003b), a previous study of M13 phage coat protein integration found no evidence for a role in post-translational integration at the ER (Wiech et al., 1993). We find that purified Hsp90 can mediate very little, if any, stimulation of Sec61βG integration, and found no synergistic effect with the actions of Hsc70-Hsp40. Thus, any role for Hsp90s during TA protein integration remains unclear.

By comparing the kinetics of Sec61β integration in the presence of different components, we found experimental evidence to support our earlier hypothesis that the SRP-mediated pathway for TA protein biogenesis operates primarily during a short period after the release of the nascent chain from the ribosome (Abell et al., 2004). By contrast, we show that the Hsc70-Hsp40-mediated route remains active throughout the course of the experiment. When complete lysate is used to better reflect the physiological integration process for Sec61β, we find that the process appears to reflect a combination of the SRP and Hsc70-Hsp40-mediated pathways. In *S. cerevisiae*, the operation of two parallel ER-

targeting pathways is well-established, with the route taken being determined by the properties of at the signal sequence of a precursor, and a number of precursors being shown to exploit both targeting routes (Ng et al., 1996). We propose that a comparable system may operate for TA proteins and that, in this case, a combination of SRP-dependent and Hsc70-Hsp40-dependent routes are used for their delivery to the ER membrane (Fig. 6). Presumably, the relative importance of each route is also determined by the properties of the TA protein, for example the length and/or hydrophobicity of the TA sequence, although this has yet to be studied in any detail.

Our conclusion that the Hsc70 chaperone system is the primary mediator for the post-translational integration of TA proteins at the ER raises the question as to the mechanism of this function. One possibility is that Hsc70 simply maintains newly made TA proteins in an 'integration-competent' form by keeping the transmembrane domains soluble, thereby inhibiting protein aggregation. A similar mechanism has been suggested for yeast pre-pro-α-factor, where Hsc70 (Ssa1p) prevented aggregation of the precursor before translocation (Ngosuwan et al., 2003). Alternatively, or in addition to any such role, there may also be ER-specific receptors or co-chaperones that recognise the Hsc70-Hsp40-bound TA proteins. For organelles such as mitochondria and chloroplasts, there is good evidence that precursor/chaperone complexes can bind to specific receptors on the cytosolic face of the membrane (Qbadou et al., 2006; Soll and Schleiff, 2004; Young et al., 2003a). However, the identities of any membrane components that mediate the actual integration of TA proteins at the ER are poorly defined and controversial (Fig. 6). Current models range from those that suggest the process maybe entirely lipid dependent (Brambillasca et al., 2006) move through those that conclude novel integration sites may be used (Steel et al., 2002; Yabal et al., 2003), and include the possibility that the well-defined Sec61 translocon may mediate integration (Abell et al., 2003). The in vivo role of Hsc70-Hsp40 chaperones during TA protein biogenesis and the identity of any ER specific receptors for these components are a key questions for future studies.

Materials and Methods

Materials

Anti-SRP54 was a gift from B. Dobberstein (ZMBH, Heidelberg, Germany), whereas anti-Hsp40 and anti-Hsp70 antibodies were from Stressgen. Canine SRP was prepared using established protocols (Walter and Blobel, 1983b), but omitting low concentrations of the detergent Nikkol in any buffers. Canine pancreatic microsomes (Walter and Blobel, 1983a) were depleted of endogenous SRP (supplementary material Fig. S1A) by washing in high-salt buffer (Walter and Blobel, 1983b). Hsc70 was purified from bovine brain by chromatography on DEAE-cellulose, ATP-agarose and hydroxyapatite (supplementary material Fig. S2). Recombinant human Hsp40 and Hsp90 were obtained from Stressgen. The C-terminal domain of human Bag-1M [C-BAG, residues 151-264) in the vector pPROEXHTa (Invitrogen)] was expressed in BL21(DE3) *E. coli* and purified by Ni-Sepharose and Mono Q chromatography (supplementary material Fig. S2) as previously described (Sondermann et al., 2001).

Transcription

cDNAs encoding human Sec61β and rat synaptobrevin 2 were cloned in to pSPUTK (Abell et al., 2004) and transcription templates incorporating a C-terminal glycosylation tag or replacing the hydrophobic tail-anchor region were prepared by PCR using appropriate reverse primers (see supplementary material Table S1). Sec61βOPG was created in pCDNA5 (Invitrogen) by mutagenesis and the transcription template obtained by PCR from the resulting construct (supplementary material Table S1). In all cases, the mRNAs lacked a stop codon causing the resulting polypeptides to remain associated with the ribosome after synthesis (see Fig. 1A for protein sequences). Transcripts were synthesised using SP6 or T7 RNA polymerase, according to manufacturer's instructions (New England Biolabs or Promega, respectively).

Translation and membrane insertion

Proteins were synthesised using rabbit reticulocyte lysate with incubations at 30°C in the presence of [^{35}S]-methionine, according to manufacturer's instructions (Promega). Puromycin was used at 1 mM with subsequent incubation at 30°C for 5 minutes to elicit efficient release of the stalled peptidyl-tRNAs from the ribosome (Abell et al., 2004). SRP-depleted microsomes (K-RM) were added to a final concentration of 1.5-2.0 OD_{280} per ml, and were analysed for TA protein insertion on the basis of relative N-glycosylation efficiency following recovery by centrifugation through 100 μl HSC (500 mM sucrose, 500 mM KOAc, 5 mM $Mg(OAc)_2$, 50 mM Hepes-KOH pH 7.9) at 100,000 ***g*** for 10 minutes or 132,000 ***g*** for 5 minutes. Where indicated, the resulting membrane pellet was resuspended in 100 μl of cold 0.1 M Na_2CO_3, incubated on ice for 10 minutes and recovered by centrifugation at 132,000 ***g*** for 5 minutes to confirm membrane integration. De-glycosylation was performed with endoglycosidase H (EndoH) according to manufacturer's instructions (New England Biolabs).

Nucleotide depletion

Reticulocyte lysate was depleted of nucleotides by loading 70 μl onto a Biospin 6 column (Bio-Rad) equilibriated with LSC buffer (100 mM sucrose, 100 mM KOAc, 5 mM $Mg(OAc)_2$, 50 mM Hepes-KOH pH 7.9, 1 mM DTT), following manufacturer's instructions, repeating the process once. A parallel depletion using a translation of Syb2 showed a 49% recovery rate and a double volume of depleted lysate was used for comparative experiments with non-depleted lysate.

Crosslinking and immunoprecipitation

Following puromycin treatment, translation products were treated with 1 μg of apyrase per 40 μl volume for 5 minutes at 30°C, then incubated on ice for 5 minutes followed by incubation at 30°C for 5 minutes with either 1 mM disuccinimidyl suberate (DSS; Pierce), 1 mM succinimidyl *trans*-4-(maleimidylmethyl) cyclohexane-1-carboxylate (SMCC; Pierce) or bismaleimidohexane (BMH; Pierce) diluted from a 20 mM stock in DMSO. Crosslinking was stopped with 50 mM glycine (DSS), 10 mM 2-mercaptoethanol (BMH) or both (SMCC). Samples were denatured with SDS unless otherwise stated; specific adducts were recovered by immunoprecipitation (Abell et al., 2003).

Reconstitution of ER integration

Ribosome–nascent-chain complexes (RNCs) were generated by translating transcripts lacking a stop codon for 7 minutes. Reactions of 200 μl were supplemented with 2.5 mM cycloheximide and 500 mM KOAc, and the final 240 μl sample was layered over 400 μl HSCC (HSC with 2.5 mM cycloheximide and 1 mM DTT), followed by centrifugation at 213,000 ***g*** for 20 minutes. The pellet was resuspended in 50 μl HSCC with reduced sucrose (100 mM), layered onto 150 μl HSCC, and centrifuged at 213,000 ***g*** for 20 minutes. The pellet was finally resuspended in 40 μl LSC. Membrane-insertion reactions comprised 2 μl of isolated RNCs made up to a final volume of 10 μl by LSC and various additions. Hsp40 was added at 3 μM, Hsc70 was added at 1.7 μM, Hsp90 was added at 1.3 μM, TRiC (gift from Judith Frydman, James Clark Center, Stanford University, CA) was added at 0.6 μM, SRP was added at ~12.5 nM, prespun reticulocyte lysate was added at 20% v/v, and depleted lysate was added at 40% v/v. ATP or GTP was added at 1 mM. Following the addition of all cytosolic targeting factors and treatments, puromycin was added at 1 mM and the sample incubated for 5 minutes at 30°C. Membrane insertion was achieved by incubation with K-RMs (final concentration of 1.5-2.0 OD_{280} per ml) at 30°C.

Gel electrophoresis

Samples were heated to 70°C for 10 minutes in SDS-PAGE sample buffer and then resolved on 16% polyacrylamide Tris-glycine gels under denaturing conditions. Gels were fixed, dried and then exposed to phosphorimage plates, which were read using a Fuji BAS-3000 phosphorimager. Radiolabelled products separated by SDS-PAGE were quantified using Aida software.

This work was supported by a Biotechnology and Biological Sciences Research Council (BBSRC) Professorial Fellowship and a BBSRC grant (both to S.H.) and a Canadian Institutes of Health Research operating grant (to J.C.Y.). J.C.Y. holds a Canada Research Chair in Molecular Chaperones. We thank Judith Frydman (Stanford) for supplying purified TRiC and Bernhard Dobberstein (ZMBH) for antibodies. Thanks to C. Y. Anna Fan for assistance with protein purifications, and Martin Pool and Phil Woodman for their help during the preparation of the manuscript.

Note added in proof

While this work was under review, the Asna-1 protein was independently identified as a cytosolic ATPase that can promote the membrane insertion of TA proteins (Stefanovic and Hegde, 2007). We therefore conclude that the ATP-dependent integration of TA proteins at the ER is most probably complex and multifaceted.

References

Abell, B. M., Jung, M., Oliver, J. D., Knight, B. C., Tyedmers, J., Zimmermann, R. and High, S. (2003). Tail-anchored and signal-anchored proteins utilize overlapping pathways during membrane insertion. *J. Biol. Chem.* **278**, 5669-5678.

Abell, B. M., Pool, M. R., Schlenker, O., Sinning, I. and High, S. (2004). Signal recognition particle mediates post-translational targeting in eukaryotes. *EMBO J.* **23**, 2755-2764.

Beilharz, T., Egan, B., Silver, P. A., Hofmann, K. and Lithgow, T. (2003). Bipartite signals mediate subcellular targeting of tail-anchored membrane proteins in Saccharomyces cerevisiae. *J. Biol. Chem.* **278**, 8219-8223.

Borgese, N., Gazzoni, I., Barberi, M., Colombo, S. and Pedrazzini, E. (2001). Targeting of a tail-anchored protein to endoplasmic reticulum and mitochondrial outer membrane by independent but competing pathways. *Mol. Biol. Cell* **12**, 2482-2496.

Borgese, N., Colombo, S. and Pedrazzini, E. (2003). The tale of tail-anchored proteins: coming from the cytosol and looking for a membrane. *J. Cell Biol.* **161**, 1013-1019.

Brambillasca, S., Yabal, M., Makarow, M. and Borgese, N. (2006). Unassisted translocation of large polypeptide domains across phospholipid bilayers. *J. Cell Biol.* **175**, 767-777.

Chirico, W. J., Waters, M. G. and Blobel, G. (1988). 70 K heat shock related proteins stimulate protein translocation into microsomes. *Nature* **332**, 805-810.

Flanagan, J. J., Chen, J. C., Miao, Y., Shao, Y., Lin, J., Bock, P. E. and Johnson, A. E. (2003). Signal recognition particle binds to ribosome-bound signal sequences with fluorescence-detected subnanomolar affinity that does not diminish as the nascent chain lengthens. *J. Biol. Chem.* **278**, 18628-18637.

Frydman, J., Nimmesgern, E., Ohtsuka, K. and Hartl, F. U. (1994). Folding of nascent polypeptide chains in a high molecular mass assembly with molecular chaperones. *Nature* **370**, 111-117.

Halic, M., Gartmann, M., Schlenker, O., Mielke, T., Pool, M. R., Sinning, I. and Beckmann, R. (2006). Signal recognition particle receptor exposes the ribosomal translocon binding site. *Science* **312**, 745-747.

High, S. and Abell, B. M. (2004). Tail-anchored protein biosynthesis at the endoplasmic reticulum: the same but different. *Biochem. Soc. Trans.* **32**, 659-662.

Hohfeld, J. and Jentsch, S. (1997). GrpE-like regulation of the hsc70 chaperone by the anti-apoptotic protein BAG-1. *EMBO J.* **16**, 6209-6216.

Humphries, A. D., Streimann, I. C., Stojanovski, D., Johnston, A. J., Yano, M., Hoogenraad, N. J. and Ryan, M. T. (2005). Dissection of the mitochondrial import and assembly pathway for human Tom40. *J. Biol. Chem.* **280**, 11535-11543.

Ismail, N., Crawshaw, S. G. and High, S. (2006). Active and passive displacement of transmembrane domains both occur during opsin biogenesis at the Sec61 translocon. *J. Cell Sci.* **119**, 2826-2836.

Kim, P. K., Janiak-Spens, F., Trimble, W. S., Leber, B. and Andrews, D. W. (1997). Evidence for multiple mechanisms for membrane binding and integration via carboxyl-terminal insertion sequences. *Biochemistry* **36**, 8873-8882.

Kutay, U., Ahnert-Hilger, G., Hartmann, E., Wiedenmann, B. and Rapoport, T. A. (1995). Transport route for synaptobrevin via a novel pathway of insertion into the endoplasmic reticulum membrane. *EMBO J.* **14**, 217-223.

May, T. and Soll, J. (2000). 14-3-3 proteins form a guidance complex with chloroplast precursor proteins in plants. *Plant Cell* **12**, 53-64.

Mayer, M. P. and Bukau, B. (2005). Hsp70 chaperones: cellular functions and molecular mechanism. *Cell. Mol. Life Sci.* **62**, 670-684.

Mihara, K. and Omura, T. (1996). Cytoplasmic chaperones in precursor targeting to mitochondria: the role of MSF and hsp 70. *Trends Cell Biol.* **6**, 104-108.

Nagai, K., Oubridge, C., Kuglstatter, A., Menichelli, E., Isel, C. and Jovine, L. (2003). Structure, function and evolution of the signal recognition particle. *EMBO J.* **22**, 3479-3485.

Ng, D. T. W., Brown, J. D. and Walter, P. (1996). Signal sequences specify the targeting route to the endoplasmic reticulum membrane. *J. Cell Biol.* **134**, 269-278.

Ngosuwan, J., Wang, N. M., Fung, K. L. and Chirico, W. J. (2003). Roles of cytosolic Hsp70 and Hsp40 molecular chaperones in post-translational translocation of presecretory proteins into the endoplasmic reticulum. *J. Biol. Chem.* **278**, 7034-7042.

Qbadou, S., Becker, T., Mirus, O., Tews, I., Soll, J. and Schleiff, E. (2006). The molecular chaperone Hsp90 delivers precursor proteins to the chloroplast import receptor Toc64. *EMBO J.* **25**, 1836-1847.

Reichert, A. S. and Neupert, W. (2004). Mitochondriomics or what makes us breathe. *Trends Genet.* **20**, 555-562.

Rial, D. V., Arakaki, A. K. and Ceccarelli, E. A. (2000). Interaction of the targeting sequence of chloroplast precursors with Hsp70 molecular chaperones. *Eur. J. Biochem.* **267**, 6239-6248.

Siegel, V. and Walter, P. (1988). The affinity of signal recognition particle for presecretory proteins is dependent on nascent chain length. *EMBO J.* **7**, 1769-1775.

Soll, J. and Schleiff, E. (2004). Protein import into chloroplasts. *Nat. Rev. Mol. Cell Biol.* **5**, 198-208.

Sondermann, H., Scheufler, C., Schneider, C., Hohfeld, J., Hartl, F. U. and Moarefi, I. (2001). Structure of a Bag/Hsc70 complex: convergent functional evolution of Hsp70 nucleotide exchange factors. *Science* **291**, 1553-1557.

Steel, G. J., Brownsword, J. and Stirling, C. J. (2002). Tail-anchored protein insertion into yeast ER requires a novel posttranslational mechanism which is independent of the SEC machinery. *Biochemistry* **41**, 11914-11920.

Stefanovic, S. and Hegde, R. S. (2007). Identification of a targeting factor for posttranslational membrane protein insertion into the ER. *Cell* **128**, 1147-1159.

Takayama, S. and Reed, J. C. (2001). Molecular chaperone targeting and regulation by BAG family proteins. *Nat. Cell Biol.* **3**, E237-E241.

Terada, K. and Mori, M. (2000). Human DnaJ homologs dj2 and dj3, and bag-1 are positive cochaperones of hsc70. *J. Biol. Chem.* **275**, 24728-24734.

Walter, P. and Blobel, G. (1983a). Preparation of microsomal membranes for cotranslational protein translocation. *Meth. Enzymol.* **96**, 84-93.

Walter, P. and Blobel, G. (1983b). Signal recognition particle: a ribonucleoprotein required for cotranslational translocation of proteins, isolation and properties. *Meth. Enzymol.* **96**, 682-691.

Wiech, H., Buchner, J., Zimmermann, M., Zimmermann, R. and Jakob, U. (1993). Hsc70, immunoglobulin heavy chain binding protein, and Hsp90 differ in their ability to stimulate transport of precursor proteins into mammalian microsomes. *J. Biol. Chem.* **268**, 7414-7421.

Wiedemann, N., Frazier, A. E. and Pfanner, N. (2004). The protein import machinery of mitochondria. *J. Biol. Chem.* **279**, 14473-14476.

Wolin, S. L. and Walter, P. (1989). Signal recognition particle mediates a transient elongation arrest of preprolactin in reticulocyte lysate. *J. Cell Biol.* **109**, 2617-2622.

Yabal, M., Brambillasca, S., Soffientini, P., Pedrazzini, E., Borgese, N. and Makarow, M. (2003). Translocation of the C terminus of a tail-anchored protein across the endoplasmic reticulum membrane in yeast mutants defective in signal peptide-driven translocation. *J. Biol. Chem.* **278**, 3489-3496.

Young, J. C., Barral, J. M. and Hartl, F. U. (2003a). More than folding: localized functions of cytosolic chaperones. *Trends Biochem. Sci.* **28**, 541-547.

Young, J. C., Hoogenraad, N. J. and Hartl, F. U. (2003b). Molecular chaperones Hsp90 and Hsp70 deliver preproteins to the mitochondrial import receptor Tom70. *Cell* **112**, 41-50.

Young, J. C., Agashe, V. R., Siegers, K. and Hartl, F. U. (2004). Pathways of chaperone-mediated protein folding in the cytosol. *Nat. Rev. Mol. Cell Biol.* **5**, 781-791.

Zimmermann, R., Sagstetter, M., Lewis, M. L. and Pelham, H. R. B. (1988). Seventy-kilodalton heat shock proteins and an additional component from reticulocyte lysate stimulate import of M13 procoat protein into microsomes. *EMBO J.* **7**, 2875-2880.

Journal of Cell Science